Faculty of Science

Department of Inorganic and Physical Chemistry

Novel Ruthenium Indenylidene Catalysts: From Homogeneous to Heterogeneous

Fatma B. Hamad

Promoter: Prof. Dr. F. Verpoort

Thesis Submitted in Fulfillment of the Requirements for the Degree of Doctor of Science: Chemistry

2013

Examination Committee

Prof. F. Verpoort

Prof. A. Adriaens

Prof. K. Van Hecke

Prof. I. Dragutan

Prof. C. Stevens

Prof. V. Dragutan

Acknowlodgement

This thesis is the end of my journey toward getting Ph.D. I have not traveled in a vacuum in this journey. This thesis has been kept on track and been seen through to completion with the support and encouragement of numerous people. It is a pleasure to thank all those who contributed in any ways to the success of this study, made this thesis possible and an unforgettable experience for me.

First of all, I would like to thank my promoter, Prof. Dr. Francis Verpoort not only for accepting me to join his research group but also for his patience in supervising, critics and giving thoughtful guidance with knowledge towards the completion of this research.

I take this opportunity to sincerely acknowledge the Science and Technology Higher Education project (STHEP) for providing financial support which buttresses me to perform my work comfortably.

Special thanks are due to Dr. Ana for her encouragement and support in working with homogeneous metathesis catalysis. I would like thank my colleagues: Stijn, Agata, Heriberto, Yu, Fu, Zhixhu, Karen, Els, Ilke, Yingya, Doleres, Shyam and Matthias for the stimulating discussions. Technical support from Danny, Tom, Pat, Philip and Bart is gratefully acknowledged. Thanks to Pierre and Claudine, their help exceeded that of administrative one.

Finally, I am very thankful to my mother, my husband and my beloved daughters and son, my sisters and brothers for their love, understanding, encouragement and support.

Preface

The term olefin metathesis was coined by Calderon and co-workers after discovery of tungsten based catalysts that bring about both ring-opening polymerization and the disproportionation of acyclic olefins.

After establishment of Chauvin's olefin metathesis mechanism and of its experimental support several well-defined, single-species catalysts based on different transition metals have been developed. These include the Tebbe's reagent, Schrock's molybdenum and tungsten alkylidene catalysts. However, these catalysts are limited by the high oxophilicity of the metal centers and by poor functional group tolerance.

In 1996, Grubbs' 1st generation catalyst was introduced which displayed not only functional groups tolerance but also improved activity**.** Since that discovery several research groups have dedicated their efforts to synthesize structurally-related catalysts, with improved properties. Interestingly, several ruthenium carbene that initially meant for metathesis reaction turned out to be active catalysts for other kind of reactions such as hydrogenation, isomerisation, Kharasch reaction, oxidations etc. In addition, it is possible to immobilize this kind of carbenes to afford heterogeneous catalysts which can be easily separated from reaction mixture and reused.

Although ruthenium indenylidene metathesis initiators proved to have higher thermal stability than their benzylidene counterpart, the state-of-the-art of these carbenes is lagging behind that of alkylidene analogs in many respects. As our contribution in this field, we have started by fine tuning the ligand environment of the second generation ruthenium indenylidene catalyst to afford *N*-alkyl, *N*'-aryl NHC coordinated catalysts followed by investigating the stability and activity of indenylidene ruthenium catalysts immobilized on silica supported niobic acid and on silica supported methylaluminoxane.

Outline

This thesis is made up of mainly three parts; part one comprises of literature review, part two results and discussions and part three concerns with summary, conclusion and outlook.

Part I: Literature Review

Chapter 1: Presents general introduction to olefin metathesis, it includes chronological development of first generation and second generation ruthenium alkylidene and indenylidene catalysts.

Chapter 2: Provides current state-of-the- art on unsymmetric NHC carbenes bearing ruthenium metathesis initiators. It mostly discusses the synthesis, characterization and applications of ruthenium complexes coordinated with unsymmetric NHC carbenes in metathesis processes. The progress involved and advantages offered by the unsymmetrical ligands as compared to the related symmetrical analogs are also discussed in detailed and critical manner.

Chapter 3: Summarizes the application of ruthenium catalysts in non-metathesis reactions particularly isomerization of allylic alcohols, isomerization of alkenes and Kharasch addition.

Chapter 4: Presents heterogenization of ruthenium based metathesis initiators on solid supports.The immobilization of the catalysts on polymeric beads, monolithic materials and siliceous supports both mesoporous as well as nonporous is discussed. In addition, the performance of the supported catalysts is compared with that of homogeneous analogs.

Part II: Results and Discussion

Chapter 5: Illustrates the coordination of unsymmetrical NHCs bearing *N*-alkyl, *N'*-aryl on ruthenium indenylidene and their catalytic activity in the ROMP of 1,5-*cis,cis*-cyclooctadiene and RCM of diethyl diallyl malonate.

Chapter 6: Summarizes the application of ruthenium catalysts bearing unsymmetrical NHCs in non-metathesis reactions mainly isomerization of allylic alcohol, isomerization of alkene and Kharasch addition.

Chapter 7: Discusses the stability and activity ruthenium indenylidene catalysts immobilized on silica supported niobic acid.

Chapter 8: Describes the suitability of strong Lewis acidic-methylaluminoxane supported on silica as alternative support for ruthenium indenylidene catalysts.

Part III: Summary, Conclusion and Outlook

Chapter 9: Provides the summary of the previous chapters, conclusion and recommendation for future work.

Chapter 10: Concerns with the Dutch summary and outlook.

List of Abbreviations

NHC	*N*-Heterocyclic Carbene
ROMP	Ring Opening Metathesis Polymerization
CM	Cross Metathesis
RCM	Ring Closing Metathesis
ROM	Ring Opening Metathesis
ADMET	Acyclic Diene Metathesis Polymerization
Mes	2,4,6-trimethylphenyl
THF	Tetrahydofuran
RO-RCM	Ring Opening Ring Closing Metathesis
DEDAM	Diethyl Diallyl Malonate
TON	Turn Over Number
NBE	Norbornene
COE	Cyclooctene
CPE	Cyclopentene
RO-RCM	Ring Opening-Ring Closing Metathesis
DRRM	Diastereoselective Ring Rearrangement Metathesis
REMP	Ring Expansion Metathesis Polymerization
NMR	Nuclear Magnetic Resonance
PCy_3	Tricyclohexylphosphine
PPh_3	Triphenylphosphine
AROCM	Asymmetric Ring opening Cross Metathesis
COD	cyclooctadiene
CAAC	A cyclic (Alkyl) (Amino) Carbene
Cp	Cyclopentadienyl
ATRA	Atom Transfer Radical Addition
AIBN	Azobisisobutyronitrile
PS-DVB	polystyrene Divinyl Benzene
PS-BES	Polystyrene-Butyldiethylsilyl
PEGA	Polystyrene polyethylene glycol
TEOS	Tetraethoxysilane
SBA-15	Santa Barbara Amorphous-15
MCM-41	Mobil Composite Materials-41
MCF	Mesocellular Foam
KHMDS	Potassium bis(trimethylsilyl) amide
LiHMDS	Lithium bis(trimethylsilyl) amide
NOESY	Nuclear Overhauser effect spectroscopy
FTIR	Fourier Transform Infrared Spectroscopy
IUPAC	International Union for Pure and Applied Chemistry
BHT	Butylated Hydroxytoluene
MAO	Methylaluminoxane
TMA	Trimethylaluminium

Contents

Part I: Literature Review

1.1 Development of First Generation Ruthenium Alkylidene

The olefin metathesis was discovered incidentally and independently in 1950s by different researchers on their attempt to polymerize olefins by the Ziegler process [1-5]. The earliest discoveries were the basic exchange olefin metathesis of the inter-conversion of propylene, ethylene and butane-2 as well as ROMP of norbornene and cylcopentene. However, the connection between the two types of reactions was not immediately apparent mainly because different catalysts and conditions were generally involved.

The discovery of the tungsten based catalyst by Calderon and co-workers that bring about both rapid polymerization of cyclooctene and cyclooctadiene [6] and the disproportionation of pent-2-ene [7-9] provided the connection that led to the realization that both ring-opening polymerization and the disproportionation of acyclic olefins were the same kind of reaction. Henceforward, the reaction became known as olefin metathesis, to mean the metal-catalyzed redistribution of carbon-carbon double bonds.

The most common variations of olefin metathesis are represented in Scheme 1. Cross metathesis (CM) where groups between acyclic olefins are exchanged [10,11], ring closing metathesis (RCM) where acyclic dienes are ring closed [12], ring-opening metathesis (ROM) where dienes are formed from cyclic olefins [13], ring-opening metathesis polymerization (ROMP) where cyclic olefins are polymerized [14,15] and acyclic diene metathesis polymerization (ADMET) where acyclic dienes are polymerized [16].

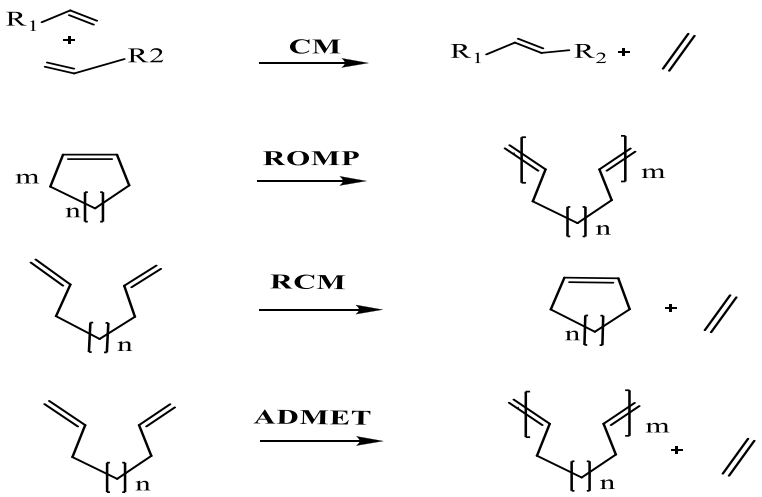

Scheme 1: Types of olefin metathesis reactions.

However, from its discovery in 1950s to the early 1980s, all olefin metathesis were accomplished with poorly defined, multi-component systems which are formed *in-situ* from transition metal halide catalysts and main group metal alkyl co-catalysts. Some representative examples include; $WCl_6/EtAlCl_2$, $WCl_6/BuSn_4$, and MoO_3/SiO_2 [14]. Sometime a third component, for instance, in the Calderon's catalyst ($WCl_6/EtAlCl_2/EtOH$) [8] had to be added to the catalytic system as an activator. Nevertheless, the utility of these catalysts was limited by the harsh conditions and strong Lewis acids that are required which made them incompatible with most functional groups.

In addition, the reactions were difficult to initiate and control because of very little active species formed in the catalyst mixtures. These problems motivated researchers to perform extensive work focused on better understanding of olefin metathesis and its mechanism.

The initial proposed mechanism was that of a pair-wise exchange of alkylidenes through a 'quasi-cyclobutane' mechanism in which two olefins coordinated to the metal and exchanged alkylidene groups through a symmetrical intermediate [17]. However, Chauvin found that this mechanism could not explain some of the experimental observations. For instance, he found that, at the end acyclic olefin became disconnected, resulting in a statistical mixture of kinetic products. Based on that observation, he suggested a non-pair wise mechanism in which a metal carbene reacts with an olefin to form a metallacyclobutane intermediate. This intermediate then proceeds by cycloreversion either non-productively resulting in the reformation of the starting materials or productively resulting in the new olefin and a new metal carbene [18] (Scheme 2).

Establishment of the experimental support to Chauvin's mechanism by Katz [20-22] and Grubbs [23,24] made the design of rational catalysts possible. Consequently, several well-defined, single-species catalysts based on different transition metals have been developed. In particular, Tebbe's reagent [25] **1** and Schrock's molybdenum and tungsten alkylidene catalysts [26-30] **2** made a great contribution in olefin metathesis (Scheme 3). However, these catalysts and others based on the early transition metals are limited by the high oxophilicity of the metal centers and by moderate to poor functional groups tolerance.

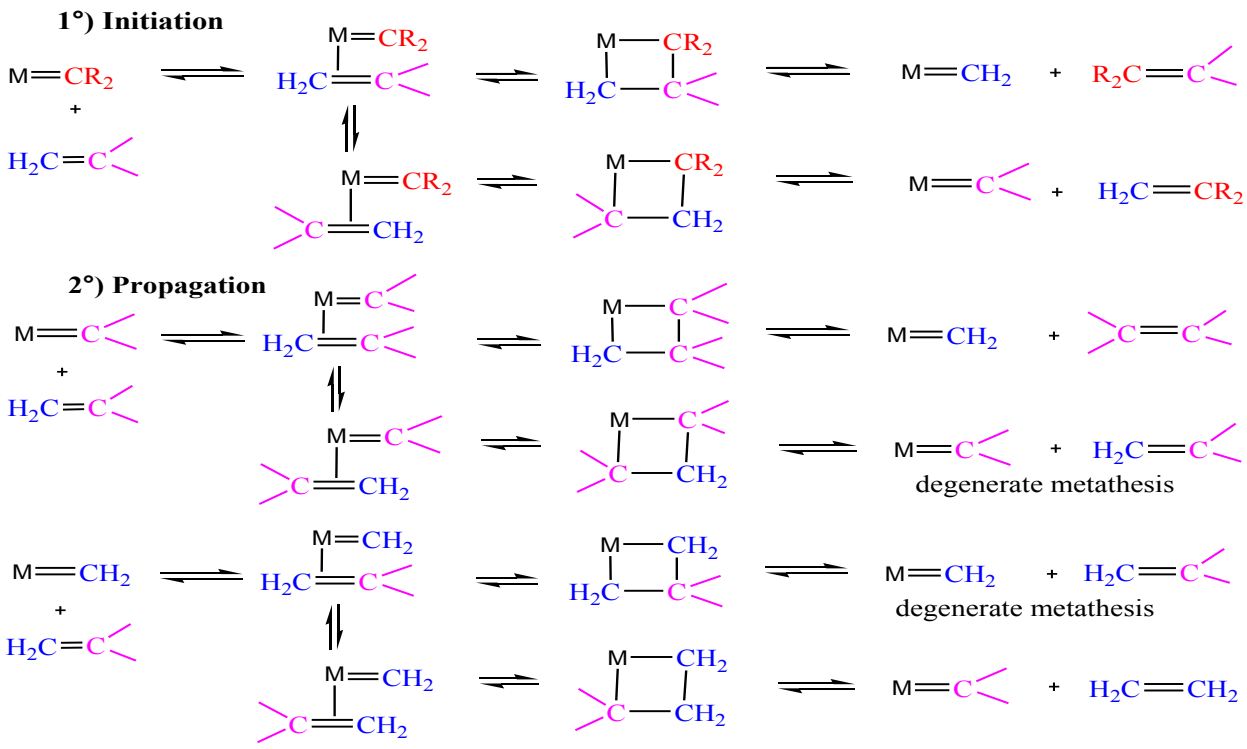

Scheme 2: General mechanism of olefin metathesis [19].

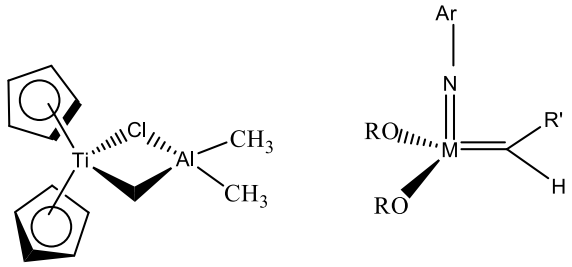

1 **2:** M = Mo, W

Scheme 3: Tebbe's reagent **1** and Schrock's alkylidene catalyst **2**.

In 1992 Grubbs and coworkers [31] developed ruthenium catalyst **3** from commercially available diphenylcyclopropene and $RuCl_2(PPh_3)_3$ (Scheme 4). Although this catalyst is stable in protic and aqueous solvents, it exhibits limited reactivity compared to Schrock's catalysts and is only effective in the ROMP of highly strained olefins.

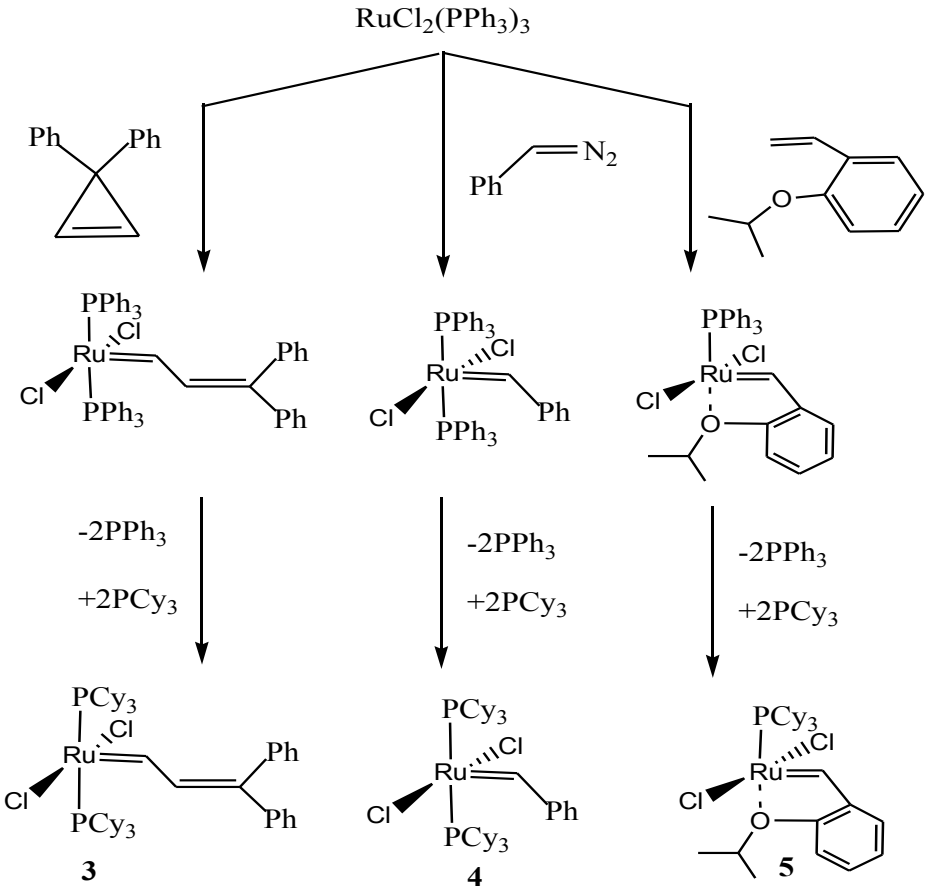

Scheme 4: Preparation of the catalysts **3**-**5**.

Modifications of the ruthenium catalyst **3** were conducted and eventually in 1996, Grubbs' 1st generation catalyst **4** was introduced from reaction of $RuCl_2(PPh_3)_3$ with phenyl diazoalkane (Scheme 4) [32], which displayed not only functional groups tolerance compared with ruthenium catalyst **3** but also improved activity**.** The substitution of one phosphine ligand for a bidentate alkylidene led to the development of ruthenium catalyst **5** with even higher thermal stability [33-35].

Soon after the discovery of Grubbs' 1st generation, the effort to understanding its mechanism in olefins metathesis began. Various reports show that ruthenium complexes, $L_2X_2Ru{=}CHR$, are arranged in a distorted square pyramidal geometry with the alkylidene in the axial position and the phosphines and halides in the equatorial plane [32]. Based on extensive kinetic studies Grubbs and co-workers proposed a mechanism that is consistent with the observed activity trends [36].

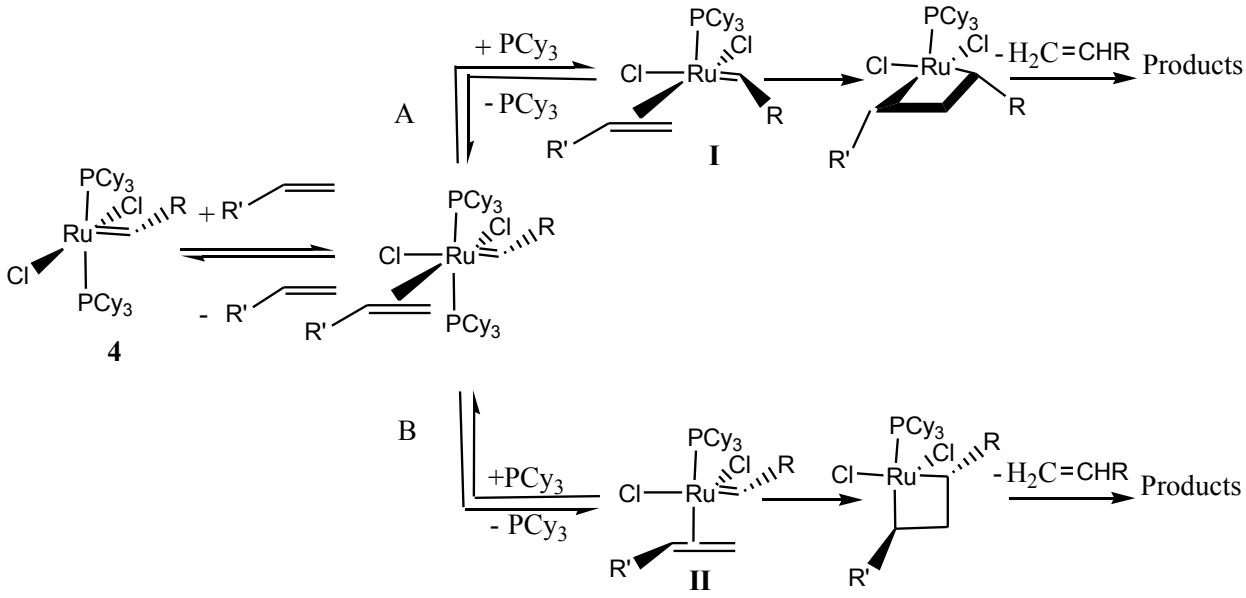

Scheme 5: Proposed mechanism for catalyst **4** in olefin metathesis [42].

As illustrated in Scheme 5, the first step involves olefin coordination to the metal center. Two pathways are possible at this stage. Pathway (**A**) phosphine dissociation and alkylidene rotation occur in order to generate the 16-electrons intermediate **I**, in which the olefin remains *cis* to the alkylidene. This intermediate then undergoes metallocyclobutane formation *cis* to the bound phosphine, followed by cleavage to release the metathesis products. An alternative pathway (**B**) involves phosphine dissociation and rearrangement of the olefin in order to generate intermediate (**II**). The intermediate (**II**) then undergoes metallocyclobutane formation *trans* to the phosphine.

1.2 Development of Second Generation Ruthenium Alkylidene

In 1998, Herrmann and co-workers reported the synthesis of the first heterocyclic carbene coordinating ruthenium catalysts (**6-10**) (Scheme 6) in which both phosphine ligands were replaced by NHCs [37]. Despite their high stability, these complexes did not show a significant improvement in metathesis activity, mostly due to their slow initiation rates. In these complexes, one of the NHCs [38, 39] has to dissociate from the metal center for the catalyst to be initiated.

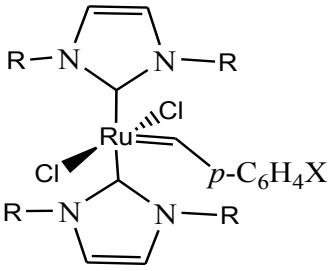

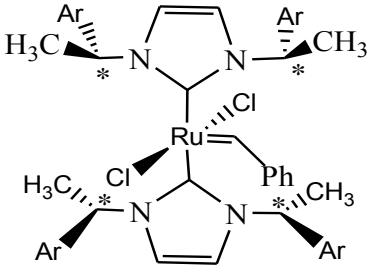

6: R = *i*Pr, X=H
7: R = cyclohexyl, X = H
8: R = *i*Pr, X= Cl

9: Ar = Ph
10: Ar = naphthyl

Scheme 6: First reported ruthenium-based carbene-coordinated metathesis catalysts.

Soon thereafter, the synthesis of heteroleptic ruthenium complexes **11** and **12** (Scheme 7), which combinine a non-labile NHC with a labile phosphine ligands was reported [39]. Complexes **11** and **12** exhibited not only higher RCM activity affording even tetrasubstituted cycloolefins, at that time out of reach of ruthenium catalysts, [39] but also improved thermal stability relative to the parent complex **4**. These first reports on NHCs-coordinated ruthenium catalysts paved the way for the development of Grubbs' second-generation complex **13** (Scheme 7) [40].

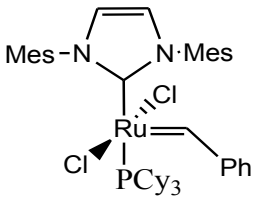

11

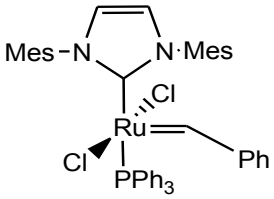

12

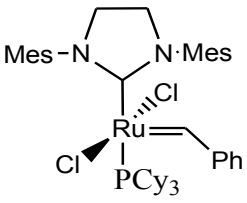

13

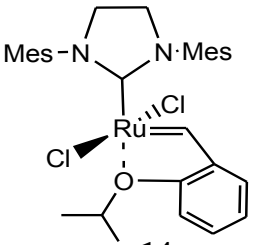

14

Mes = 2,4,6-trimethylphenyl

Scheme 7: Ruthenium-based metathesis catalysts **11-14** bearing NHC ligands.

The motivation for the preparation of complex **13** originated from the expectation that the increased basicity of the corresponding saturated NHCs, relative to their unsaturated counterparts will lead to the resulting ruthenium complexes with increased activity [40,41]. Complex **13** expanded the scope of ruthenium metathesis catalysts significantly, as it was proved to be not only air, water, and functional group tolerant [42] but also highly efficient in the RCM of

sterically demanding dienes, [40] in the ROMP of low-strain substrates, [43] and in the realization of challenging CM reactions [42].

In another significant contribution to the field of ruthenium based metathesis, the Hoveyda [44] and Blechert [45] groups almost simultaneously reported the synthesis of isopropoxystyrene-coordinated catalyst **14** (Scheme 7). Compared to its phosphine-containing analogue **13**, catalyst **14** shows improved thermal stability, oxygen and moisture tolerance.

The proposed catalytic mechanism of the Hoveyda's type complexes is slightly different from that of the phosphine-containing complexes (Scheme 5). Initially, 14-electron intermediate **III** is formed through the dissociation of the benzylidene ether chelating group (Scheme 8). Coordination of the alkene substrate to form **IV**, followed by metathesis, leads to the formation of the catalytically active species **V** and a molecule of isopropoxystyrene (or a related derivative) [46]. When the alkene is completely consumed, the catalyst may return to its original state by rebinding the isopropoxy styrene that was eliminated at the first step [46].

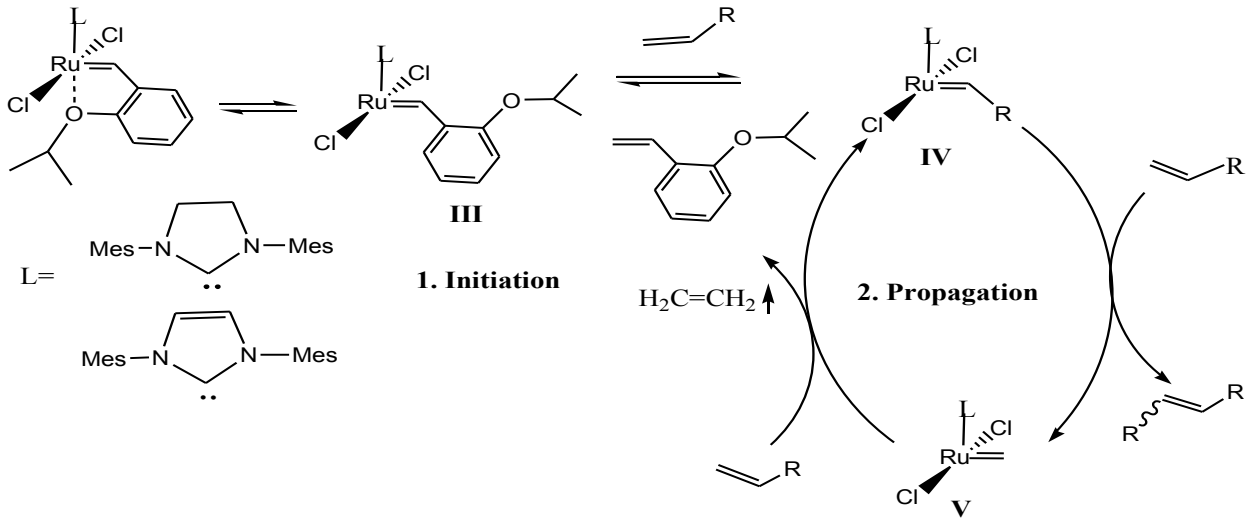

Scheme 8: Proposed catalytic mechanism of isopropoxystyrene coordinated ruthenium catalysts.

1.3 Ruthenium Indenylidene Metathesis Initiators

On their attempt to synthesize a ruthenium-allenylidene complex Fürstner *et al.* [47] obtained the related indenylidene complex **15.** Complex **15** can be synthesized by the reaction of $(PPh_3)_3$-$_4RuCl_2$ with 1,1-diphenyl-2-propyn-1-ol in THF under reflux to afford complex **16** which then

react with the starting complex, $(PPh_3)_{3\text{-}4}RuCl_2$, to afford a binuclear complex **17** as intermedeate (Scheme 9). The reaction of complex **17** with 1 equivalent of 1,1-diphenyl-2-propyn-1-ol, 2 equivalent of PPh_3 and 0.1 equivalent of acetyl chloride in refluxing THF forms the desired complex **15** (Scheme 9). However, the reaction is slow and the conversion does not go to completion. It has been demonstrated, however, adding catalytic amounts of acetyl chloride under otherwise similar reaction conditions results in complete and reliable formation of compound **15** (Scheme 9) [48].

While complex **15** it self is slightly metathesis active, is highly useful. In solid, dry form, it is highly stable, can be stored for months in air without noticeable decomposition in contrast to Grubbs' complex **4**. This stability makes complex **15** an ideal precursor to access a collection of differently substituted olefin metathesis catalysts. Now the PPh_3 ligands from **18** have been subsequently replaced by a better donating ligand PCy_3, affording complex [49] **18** with improved activity and stability (Scheme 9).

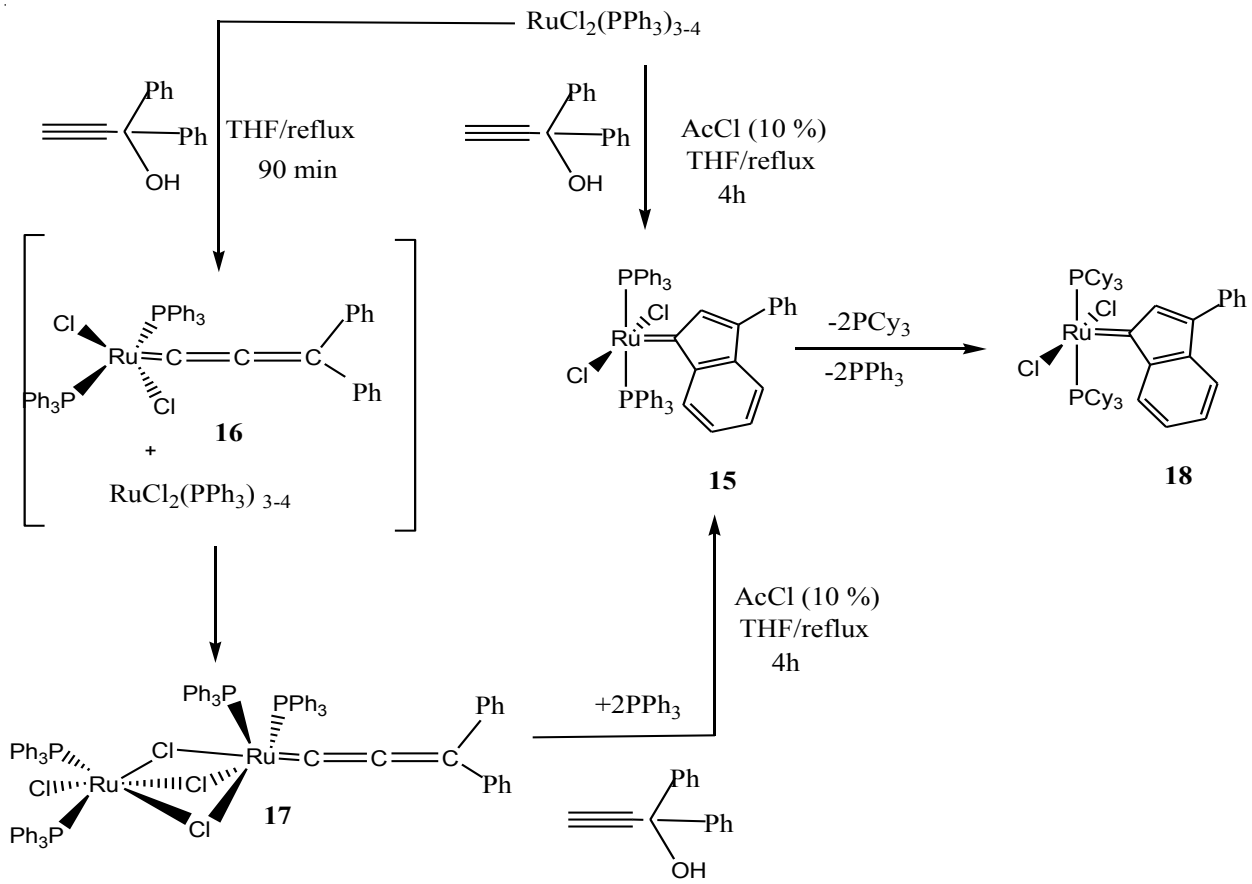

Scheme 9: Preparation of ruthenium indenylidene catalysts **15** and **18**.

Further substitution of phosphine ligands by imidazol-2-ylidene or imidazolin-2-ylidene, enabled Nolan to introduce the 2nd generation ruthenium indenylidene complexes [50] **19** which is in line with the synthesis of **20** by Verpoort [51] and Nolan [52] (Scheme 10). The resulting initiators show excellent catalytic properties.

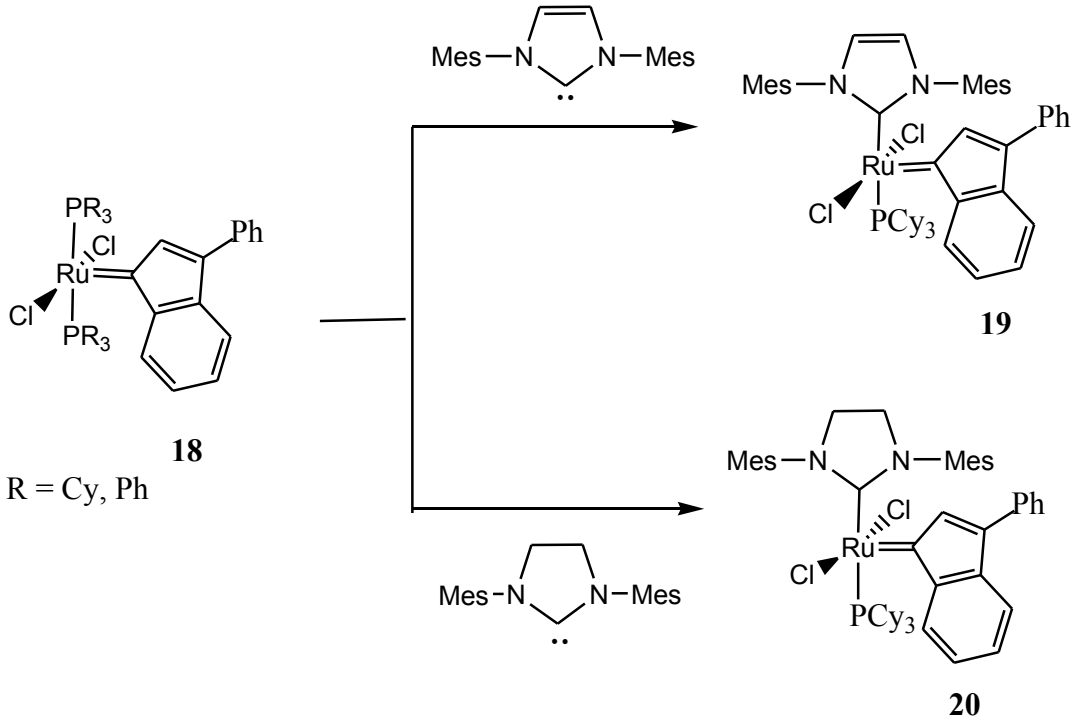

Scheme 10: Ruthenium indenylidene metathesis initiators **19** and **20**.

According to the generally accepted mechanism (Scheme 5) phosphine bearing catalysts are initiated by the dissociation of a phosphine group to form the 14-electron complex [53,54]. This mechanistic scheme can be used to explain observed differences between the second-generation Grubbs' and indenylidene complexes. The release of indenylidene species and the formation of the common propagating species **IV** and **V** (Scheme 11) proceed much more slowly in the case of **19** and **20**, whereas **11** and **13** easily lose phosphine in the analogous transformation. Therefore, catalysts **19** and **20** initiate much more slowly than **11** and **13** and need a higher temperature to reach reasonable activity.

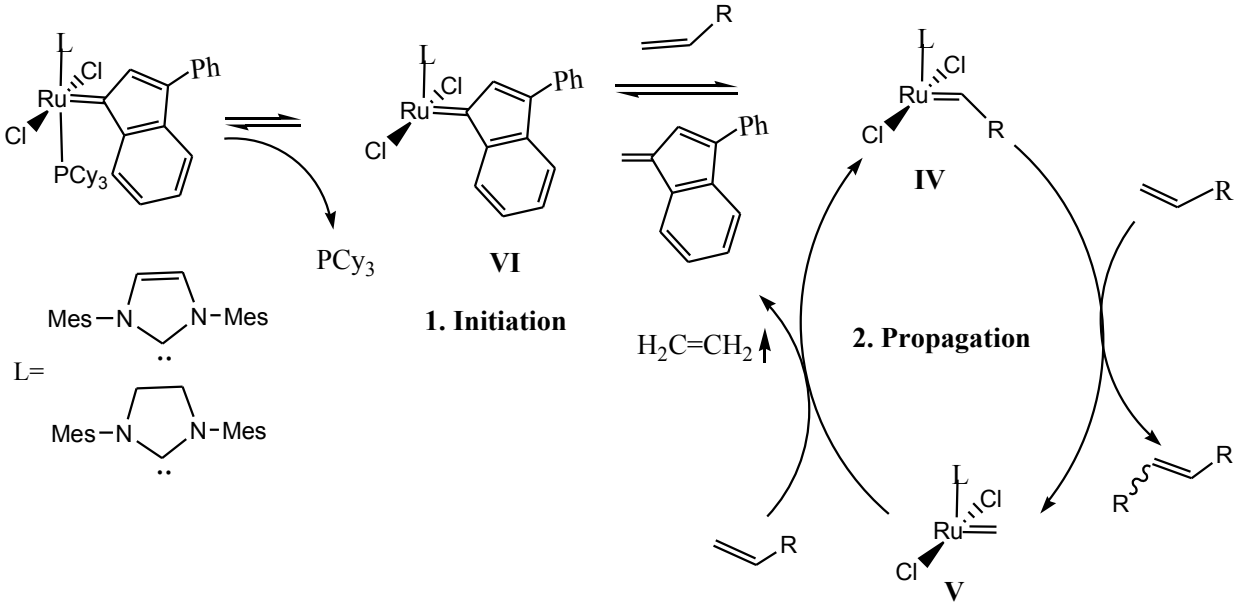

Scheme 11: Proposed catalytic mechanism of indenylidene coordinated ruthenium catalysts.

Verpoort *et al*. reported ruthenium indenylidene Schiff base complexes **21** (Scheme 12) as effective metathesis initiators [55,56]. These catalysts exhibited high thermal stability with moderate room temperature activity. In addition, Verpoort introduced for the first time N,O Schiff base ligand in NHC-coordinated indenylidene complex **22** [57-61]. Activation of this group of catalysts by a Lewis acid resulted in to efficient catalysts in the RCM and ROMP of a series of substrates [62-64].

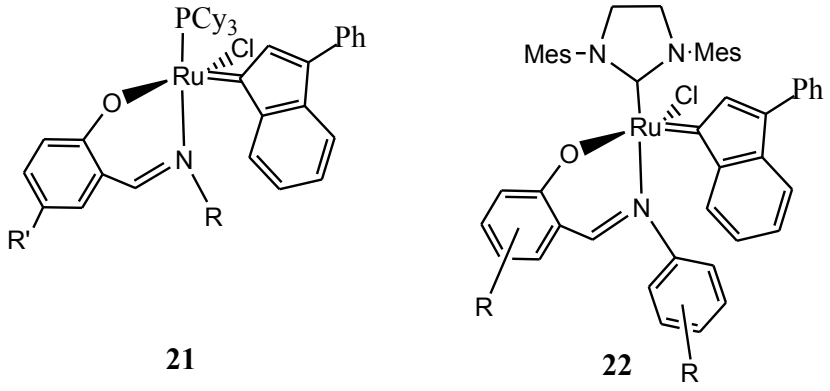

Scheme 12: Ruthenium indenylidene Schiff base metathesis initiators.

1.4 References

[1] H. S. Eleuterio, *German Patent* 1, 072, 811, 1960.

[2] H. S. Eleuterio, *US Patent* 3, 074, 918, 1963.

[3] A. W. Anderson, N. G. Meckling, *US Patent* 2, 721, 189, 1955.

[4] E. F. Peters, Lansing, B. L. Evering, *US Patent* 2, 963, 447, 1960.

[5] R. L. Banks, *Chem. Technology*, 1986, 112.

[6] N. Calderon, E. A. Ofstead, W. A. Judy, *J. Polymer Sci., A-1,* 1967, 52209.

[7] N. Calderon, *et al*. *Chem. Eng. News*, 1967, **45**, 51.

[8] N. Calderon, H. Y. Chen, K. W. Scott, *Tetrahedron lett*.,1967, 3327.

[9] N. Calderon, E. A. Ofstead, J. P.Ward, W. Judy, *J. Am. Chem. Soc.,*1968, **90**, 4133.

[10] S. J. Connon, S. Blechert, *Angew. Chem. Int. Ed.,* 2003, **42**, 1900.

[11] A. K. Chatterjee, T.-L. Choi, D. P. Sanders, R. H. Grubbs, *J. Am. Chem. Soc.,* 2003, **125**, 11360.

[12] R. H. Grubbs, S. J. Miller, G. C. Fu, *Acc. Chem. Res.,* 1995, **28**, 446.

[13] J. A. Tallarico, M. L. Randall, M. L. Snapper, *Tetrahedron,* 1997, **53**, 16511.

[14] R. H. Grubbs, Handbook of Metathesis 2003, Wiley-VCH, volume **1-3**.

[15] C. W. Bielawski, R. H. Grubbs, *Prog. Polym. Sci*., 2007, **32**, 1.

[16] J. E. Schwendeman, A. C. Church, K. B. Wagener, *Adv. Synth. & Cat.,* 2002, **344**, 597.

[17] N. Calderon, H. Y. Chen, K. W. Scott, *Tetrahedron Lett.,* 1967, 3327.

[18] J. L. Herisson, Y. Chauvin, *Makromol. Chem.,* 1971, **141**, 161.

[19] D. Astruct, *New J. Chem.,* 2005, **29**, 42.

[20] T. J. Katz, J. McGinnis, *J. Am. Chem. Soc.,* 1975, **97**, 1592.

[21] T. J. Katz, R. Rothchild, *J. Am. Chem. Soc.,* 1976, **98**, 2519.

[22] T. J. Katz, J. McGinnis, *J. Am. Chem. Soc.,* 1977, **99**, 1903.

[23] R. H. Grubbs, P. L. Burk, D. D. Carr, *J. Am. Chem. Soc.,* 1975, **97**, 3265.

[24] R. H. Grubbs, D. D. Carr, C. Hoppin, P. L. Burk, *J. Am. Chem. Soc.,* 1976, **98**, 3478.

[25] F. N. Tebbe, G. W. Parshall, G. S. Reddy, *J. Am. Chem. Soc.,* 1978, **100**, 3611.

[26] R. R. Schrock, *Tetrahedron,* 1999, **55**, 8141.

[27] R. R. Schrock, In Alkene Metathesis in Organic Synthesis, A., Fürstner, Ed., Springer: Berlin, 1998, pp 1-36.

[28] R. R. Schrock, *The Strem Chemiker.,* 1992, **14**, 1.

[29] J. Feldman, R. R. Schrock, *Prog. Inorg. Chem.,* 1991, **39**, 1.

[30] R. R. Schrock, *Acc. Chem. Res.,* 1990, **23**,158.

[31] S. T. Nguyen, L. K. Johnson, R. H. Grubbs, J. W. Ziller, *J. Am. Chem. Soc.,* 1992, **114**, 3974.

[32] P. Schwab, R. H. Grubbs, J. W. Ziller, *J. Am. Chem. Soc.,* 1996, **118**, 100.

[33] J. S. Kingsbury, J. P. A. Harrity, P. J., Jr. Bonitatebus, A. H. Hoveyda, *J. Am. Chem. Soc*., 1999, **121**, 791.

[34] S. B. Garber, J. S. Kingsbury, B. L. Gray, A. H. Hoveyda, *J. Am. Chem. Soc*., 2000, **122**, 8168.

[35] S. Gessler, S. Randl, S. Blechert, *Tetrahedron Lett.,* 2000, **41**, 9973.

[36] E. L. Dias, S. T. Nguyen, R. H. Grubbs, *J. Am. Chem. Soc.,* 1997, **119**, 3887.

[37] T. Weskamp, W. C. Schattenmann, M. Spiegler, W. A. Herrmann, *Angew. Chem., Int. Ed.,* 1998, **37**, 2490.

[38] W. A. Herrmann, C. Kocher, *Angew. Chem., Int. Ed. Engl*., 1997, **36**, 2162.

[39] M. Scholl, T. M. Trnka, J. P. Morgan, R. H. Grubbs, *Tetrahedron Lett.,* 1999, **40**, 2247.

[40] M. Scholl, S. Ding, C. W. Lee, R. H.,*Grubbs, Org. Lett.,* 1999, **1**, 953.

[41] S. Diez-Gonzalez, S. P. Nolan, *Coord. Chem. Rev.,* 2007, **251**, 874.

[42] A. K. Chatterjee, J. P. Morgan, M. Scholl, R. H. Grubbs, *J. Am. Chem. Soc.,* 2000, **122**, 3783.

[43] C. W. Bielawski, R. H. Grubbs, *Angew. Chem., Int. Ed.,* 2000, **39**, 2903.

[44] S. B. Garber, J. S.Kingsbury, B. L. Gray, A. H. Hoveyda, *J. Am. Chem. Soc.,* 2000, **122**, 8168.

[45] S. Gessler, S. Randl, S. Blechert, *Tetrahedron Lett.,* 2000, **41**, 9973.

[46] J. S. Kingsbury, J. P. A. Harrity, P. J., Jr. Bonitatebus, A. H. Hoveyda, *J. Am. Chem. Soc.,* 1999, **121**, 791.

[47] Fürstner, A. F. Hill, *et al., J. chem. Soc. chem. commun.,* 1999, 601.

[48] E. A. Shaffer, C. Chen , A. M. Beatty , E. J. Valente, H. Schanz, *J. Organometallic Chem.,* 2007, **692**, 5221.

[49] L. Jafarpour, H. J. Schanz, E. D. Stevens, S. P Nolan, *Organometallics,* 1999, **18**, 5416.

[50] H. Clavier, J. L. Petersen *et al., J. Organomet. Chem.,* 2006, **691**, 5444.

[51] S. Monsaert, R. Drozdzak, V. Dragutan, I. Dragutan, F. Verpoort, *Eur. J. Inorg. Chem.,* 2008, **3**, 432.

[52] H. Clavier, S. P. Nolan, *Chem.Eur. J.* 2007, 8029.

[53] J. A. Love, J. P. Morgan, T. M. Trnka, R. H. Grubbs, *Angew. Chem., Int. Ed.,* 2002, **41**, 4035.

[54] J. S. Kingsbury, A. H. Hoveyda, *J. Am. Chem. Soc.,* 2005, **127**, 4510.

[55] T. Opstal, F. Verpoort, *Synlett.,* 2002, **6**, 935.

[56] T. Opstal, F. Verpoort, *New J. Chem.,* 2003, **27**, 257.

[57] A. M. Lozano Vila, S. Monsaert, R. Drozdzak, S. Wolowiec, F. Verpoort, *Adv. Synth. Catal.,* 2009, **351**, 2689.

[58] B. de Clercq, F. Verpoort, *Tetrahedron Lett.,* 2002, **43**, 9101.

[59] B. de Clercq, F. Verpoort, *J. Organomet. Chem.,* 2003, **672**, 11.

[60] R. Drozdzak, B. Allaert, N. Ledoux, I. Dragutan, V. Dragutan, F. Verpoort, *Adv. Synth. Catal.,* 2005, **347**, 1721.

[61] R. Drozdzak, N. Ledoux, B. Allaert, I. Dragutan, V. Dragutan, F. Verpoort, *Cent. Eur. J. Chem.,* 2005, **3**, 404.

[62] R. Drozdzak, B. Allaert, N. Ledoux, I. Dragutan, V. Dragutan, F. Verpoort, *Coord. Chem. Rev.,* 2005, **249**, 3055.

[63] F. Ding, Y. G. Sun, S. Monsaert, R. Drozdzak, I. Dragutan, V. Dragutan, F. Verpoort, *Curr. Org. Synth.,* 2008, **5**, 291.

[64] B. Allaert, N. Dieltiens, N. Ledoux, C. Vercaemst, P. van der Voort, C. V. Stevens, A. Linden, F. Verpoort, *J. Mol. Catal. A: Chem.,* 2006, **260**, 221.

2.1 Introduction

Catalytic olefin metathesis has become a powerful tool for carbon-carbon bond formation in organic chemistry [1].Whereas several well-defined, single-species metathesis catalysts based on different transition metals have been developed, ruthenium based catalysts are highly applicable due to their high tolerance towards functional groups, moisture and air [2]. In particular, ruthenium benzylidene complexes have been studied in the greatest detail and are most widely used for many applications [1]. These complexes include Grubbs' catalysts **1** [3] and its NHC coordinated derivative **2** [4] but also the first- and second-generation Hoveyda-Grubbs catalysts **3** [5] and **4** [6] (Scheme 1).

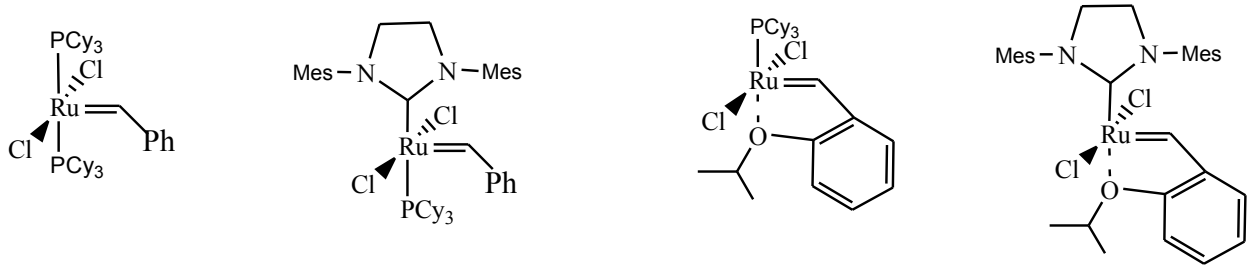

1 **2** **3** **4**

Mes = 2,4,6-trimethylphenyl

Scheme 1: Ruthenium alkylidene metathesis initiators [3-6].

NHCs are strong σ-donor and weak π-acceptor ligands [7] which can lead to very strong NHC-metal bonds [8]. These properties can be translated into catalysts with superior stability relative to the first generation catalysts and increased activity for olefin metathesis. In addition, it is possible to fine-tune the catalytic activity of the NHC coordinated catalysts by altering the steric and electronic properties of the ligands. This can be done through modification of the NHC ligands both at nitrogen and on the carbon backbone [9].

Unsymmetrical modifications of NHC ligands in the ruthenium catalysts have been successfully performed and resulted in catalysts with attractive applications. The introduction of unsymmetrical NHC ligands with an aliphatic amino side group was based on anticipation that the increased σ-donation of the aliphatic-substituted NHCs relative to the aromatic mesityl analogues would lead to the catalysts with enhanced stability and activity [10].

In addition, unsymmetrical NHC ligands may stabilize key intermediates [11] to effect E:Z selectivity in cross metathesis (CM) reactions and selectivity in diastereoselective ring-closing metathesis (RCM) reactions. *Z*-selective cross metathesis is among the challenges in olefin metathesis, as it not only requires the reaction to have a preference for the thermodynamically less favored Z-isomer but also a condition in which the key metathesis intermediate fails to react with the more reactive *Z*-olefin through secondary metathesis [12].

Furthermore, unsymmetrical NHC ligands may selectively produce predominantly alternating copolymers by Ring Opening Metathesis Polymerization (ROMP) of two monomers. This success is attributed to the ability of these dual-site catalysts to swing back and forth thereby discriminating between two substrates in the same catalytic reaction [13].The alternating site reactivity also explains the selectivity toward formation of cyclic oligomers by ring opening-ring-closing metathesis (RO-RCM) of a single substrate by alternating one reaction with another.

2.2 *N*-aryl, *N'*-alkyl NHC Coordinated Ruthenium Metathesis Catalysts

The metathesis activity of the catalysts incorporating an NHC ligand that combines one alkyl and one aryl side chain has been examined by many researchers. However, the expected higher activity through enhanced σ-electron donation of the NHCs bearing alkyl side chain was not revealed in RCM and in most cases steric effects played an important role in influencing the metathesis activity in this reaction. The relatively less efficiency of the catalysts comprising unsymmetrical alkyl-aryl NHCs in RCM has been attributed to a strong preference of these catalysts to propagate as methylidene species in the catalytic cycle [14, 15].

Catalyst **5** and **6** (Scheme 2) perform a nearly equal number of degenerate and productive metathesis events in the RCM of diethyl diallyl malonate (DEDAM) and two or more nonproductive reactions for every productive event in RCM of allyl methallyl malonate [14].

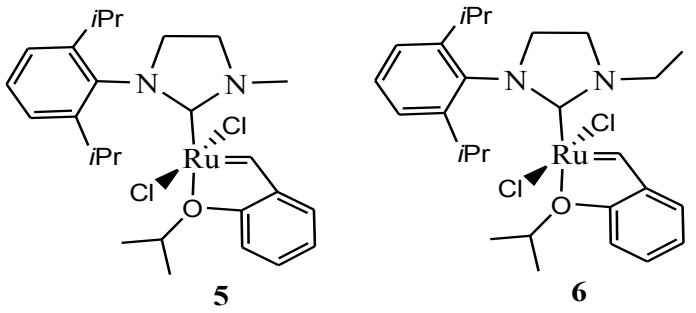

Scheme 2: Ruthenium catalysts **5** and **6** bearing unsymmetrical NHC ligands [14].

However, the selectivity for degenerate metathesis was beneficial in some applications such as the ethenolysis reaction. In this respect, a variety of ruthenium metathesis catalysts (**7-16**) bearing *N*-aryl, *N'*-alkyl heterocylic carbene have been developed and applied in the ethenolysis of methyl oleate (Scheme 4) [16]. These catalysts exhibit high selectivity toward the formation of kinetic products **II** and **III** over the thermodynamic products **IV** and **V** of self-metathesis (Scheme 3). The observed selectivity is a function of steric bulkiness of the NHC ligand substituents as increasing the sterics of the NHC substituents enhances selectivity. Catalyst **14** showed excellent kinetic selectivity (95%), which is higher than those reported for other ruthenium NHC catalysts and comparable with those of first-generation ruthenium catalysts [17]. For all catalysts, rising temperature to 50 °C increased the TON and yield significantly; however, further increase led to catalyst decomposition.

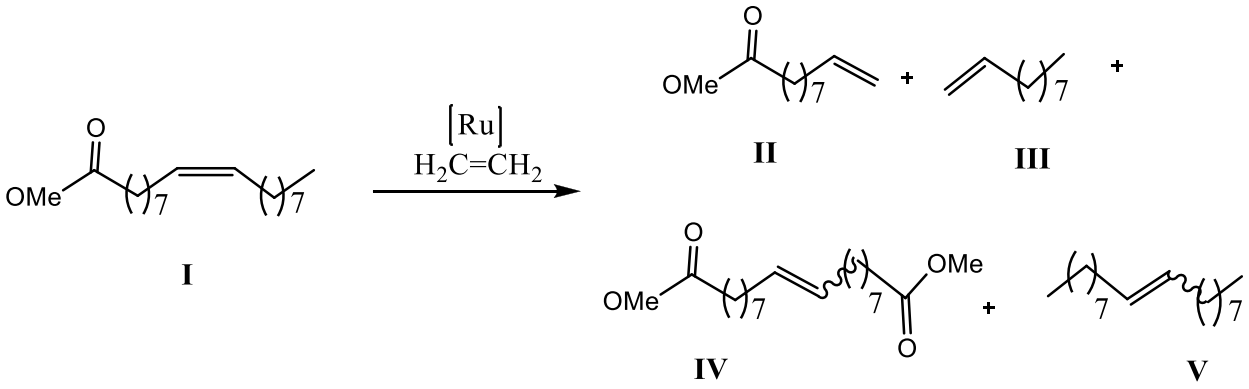

Scheme 3: Ethenolysis of methyl oleate [16].

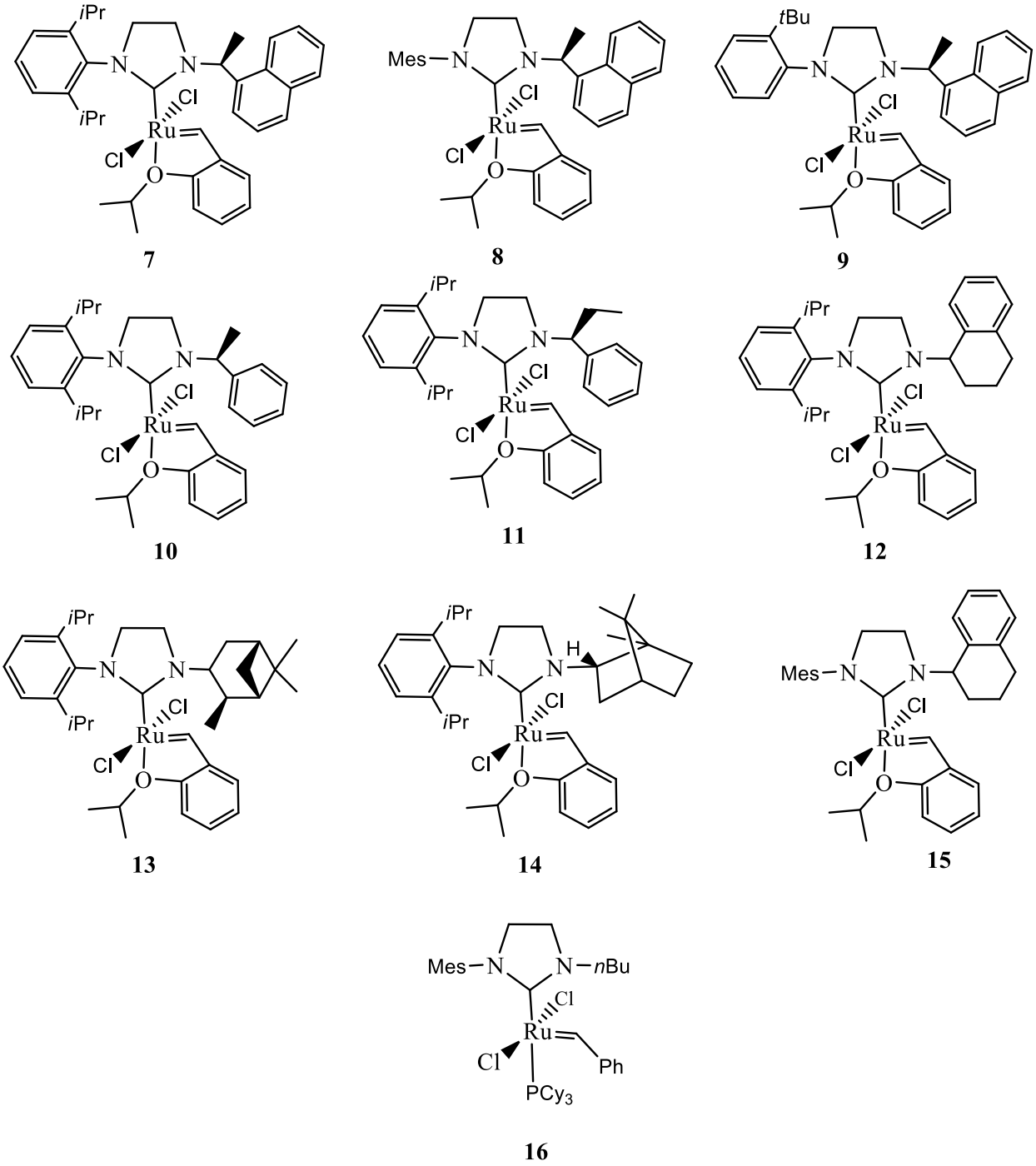

Scheme 4: Ruthenium based catalysts designed for ethenolysis reaction [16].

The steric effect was studied [18] by replacing the mesityl group from Grubbs' catalyst **2** with the more sterically demanding adamantly group to afford a single isomer (**17**). However, the anticipated enhanced catalytic activity was not observed, as complex **17** (Scheme 5) is only a very poor olefin metathesis catalyst.

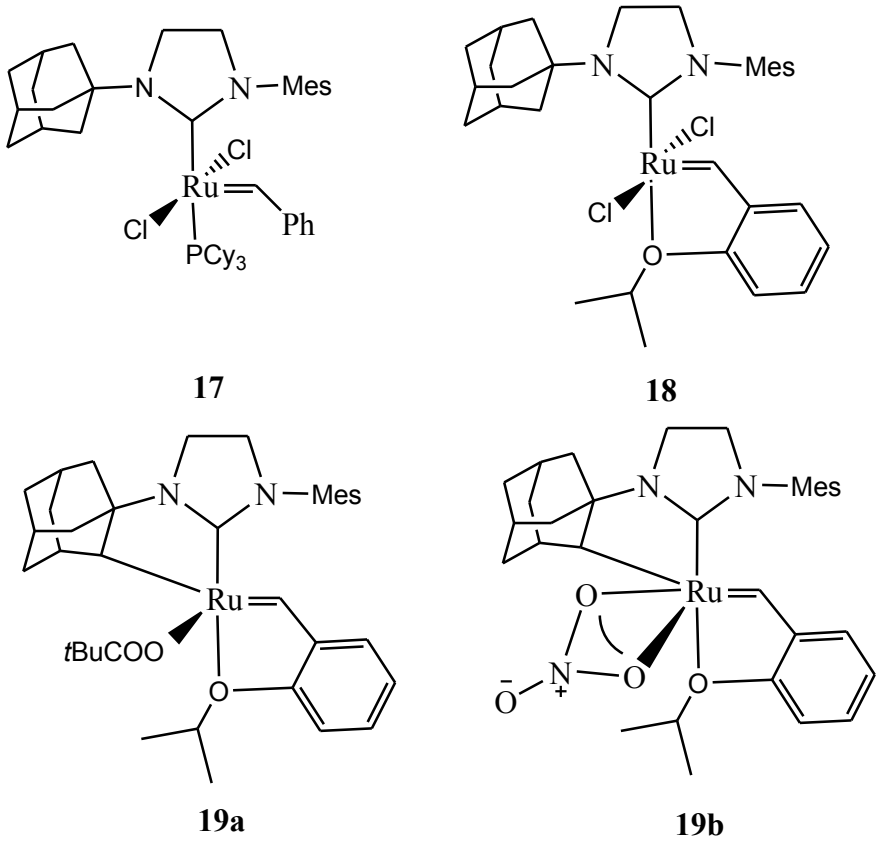

Scheme 5: Unsymmetrical NHC bearing adamantyl ligand in ruthenium complexes [18, 19].

Grubbs *et al.* [19] reported the first *cis* selective ruthenium-based catalysts **19 ab** (Scheme 5). The synthesis of catalyst **19a** involves treatment of complex **18** with silver pivalate, which leads to a subsequent intramolecular C-H activation of the CH_2 group of the adamantyl substituent. This marks the first report of such C-H activated chelates providing metathesis active complexes. Surprisingly, employing the standard cross metathesis of allylbenzene and *cis*-1,4-diacetoxy-2-butene, the chelated-adamantyl catalyst provides a much lower E/Z ratio of the cross-coupled product compared with its parent non-chelated catalysts **18**. The obtained E/Z ratio of 0.12 (90% Z-isomer) is among the smallest reported for ruthenium-based olefin metathesis catalysts. Interestingly, allylbenzene also undergoes self-metathesis during the above cross metathesis,

providing the homo-coupled product in >95% Z-selectivity. On the other hand catalyst **19b** can efficiently mediate *cis*-selective ring opening polymerization of several monomers to afford polymers with significantly higher *cis* percentage relative to those prepared by Grubbs' complex **2** [19b].

The poor olefin metathesis activity of **17** was associated with the excessive steric crowding imparted by the adamantyl moiety towards the position *trans* to the benzylidene group. Blechert [20] developed unsymmetrical NHC ligands with decreased steric bulkiness and coordinated them to ruthenium giving novel olefin metathesis initiators (**20-23**) (Scheme 6). In RCM of *N,N*-diallyl-*p*-toluenesulfonamide, the metathesis initiators displayed activities similar to those of their symmetrical counterparts bearing only mesityl groups (**2, 4**). Interestingly, complexes **20** and **22** gave significantly different *E:Z* ratios in cross metathesis reactions, and improved selectivity in diastereoselective ring-closing metathesis.

The initiators **20** and **21** together with **24** prepared by Buchmeiser as well as their pyridine-containing analogues **25-27** (Scheme 6) were used for alternating co-polymerization of norbornene (NBE) with *cis*-cyclooctene (COE) and cyclopentene (CPE) respectively [21]. The pyridine-containing initiators **25-27** were prepared from the phosphine-based catalysts (**20**, **21** and **24**) by using a polymer-bound triphenylphosphane-CuCl complex as phosphane scavenger. Where as initiators **25** and **26** were obtained as monopyridine adducts, initiators **27** were obtained as a mixture of the mono- and bis(pyridine) adduct in a 42:58 ratio. In the copolymerization of NBE with COE using 1:50 ratio of NBE/COE the corresponding copolymers contain 95-97% alternating diads with high *cis*-content in poly(NBE-alt-COE)$_n$ were obtained. In copolymerizations of NBE with CPE using a ratio of NBE/CPE of 1:7, copolymers containing 79-91% of alternating diads were obtained. This percentage of alternating units is among the highest values found so far.

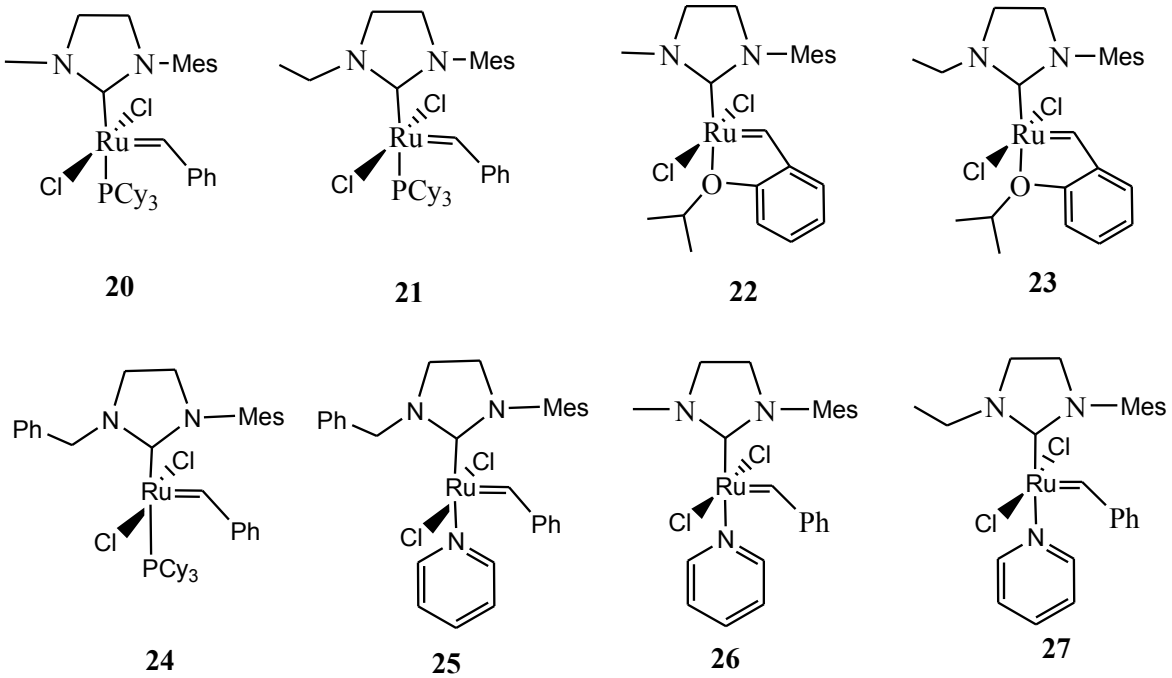

Scheme 6: Unsymmetrical NHC bearing alkyl group in ruthenium complexes **20-27** [20, 21].

Verpoort [22] extended the study by coordinating a series of unsymmetrical heterocyclic carbene on Grubbs' second generation (Scheme 7). In addition to the catalyst **20** reported by Blechert [20] four new catalysts (**28-31**) were afforded. While catalysts **20, 28**, **30** and **31** demonstrated activities comparable with that of complex **2** in ROMP of 1,5-cyclooctadiene, catalyst **29** is considerably less active. The activity of the new catalysts on RCM diethyl diallyl malonate showed a significant dependence on the steric bulkiness of the NHC entities, as an increase in the size of alkyl chain led to lower activity. Catalyst **20**, bearing an NHC ligand with a small methyl amino moiety is substantially more active than the Grubbs' complex **2.**

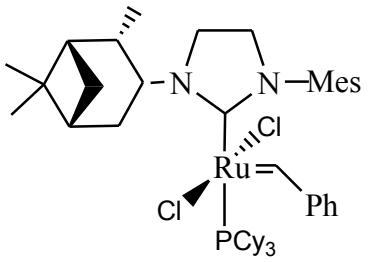

28

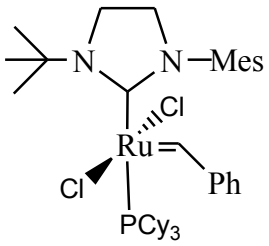

29

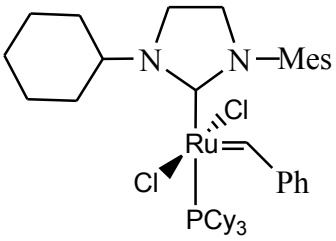

30

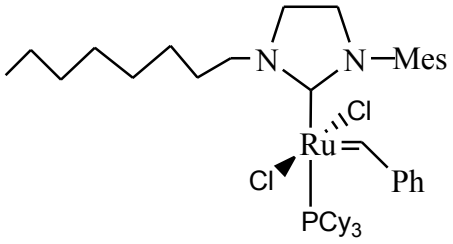

31

Scheme 7: Unsymmetrical NHC bearing an alkyl group in ruthenium initiators **28-31**[22].

Ring Opening-Ring Closing Metathesis (RO-RCM) of cyclooctene was investigated with unsymmetrical catalysts **32** and **33** (Scheme 8) [23]. A higher mass balance was reached by these catalysts at low conversion (80% after 10% conversion), implying that the catalysts selectively produce smaller cyclic oligomers (preferably dimers and trimers) instead of polymers in contrast to complexes **2** and **34** which form polymers (or large oligomers) at lower conversion and then converted to smaller oligomers via backbiting at higher conversion. The selective formation of cyclic oligomers over polymers originates from the catalyst system having a dual-site configuration due to two different steric environments.

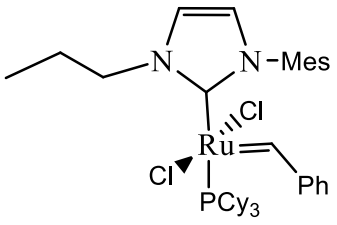

32

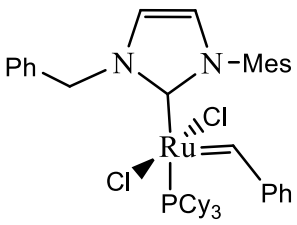

33

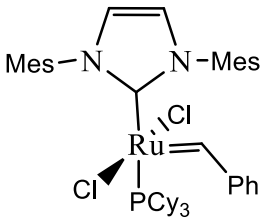

34

Scheme 8: Ruthenium based catalysts **32-34** [23].

Ruthenium indenylidene catalysts **35a-c** incorporating NHC ligands with a benzyl group bearing a donor substituent as one of the side groups have been reported [24] (Scheme 9). The catalytic activity of complexes **35a,b** out perform catalyst **37** in RCM of various substrates. In cross metathesis of allylbenzene and 1,4-*cis*-diacetoxy-2-butene both catalysts **35a,b** showed *E*-selectivity comparable with complex **37**.

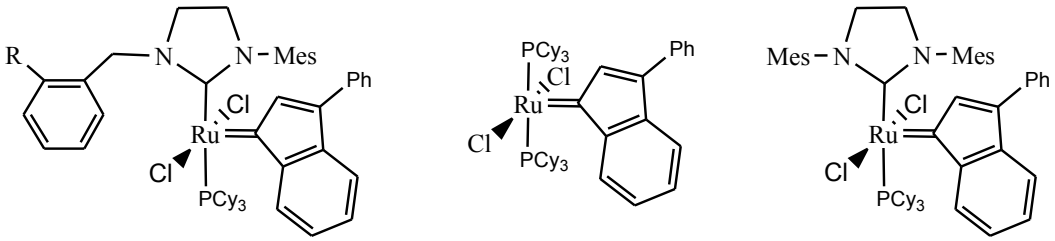

35a: R = OMe
35b: R = NMe_2
35c: R = SMe

36

37

Scheme 9: Ruthenium indenylidene based catalysts **35-37** [24].

In addition, application of the catalysts **35a,b** in Diastereoselective Ring Rearrangement Metathesis (DRRM) of protected cyclopentene **VI** (Scheme 10) resulted in much higher diastereoselectivity than shown by **37**. The diastereoselectivity shown by catalyst **35a** for the substrate **VI** is the highest reported to date. In contrast, complex **35c** containing the -SMe substituent, showed practically no reactivity in RCM.

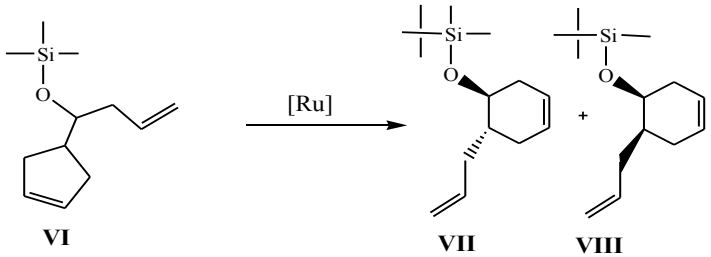

VI **VII** **VIII**

Scheme 10: Diastereoselective Ring Rearrangement Metathesis by catalysts **35a,b**.

Catalysts coordinated with unsymmetrical NHC bearing an olefinic side chain (such as **38**) (Scheme 11) have the unique ability to metathesize their own ligands to form cyclic complexes in which the *N*-heterocyclic carbene and the regular carbene unit Ru=CHR are tethered [25]. In this respect, a series of cyclic ruthenium-alkylidene catalysts (**39a-d** and **40a,b**) (Scheme 11)

have been prepared from their corresponding non-chelating complexes [25-27]. These complexes efficiently mediate the synthesis of cyclic polymers from cyclic monomers by Ring Expansion Metathesis Polymerization (REMP) [26,27]. During this process the monomer (e.g. *cis*-cyclooctene) is incorporated in to the cycle and polymerized to form a macrocyclic complex, which then undergoes intramolecular chain transfer to yield cyclic polymer and catalyst (Scheme 12). In the case of unsaturated NHC backbones, catalyst stability and activity were strongly influenced by the length of the chelating tether. In general, the stable catalysts are the ones with shorter tether lengths (between 4-6 carbon tethers), however, these catalysts exhibit lower activity than the catalysts with longer tethers. Interestingly, combination of shortened tether lengths and saturated NHC backbones provided REMP catalysts of high stabilities and activities [27].

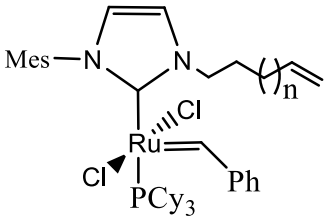

38a: n = 1
38b: n = 2
38c: n = 4

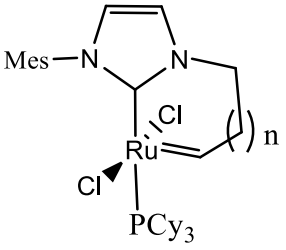

39a: n = 2
39b: n = 3
39c: n = 4
39d: n = 5

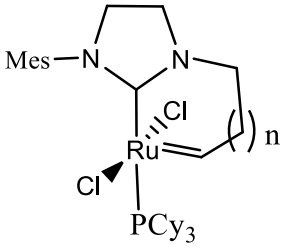

40a: n = 3
40b: n = 4

Scheme 11: Ruthenium based catalysts **38**-**40** [25-27].

Complexes (**38 a-c**) (Scheme 11) together with complex **41** and **42** (Scheme 13) reported by Fürstner and co-workers [25] were efficient in RCM of *N,N*-bis(2-methylallyl)-*p*-toluenesulfonamide to the corresponding tetra-substituted cycloalkene, a transformation which cannot be performed by complex **1**. However, the catalytic activity of the homologous series **38a-c** shows a significant dependence of the reactivity on the tether length between the alkene entity and the metal core.

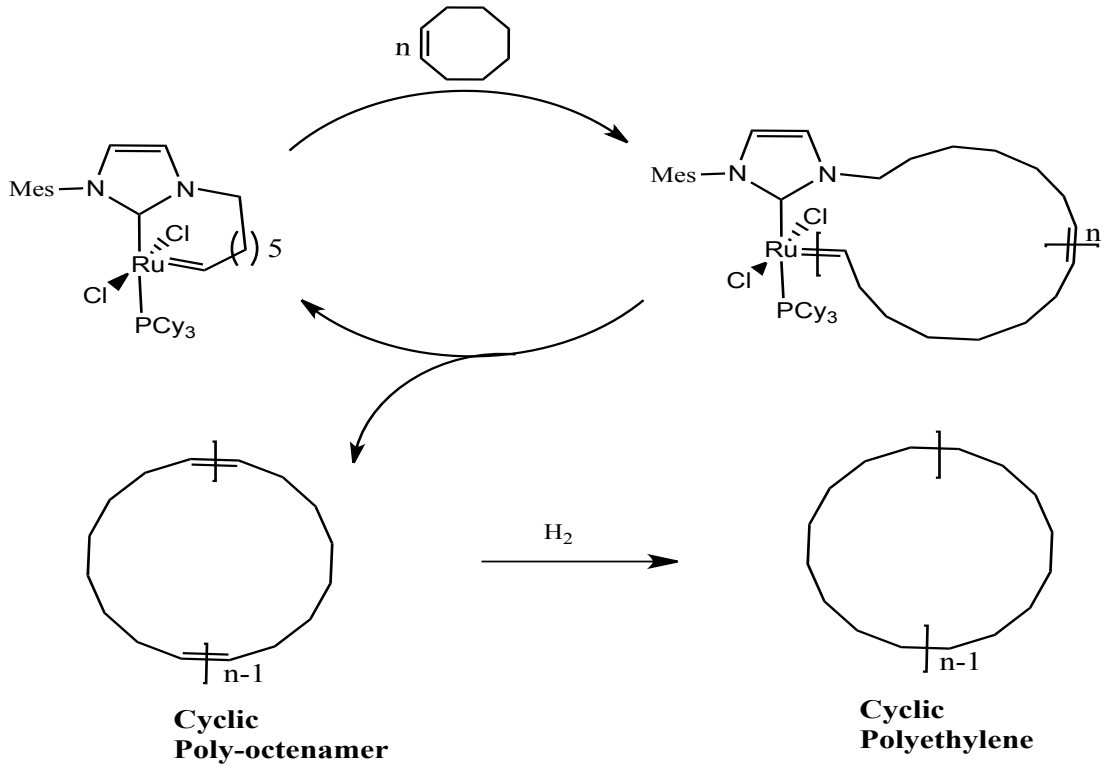

Scheme 12: Ring expansion metathesis polymerization of cyclooctene by catalyst **39d** [26, 27].

Furthermore, ruthenium-carbene complex **43** (Scheme 13) bearing a hydroxyalkyl group on its NHC ligand, which might lend themselves for immobilization on various supports, was also reported by the Fürstner's group [28]. In RCM complex **43a** gave yields similar to those obtained with its homogeneously soluble analogues, although a longer reaction time was necessary to reach full conversion.

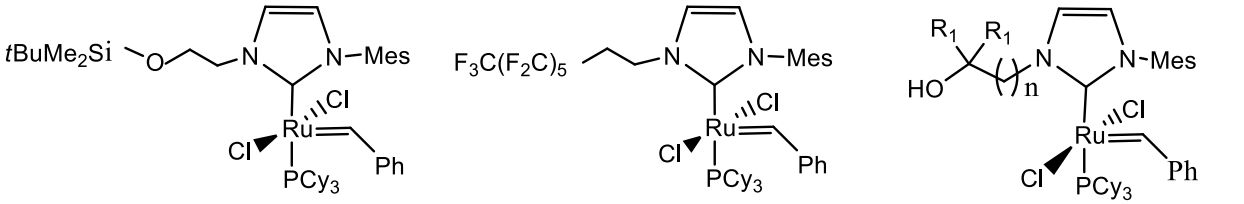

41 **42**

43a: n = 5, R_1 = H
43b: n = 2, R_1 = H
43c: n = 2, R_1 = Me
43d: n = 1, R_1 = H

Scheme 13: Ruthenium based complexes **41-43** bearing unsymmetrical NHC ligands [25, 28].

An addition of one equivalent of bidentate NHC ligand containing a mesityl amine tether, 2,4,6-$Me_3C_6H_2NC_3H_2NCH_2CH_2NH$-2,4,6-$Me_3C_6H_2$, to a toluene solution of complex **1** at room temperature generated a fairly air and moisture stable complex **44** in good yield [29] (Scheme 14). The NMR spectrum of the concentrated samples of **44** revealed the presence of isomer **44a** although in small quantities. Since the isolation of complex **44a** was not possible, it was partially characterized in solution spectroscopically. Two possible structures for the minor isomer **44a** were suggested. One is *syn*-**44a**, in which the two chloro ligands are *cis*-disposed and the PCy_3 unit is *cis* to both the NHC and the benzylidene and another one is a geometric isomer of *syn*-**44a**, (*anti*-**44a**) with the orientation of the PCy_3 unit and benzylidene C-H *trans* across the Ru=CHPh double bond.

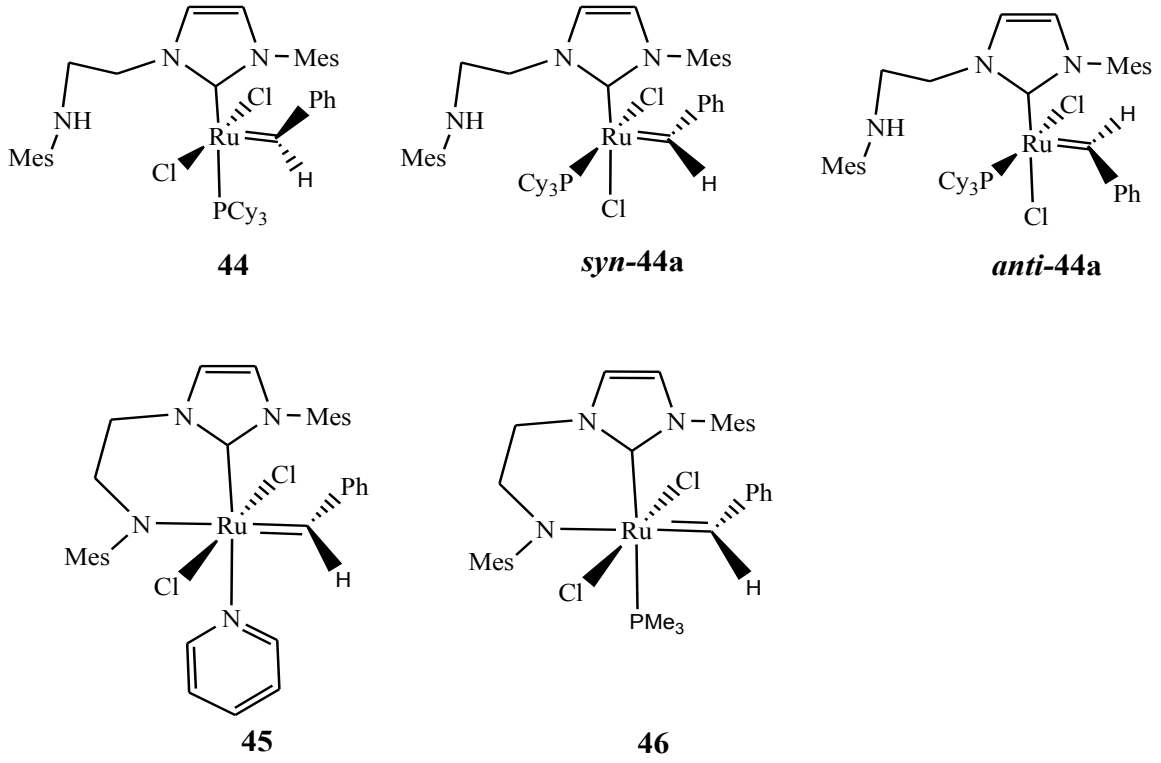

44 ***syn*-44a** ***anti*-44a**

45 **46**

Scheme 14: Ruthenium based complexes **44-46** bearing amine-tethered NHC [29].

When excess pyridine was added to complex **44**, it resulted into the monopyridine product **45**, which has the pendant amine arm coordinated to the ruthenium center. The complex **45** marks the first example of a Grubbs' catalyst derivative incorporating a bidentate amino- NHC ligand. While complex **45** is unreactive to the addition of triphenylphosphine, it reacted with a

phosphine such as trimethyl phosphine to yield complex **46**. The complex **44** underperformed in both RCM and ROMP when compared with the Grubbs' complexes **1** and **2**; however, it performed better than **45**.

The presence of Ru-C (benzylidene) rotamers (**47a** *syn* and **47a** *anti*) (Scheme 15) at room temperature has also been observed in catalyst **47a** developed by Grubbs *et al*. [30]. Catalysts **47a** and **47b** incorporating carbohydrate containing NHCs derived from glucose and galactose respectively were synthesized and showed excellent stability different from many *N*-alkyl NHCs. Complex **47a** was isolated as a single anomer (β), while **47b** was isolated as a ca. 1.2:1 mixture of β:α anomers.

The effectiveness of catalysts **47a,b** was investigated in a variety of olefin metathesis reactions, including ROMP, RCM, CM, and AROCM (Asymmetric Ring opening Cross Metathesis). In ROMP of cyclooctadiene (COD) both **47a** and **47b** outperform in activity Grubbs' complex **1** and showed similar activity to **34**; however, compared with complex **2** they are less active. Interestingly, **47a,b** showed different kinetic behavior in RCM of DEDAM. While **47b** displayed activity similar to that of catalyst **1**, catalyst **47a** underperformed in this reaction relative to **2** and **34** as well as catalyst **1**.

On the other hand, both **47a** and **47b** maintained lower E/Z ratio in the CM of allylbenzene and *cis*-diacetoxybutene, however, the observed selectivity was associated with catalyst decomposition, as it decreased when a fresh batch of catalyst was added. In contrast, the catalysts exhibit poor *ee's* in the AROCM of substituted norbornenes with terminal olefins.

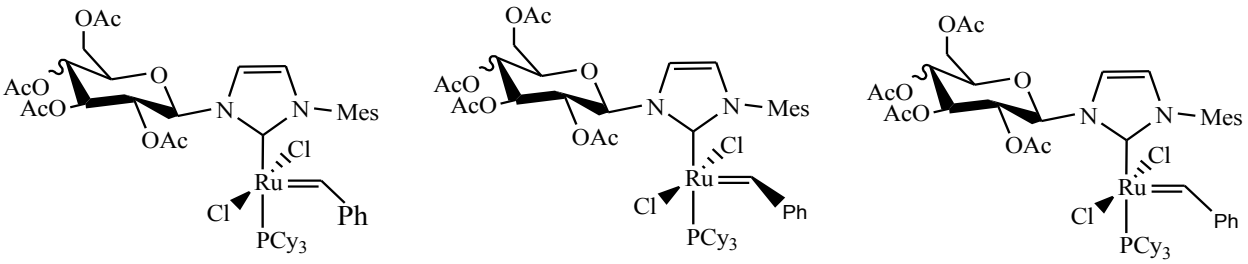

47a: When glucose is used
47b: When galactose is used

47a *Anti*

47a *Syn*

Scheme 15: Ruthenium metathesis catalysts bearing carbohydrate containing NHC [30].

2.3 *N*-aryl, *N'*-aryl NHC Coordinated Ruthenium Metathesis Catalysts

Replacing one mesityl group from the Hoveyda-Grubbs' catalyst **4** by a phenyl group afforded ruthenium complex **48** [31] (Scheme 16). The same group also reported a phosphine-free second generation ruthenium complex **49** with *N*-aryl ligands. Under inert conditions, the crude product contained only **48**, which is analogous to the Hoveyda–Grubbs' catalyst **4**. However, two different green compounds were isolated from the chromatographic purification. The olive green complex **48** was isolated (67% yield), but also the dark green, crystalline C-H inserted product **49** in 10% yield was obtained. Both solids are air-stable, although in CH_2Cl_2, **48** converts completely into **49** within a few hours. The isolated complex **49** is completely inactive in various metathesis reaction protocols.

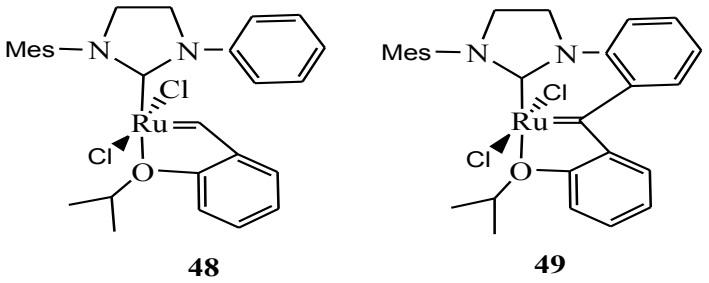

48 **49**

Figure 16: Unsymmetrical NHC bearing phenyl in ruthenium complexes **48** and **49** [31].

A series of ruthenium catalysts **50-57** (Scheme 17) bearing a fluorinated *N*-aryl group in the NHC ligands have been prepared [32, 33]. Phosphine-containing catalysts **50, 52** and **54** are more efficient than complex **2** in RCM of various substrates with catalyst **52** being the most efficient of all. On the other hand, phosphine-free catalysts **51, 53** and **55** are less efficient than parent complex **2**. In general, an increase in the number of fluorine atoms on the *N*-aryl substituent results in lower activity of phosphine-free catalysts, with catalyst **55** being the least efficient of all. Differing from the RCM reaction, catalyst **55** is the most reactive among fluorinated phosphine-free catalysts in the ROMP of 1,5-cyclooctadiene. In this reaction, complex **52** is the most efficient catalyst, showing a very similar reactivity pattern with complex **2**. In the CM of allylbenzene with 1,4-*cis*-diacetoxy-2-butene catalysts **50-55** are more Z selective than catalysts **2** and **4**, at conversions above 60% and demonstrated activity analogous to the second-generation catalysts **2** and **4**.

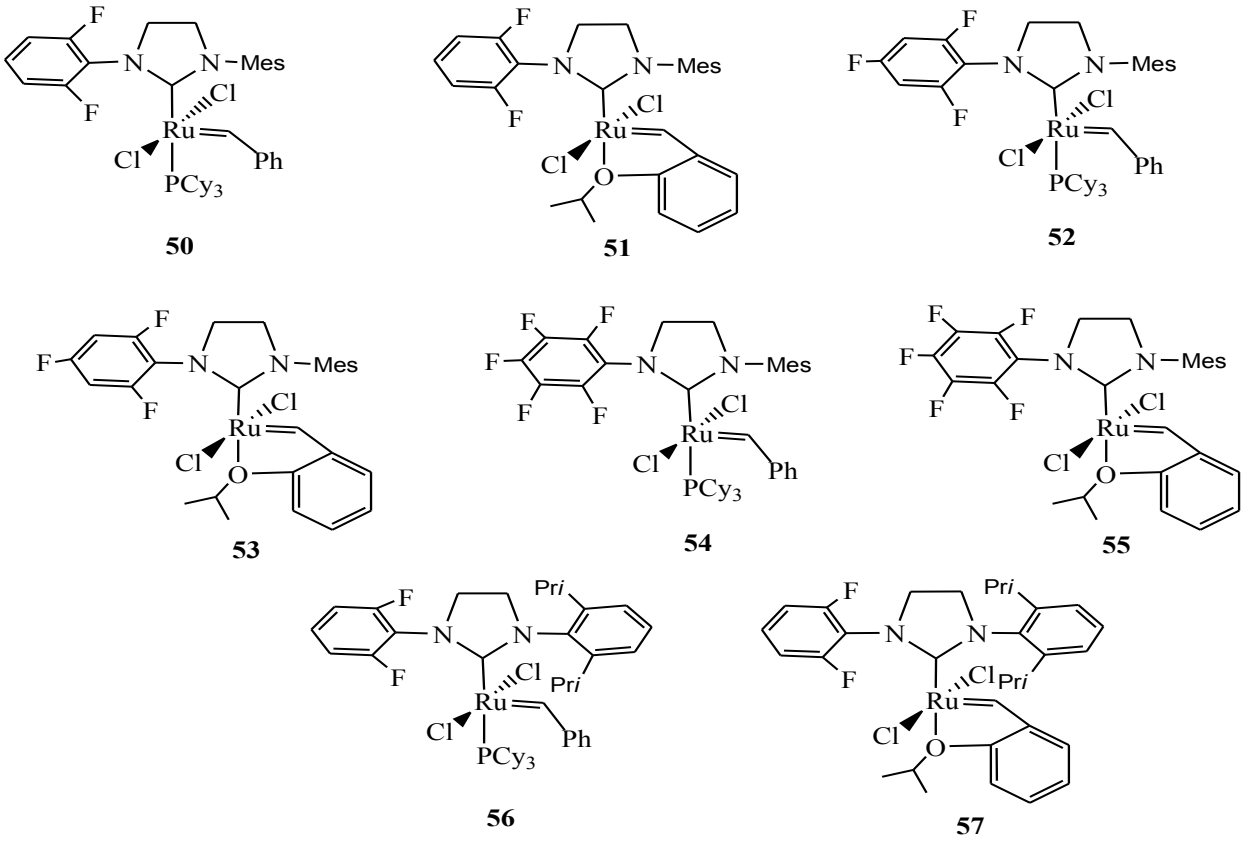

Scheme 17: Unsymmetrical NHC bearing fluorinated *N*-aryl group in ruthenium complexes **50-57** [32, 33].

Further fine-tuning of complex **2** was made and catalysts **58a-c** (Scheme 18) bearing different 4,4'-substituents on the phenyl ring were reported [34]. These complexes exist as two atropisomers which are characterized by different orientations of the 4,4'-substituents relative to the ruthenium-benzylidene unit and more importantly also by different redox potentials.The aryl group located above the Ru=CHPh unit is primarily responsible in controlling the redox potentials of these catalysts.

Pincer system comprising carbene-bipyridyl ligand (C-N-N) has been coordinated to the Grubbs' catalyst to afford catalyst **59** (Scheme 19) [35]. This type of chelating ligand tightly binds to the metal center in meridional configuration and therefore stabilizes the resulting complex. However, the in flexibility of the pincer-ruthenium interaction has limited the catalytic activity in metathesis reactions as it is less active in bench mark RCM and ROMP relative to both Grubbs' complex **1** and **2**.

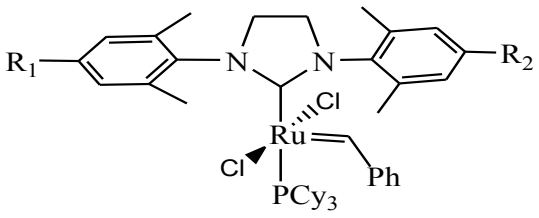

58a: $R_1 = NEt_2$, $R_2 = H$
58b: $R_1 = Br$, $R_2 = H$
58c: $R_1 = NEt_2$, $R_2 = Br$

Scheme 18: Unsymmetrical NHC bearing aryl groups in ruthenium initiators **58a-c** [34].

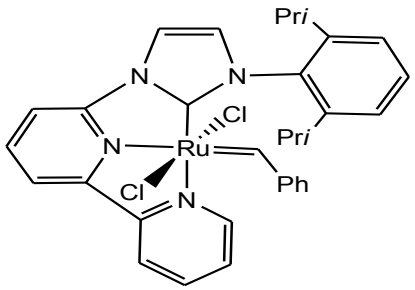

59

Scheme 19: Unsymmetrical NHC bearing carbene-bipyridyl in ruthenium initiators [35].

2.4 Ruthenium Initiators Bearing Two Unsymmetrical NHCs

In an effort to replace the NHC's mesityl group from Grubbs' 2nd generation **2** with a 2,6-diisopropylphenyl group, Verpoort [36] found that two of these NHCs were always coordinating on the ruthenium center. The resulting complexes **60a,b** (Scheme 20) show substantial olefin metathesis activity at elevated temperature. The exchange of one NHC in **60b** with PCy_3 allowed the isolation of a new complex **61b**, which displays moderate olefin metathesis activity with a higher initiation rate relative to the Grubbs 2nd generation catalyst **2**. On the other hand, the isolation of complex **61a** was not possible due to its instability and low ratio present in the reaction mixture.

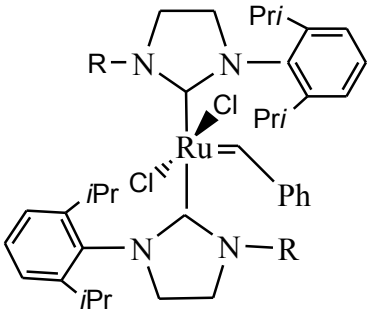

60a: R= Me
60b: R = Cy

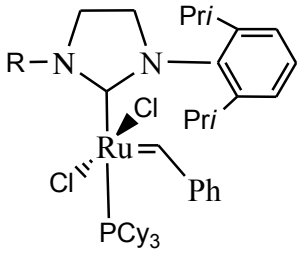

61a: R= Me
61b: R = Cy

Scheme 20: Ruthenium initiators **60** and **61** bearing unsymmetrical NHC ligands [36].

Grubbs [37] observed the same difficulty in his attempt to prepare phosphine-containing ruthenium complex bearing a 3-(2,6-diisopropylphenyl)-4,5-dimethylthiazol-2-ylidene, only the formation of complex **62** was observed (Scheme 21). Complex **62** is not stable enough to be isolated by column chromatography.

Complex **63** (Scheme 22) coordinated with tridentate ligand made up of a pyridine-dicarbene (C-N-C) has been reported [35]. The very low yield of complex **63** prepared *in situ*, has prevented its detailed study as a metathesis catalyst. In addition, metathesis inactive ruthenium alkylidene complexes **64** and **65** (Scheme 22) coordinated by two-bidentate aryloxy-NHC ligands were prepared and separated by flash chromatography [38]. The inactivity of these complexes was associated with low lability of NHCs as the only dative ligands.

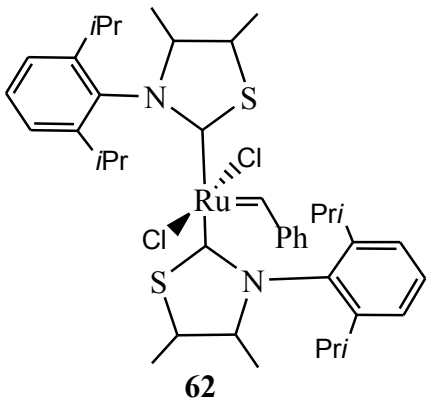

62

Scheme 21: Ruthenium complex **62** coordinated with two unsymmetrical NHC ligands [37].

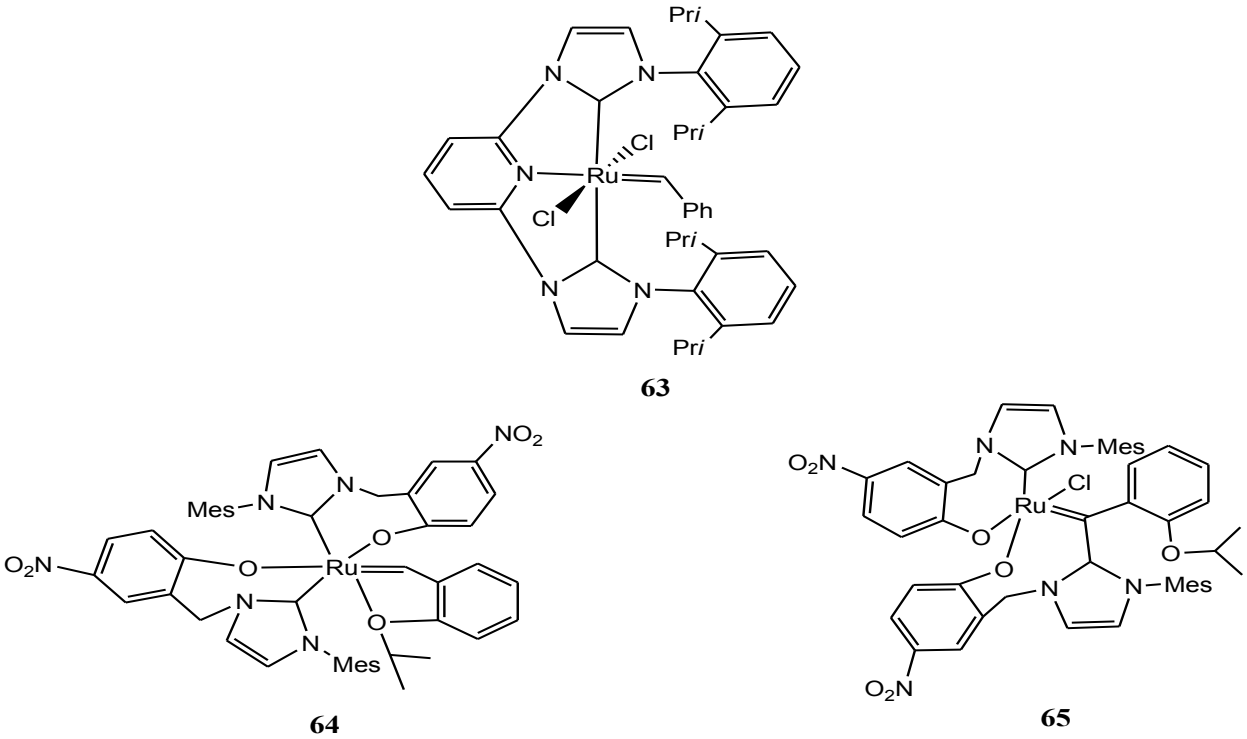

Scheme 22: Ruthenium complex **63-65** coordinated with two unsymmetrical NHC ligands [35, 38].

2.5 Ruthenium Complexes Bearing Cyclic (Alkyl) (Amino) Carbenes

A cyclic (alkyl) (amino) carbene (CAAC) in which an alkyl group has replaced one amino group from an NHC has also been coordinated to the ruthenium olefin metathesis initiators [39]. Grubbs *et al.* synthesized pyridine adduct complexes **66a,b** (Scheme 23) that were obtained by treating pyridine substituted Grubbs 1st generation catalyst with prepared CAAC ligands. However, the efficiency of catalyst **66a**, on RCM of diethyl diallyl malonate is low due to catalyst decomposition. Air and moisture stable catalysts **67a,b** and **68** were reported with improved activity relative to **66**. Catalyst **68** with decreased steric bulk of the *N*-aryl ring demonstrated a significant increase in activity which is comparable with standard second generation catalysts **2** and **4** in the formation of di- and trisubstituted olefins.

Catalysts **67ab** and **68** were further tested for activity in the cross metathesis of *cis*-1,4 diacetoxy-2-butene with allylbenzene and in the ethenolysis of methyl oleate [40]. In cross metathesis the catalysts exhibit lower E/Z ratios even at higher conversion (3:1 at 70% conversion) as compared with catalysts **1-4**. In the ethenolysis of methyl oleate (**I**) the catalysts

outperformed NHC-containing systems **2** and **4** in selectivity (73-94%) toward the production of terminal olefins 9-methyl decenoate (**II**) and 1-decene (**III**) (Scheme 4).

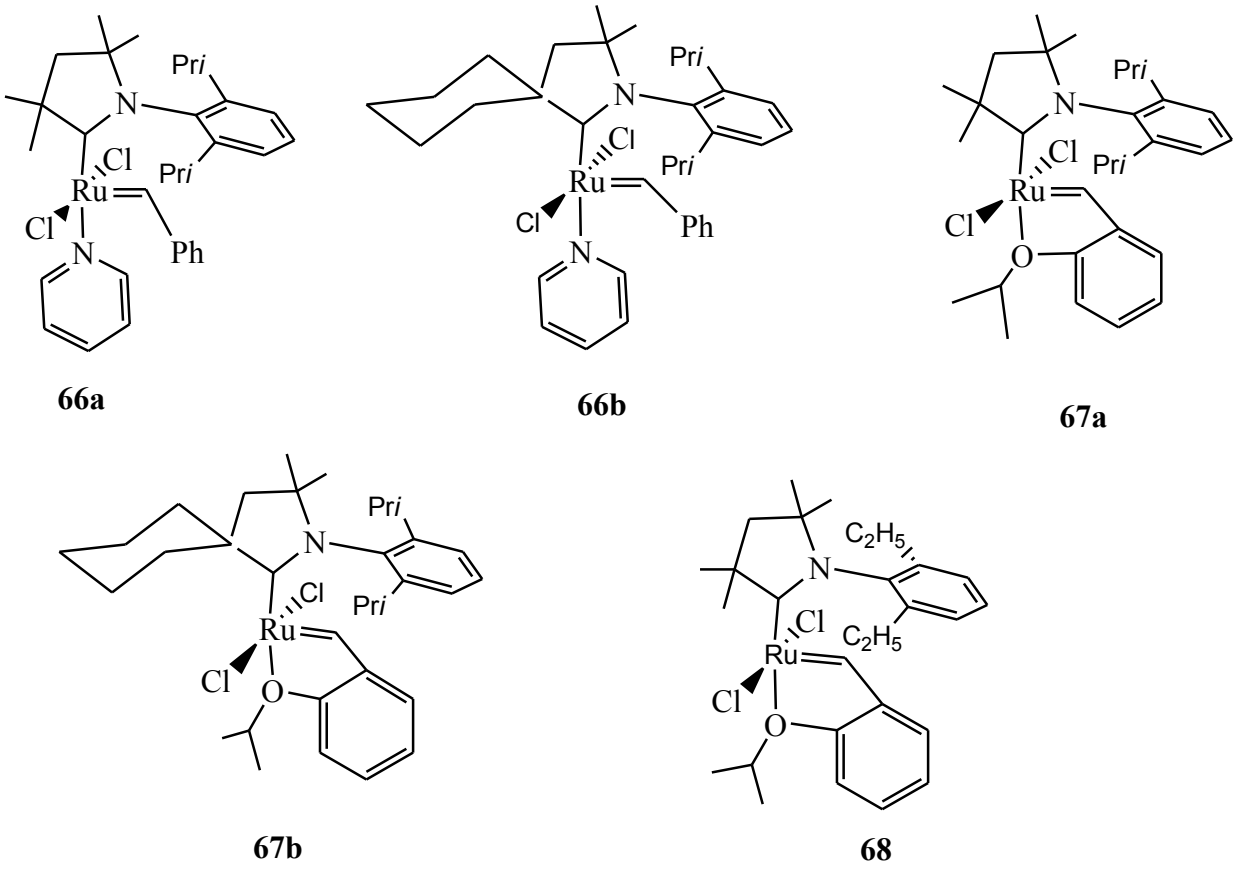

Scheme 23: Cyclic (alkyl) (amino) carbenes coordinated to ruthenium complexes [39].

2.6 Ruthenium-Based Initiators Coordinated by Thiazol-2-ylidene Ligands

Grubbs *et al.* [37] described a new family of ruthenium olefin metathesis initiators bearing thiazol-2-ylidene ligands [Scheme 24]. Two variants of this kind of catalyst, namely, phosphine free catalysts (**69-73)** and phosphine containing catalysts (**74** and **75)** have been prepared from commercially available complexes **1** and **4** respectively. The performance of these catalysts (**69-75**) was evaluated in ring closing metathesis of diethyl diallyl malonate and diethyl allylmethylallyl malonate, cross metathesis of allylbenzene with *cis*-1,4-diacetoxy-2-butene, ring-opening metathesis polymerization reactions of 1,5-cyclooctadiene and norbornene and the macrocyclic ring-closing of a 14-membered lactone. Although all the catalysts were active in these reactions, thephosphine-free variant of this family is more stable than its phosphine-

containing counter parts and demonstrated activity and stability similar to the second-generation catalysts **2** and **4.** Importantly, the fine-tuning of thiazol-2-ylidene ligand environment has substantial effect on reactivity profile of the corresponding catalysts. For instance, catalyst induction period increased with the steric bulk of the carbene ligand and in cross metathesis reaction, more Z-olefins were produced upon increasing the bulkiness of the carbene ligand.

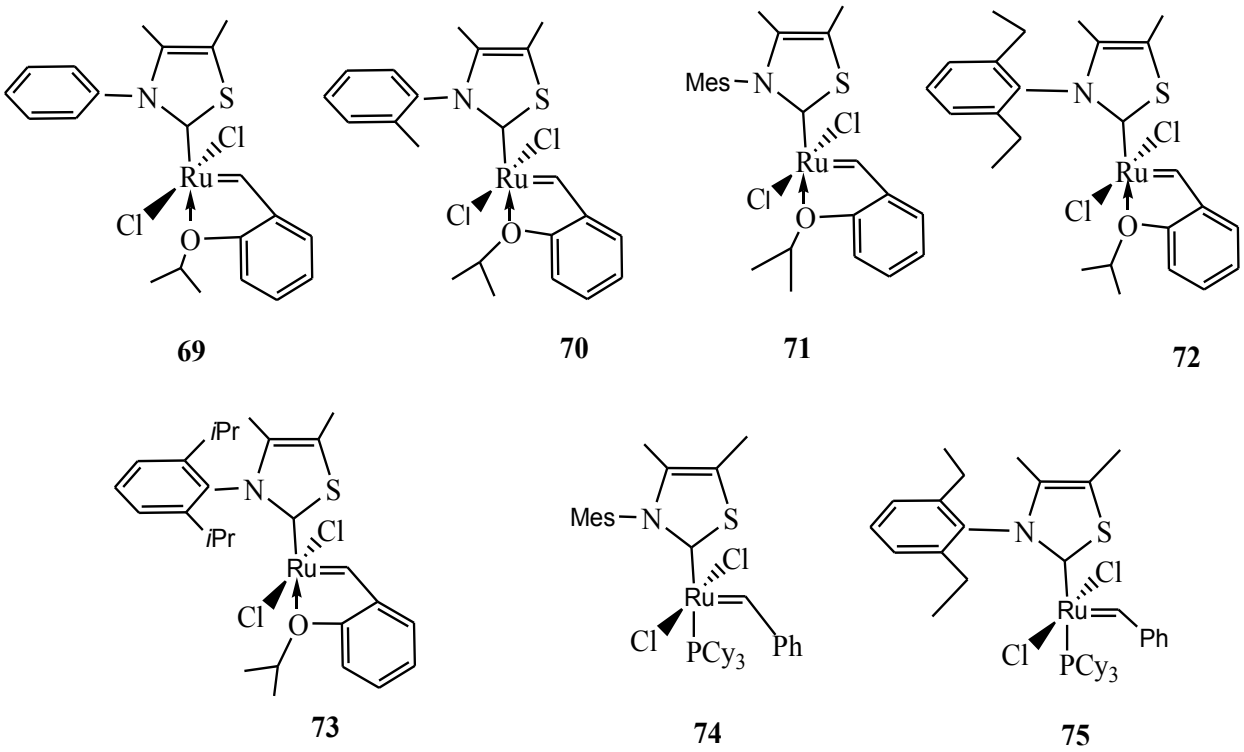

Scheme 24: Ruthenium-based olefin metathesis initiators coordinated with thiazol-2-ylidene ligands [37].

2.7 References

[1] See review articles (a) A. Fürstner, *Angew. Chem., Int. Ed*., 2000, **39**, 3013. (b) T. M. Trnka, R. H. Grubbs, *Acc. Chem. Res.,* 2001, **34**, 18. (c) Handbook of Metathesis; R. H. Grubbs, Ed.;Wiley-VCH: Weinheim, 2003, 1204. (d) D. Astruc, *New J. Chem*., 2005, **29**, 42. (e) P. H. Deshmukh, S. Blechert, *Dalton Trans*., 2007, 2479. (f) C. Samojłowicz, M. Bieniek, K. Grela, *Chem. Rev.,* 2009, **109**, 3708. (g) I. Drugutan, V. Dragutan, L. Delaude, A. Demonceau, *ChimicaOggi*/*Chem. Today,* 2009, **27**, 13. (h) S. Díez-González, N. Marion, S. P. Nolan, *Chem. Rev.,* 2009, 109, 3612. (i) G. C. Vougioukalakis, R. H. Grubbs, *Chem. Rev.,* 2010, **110**, 1746. (j) A. M. Lozano-Vila, S. Monsaert, A. Bajek, F. Verpoort, *Chem. Rev.,* 2010, **110**, 4865. S. Kress, S. Blechert, *Chem. Soc. Rev.,* 2012, **41**, 4389.

[2] S.T. Nguyen, L.K. Johnson, R.H. Grubbs, W. Z. Joseph, *J. Am. Chem. Soc.,* 1992, **114**, 3974.

[3] (a) P. Schwab, M. B. France, J. W. Ziller, R. H. Grubbs, *Angew. Chem. Int. Ed.,* 1995, 2039. (b) P. Schwab, R. H. Grubbs, J. W. Ziller, *J. Am. Chem. Soc.,* 1996, **118**, 100. (c) E. L. Dias, S. T. Nguyen, R. H. Grubbs, *J. Am. Chem. Soc.,* 1997, **119**, 3887.

[4] (a) M. Scholl, T. M. Trnka, J. P. Morgan, R. H. Grubbs, *Tetrahedron Lett.,* 1999 **40**, 2247. (b) M. Scholl, S. Ding, C. W. Lee, R. H. Grubbs, *Org. Lett.,* 1999, **1**, 953.

[5] J. S. Kingsbury, J. P. A. Harrity, P. J. Jr. Bonitatebus, A. H. Hoveyda, *J. Am. Chem. Soc.,* 1999, **121**, 791.

[6] (a) S. B. Garber, J. S. Kingsbury, B. L. Gray, A. H. Hoveyda, *J. Am. Chem. Soc.,* 2000, **122**, 8168. (b) S. Gessler, S. Randl, S. Blechert, *Tetrahedron Lett.,* 2000, **41**, 9973.

[7] See reviews articles: (a) S. Díez-González, S. P. Nolan, *Coord. Chem. Rev.,* 2007, **251**, 874. (b) L. Cavallo, A. Correa, C. Costabile, H. Jacobsen, *J. Organomet. Chem.,* 2005, **690**, 5407.

[8] H. Jacobsen, A. Correa, A. Poater, C. Costabile, L. Cavallo, *Coord. Chem. Rev.,* 2009, **253**, 687.

[9] (a) N. Hadei, E. A. B. Kantchev, C. J. O'Brien, M. G. Organ, *Org. Lett.* 2005, **7**, 1991. (b) P. de Fremont, N. M. Scott, E. D. Stevens, S. P. Nolan, *Organometallics,* 2005, **24**, 2411.

[10] L. Jafarpour, S. P. Nolan, *J. Organomet. Chem.,* 2001, **617-618**, 17.

[11] A. G. Wenzel, R. H. Grubbs, *J. Am. Chem. Soc.,* 2006, **128**, 16048.

[12] (a) M. Ulman, R. H. Grubbs, *Organometallics,* 1998, **17**, 2484. (b) T. Ritter, A. Hejl, A. G. Wenzel, T. W. Funk, R. H. Grubbs, *Organometallics,* 2006, **25**, 5740.

[13] (a) M. Bornand, P. Chen, Angew. *Chem. Int. Ed.,* 2005, **44**, 7909. (b) M. Bornand, S. Torker, P. Chen, *Organometallics,* 2007, **26**, 3585.

[14] I. C. Stewart, B. K. Keitz, K. M. Kuhn, R. M. Thomas, R. H. Grubbs *J. Am. Chem. Soc.,* 2010, **132**, 8534.

[15] B. K. Keitz, R. H. Grubbs, *J. Am. Chem. Soc.,* 2011, **133**, 16277.

[16] R. M. Thomas, B. K. Keitz, T. M. Champagne, R. H. Grubbs, *J. Am. Chem. Soc.,* 2011, **133**, 7490.

[17] (a) J. Patel, S. Mujcinovic, W. R. Jackson, A. J. Robinson, A. K. Serelis, C. Such, *Green Chem*. 2006, **8**, 450. (b) X. Bei, D. P. Allen, R. L. Pedersen, Pharm. *Technol.* 2008, s18.

[18] M. B. Dinger, P. Nieczypor, J. C. Mol, *Organometallics,* 2003, **22**, 5291.

[19] (a) K. Endo, R. H. Grubbs, *J. Am. Chem. Soc.,* 2011, **133**, 8525. (b) B. K. Keitz, A. Fedorov, R. H. Grubbs, *J. Am. Chem. Soc.,* 2012, **134(4),** 2040. (c) M. B. Herbert, Y. Lan, B. K. Keitz, P. Liu, K. Endo, M. W. Day, K. N. Houk, R. H. Grubbs, *J. Am. Chem. Soc*., 2012, **134(18)**, 7861.

[20] K. Vehlow, S. Maechling, S. Blechert, *Organometallics,* 2006, **25**, 25.

[21] M. Lichtenheldt, D. Wang, K. Vehlow, I. Reinhardt, C. Kühnel, U. Decker, S. Blechert, M. R. Buchmeiser, *Chem. Eur. J.,* 2009, **15**, 9451.

[22] N. Ledoux, B. Allaert, S. Pattyn, H. V. Mierde, C. Vercaemst, F. Verpoort, *Chem. Eur. J*., 2006, **12**, 4654.

[23] S. Kavitake, M. K. Samantaray, R. Dehn, S. Deuerlein, M. Limbach, J. A. Schachner, E. Jeanneau, C. Copéret, C. Thieuleux *Dalton Trans*., 2011, **40**, 12443.

[24] O. Ablialimov, M. Kędziorek, C. Torborg, M. Malińska, K. Woźniak, K. Grela, *Organometallics,* 2012, **31**, 7316.

[25] A. Fürstner, L. Ackermann, B. Gabor, R. Goddard, C. W. Lehmann, R. Mynott, F. Stelzer, O. R. Thiel, *Chem. Eur. J.,* 2001, **7**, 3236.

[26] C. W. Bielawski, D. Benitez, R. H. Grubbs, *Science,* 2002, **297**, 2041.

[27] A. J. Boydston, Y. Xia, J. A. Kornfield, I. A. Gorodetskaya, R. H. Grubbs *J. Am. Chem., Soc.* 2008, **130(38),** 12775.

[28] S. Prühs, C. W. Lehmann, A. Fürstner, *Organometallics,* 2004, **23**, 280.

[29] H. Jong, B. O. Patrick, M. D. Fryzuk, *Organometallics*, 2011, **30**, 2333.

[30] B. K. Keitz, R. H. Grubbs, *Organometallics,* 2010, **29**, 403.

[31] K. Vehlow, S. Gessler, S. Blechert, *Angew. Chem. Int. Ed.,* 2007, **46**, 8082.

[32] G. C. Vougioukalakis, R. H. Grubbs, *Organometallics,* 2007, **26**, 2469.

[33] G. C. Vougioukalakis, R. H. Grubbs, *Chem. Eur. J.,* 2008, **14**, 7545.

[34] S. Leuthäußer, V. Schmidts, C. M. Thiele, H. Plenio. *Chem. Eur. J.,* 2008, **14**, 5465.

[35] J. A. Wright, A. A. Danopoulos, W. B. Motherwell, R. J. Carroll, S. Ellwood, *J. Organomet. Chem.,* 2006, **691**, 5204.

[36] N. Ledoux, B. Allaert, A. Linden, P. Van Der Voort, F. Verpoort, *Organometallics,* 2007, **26**, 1052.

[37] G. C. Vougioukalakis, R. H. Grubbs, *J. Am. Chem. Soc.,* 2008, **130**, 2234.

[38] G. Occhipinti, H.-R. Bjørsvik, K. W. Törnroos, A. Fürstner, V. R. Jensen, *Organometallics,* 2007, **26**, 4383.

[39] D. R. Anderson, V. L. Daniel, J. O' Leary, G. Bertrand, R. H. Grubbs, *Angew. Chem. Int. Ed.,* 2007, **46**, 7262.

[40] D. R. Anderson, T. Ung, G. Mkrtumyan, G. Bertrand, R. H. Grubbs, Y. Schrodi, *Organometallics,* 2008, **27(4),** 563.

3.1 Introduction

The area of ruthenium catalyzed olefin metathesis has become remarkable topic in current chemistry because of its relevance as an efficient and elegant method for carbon-carbon bond formation [1]. Several well-defined ruthenium-based catalysts have been introduced showing high activity in olefin metathesis and excellent tolerance to many functional groups. A growing number of these carbenes has broadened their utility beyond olefin metathesis. This chapter summarizes the application of ruthenium carbenes in non-metathesis reactions particularly isomerization of allylic alcohols, isomerization of alkenes and Kharasch addition.

3.2 Isomerization of Allylic Alcohols

The conversion of allylic alcohols to saturated carbonyl compounds is a useful synthetic process. Conventionally this process requires two-steps that are oxidation and reduction reactions (Paths B and C respectively, Scheme 1). This is undesirable method due to the fact that stoichiometric or even excess amounts of reductant and oxidant are needed. A one-pot catalytic transformation (path A, Scheme 1), equivalent to an internal redox process is an attractive strategy [2] as it not only maintains total atom economy but also avoids the use of costly and toxic reagents [3, 4].

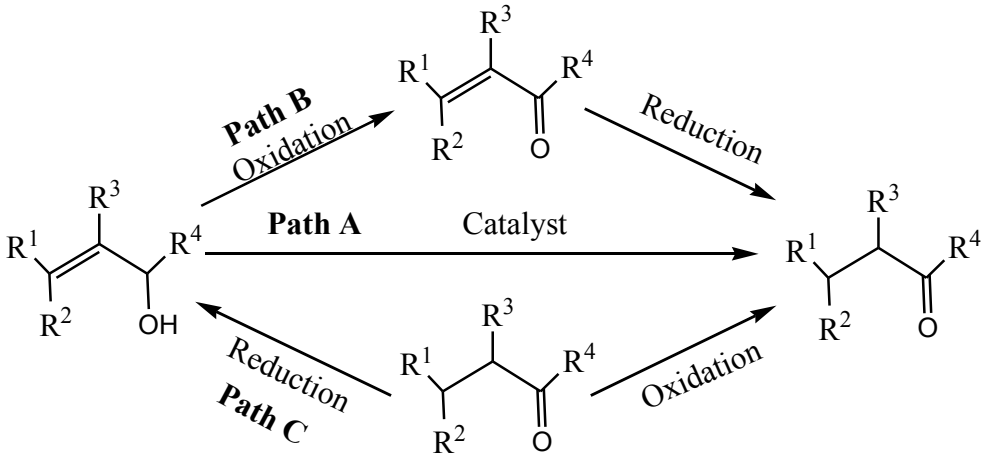

Scheme 1: Isomarization of allylic alcohols into carbonyl compounds.

In this regard, a number of methods have been developed harnessing the ability of transition metal complexes to effect the isomerization of allylic alcohols. From a mechanistic point of view, the transition-metal complex turns the allylic alcohol into an enol which readily tautomerizes to the corresponding carbonyl compound [5, 6]. Three general mechanisms are commonly known [7, 8]. In the first one (path **a**, Scheme 2), an alkyl metal complex is formed as

an intermediate. The alkyl metal intermediate is generated by insertion of the olefinic unit of the allylic alcohol into the M-H bond of a metal hydride catalyst which is either isolated or generated *in situ*. Subsequent *β*-hydrogen elimination, followed by decomplexation, liberates the enol and regenerates the active species [9]. In the second mechanism (Path **b** in Scheme 2), the enol is generated via a *π*-allyl metal hydride intermediate formed by oxidative addition of the allylic C-H bond to the catalyst [10]. Finally, in path **c**, the allylic alcohol coordinates to the metal center to form a metal alkoxide complex, followed by a formation of a key *π*-oxoallyl complex. After protonation, enol is the released and the starting complex is regenerated.

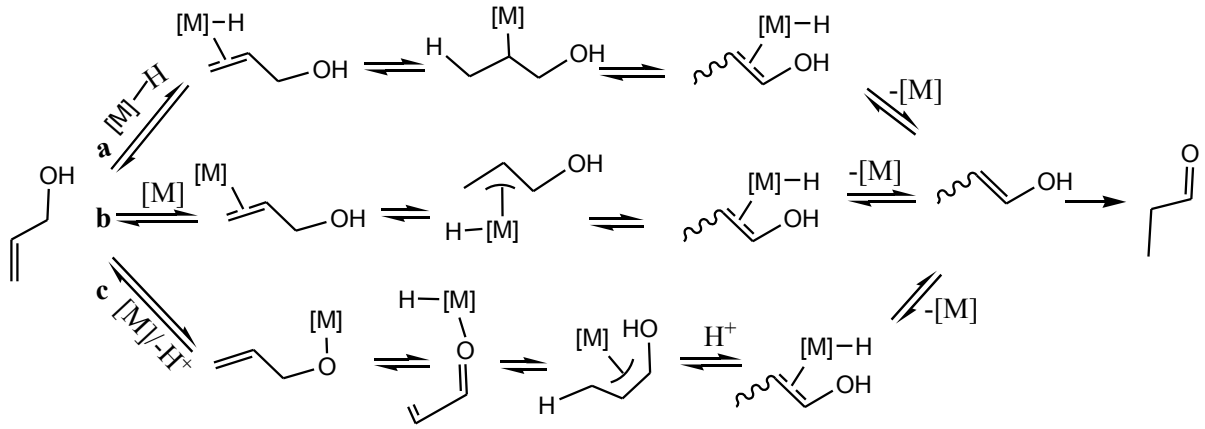

Scheme 2: Mechanism of catalytic isomerization of allylic alcohols.

A variety of ruthenium derivatives have been employed in the isomerization of allylic alcohols. In the early experiments $RuCl_3$ found to be capable of catalyzing isomerization of allyl alcohols [11] and glycols [12]. When a 1:1 mixture of $RuCl_3$ and NaOH was used, the reaction was quantitative after 5 minutes at 130 °C. Furthermore, on using chiral non-racemic alcohols, the transposition occurred with a significant chirality transfer (Scheme 3) [13].

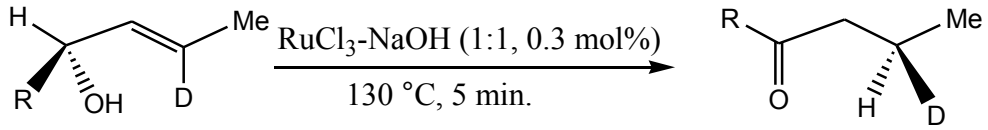

R = Me, Et

Scheme 3: Isomerization of chiral nonracemic alcohols.

Furthermore, $Ru(acac)_3$ (acac = acetylacetonato: 2,4-pentanedionato) also proved to be an effective catalyst for the isomerization of allylic alcohols [14-16]. Worth noting is the fact that a combination of $Ru(acac)_3$ with some other reagents improved its efficiency. For instance, a mixture of Ph_3P and $Ru(acac)_3$ (2:1) isomerized 3-buten-2-ol to methylethyl ketone [17]. In addition, a combination of some Brønsted acids such as TsOH with cationic ruthenium complexes which is obtained from $Ru(acac)_3$ with 2 equivalent 1,10-phenanthroline led to efficient catalyst for isomerization of sterically less hindered allylic alcohols [17].

The ruthenium complexes $Ru(H_2O)_6(tos)_2$ [18,19] and $Ru(H_2O)_6(trif)_2$ [20] efficiently catalyze the isomerization of simple allylic ethers and alcohols under mild conditions to give carbonyl compounds, although, in some cases oxidation products were observed [18,20].

The oxoruthenium complex $Ru_3O(OCOCH_3)_7$, on the other hand, was found to be an interesting catalyst for the isomerization of simple secondary alcohols. Its solubility in ethylene glycol permitted the isolation of the resulting ketone (insoluble in ethylene glycol) by decantation and the catalytic system could be recycled several times [21].

A wide range of organometallic ruthenium chloride complexes both homogeneous and heterogeneous have been studied [22]. It has been demonstrated that homogeneous catalysts efficiently mediate rearrangement of simple secondary allylic alcohols with higher initiation rate than the corresponding supported one.

Trost *et al*. [23, 24] reported on the scope and limitations of the rearrangement of allylic alcohols with $CpRu(PPh_3)_2Cl$ and the corresponding indenyl complex. Under standard reaction conditions (5 mol % catalyst in dioxane at 100 °C), using Et_3NHPF_6 for sequestering the chloride anion, the isomerization proceeded in good yield for cinnamyl alcohol as well as for a wide range of allylic secondary alcohols. In addition, these catalysts exhibit a remarkable chemoselectivity since non-allylic alcohols are not isomerized (Scheme 4) and remote double bonds migrate slowly compared to that of allyl alcohols [25]. Furthermore, with these catalysts sterically hindered alcohols and six-membered substrates are not isomerized.

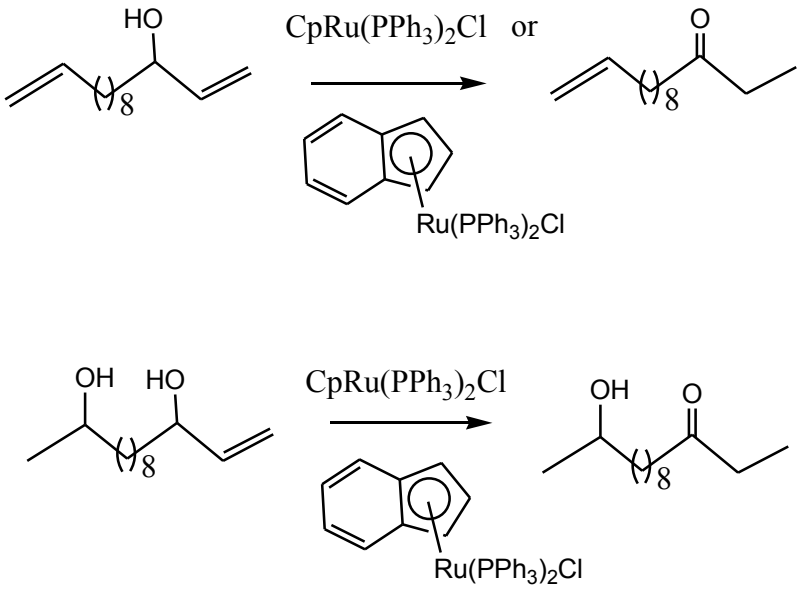

Scheme 4: Chemoselectivity of $CpRu(PPh_3)_2Cl$ and the corresponding indenyl complex in the isomerization allylic alcohol.

A strong increase in reactivity of catalyst complexes was observed when the reaction was carried out using AgOTs instead of Et_3NHPF_6, this because Ag^+ abstracts a chloride anion easier [25]. However, its Lewis acid character often leads to the products resulting from competitive nucleophilic addition by the solvent [26].

In yet another study, a series of $[RuCp(PR_3)(CH_3CN)_3][PF_6]$ type complexes were tested [27]. Such derivatives have more labile ligands and therefore, would generate the 14-electron cationic ruthenium species more readily. The reaction of simple disubstituted allylic alcohols with these catalysts (1 mol %) at 57 °C gave the corresponding carbonyls in good yields. However, from a synthetic point of view, there appears to be strong limitations since neither C_1 nor C_3 disubstituted alcohols could be isomerized under these conditions.

Several ruthenium hydride type complexes such as $(RuClH(PPh_3)_3$, $RuH_2(PPh_3)_3$, $RuH_2(PnBu_3)_4)$ form another class of active catalysts for the isomerization of allylic alcohols. These ruthenium complexes can be generated *in situ*, however, they can only be used for isomerization of less hindered secondary allylic alcohols while primary allylic alcohols do not react in the presence of these catalysts [21, 10, 12].

Ruthenium complexes **1** and **2** (Scheme 5) with Cp-functionalized N-heterocyclic carbenes have been found to be efficient catalysts in the isomerization of allylic alcohols without base [28]. The more sterically crowded complex, **2**, showed very low activity, while **1** was very active. The isomerization of O-deuterated allylic alcohol provides the corresponding ketone with the deuterium at the *α*-carbon, which is in agreement with previously reported results by Grubbs and co-workers.

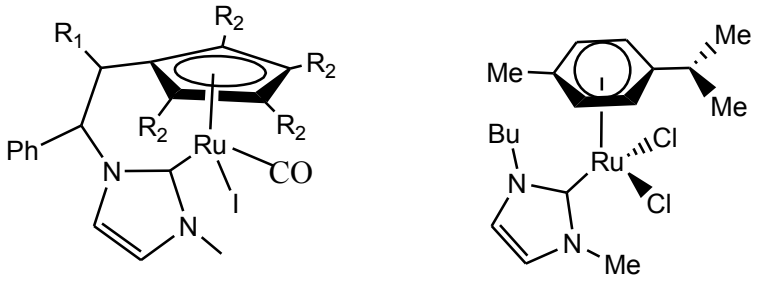

1: R_1 =H, R_2 = Me
2: R_1 =Ph, R_2 = Br

3

Scheme 5: Ruthenium complexes **1**-**3** bearing *N*-heterocyclic carbenes.

Allyl alcohols were also isomerized to ketones or aldehydes in aqueous–organic biphasic systems by water-soluble N-heterocyclic carbene complex **3** using hydrogen as an initiator of the [29]. It was found that the reactions were strongly influenced by the pH and the chloride of the aqueous phase and highest activity and selectivity was obtained at pH 7 and 0.2 M NaCl. The catalyst could be recycled in the aqueous phase for at least four times without a significant change in activity and selectivity.

Another set of ruthenium catalysts for isomerization of allylic alcohols (**4-7**) working in homogeneous aqueous solutions or in two-phase reactions have been developed (Scheme 6) [30]. Catalysts **4-6** showed good to excellent catalytic activities in the isomerization of simple allylic alcohols in homogeneous aqueous solutions or in two-phase. Replacement of chloride in **6** by a strongly bound CO to afford catalyst **7** led to a substantial drop in the catalytic activity implying that the presence of a labile ligand is essential for good catalytic activity.

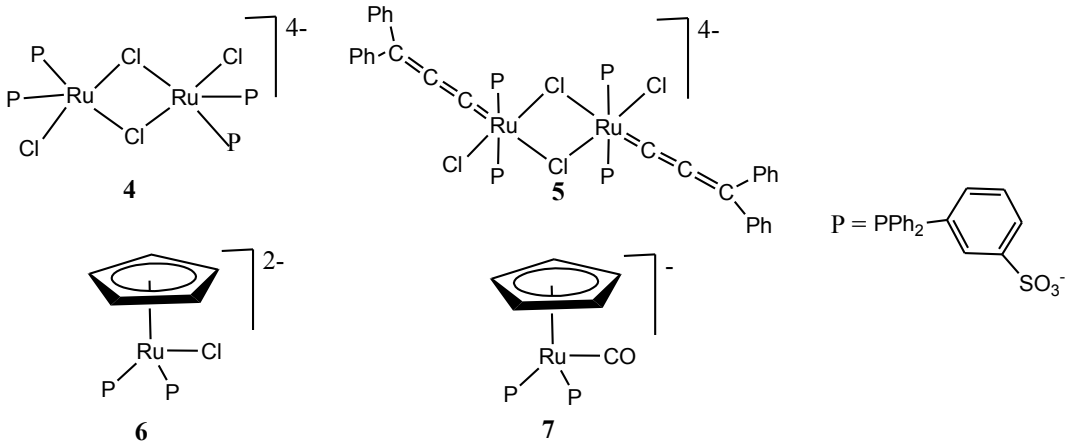

Scheme 6: Ruthenium based catalysts **4-7** for isomerization of allylic alcohols.

3.3 Isomerization Reactions of Allylic Alcohols Catalyzed by Ruthenium Carbenes

Tori and coworkers [31, 32] reported that under ring closing olefin metathesis reaction (RCM) conditions using the Grubbs' complex **8** the allylic alcohol **10** rearranged into the ketones in a ratio of 2:1 with 68% yield and the expected 10-membered carbocycle was not formed (Scheme 8).

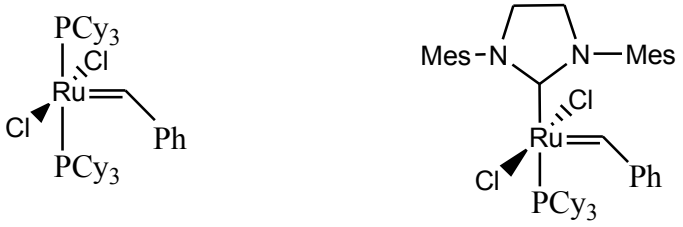

Scheme 7: Grubbs' catalysts **8** and **9**.

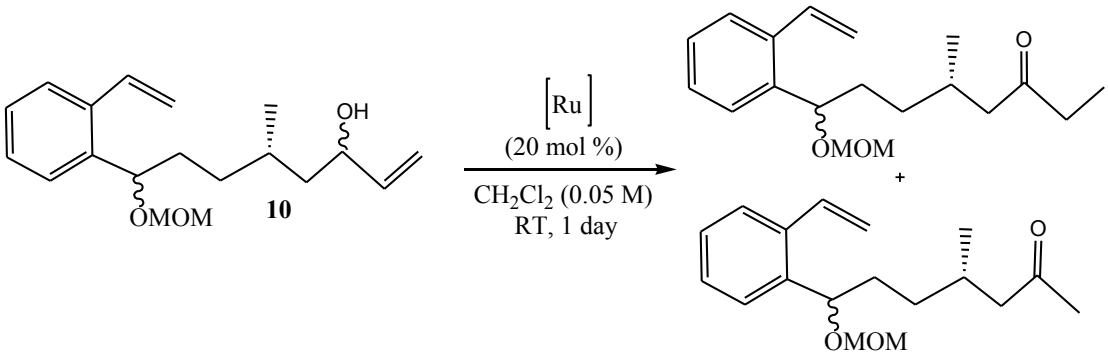

Scheme 8: Rearrangement of the allylic alcohol **10** catalyzed by complex **8**.

Thereafter, some different allylic alcohols were tested revealing that more hindered alcohols are stable under these conditions. Only the simple allylic alcohols tend to isomerize producing ethyl ketone and the corresponding degraded methyl ketone. The degradation of secondary allylic alcohols by Grubbs' catalyst **8** to produce a methyl ketone has also reported by Yakambram and cowokers [33]. They observed that secondary allylic alcohols with 10 mol% of Grubbs catalyst undergo isomerization to ethyl ketones whereas with 100 mol% of Grubbs catalyst at room a net fragmentation reaction with the loss of a carbon atom occurs, to provide a methyl ketone.

The mechanism for the formation of the one-carbon degraded methyl ketone has been reported and is depicted in Scheme 9 [31]. The Grubbs' reagent attacks compound **11** to produce another carbene complex **12**, which rearranges into enol **13**. Then, tautomerization to **14** and reductive elimination affords the degraded ketone **15**.

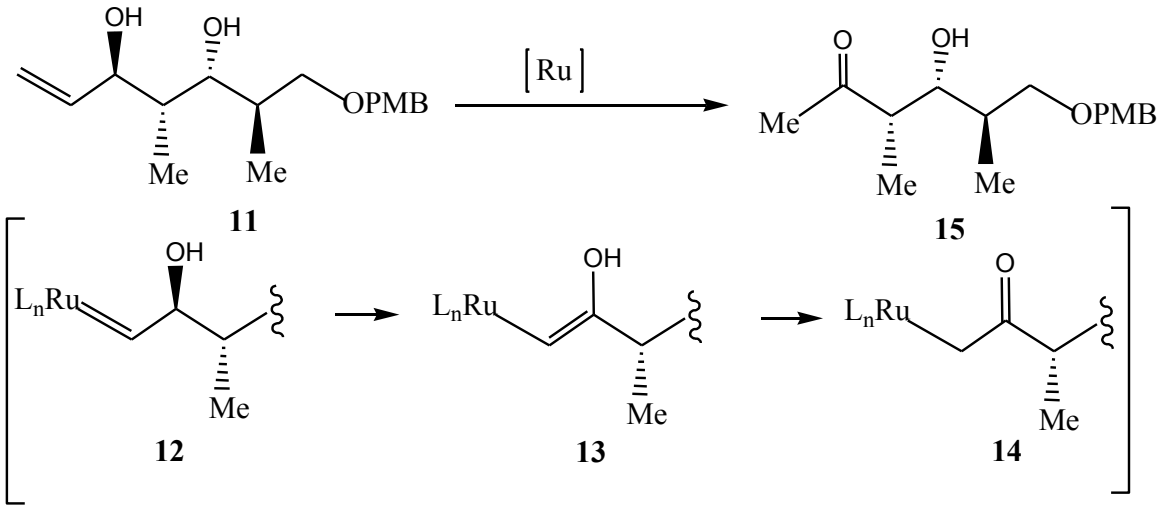

Scheme 9: Mechanism for the formation of the one-carbon degraded methyl ketone.

The Grubbs'catalyst **9** is also able to mediate isomerization of O- and N-allyl as well as O-homoallyl groups to produce the corresponding enol ethers and enamines. The resulting enol ethers and enamines can be transformed to the corresponding alcohols and amines by acidic work-up [34] (Scheme 10).

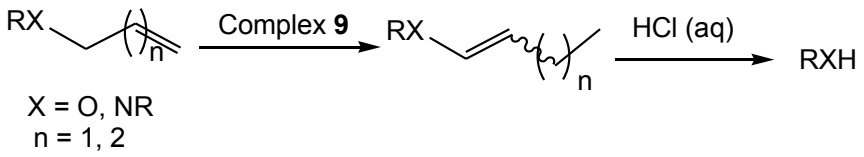

Scheme 10: Isomerization of O- and N-allyl catalyzed by complex **9**.

On the other hand, Rutjes *et al.* [35] encountered an interesting ruthenium-induced isomerization of allenamides to dienamides catalyzed by complex **9** (Scheme 11) in the ring-closing metathesis reactions of olefin containing-enamides. Furthermore, it has been outlined that in some cases the isomerization to the internal double bond in N-allyllactam is favored over ring-closing metathesis by using Grubbs' catalyst (Scheme 12) [36].

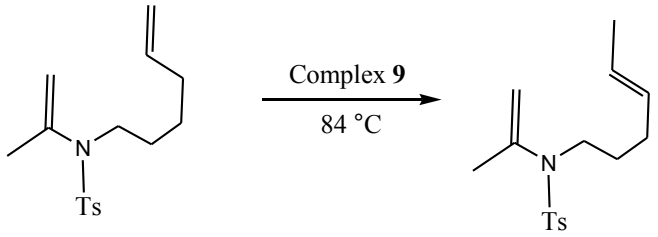

Scheme 11: Grubbs' catalyst-promoted isomerization of allenamides.

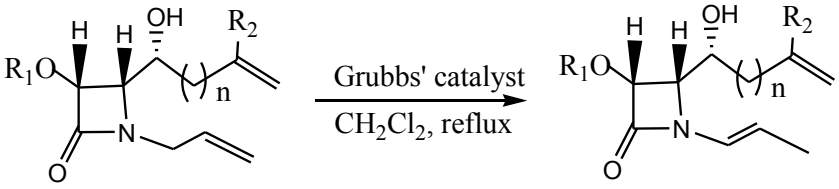

Scheme 12: Grubbs' catalyst-promoted isomerization of allylamides.

3.4 Isomerization of Olefins

Two pathways for transition-metal-catalyzed olefin isomerization are commonly known [37, 38]. The first pathway is the metal hydride addition-elimination mechanism (Scheme 13) in which free olefin coordinates to a metal hydride species with a subsequent insertion into the metal-hydride bond yielding a metal alkyl. Formation of a secondary metal alkyl followed by β-elimination yields isomerized olefins and regenerates the initial metal hydride.

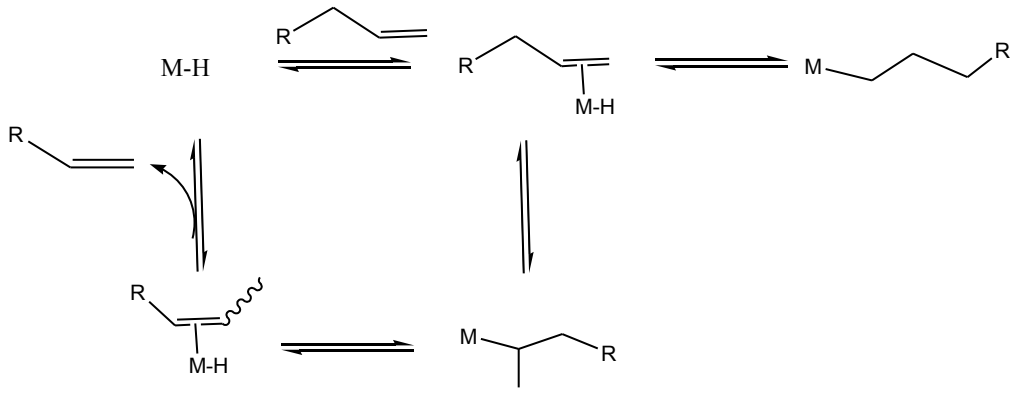

Scheme 13: The metal hydride addition-elimination mechanism of olefin isomerization.

The second pathway is the π-allyl hydride mechanism (Scheme 14) in which a free olefin coordinates to a transition metal fragment that does not contain a hydride ligand. Oxidative addition of an activated allylic C-H bond to the metal yields a π-allyl metal hydride. Transfer of the coordinated hydride to the opposite end of the allyl group yields isomerized olefin.

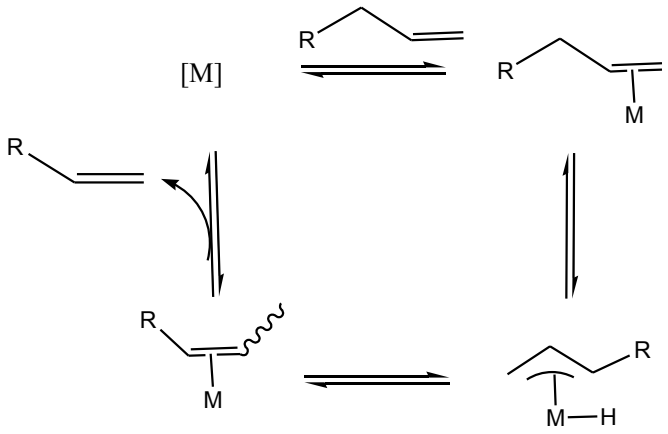

Scheme 14: The π-allyl hydride mechanism of olefin isomerization.

Isomerization of hexene catalyzed by $RuCl_3$ in ethanol at 65 °C using catalyst concentration of 0.5 mol% was reported [39]. In this case a longer induction period was observed (distinctly about 1 h), in which ruthenium(III) was reduced to the active ruthenium(II). Corresponding to this change, the formation of *n*-hexanal and hexanone were confirmed in the reaction mixture in addition to the isomerization products.

The isomerization of pentene-1 to *cis*-pentene-2 (60%) and trans-pentene-2 (40%) is catalyzed by $RuHCI(PPh_3)_3$ solutions in benzene [40]. The reaction is the first order with respect to both

the complex and to pentene-1 at low concentrations although the order decreased after enough conversion of pentene-1. The change from first-order behavior occurs because the catalytically active species are formed by dissociation of the complex and because of the changes in the nature of the solvent at the higher pentene concentrations. Isomerization of deuterium-labelled pentene-1revealed that (i) the equilibrium is established between uncoordinated and co-ordinated pentene-1, (ii) redistribution of deuterium in pentene-1accompanies its isomerization, (iii) normally isomerization involves the movement of the double bond to the adjacent position only, (iv) *cis*- and *trans*-pentene-2 are each formed by a mechanism involving a pentyl intermediate, (v) a mechanism involving allylic intermediate also contributes to the formation of the *trans*-isomer, and (vi) some processes require the formation of transient species having two hydrogen atoms as ligands on ruthenium and in which two phosphine ligands have been lost by dissociation.

The isomerization of hexane-1 was performed in a hydrocarbon solvent, in the presence of the phosphine-substituted ruthenium carbonyls $Ru(CO)_3(PR_3)_2$, $Ru_3(CO)_9(PR_3)_3$ and $Ru(CO)_2(OAc)_2(PR_3)_2$ [R-Bu, Ph] [41]. The rate of the reaction was found to depend on the concentration of the catalyst and substrate, solvent used and additional gas. The rate of the reaction significantly changed when an alcohol was used as solvent which was attributed to a modification of the catalytic precursor with formation of a ruthenium hydride. While the addition of dinitrogen, argon and xenon led to the retardation of the rate of reaction, helium did not display any influence.

3.5 Ruthenium Promoted Radical Reactions

The origin of atom transfer radical addition (ATRA) can be traced back to1937 when Kharasch and co-workers discovered the peroxide effect in the anti-Markovnikof addition of HBr to unsymmetrical alkenes in the presence of peroxide initiators [42]. The generally accepted mechanism for this reaction involves free-radical intermediates as outlined in Scheme 15.

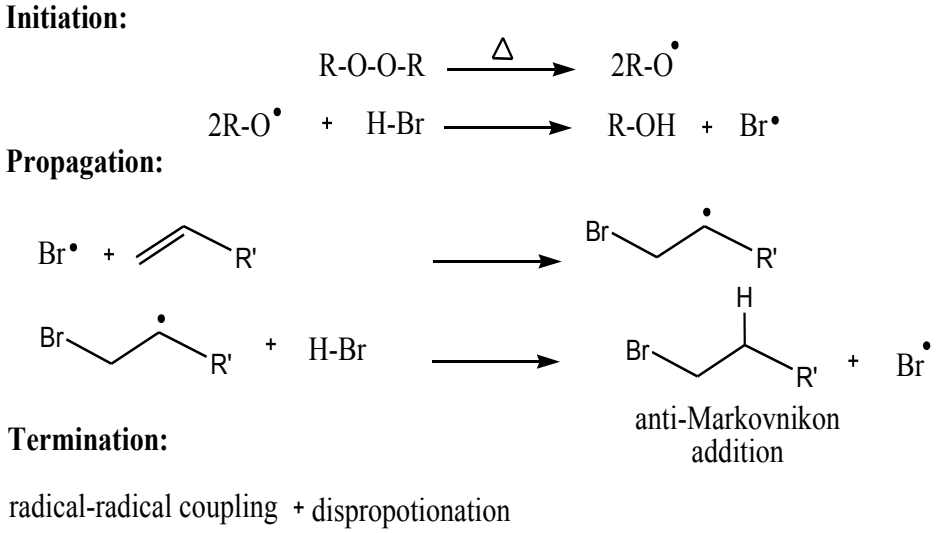

Scheme 15: Anti-Markovnikov addition of HBr to unsymmetrical alkenes.

It was then recognized that a variety of substrates including polyhalogenated alkanes could be used in the radical addition to alkenes. In particular, Kharasch investigated the addition of polyhalogenated alkanes (CBr_4, CCl_4, CBr_3Cl and CCl_3Br) to alkenes in the presence of free-radical initiators or light (Scheme 16). This reaction is today widely known as the Kharasch addition or atom transfer radical addition (ATRA) [43, 44]. Very high yields of the mono-adduct were obtained in the case of simple olefins (hexane-1, octane-1 and decene-1), but were significantly decreased for more reactive monomers such as styrene, methyl acrylate and methyl methacrylate. The main reason for the decreased yield of the mono-adduct was radical-radical coupling and repeating radical addition to the alkene to generate oligomers and polymers.

Although, radical-radical termination reactions by coupling and disproportionation could be suppressed by decreasing the radical concentration (R_t α [radicals]^2), telomerization reactions could not be avoided due to the low chain transfer constant (k_{tr}/k_p, Scheme 16). The research was thus shifted in a direction of finding means to selectively control the product distribution.

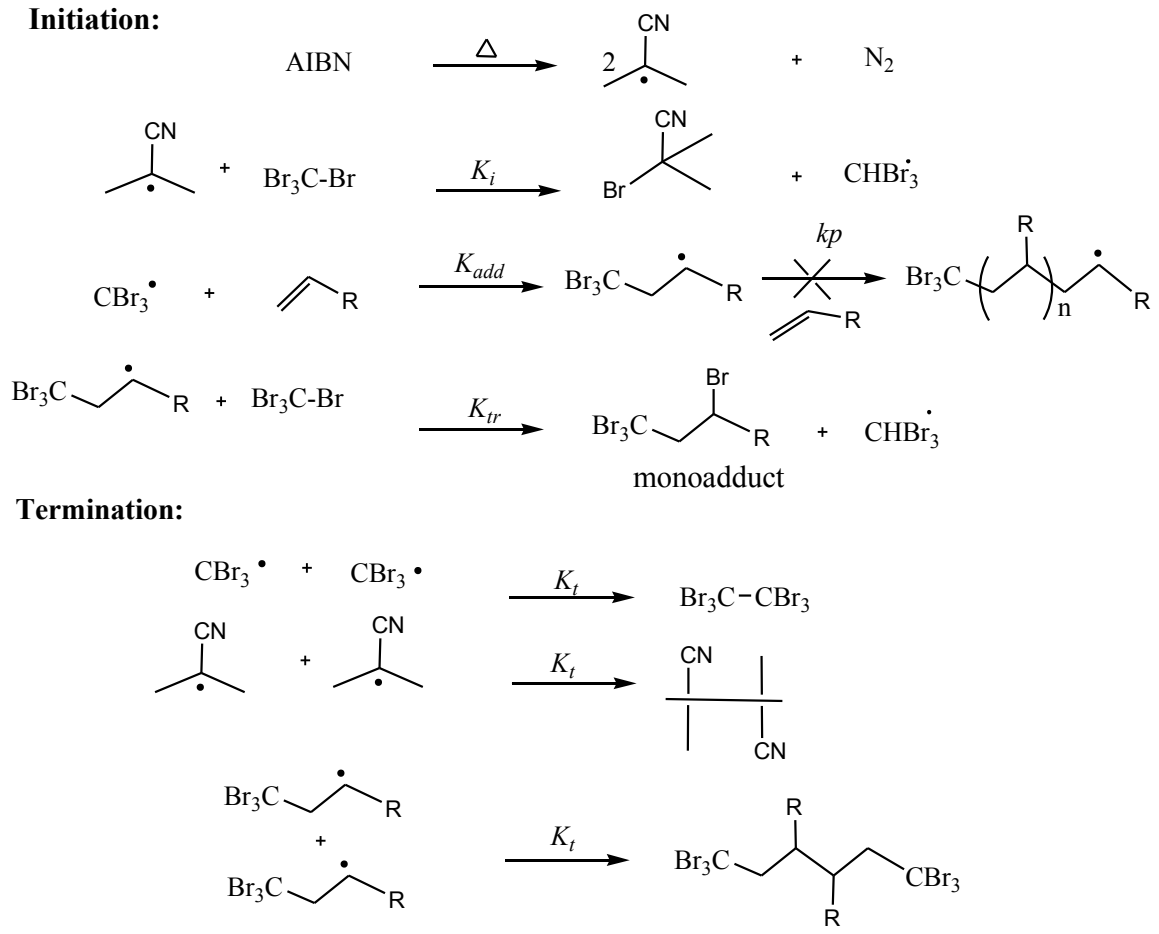

Scheme 16: AIBN initiated Kharasch addition of CBr_4 to alkene.

In 1956, Minisci *et al.* attempted thermal polymerization of acrylonitrile in CCl_4 and $CHCl_3$ in a steel autoclave and observed a considerable amount of mono-adduct (CCl_3-CH_2-CHClCN with CCl_4 and $CHCl_2$-CH_2-CHClCN with $CHCl_3$) [45]. In 1961 further investigation of the phenomena by the same authors revealed that, iron chlorides arising from corrosion of the autoclave played a major role in this process [46–51]. This reaction marked the beginning of transition metal catalyzed ATRA.

Based on chemo-, regio-, and stereoselectivity, it is generally accepted that the mechanism of transition metal catalyzed ATRA involves free radical intermediates [52]. In particular, the treatment of organic halides (R-X) with various low-valent transition metal complexes (M) results in abstraction of halogen atom from the organic halides to produce organic radicals ($R^{\cdot}$) (Scheme 17, Equation 1). The formal oxidation state of the metal complex is increased by one,

and M-X is formed by the halogen abstraction (Equation 2). If the formed organic radicals are able to promote an addition reaction to unsaturated compounds (Equation 3), the the resulting adduct radicals are capable of abstracting the halogen atom from the high-valent metallic species M-X (equation 4), in this manner the full catalytic sequence shown in Scheme 17 is established [54].

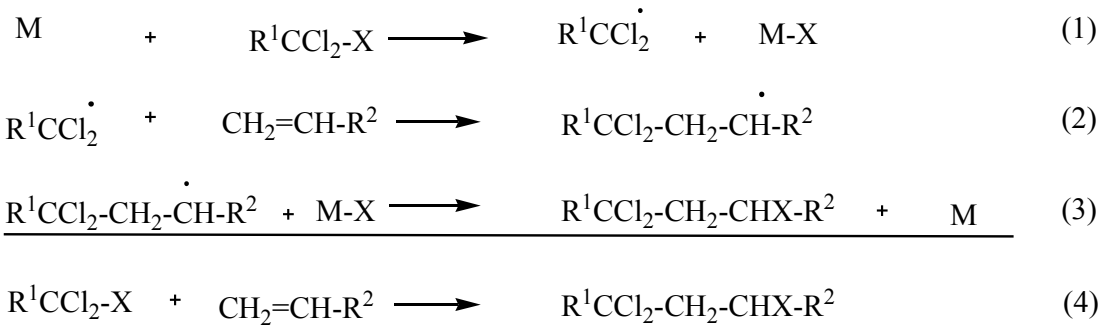

Scheme 17: Metal catalyzed Kharasch addition.

Now various polyhalogenated compounds such as CX_3Y (X = halogen, Y = H, halogen, CF, or another electronegative group) are used as the organic halides and a number of transition metal species including complexes of Cu, Fe, Ru and Ni [53-55], as well as metal oxides [56, 57] and zero valent metals such as Cu(0) [58, 59], and Fe(0) [60–62] were found to be active in Kharasch reactions. In particular, certain ruthenium complexes sometimes show distinctly different activity and selectivity from other catalysts. The detailed description of ruthenium complexes as Kharasch reactions initiators and their trend in catalytic activity will be discussed in the following section.

As the first ruthenium catalyst, Nagai and coworkers identified that, $RuCl_2(PPh_3)_3$ and $RuCl_2(PPh_3)_4$ catalyzed effectively the addition of poly-chloromethanes such as carbon tetrachloride and chloroform to 1-olefins to afford the corresponding 1:1 adducts with little telomerization even in the case of styrene. By using these catalysts the reaction proceeded smoothly under mild conditions and the use of polar solvents such as alcohols or nitriles is no longer necessary contrary to cuprous or ferrous chloride catalysts [63].

Mechanistic investigations of the addition of CCl_4 to alkenes catalyzed by $RuCl_2(PPh_3)_3$ have been reported by J. L. A. Durrant *et al*. (Scheme 18) [64,65]. In their investigation they noticed

the decrease in reaction rates when triphenylphosphine was added, which indicates that an initial dissociation of a PPh_3 ligand has to take place. The fourteen-electron fragment $[RuCl_2(PPh_3)_2]$ formed was suggested to be the catalytic active species, which reacts with CCl_4 to give the oxidized Ru(III) fragment $RuCl_3(PPh_3)_2$ and the radical $CCl_3^{\cdot}$. Further reaction of the $CCl_3^{\cdot}$ radical with the alkene yields the radical $R^{\cdot}CHCH_2CCl_3$. Final elimination of the 1:1 adduct, with the abstraction of one chlorine atom from the oxidized form of the catalyst, recycles the active Ru(II) fragment.

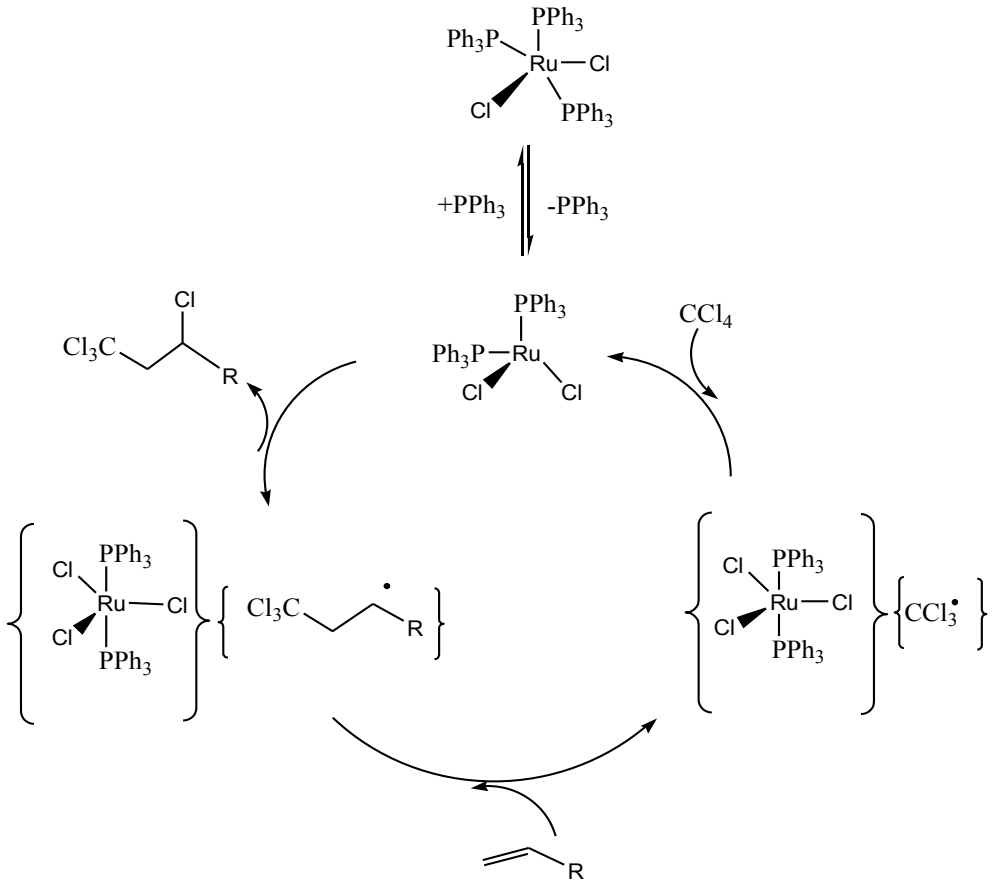

Scheme 18: Ruthenium catalyzed Kharasch addition.

Nagai and coworkers expanded their study to highly stereoselective addition of carbon tetrachloride to cyclohexene catalyzed by $RuCl_2(PPh_3)_3$ to afford *trans*-1-trichloromethyl-2-chlorocyclohexane (**16)** in good yield. However, the reaction was accompanied by the formation of 3-trichloromethyl-1-cyclohexene (**17**) (trace), 3-chloro-l-cyclohexene 2 (**18**) (trace), 1,2-dichlo rocyclohexane (**19**) (6% yield) and chloroform (25% yield), however, these by-products were easily separated from **16** by distillation (Scheme 19) [66].

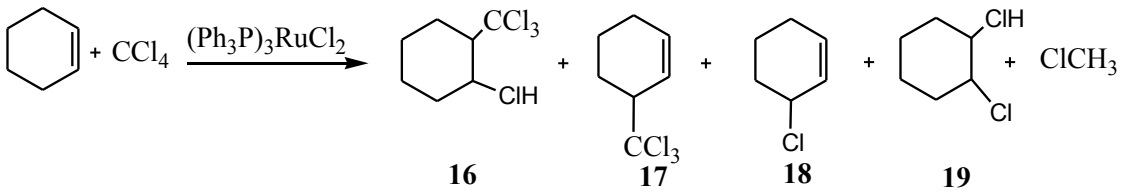

Scheme 19: Stereoselective addition of carbon tetrachloride to cyclohexene.

Selective 1,4-addition of CCl_4 to conjugated 1,3-dienes such as 1,3-butadiene, 1,3-pentadiene, isoprene, 1,3-cyclohexadiene and 1,3-cyclooctadiene proceeded smoothly under mild conditions in the presence of $RuCl_2(PPh_3)_3$ (Scheme 20). Interestingly, the addition of CCl_4 to isopropene proceeded with a high regioselectivity to give 1,1,1,5-tetrachloro-3-methylpentene-3 only (Scheme 20) [67].

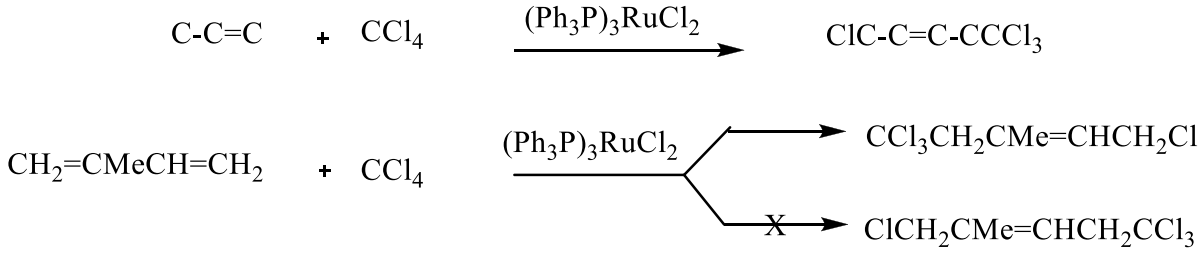

Scheme 20: 1,4-addition of CCl_4 to conjugated 1,3-dienes.

Methyl and ethyl trichloroacetates or a further extension of the $RuCl_2(PPh_3)_3$ catalyzed Kharasch reaction, the addition of CF_2ClCCl_3 to silyl enol ether was also reported to give halogenated enone **21** as the product which is formed by dehydrochlorination of the primary addition-desilylation product **20** (Scheme 21) [69].

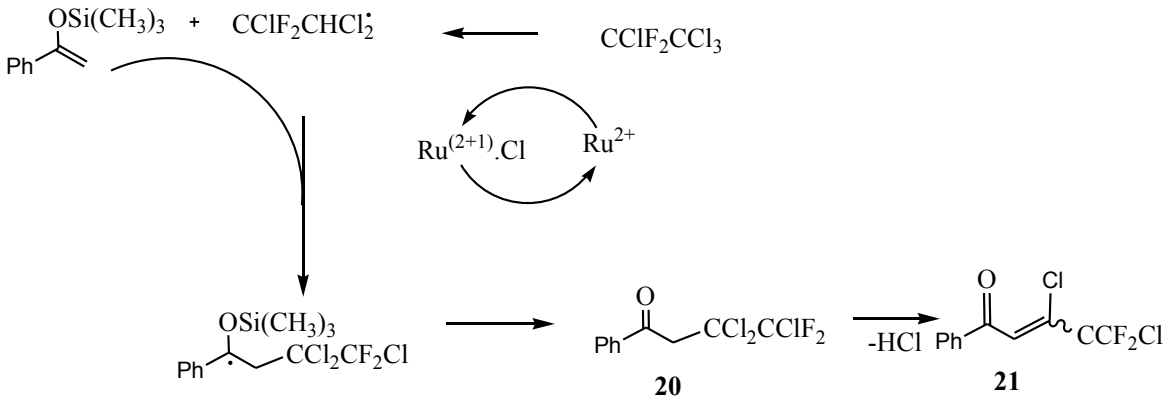

Scheme 21: Ruthenium catalyzed reaction of silyl enol ether with CF_2ClCCl_3.

Although Ru-based precatalyst, $RuCl_2(PPh_3)_3$ has been extensively employed to promote the addition of halocarbons to various olefinic substrates, it surfer from major draw backs in that relatively higher catalyst loading (≥ 0.5 mol%) and temperature (≥ 80 °C) are often needed to achieve acceptable yields.

The isoelectronic complexes **22** and **23** (Scheme 22) were displayed good to excellent ATRA activities [70]. For all the reactions investigated, the {Cp*Ru} complex **22** gave lower yields than complexes **22** and **23**. The latter, however, are among the most active catalysts for the addition of CCl_4 and $CHCl_3$ to olefins at that time. Complex **22** allows the Kharasch addition of CCl_4 to olefins to be carried out at ambient temperature.

Verpoort *et al.* reported the synthesis and the catalytic activity of half-sandwich ruthenium (II) complexes, which contain neither phosphine nor N-heterocyclic carbene (NHC) ligands but bidentate Schiff base ligands (**24**) [71]. The advantage of using Schiff base ligands is that their steric and electronic properties can be modified easily.

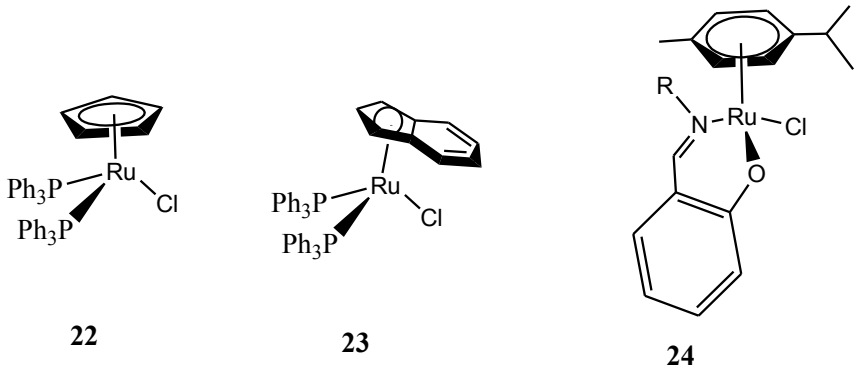

R = Me, *t*Bu, or 2, 6-Me-4-BrC_6H_2

Scheme 22: Ruthenium based ATRA catalysts **22-24**.

Demonceau *et al.* described a half-sandwich complex with *N*-heterocyclic (NHC) ligand (**25**), which was active for the ATRA of CCl_4 to styrene [72]. Optimization of the steric and electronic properties of the NHC ligand, however, was necessary to control the catalytic activity of the catalysts. For example, when the chloro atoms in complex **25** were substituted with hydrogen atoms, the catalytic activity of the resulting catalyst decreased significantly.

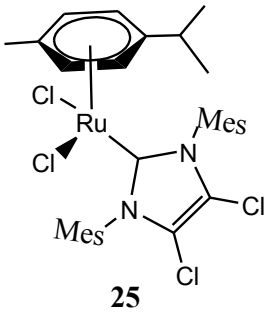

25

Scheme 23: Half-sandwich ruthenium complexes **25**.

3.6 Ruthenium Carbene Catalyzed Kharasch Addition

Grubbs' ruthenium benzylidene complex **8** was found to be active for the chemo- and region-selective addition of chloroform across various olefins [73]. In fact, during an investigation on cross-metathesis, Snapper and coworkers isolated a product not derived from olefin metathesis but from ruthenium catalyzed addition of $CHCl_3$ across alkenes (Scheme 24).

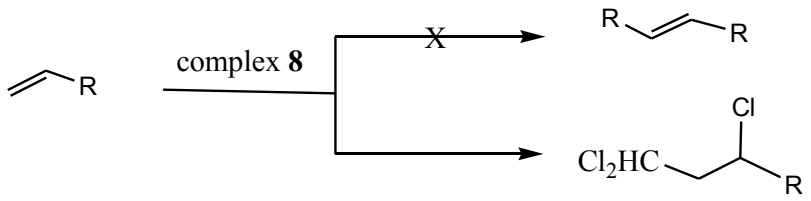

Scheme 24: Kharasch addition catalyzed by Grubbs' ruthenium benzylidene complex **8**.

In comparison to previously described ruthenium-based Kharasch catalysts, Grubbs' carbene affects the addition of $CHCl_3$ under mild conditions. While higher temperatures (>120 °C) and prolonged reaction times (>8 h) were usually required applying $[Cl_2Ru(PPh_3)_3]$ catalyst, exposure of styrene to $CHCl_3$ in the presence of complex **8** for only 2 h at 65 °C resulted in a quantitative yield. The same reaction conditions with $[Cl_2Ru(PPh_3)_3]$ provided < 5% of the addition product. However, it was noted that in $CHCl_3$ using Grubbs' catalyst, readily metathesizable olefins, such as unhindered alkenes, are susceptible to both reactions pathways.

On the other hand, Demonceau and coworkers reported the ability of complex **8** and the related compounds **26** and **27** (Scheme 25) in catalyzing the Kharasch addition reaction [74].

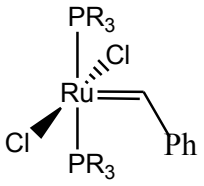

26: R = Ph
27: R = c-C_5H_9

Scheme 25: Ruthenium based ATRA initiators **26** and **27**.

The group of Verpoort also developed various other ruthenium carbenes which were used as ATRA catalysts. The vinylidene complexes **28** and **29** [75], the mixed carbene complexes **30** [76] and ruthenium Schiff base **31** [77] and **32** [78] (Scheme 26) were found to be particularly active.

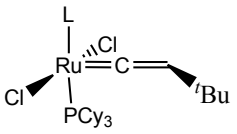

28: L = PCy_3

29: L = 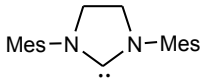

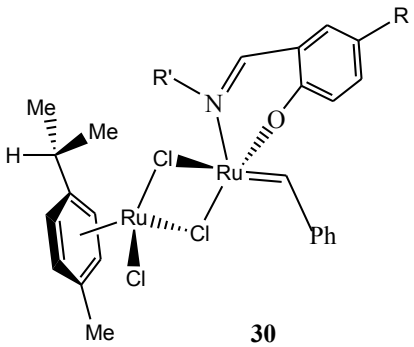

30

a: R = H, R' =Me
b: R = NO_2, R' =Me
c: R = H, R' = 2,6-Me-4-BrC_6H_2
d: R = NO_2, R' = 2,6-Me-4-BrC_6H_2
e: R = H, R' =2,6-*i*PrC_6H_3
f: R = NO_2, R' =2,6-*i*PrC_6H_3

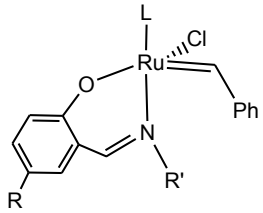

31

L = PCy_3 or 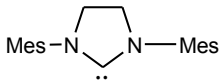

R = H or NO_2
R' = Me, 2,6-Me-4-BrC_6H_2, or 2,6-^{i}PrC_6H_3

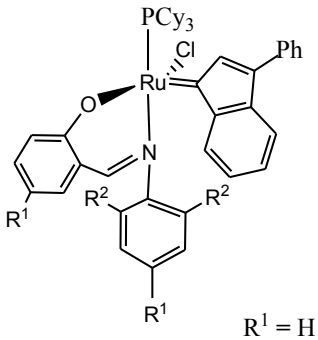

32

R^1 = H or NO_2
R^2 = ^{i}Pr or Me
R_3 = H or Br

Scheme 26: Ruthenium based ATRA initiators **28-32**.

3.7 References

[1] A. Fürstner, *Angew. Chem., Int. Ed*., 2000, **39**, 3013. (b) T. M. Trnka, R. H. Grubbs, *Acc. Chem. Res.,* 2001, **34**, 18. (c) Handbook of Metathesis; R. H. Grubbs, Ed.; Wiley-VCH: Weinheim, 2003, 1204. (d) D. Astruc, *New J. Chem*., 2005, **29**, 42. (e) P. H. Deshmukh, S. Blechert, *Dalton Trans*., 2007, 2479. (f) C. Samojłowicz, M. Bieniek, K. Grela, *Chem. Rev.,* 2009, **109**, 3708. (g) I. Drugutan, V. Dragutan, L. Delaude, A. Demonceau, *ChimicaOggi*/*Chem. Today,* 2009, **27**, 13. (h) S. Díez-González, N. Marion, S. P. Nolan, *Chem. Rev.,* 2009, **109**, 3612. (i) G. C. Vougioukalakis, R. H. Grubbs, *Chem. Rev.,* 2010, **110**, 1746. (j) A. M. Lozano-Vila, S. Monsaert, A. Bajek, F. Verpoort, *Chem. Rev.,* 2010, **110**, 4865. S. Kress, S. Blechert, *Chem. Soc. Rev.,* 2012, **41**, 4389.

[2] (a) L. A. Yanovskaya, Kh. Shakhidayatov, *Russ. Chem. Rev.,* 1970, **39**, 859. (b) R. C. Van der Drift, E. Bouwman, E. Drent, *J. Organomet. Chem.,* 2002, **650**, 1.

[3] B. M. Trost, *Science,* 1991, **254**, 1471.

[4] B. M. Trost, *Angew. Chem., Int. Ed. Engl.,* 1995, **34**, 259.

[5] C. Masters, *in Homogeneous Transition-Metal Catalysis*, Chapman and Hall, London, 1981, p. 70-89.

[6] G. W. Parshall, S. D. Ittel, *in Homogeneous Catalysis*, Wiley, New York, 1992, p.9-24.

[7] R. Uma, C. Crévisy, R. Grée, *Chem. Rev.,* 2003, **103**, 27.

[8] R. C. van der Drift, E. Bouwman, E. Drent*, J. Organomet. Chem.,* 2002, **650**, 1.

[9] D. V. McGrath, R. H. Grubbs, *Organometallics,* 1994, **13**, 224.

[10] V. Branchadell, C. Crévisy, R. Grée, *Chem. Eur. J.,* 2003, **9**, 2062.

[11] J. K. Nicholson, B. L. Shaw, *Proc. Chem. Soc.,* 1963, **282**.

[12] M. Dedieu, J.-Y. Pascal, *J. Mol. Catal.,* 1980, **9**, 59.

[13] W. Smadja, G. Ville, C. Georgoulis, *J. Chem. Soc., Chem. Commun.,* 1980, **594**.

[14] C. Georgoulis, J. M. Valery, G. Ville, *Synth. Comm.,* 1984, **14**, 1043.

[15] S. Krompiec, J. Suwinski, *Pol. J. Chem.* 1990, **64**, 505.

[16] S. Krompiec, J. Suwinski, R. Grobelny, *J. Mol. Cat.,* 1994, **89**, 303.

[17] F. Stunnenberg, F. G. M. Niele, E. Drent, *Inorg. Chim. Acta*, 1994, **222**, 225.

[18] D. V. McGrath, R. H. Grubbs, *Organometallics,* 1994, **13**, 224.

[19] D. V. McGrath, R. H. Grubbs, J. W. Ziller, *J. Am. Chem. Soc.,* 1991, **113**, 3611.

[20] M. Karlen, A. Ludi, *Helv. Chim. Acta,* 1992, **75**, 1604.

[21] Y. Sasson, G. L. Rempel, *Tetrahedron Lett.,* 1974, **47**, 4133.

[22] A. Zoran, Y. Sasson, J. Blum, *J. Org. Chem.,* 1981, **46**, 255.

[23] B. M. Trost, R. J. Kuliawec, *Tetrahedron Lett.,* 1991, **32**, 3039.

[24] B. M. Trost, R. J. Kuliawec, *J. Am. Chem. Soc*., 193, **115**, 2027.

[25] R. C. van der Drift, M. Vailati, E. Bouwman, E. Drent, *J. Mol. Catal. A: Chem.,* 2000, **159**, 163.

[26] R. Uma, M. K. Davies, C. Crévisy, R. Grée, *Eur. J. Org. Chem.,* 2001, 3141.

[27] C. Slugovc, E. Rüba, R. Schmid, K. Kirchner, *Organometallics,* 1999, **18**, 4230.

[28] A. P. Costa, J. A. Mata, B. Royo, E. Peris, *Organometallics*, 2010, **29**, 1832.

[29] M. Fekete, F. Joó, *Catal. Commun.*, 2006, **7**, 783.

[30] T. Campos-Malpartida, M. Fekete, F. Joó, Á. Kathó, A. Romerosa, M. Saoud, W. Wojtkówc, *J. Organometal. Chem.,* 2008, **693**, 468.

[31] K. Nakashima, S. Okamoto, M. Sono, M. Tori, *Molecules,* 2004, **9**, 541.

[32] K. Nakashima, R. Ito, M. Sono, M. Tori, *Heterocycles*, 2000, **53**, 301.

[33] M. K. Gurjar, P. Yakambram, *Tetrahedron Lett.,* 2001, **42**, 3633.

[34] C. Cadot, P. I. Dalko, J. Cossy, *Tetrahedron Lett.,* 2002, **43**, 1839.

[35] S. S. Kinderman, J. H. van Maarseveen, H. E. Schoemaker, H. Hiemstra, F. P. J. T. Rutjes, *Org. Lett.,* 2001, **3**, 2045.

[36] B. Alcaide, P. Almendros, J. M. Alonso, M. F. Aly, *Org. Lett.,* 2001, **3**, 3781.

[37] G. W. Parehall, *Homogeneous Catalysis;* Wiley: New York, 1980; pp 31-35.

[38] R. H. Crabtree, The *Organometallic Chemistry of the Transition Metals;* Wiley: New York, 1988; pp 188-190.

[39] H. Hirai, H. Sawai, E. I. Ochiai and Makishim, *J. Catal.,* 1970, **17**, 119.

[40] D. F. Ewing, B. Hudson, D. E. Webster, P. B. Wells, *J.C.S. Dalton.,* 1972, 1204.

[41] A. Salvini, F. Piacenti, P. Frediani, A. Devescovi, M. Caporali, *J. of Organometal Chem.* 2001, **625**, 255.

[42] M.S. Kharasch, H. Engelmann, F.R. Mayo, *J. Org. Chem.,* 1937, **2**, 288.

[43] M.S. Kharasch, E.V. Jensen, W.H. Urry, *Science,* 1945, **102**, 128.

[44] M. S. Kharasch, E. V. Jensen, W. H. Urry, *J. Am. Chem. Soc.,* 1945, **67**, 1626.

[45] M. De Malde, F. Minisci, U. Pallini, E. Volterra, A. Quilico, *Chim. Ind. (Milan),* 1956, **38**, 371.

[46] F. Minisci, *Gazz. Chim. Ital*., 1961, **91**, 386.

[47] F. Minisci, U. Pallini, *Gazz. Chim. Ital,.* 1961, **91**, 1030.

[48] F. Minisci, R. Galli, *Tetrahedron Lett.,* 1962, 533.

[49] F. Minisci, R. Galli, *Chim. Ind. (Milan)* 1963, **45**, 1400.

[50] F. Minisci, *Acc. Chem. Res.,* 1975, **8**, 165.

[51] F. Minisci, M. Cecere, R. Galli, *Gazz. Chim. Ital.,* 1963, **93**, 1288.

[52] For a review: C. Walling, E. S. Huyser, *Org. React.,* 1963, **13**, 91.

[53] J. Iqbal, B. Bhatia, N. K. Nayyar, *Chem. Rev.,* 1994, **94**, 519.

[54] R.A. Gossage, L.A. Van De Kuil, *Acc. Chem. Res.* 1998, **31**, 423.

[55] K. Severin, *Curr. Org. Chem.,* 2006, **10**, 217.

[56] M. Hajek, P. Silhavy, J. Malek, *Collection Czechoslov. Chem. Commun.,* 1980, **45**, 3488.

[57] M. Hajek, P. Silhavy, J. Malek, *Collection Czechoslov.Chem. Commun.,* 1980, **45**, 3502.

[58] E. Steiner, P. Martin, D. Bellius, *Helv. Chim. Acta,* 1982, **65**, 983.

[59] J.O. Metzger, R. Mahler, *Angew. Chem. Int. Ed.,* 1995, **34**, 902.

[60] F. Bellesia, L. Forti, F. Ghelfi, U.M. Pagnoni, *Synth. Commun*., 1997, **27**, 961.

[61] L. Forti, F. Ghelfi, E. Libertini, U.M Pagnoni, *Tetrahedron,* 1997, **53**, 17761.

[62] L. Forti, F. Ghelfi, U.M. Pagnoni, *Tetrahedron Lett.,* 1996, **37**, 2077.

[63] H. Matsumoto, T. Nakano, Y. Nagai, *Tetrahedron Lett*., 1973, 5147.

[64] W. J. Bland, R. Davis, J. L. A. Durrant, *J. Organomet. Chem.,* 1985, **280**, 397.

[65] W. J. Bland, R. Davis, J. L. A. Durrant, *J. Organomet. Chem.,* 1984, **267**, C45.

[66] H. Matsumoto, T. Nakano, T. Nikaido, Y. Nagai, *Tetrahedron Lett.* 1975, 899.

[67] H. Matsumoto, T. Nakano, T. Nikaido, Y. Nagai, *Chem. Lett.,* 1975, 115.

[68] H. Matsumoto, T. Nikaido, Y. Nagai, *J. Org.Chem.* 1976, **41**, 396.

[69] T. Okano, T. Shimizi, K. Sumida, S. Eguchi, *J. Org. Chem.,* 1993, **58**, 5163.

[70] F. Simal, L. Wlodarczak, A. Demonceau, A. F. Noels, *Eur. J. Org. Chem.,* 2001, **14**, 2689.

[71] B. De Clercq, F. Verpoort, *Tetrahedron Lett.,* 2001, **42**, 8959.

[72] A. Richel, S. Delfosse, C. Cremasco, L. Delaude, A. Demonceau, A. F. Noels, *Tetrahedron Lett.,* 2003, **44**, 6011.

[73] J. A. Tallarico, L. A. Malnick, M. L. Snapper, *J. Org. Chem.,* 1999, **64**, 344.

[74] F. Simal, A. Demonceau, A. F. Noels, *Tetrahedron Lett,.* 1999, **40**, 5689.

[75] T. Opstal, F. Verpoort, *Tetrahedron Lett.,* 2002, **43**, 9259.

[76] B. De Clercq, F. Verpoort, *Tetrahedron Lett.,* 2002, **43**, 4687.

[77] B. De Clercq, F. Verpoort, *Catalysis Lett.,* 2002, **83**, 9.

[78] T. Opstal, F. Verpoort, *New J. Chem*., 2003, **27**, 257.

4.1 Introduction

The development of easy to handle, well-defined ruthenium-based alkylidene complex **1** [1] which combine remarkable tolerance towards functional groups and moisture with high activity has tremendously broaden the scope of metathesis reactions as a powerful synthetic tool [2]. The optimization of the activity of the catalysts for various applications in metathesis reactions normally proceeds by tuning the ligand sphere around the corresponding metal center. Thus replacement of a phosphine by a highly electron donating N-Heterocyclic carbene (NHC) has afforded catalyst **2** with increased reactivity by many orders (Scheme 1) [3]. Similarly, the introduction of the bidentate alkylidene by Hoveyda resulted in metathesis catalysts **3** and **4** with increased stability and excellent recyclability (Scheme 1) [4].

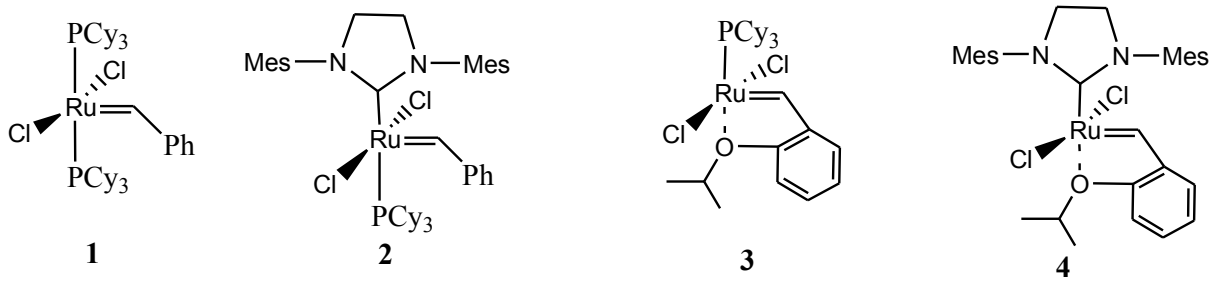

Scheme 1: Ruthenium alkylidene metathesis initiators.

However, in spite of the highly favorable properties of the homogeneous well-defined ruthenium metathesis initiators, they are difficult to separate from the reaction mixture and often impose significant challenges. Very recently, different strategies for the sequestration of ruthenium impurities from olefin metathesis post-reaction mixtures have been reviewed by G. C. Vougioukalakis [5]. Nonetheless, the residual ruthenium complex may cause problems such as olefin isomerization, decomposition of the product, and increased toxicity of the final materials. Therefore, immobilization on various supporting materials combines the advantages of conventional heterogeneous catalysts with the versatility of homogeneous ones as heterogeneous catalysts not only allow for easiness of separation and recovery from the reaction medium but also show repeated recycling potential, good stability and ease of handling.

Up to now, different soluble polymers and solid supports are used as carriers to recover catalysts. Furthermore, various solvent systems such as perfluorinated solvents, ionic liquids, and supercritical CO_2 are also employed for this purpose. The present chapter describes the current

state of the art on immobilization of ruthenium based metathesis initiators on solid supports.The immobilisation of the catalysts on polymeric beads, monolithic materials and siliceous supports both mesoporous as well as nonporous will be discussed. In addition, the performance of the supported catalysts will be compared with the homogeneous analogues.

4.2 Polymer Beads Supported Ruthenium Metahesis Catalysts

Functionalised polystyrenes present as linear or cross-linked polymers are very often used as catalyst support [6]. They are available in different bead sizes (50-500 mm) and degrees of functionalization and cross-linking [7].

Grubbs and coworkers described the first example of a polymer supported well-defined olefin metathesis catalysts [8]. They reported a series of olefin metathesis catalysts based on a ruthenium vinylcarbene complex attached on a 2% cross linked polystyrene divinyl benzene solid support (PS-DVB) (Scheme 2). The ability of vinyl carbene complexes to exchange its phosphine ligands with a variety of phosphines allowed the convenient synthesis of PS-DVB supported ruthenium bis-phosphine vinyl carbene catalysts **5-7**. However, the supported catalysts turned out to be less appropriate for polymerization relative to their homogeneous counter parts, which was attributed to phosphine chelation effects, diffusion limitations and incomplete substitution of phosphine. The general decrease in metathesis activity of these PS-DVB-supported catalysts is offset by the extended lifetime of the supported catalysts. The PS-DVB-supported ruthenium catalysts are long-lived and can be re-used in practical circumstance.

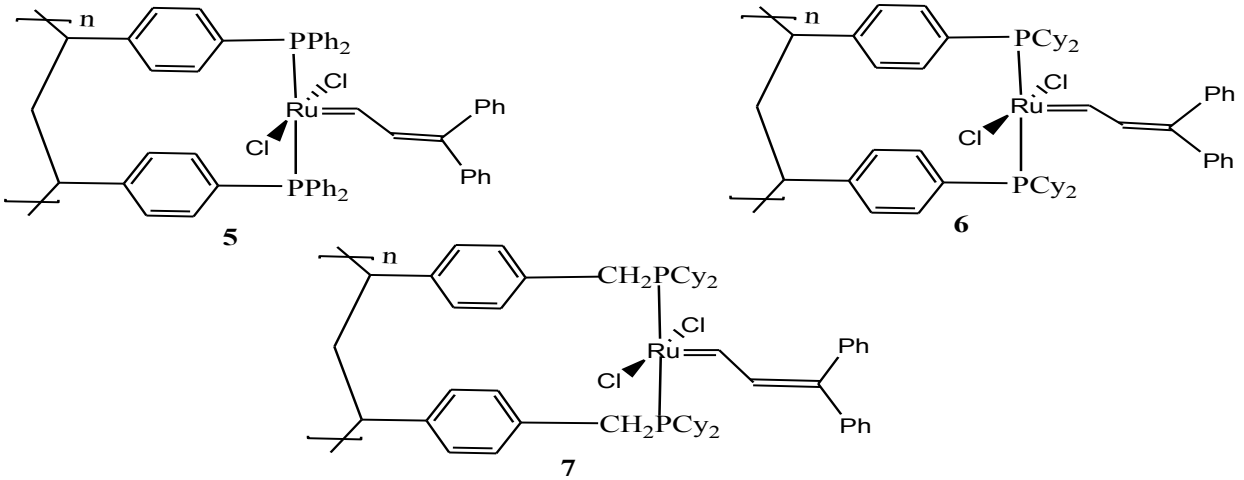

Scheme 2: The PS-supported ruthenium vinylidene catalyst **5-7**.

Blechert *et al.* [9] reported for the first time Merrifield polystyrene (1% divinyl benzene) (DVB) bound catalyst **8** anchored by a NHC ligand. They anticipated that anchorage of the catalyst through the NHC ligand could result into permanently immobilized and highly active metathesis initiator since NHC ligands remain bounded to the ruthenium center during metathesis reactions.

The supported catalyst **8** was synthesized with a loading level between 0.14 and 0.4 mmol/g of Grubbs' catalyst **2** by ligand exchange with the polymer supported 3,4-dimesityl-4-dihydroimidazoline chloride (Scheme 3). The catalyst was tested on its ring-closing metathesis (RCM) activity towards various substrates and showed full cyclization. However, the rate of cyclization is lower relative to the homogeneous analogues. Highly pure products were obtained after filtration as the only purification step. The ease of isolation allows automation and makes catalyst **8** particularly suitable for combinatorial applications.

In addition, the same group also reported on the heterogeneous Hoveyda type ruthenium catalyst **9**, obtained by immobilization on a Merrifield resin via a styrene ligand [10]. The supported catalyst **9** is an excellent initiator in olefin metathesis reactions, re-usable and tolerates a wide variety of functional groups. Krischning and coworkers applied a similar approach, however, the linkage to the polymer is of ionic character [11].

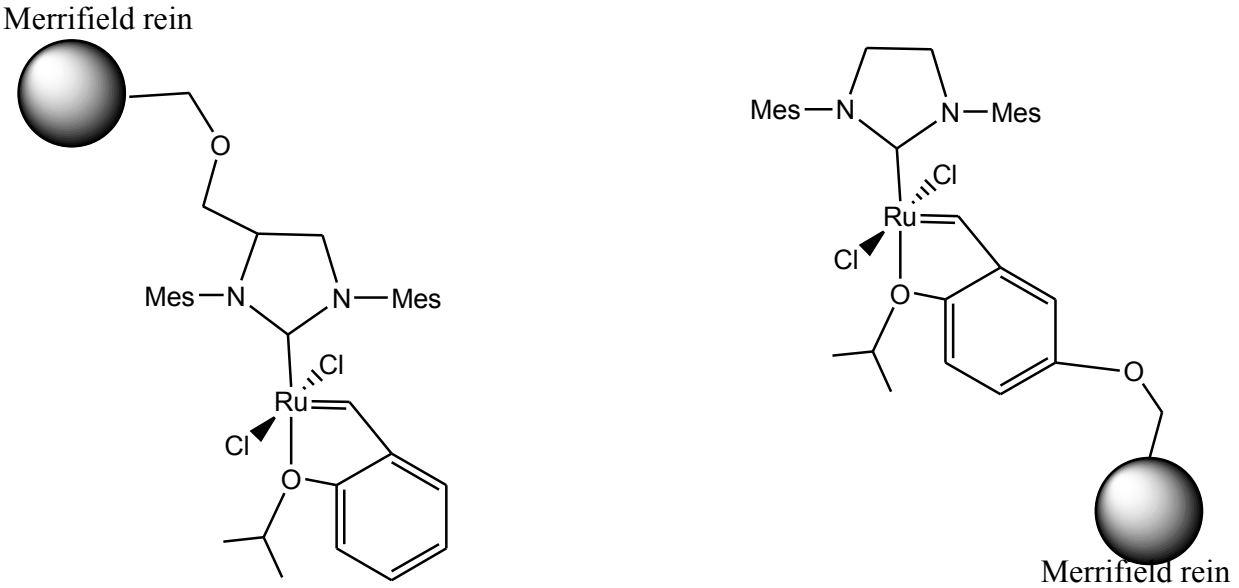

8 **9**

Scheme 3: Merrifield resin immobilized Hoveyda type ruthenium catalysts **8** and **9**.

A ruthenium alkylidene metathesis catalyst has been supported on a vinyl polystyrene polymer by means of metathesis between Grubbs' catalyst **1** and vinyl polystyrene to afford heterogeneous catalyst **10** [12]. Nevertheless, the immobilized catalyst was found to be unstable and degrades over a period of about 5 hours and if then isolated by filtration from the resin, found to be inactive. It has been suggested that the decomposition is due to the ring-closing metathesis between ruthenium alkylidene and free vinyl groups present in the resin releasing the unstable ruthenium methylidene **11** in solution (Scheme 4). This immobilized catalyst has been used to initiate ring-opening metathesis polymerization (ROMP) of norbornene derivatives onto a polymer support to prepare novel high-loading resins for use in combinatorial chemistry.

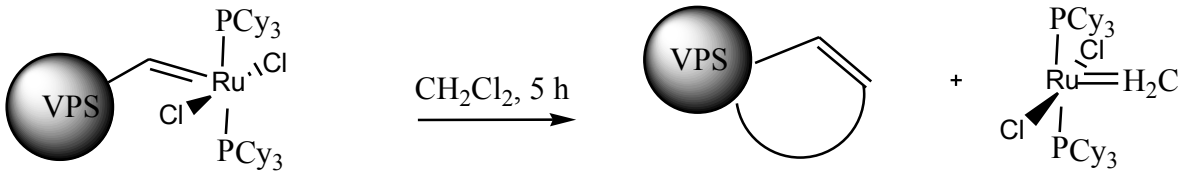

10 **11**

Scheme 4: Decomposition of vinyl polystyrene immobilized Grubbs'catalyst **10**.

Procopiou reported vinyl polystyrene polymer supported ruthenium pro-catalysts **12** and **13** that becomes homogeneous in the course of ring closing metathesis (RCM), with concomitant reaction rate advantages, and then recaptured by the resin after completion of the reaction in solution, a 'boomerang' catalysts (Scheme 5). In the preparation of the 1st generation boomerang catalyst **12** preparation time was found to be critical, longer catalyst-resin preparation times (>2 h) tended to lead to poorly active catalyst for RCM [13]. Compound **12** was found to be an effective catalyst for ring closing metathesis. The reaction rate and activity was found to be comparable to the homogeneous Grubbs' catalyst **1**. In addition, the catalyst could be recycled and re-used up to three times by simple filtration. However, deterioration of the catalyst activity was noticed and could be reduced by addition of volatile hexane. The ruthenium residues in the product mixtures were much lower compared with the reported values using catalyst **1** and comparable to the procedure reported by Grubbs applying phosphine [13]. In contrast to **12**, the second-generation boomerang catalyst **13** still retained activity in RCM after three consecutive runs [15] (Scheme 5).

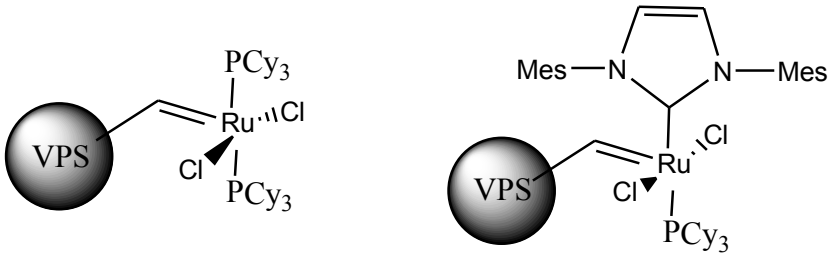

12 **13**

Scheme 5: 1st and 2nd generation boomerang catalysts.

Nolan's group reported additional boomerang catalysts [16], they used macroporous poly-DVB to prepare heterogeneous ruthenium catalysts **14-18** (Scheme 6). Macroporous poly-DVB has advantages over lightly cross-linked Merrifield resins in that the permanent well-developed porous structure in macroporous resins can be easily accessed by solvents and reactants without any need for swelling [17]. In ring-closing metathesis the immobilized catalysts show comparable or better reactivities than their homogeneous counterparts, they perform very well with dienes and moderately well with highly hindered substrates. The macroporous poly-DVB supported catalysts tolerate functional groups very well and in some cases they are recyclable.

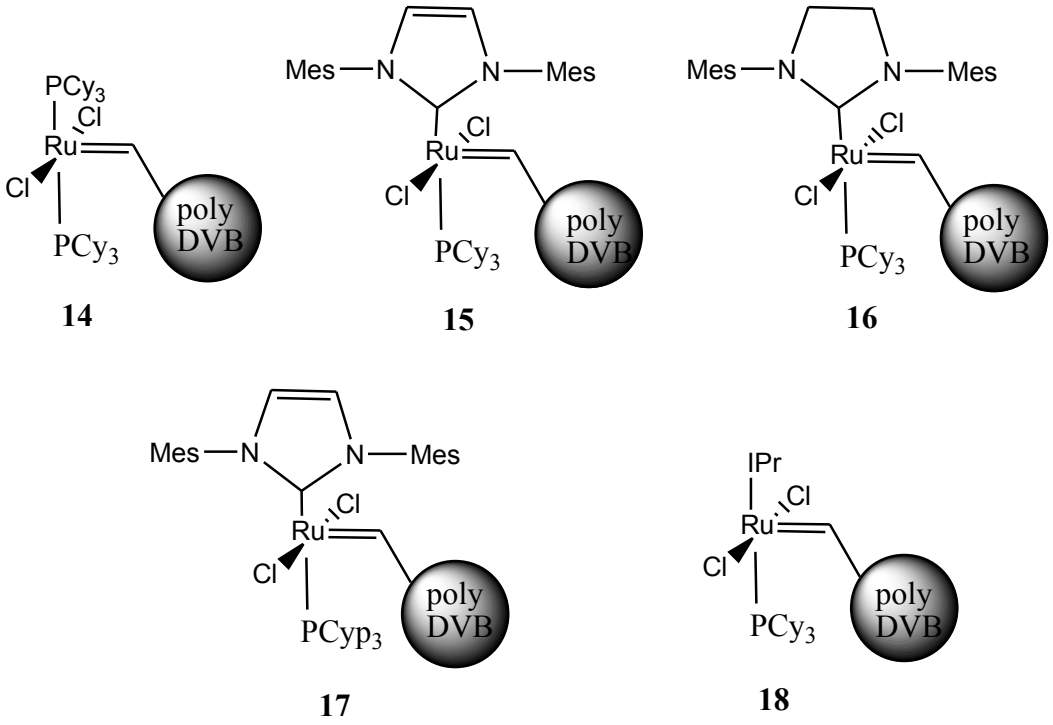

14 **15** **16**

17 **18**

Scheme 6: Macroporous poly-DVB supported boomerang ruthenium catalysts **14-18**.

A number of polymer supported catalysts (**19-22**) that can operate in a range of reagent grade, non-degassed solvents and in an air atmosphere have been reported (Scheme 7). The novel polystyrene supported catalyst **19** is a robust pro-catalyst in RCM of the representative dienes and easy to use [18]. However, the reaction rates were some what lower relative to Grubbs catalyst **1** nonetheless catalyst **19** could be recycled without the use of stabilizing additives.

Butyldiethylsilyl polystyrene (PS-BES) supported ruthenium carbene **20** has been prepared with ruthenium loadings between 0.22-0.33 mmol/g [19] (Scheme 7). The catalyst is robust in ring closing metathesis of representative substrates and easily recyclable. However, the reaction rate obtained from catalyst **20** is lower compared with the rate of the soluble analogue.

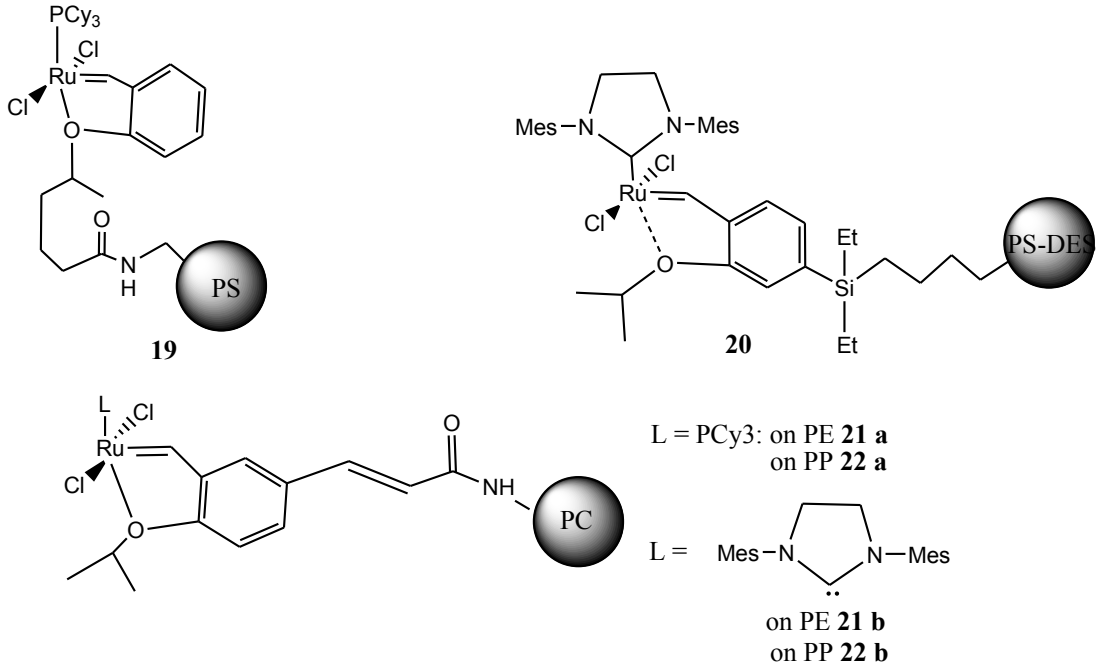

Scheme 7: Moisture stable polymer supported ruthenium catalysts **19-22**.

Furthermore, new heterogeneous Hoveyda type catalysts **21a-b** and **22a-b** attached to the surface of amino-modified sintered polyethylene plates or polypropylene membranes via an amide bond have been reported (Scheme 7). The polymeric chip is highly porous avoiding the swelling of the polymer resulting in the applicability of **21** and **22** in continuous flow-type processes. The catalysts were found to be very efficient for RCM of various substrates in reagent grade solvent and without an inert atmosphere [20].

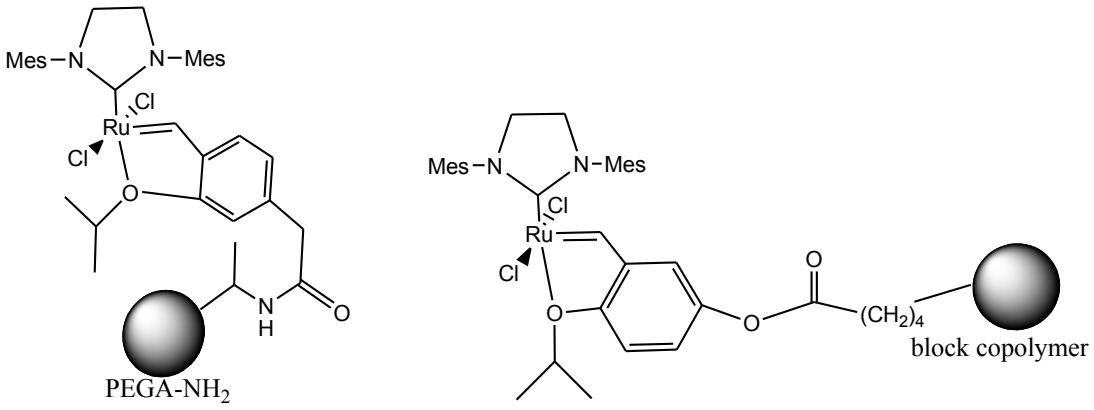

23 **24**

Scheme 8: Hydrophilic polymer supported ruthenium alkylidene metathesis initiators**.**

An innovation in the field of polymer supported metathesis initiators has led to the advent of water-soluble catalysts **23** and **24**. PEGA-NH_2 supported ruthenium alkylidene metathesis initiator **23** (Scheme 8) has been reported which serves as an active catalyst for RCM and CM in methanol and even exhibits some activity in water under air atmosphere and in non-degassed solvents [21]. The hydrophilic, PEGA-NH_2 (Figure 1) support swells four times more per unit mass in water than the polystyrene/polyethylene glycol-based TentaGel resin due the presence of amino functionalized dimethyl acrylamide and mono-2-acrylamidopropyl polyethyleneglycol, and proved to be perfectly stable under metathesis conditions.

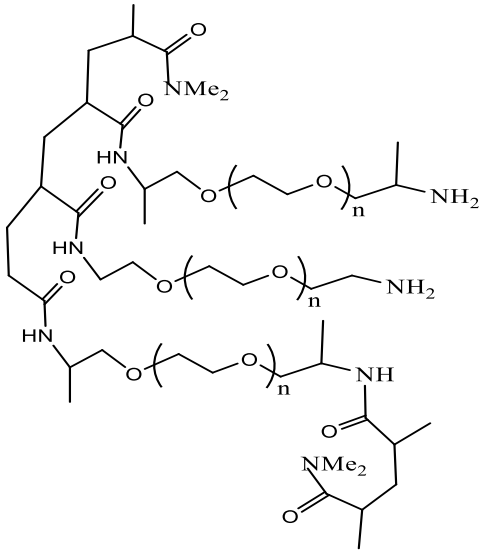

Figure 1: PEGA-NH_2 resin.

A new amphiphilic, polymer-bound variant of the Hoveyda-Grubbs catalyst was synthesized (**24**) via the coupling reaction of a carboxylic acid-functionalized poly(2-oxazoline) block copolymer with 2-isopropoxy-5-hydroxystyrene and subsequent reaction of the resulting macro-ligand (Figure 2) with Grubbs' catalyst **2** [22]. A turnover number (TON) of up to 390 was achieved for the ring-closing metathesis of diethyl diallylmalonate in water resultingin the first high value for an aqueous RCM reaction. For the first time, recycling of a ruthenium initiator in an aqueous RCM reaction has been successful to some extent. In addition, the micellar conditions accelerate the conversion of the hydrophobic diene and at the same time stabilize the active alkylidene species, although competing decomposition of the catalyst in water still impairs the catalyst performance. The residual ruthenium content was determined to be below 1 ppm in the product suggesting a very low leaching of the polymeric catalyst system.

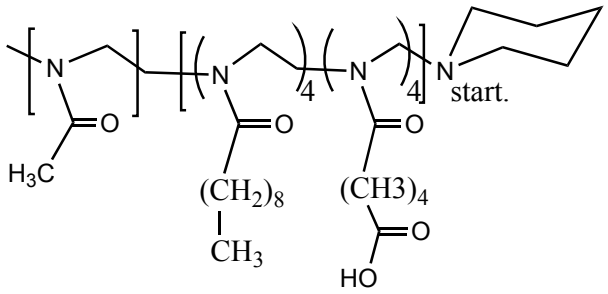

Figure 2: Carboxylic acid-functionalized block copolymer.

A series of ruthenium carbene complexes were permanently immobilized on polymer supports using carboxylate ligands as linking groups. For this objective one or both chloride ligands from parent ruthenium complexes were replaced with an immobilized carboxylic acid. For instance, polystyrene (PS) resin supported catalyst **25** was afforded as a new heterogeneous catalyst with a ruthenium loading of about 0.035 $mmol.g^{-1}$ by replacing one chloride ligand from complex **1** [23] (Scheme 9). The supported catalyst is highly active in self-metathesis of internal alkenes and performed even better than Grubbs' catalyst **1**. In the RCM of diethyl diallylmalonate, applying catalyst **25**, better results were accomplished compared with for example catalyst **19** reported by Dowden and Savovic [18]. Catalyst **25** was easily separated from the metathesis products and reused without the addition of any stabilizing agents, although some leaching and deterioration of the catalyst was observed.

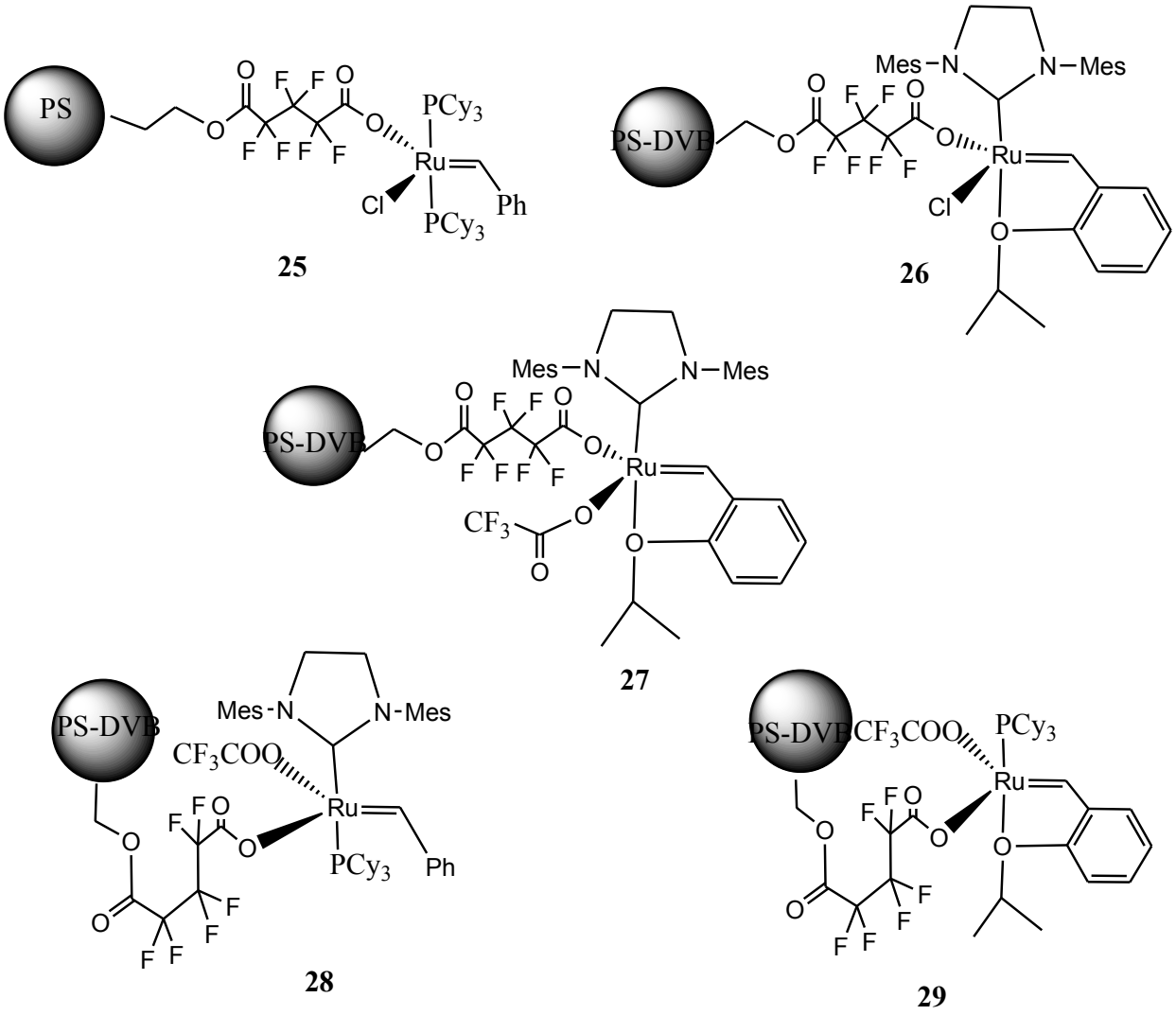

Scheme 9: Heterogeneous catalysts prepared by replacing 1 or 2 chloride ligands from the parent catalyst.

The Grubbs-Hoveyda type metathesis catalysts have also been immobilized on a perfluoroglutanic acid derivatized polystyrene-divinylbenzene (PS-DVB) by chlorine exchange [24]. While the substitution of one chloride ligand of the parent Grubbs-Hoveyda catalyst afforded catalyst **26** the substitution of both chloride ligands by addition of CF_3COOAg to **26** led to catalyst **27**. In RCM of representative substrates both catalysts possesses high activities, catalyst **27** being the superior system with TONs up to 1100 while with catalyst **26** TONs of 380 were achieved. For both systems, **26** and **27,** the leaching of ruthenium into the reaction mixture was unprecedentedly low, resulting in a ruthenium content <70 ppb in the final RCM-derived products.

Furthermore catalysts **28**, **29** were synthesized by reaction of Grubbs catalyst **2** and Grubbs-Hoveyda catalyst **3** respectively, with a perfluoroglutaric acid-derivatized poly(styrene-*co*-divinylbenzene) (PS-DVB) support [25]. Supported catalysts were prepared with high loadings (2.4 and 22.1 mg of catalyst/g PS-DVB for **28** and **29** respectively). Catalysts **28** and **29** represent the first permanently bound versions of both Grubbs' catalyst **2** and the Grubbs-Hoveyda catalyst **3**. Catalyst **28** exhibited a higher activity while catalysts **27** and **29** displayed significantly reduced activities in RCM compared to their homogeneous analogues. Hence, with **28**, turnover numbers (TONs) up to 4200 were realized in stirred-batch (carousel) RCM experiments. Leaching of ruthenium into the reaction mixture was low, resulting in ruthenium contents of 70, 83 and 15 ppb, respectively for catalysts **27**, **28** and **29**.

Polymer supported ruthenium catalyst **30** was prepared via vacuum-driven anionic ligand exchange of a polymer supported perfluorocarboxylic acid with ruthenium-bound perfluorocarboxylates in mesitylene [26] (Scheme 10).The polymer-supported catalyst **30** is active for RCM of DEDAM and can be recycled. However, the activity is considerable reduced compared to its homogenous counterpart.

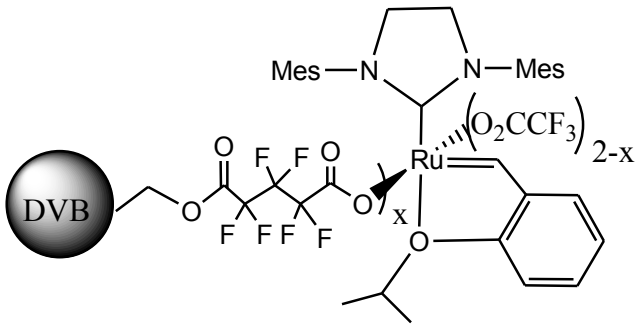

30

Scheme 10: Vacuum-driven immobilized catalysts **30**.

4.3 Monolith Supported Ruthenium Metathesis Initiators

In order to overcome the problems commonly related to heterogeneous systems, such as diffusion controlled reactions and catalyst bleedings among others, Buchmeiser was able to immobilize Grubbs' type ruthenium initiators on non-porous, ring opening metathesis polymerizationderived monolithic materials generated by well-defined transition metal

alkylidenes. This polymerization method allows for the synthesis of monolithic materials with controlled and highly reproducible porosity characteristics. In addition, it allows for the development of monolithic supports with diversity of functional groups [27].

Using Grubbs' catalyst **1** ROMP initiator, they managed to synthesize a number of functionalized monolith supports suitable for catalysts immobilization. For instance, a N-heterocyclic carbene precursor was successfully grafted onto the surface of monolithic materials [28]. The immobilized catalyst **31** (Scheme 11) with a loading of up to 1.4 mg/g was achieved from immobilized NHC following the standard procedure. The catalyst possesses a high activity towards RCM as well as towards ROMP. The *cis/trans* ratio of the polymers is exactly the same as the one obtained in homogeneous polymerizations (90% *trans*).

The prepared monolithic systems may be used either as pressure-stable reactors or (in miniaturized form) as cartridges for applications in combinatorial chemistry. Additionally, the use of NHC ligands even in RCM successfully suppresses any bleeding of the column, consequently allowing the synthesis of virtually ruthenium-free cyclization products with a ruthenium content ≤ 70 ppm.

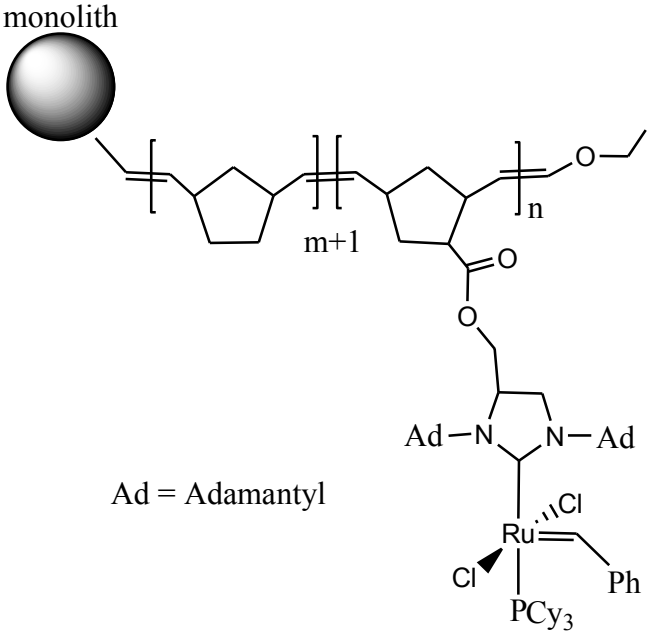

31

Scheme 11: Monolithic supported metathesis catalyst **31**.

Different versions of monolith supported metathesis catalysts were obtained by chloride exchange between Grubbs' catalyst **2** and monolith supported silver carboxylates [29] (Scheme 13). Heterogeneous catalysts **32**, **33** and **34** with loading of 10, 7 and 9 mg/g respectively were realized using this protocol. The catalysts were used in RCM of various substrates allowing turnover numbers (TON's) close to 1000. In a flow-through set-up, an auxiliary effect of pendant silver carboxylates was observed with catalyst **34**, where the silver moiety functions as a (reversible) phosphine scavenger that both accelerates initiation and stabilizes the catalyst by preventing phosphine elution. In all RCM experiments ruthenium leaching was low, resulting in a ruthenium content of the RCM products ≤ 3.5 mg/g (3.5 ppm).

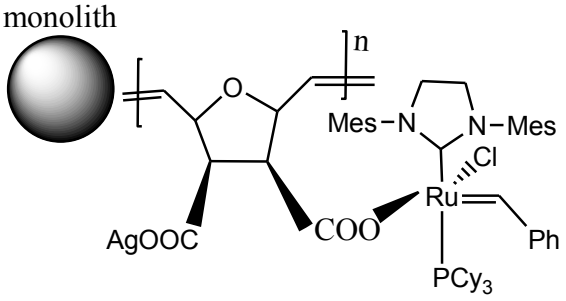

Cross-linker DMN-H_6: **32**

Cross-linker $(NBE\text{-}CH2\text{-}O)_3SiMe$: **33**

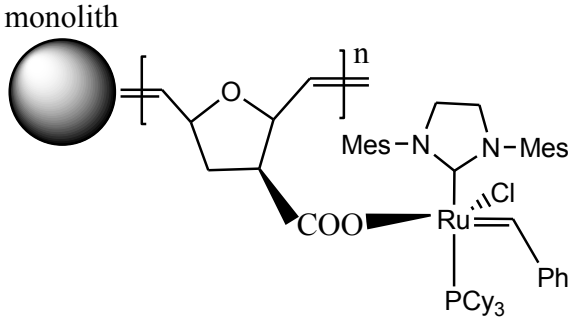

34

Scheme 12: Monolith-supported catalysts obtained via chloride exchange.

The Grubbs-Hoveyda catalyst **4** has been immobilized on a monolithic support by exchanging chloride ligands between the ruthenium initiator and a monolith supported fluorinated carboxylate [30]. For this purpose norborn-2-ene-based perfluorinated acid was grafted onto the surface of the monolith before being deprotonated and converted into the corresponding silver salt. Reaction of the thus modified support with complex **4** resulted in the formation of a mono-carboxylate substituted complex. Finally, the remaining chloride ligands were reacted with CF_3COOAg to yield the corresponding bis-carboxylate substituted catalyst **35** (Scheme 13). In this manner a ruthenium loading of the monolith-supported catalyst **35** of 0.41 mg/g was obtained.

This monolith supported Grubbs-Hoveyda catalyst **35** was successfully used in continuous flow experiments. For instance, in the RCM of diethyl diallylmalonate, turnover numbers of up to 500 were achieved. It is worth mentioning that the turnover numbers obtained with this supported version are very similar to the ones obtained with the homogeneous analogues. Most importantly, only pure product as well as unreacted adduct could be found in the eluent, which directly translates into an increased long-term stability of the catalysts. Extremely low leaching (<0.2%) was observed resulting in product contamination with ruthenium and silver of 1.8 and 0.01 ppm, respectively.

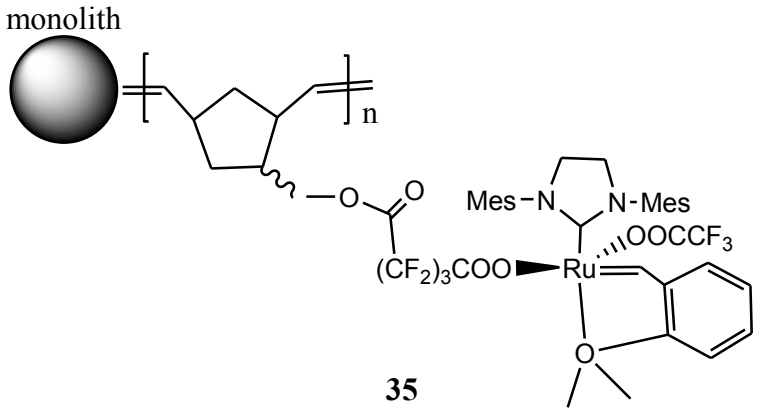

35

Scheme 13: Monolith supported Grubbs-Hoveyda type catalyst.

Buchmeiser and co-workers extended the study by focusing on disc-shaped monoliths to immobilize ruthenium initiators in contrast to previously reported one. The disc-shaped monoliths were developed by cutting the parent monolith into pieces of 1 cm in height and subsequently used in the preparation of catalysts **36** and **37** (Scheme 14). The supported catalyst **36** was prepared with loadings of about 2.5 wt% [31]. Excellent reactivities were observed in RCM and ROCM of various substrates. The monolithic disk immobilized catalyst **36** showed some what reduced activity, yet compared to the homogenous analogue, still can be regarded as good. In terms of product purity, it is noteworthy that ruthenium leaching from the supported systems **36** was very low, resulting in ruthenium contaminations of less than 0.14 ppm.

With the disc shaped monolith supported catalyst **37** [32] on the other hand, TONs in the range of 60-330 were obtained in the ring-closing metathesis of representative substrates which are comparable to those obtained with the homogeneous analogue.These relatively low activities

clearly stems from the fact that reactions within the disks were not stirred and, therefore, depended on diffusion of the substrates to the catalytic site. Nevertheless, the reactivity observed with these systems definitely justifies the use of such monolith-supported catalysts in high-through put screening, where the disk serves simultaneously as support, reaction vessel, and filtration unit and can, in principle, be directly used in combination with commercially available machines.

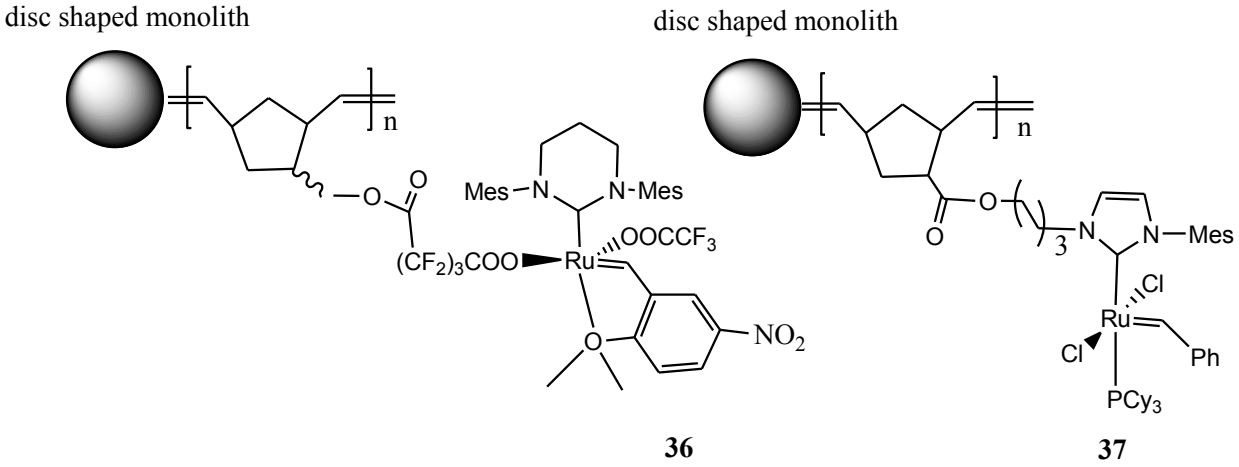

36 **37**

Scheme 14: Disc-shaped monolith-supported catalysts **36** and **37**.

Hoveyda and co-workers [33] disclosed the one-pot synthesis of ruthenium complexes **38**-**40** supported on commercially available monolithic samples of porous sol-gel glass (Scheme 15). The supported catalysts can effectively promote various olefin metathesis reactions and can be easily employed in a library synthesis format without multiple weighing, in air and with undistilled commercial reagent-grade solvents. Catalyst recovery is simply carried out with a pair of tweezers; it does not require filtration and generates minimal solvent waste. The catalyst retains its activity after multiple cycles (>15), affording products that are of high purity without recourse to any purification steps.

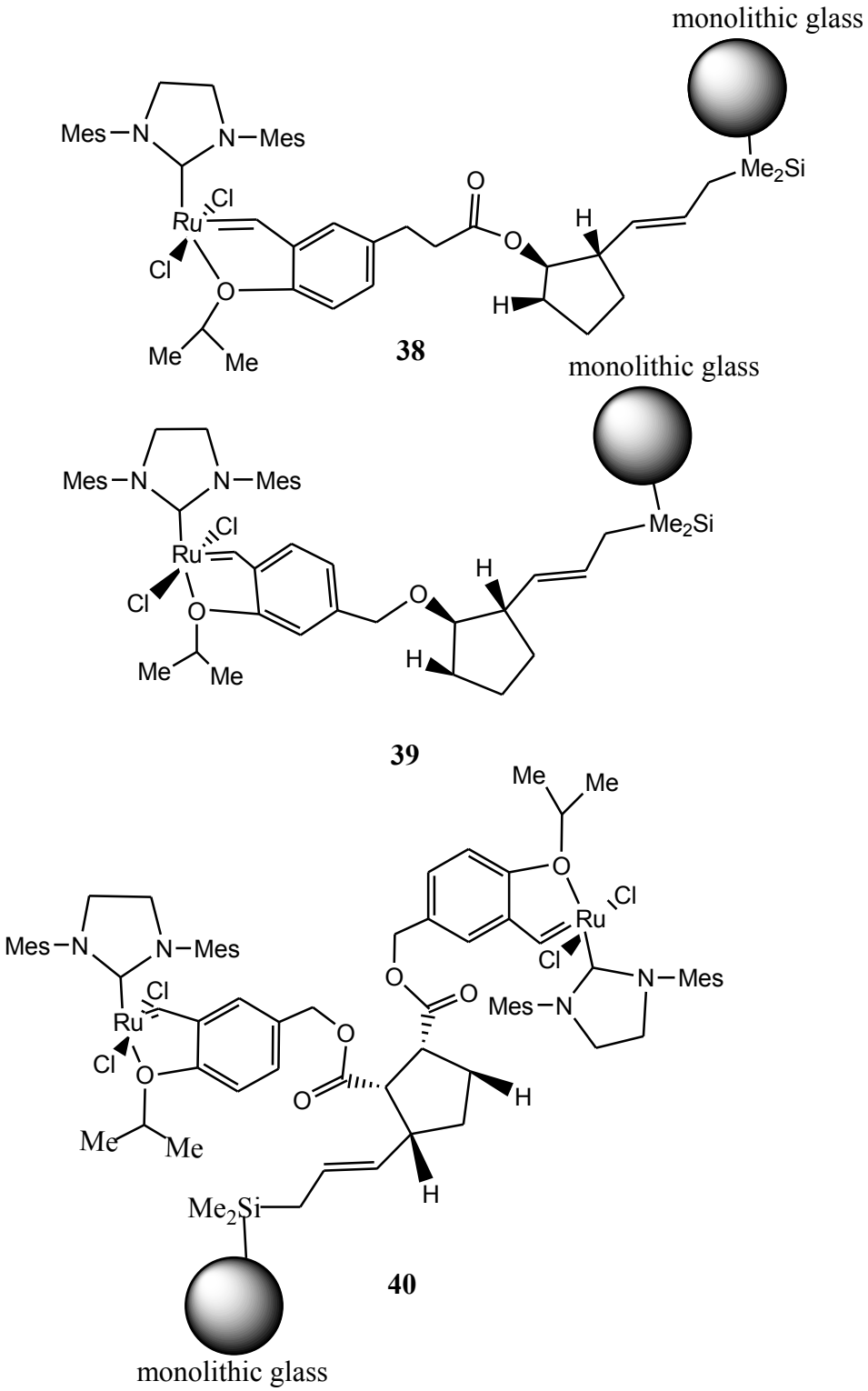

Scheme 15: Monolithic porous sol-gel glass supported ruthenium complexes **38**-**40**.

4.4 Non-porous Silica Supported Ruthenium Metathesis Initiators

Inorganic silica material is a common support for the heterogenization of molecular catalysts. It offers a considerable advantage over other supporting materials due to its excellent thermal and chemical stability, low cost, and broad solvent compatibility. It has a rigid structure, does not swell in solvents, and can be used at both high and low temperatures and pressure.

Silica-gel immobilized Hoveyda–Grubbs type catalysts **41a** and **41b** synthesized by alkylidene exchange between commercially available Grubbs' catalysts **(1** and **2)** and silica gel immobilized isopropoxystyrene has been reported by Blechert *et al.* [34] (Scheme 16). The supported catalysts showed good stability on storing at 4 °C under nitrogen over two weeks without any sign of decomposition. However, when quantitative loading of the styrene with ruthenium was achieved the catalysts decomposed within days at -20 °C. The catalysts demonstrate higher activity in a number of metathesis test reactions than the parent Grubbs' catalysts and they can be easily separated by simple filtration of the non-swelling material.

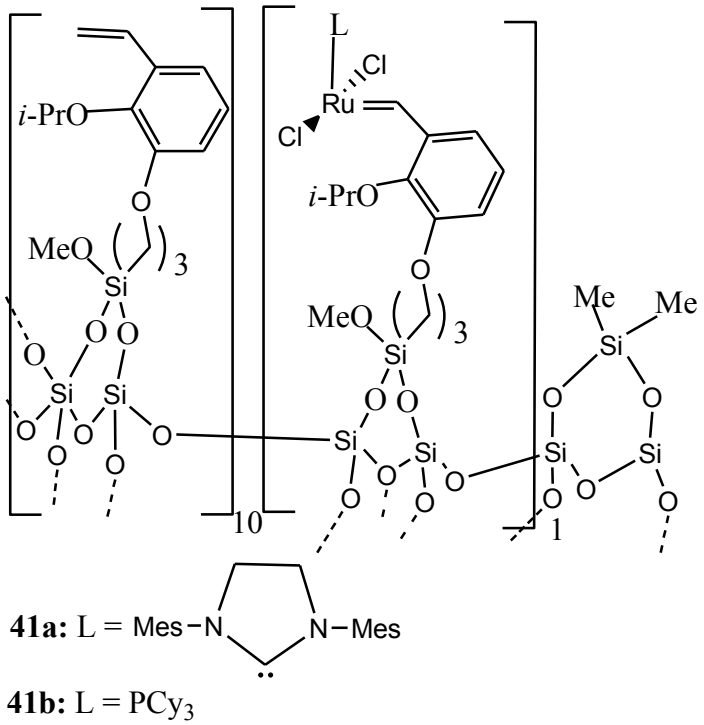

Scheme 16: Immobilized Hoveyda-Grubbs' type catalysts on silica gel.

The hybrid organic-inorganic silicas obtained as bridged silsesquioxanes from a bis-silylated Hoveyda-type monomer via the sol-gel process have been prepared for the first time by Moreau [35]. Important to note is that the sol-gel process allows the control of not only the loading of organic groups but also their distribution in the matrix in contrast with grafting approach. Three different types of hybrid materials were prepared from bis-silylated compound **42** (Scheme 17).

Co-gelification with tetraethoxysilane (TEOS) afforded **43a**, whereas hydrolytic polycondensation of monomer **42** without TEOS in the same nucleophilic conditions gave **43b**. Another sol-gel condition was tested with neat monomer **42** in order to get an organized and porous material, using dodecylamine both as basic catalyst and surfactant, and gave rise to material **43c**. Capping of the residual silanol groups was performed before charging with the metal in order to test if improved materials could be obtained, as the silylated hybrid is less hygroscopic than its parent one and gave rise to **43aSi**. All materials (**43a-c** and **43aSi**) were charged with the metal by treating them with the Grubbs' catalyst **2**. The catalysts proved their efficiency as recyclable catalysts in the ring-closing metathesis of dienes and enynes. The materials prepared from the sol-gel are superior to the same catalysts deriving from anchorage to meso-structured silica. Furthermore, end capping of residual silanol groups before charging with the metal does not improve the materials.

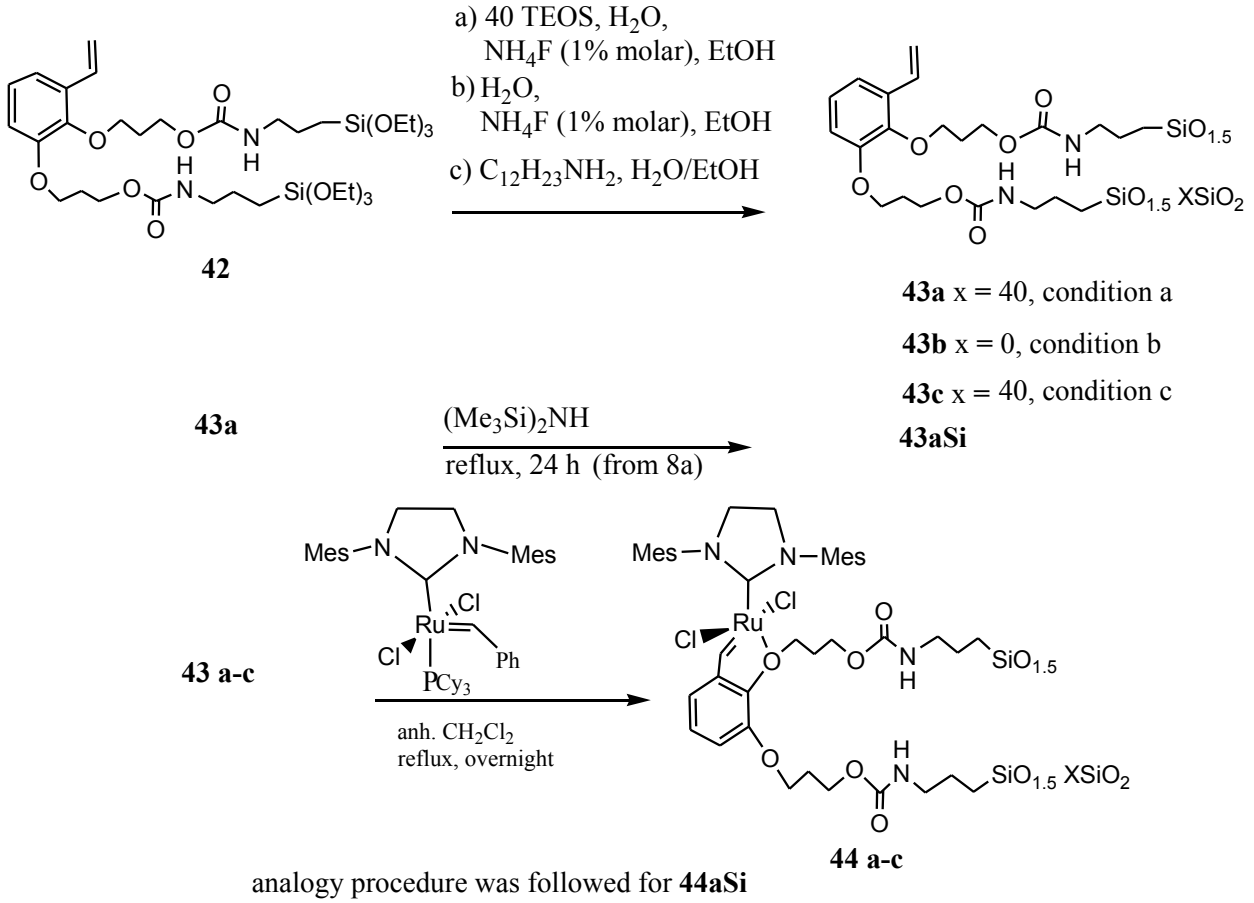

Scheme 17: Preparation of ruthenium heterogeneous catalysts **44a-c** and **44aSi**.

The second-generation Grubbs catalyst type has been successful immobilized on both porous and non-porous silica via the NHC ligand [36]. For this purpose the porous and nonporous silica were functionalized with a NHC-precursor and subsequently converted to heterogeneous **45** and **46** applying the standard procedure (Scheme 18). Ruthenium loadings of 5.3 and 1.3 mol.g^{-1} were realized. Additionally, coating techniques were applied, where C_{18}-derivatized silica-60 was used to attain a heterogeneous catalyst witha 4.1 mol.g^{-1} ruthenium loading.

In RCM of DEDAM, the catalysts immobilized onto non-porous silica reached the maximum turnover number (TON) of 75. Interestingly, basically identical results (TON = 80) were obtained with catalysts immobilized onto porous silica. Nevertheless, the low TON's (5) obtained with other less reactive compounds such as 1,7-octadiene, *N,N*-diallyltrifluoroacetamide, diallyl ether, and diallyldiphenylsilane suggest that the stirred batch

setup with this type of support is highly diffusion controlled, where reaction is too slow and decomposition of the intermediary ruthenium methylidene dominates.

Catalytic results obtained with coated supports exceed the data for TON of all other silica supports by far. This can be interpreted in a way that a support containing only macropores facilitates diffusion. It is worth mentioning that in all cases a quantitative retention of the original amount of ruthenium at the support was revealed thus offering access to metal-free products.

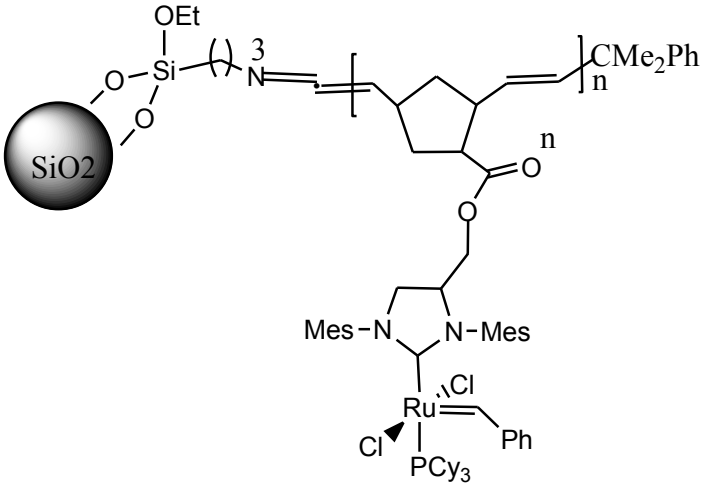

45 = on nonporous silica
46 = on porous silica

Scheme 18: Silica gel supported catalysts **45** and **46**.

A ruthenium-carbene complex **47** bearing a hydroxylalkyl group on the N-substituent of its NHC ligand reported by the Fürstner group [36] has been covalently immobilized on chloro-functionalized silica (Scheme 19). Although a longer reaction time is necessary to reach complete conversion, the immobilized catalysts **48a,b** posses a RCM performance comparable to its homogeneous analogues. These catalysts **48a,b** offer the advantage to be reusable up to three times. However, in case the immobilization of the hydroxyalkyl-functionalized ruthenium carbene complex is done by physisorption rather than chemisorption, rearrangement of **47** to isomer **49** was observed bearing the neutral ligands in a *cis* rather than the usual *trans* position (Scheme 20), which is a characteristic of the highly conserved structural feature of the Grubbs type ruthenium carbene complexes.

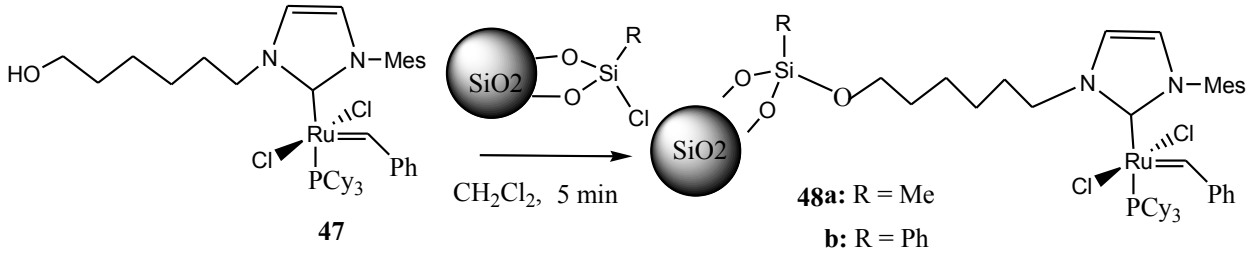

47

Scheme 19: Immobilization of complex **47** by chemisorption**.**

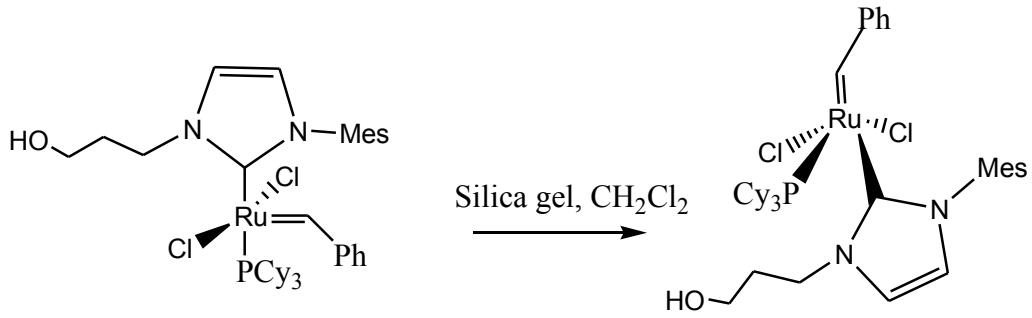

47 **49**

Scheme 20: Immobilization of complex **47** by physisorption.

The silica-supported catalysts **50** and **51** have been successfully prepared via triethoxysilyl-functionalized NHC ligands [37] (Scheme 21). These species were shown to be competent catalysts for a variety of olefin metathesis reactions, mimicking their homogeneous counterparts. Likewise, the activity of the supported catalysts is truly heterogeneous in nature as revealed by split test, moreover, they can be recycled multiple times. More significant is that the catalysts do not leach ruthenium under the standard reaction conditions as ruthenium concentration of the filtrate of less than 5 ppb in all cases are obtained.

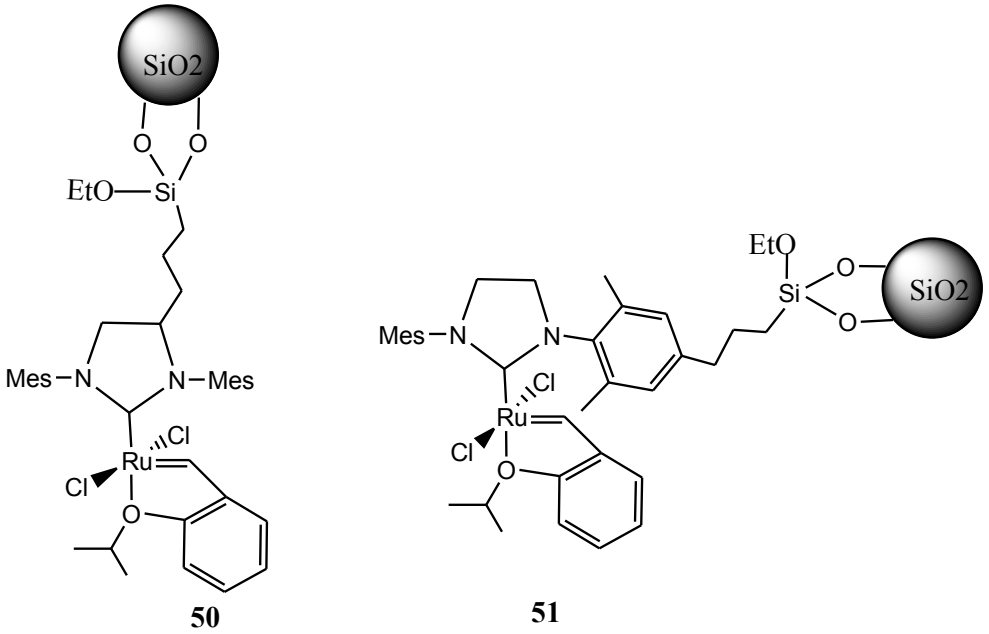

50 **51**

Scheme 21: Silica-supported catalysts **50** and **51**.

Buchmeiser *et al*. [38] reported catalysts **52** and **54** developed by exchange of chloride from Grubbs' catalyst **2** with immobilized silver carboxylates (Scheme 22). Interesting to mention is that only one chloride ligand was exchanged. Catalyst loadings of 42 and 63 mg/g respectively were achieved. These heterogeneous catalysts are competent catalysts in ring-closing metathesis of various substrates allowing turnover numbers (TONs) close to 1000. In all RCM experiments ruthenium leaching was low, resulting in a ruthenium content in the RCM products ≤ 3.5 g/g (3.5 ppm).

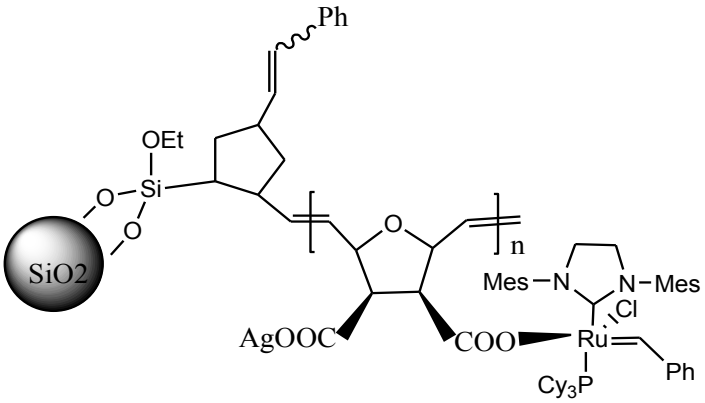

Nucleosil 300-7: **52**
LiChrospher 300-5: **53**

Scheme 22: Preparation of heterogeneous catalysts **52** and **53**.

One or both chlorides in the Hoveyda-Grubbstype catalysts have also been selectively substituted in the preparation of heterogeneous catalysts containing mixed anionic ligands as well as disubstituted catalysts. After heterogenization of the catalysts, the remaining free SiOH groups on the silica surface were subsequently capped with dimethoxydimethylsilane. Loadings between 31 and 65 μmol/g were achieved for catalysts **54-59** [39] (Scheme 23). These heterogeneous catalysts showed good stability when stored at +4 °C under argon for 4 weeks without any sign of decomposition.The silica gel bound catalysts containing mixed anionic ligands **54** and **55** were more active in RCM reaction with *N,N*-diallyl-4-methylbenzene sulfonamide than their disubstituted counterparts **56** and **57**, however, there was not such a marked difference. The supported catalysts **54-59** displayed considerable lower TONs than their homogeneous counterparts. Nonetheless, compared to similar polymer-bound systems reported by Buchmeiser *et al.* the prepared silica bound catalysts performed better.

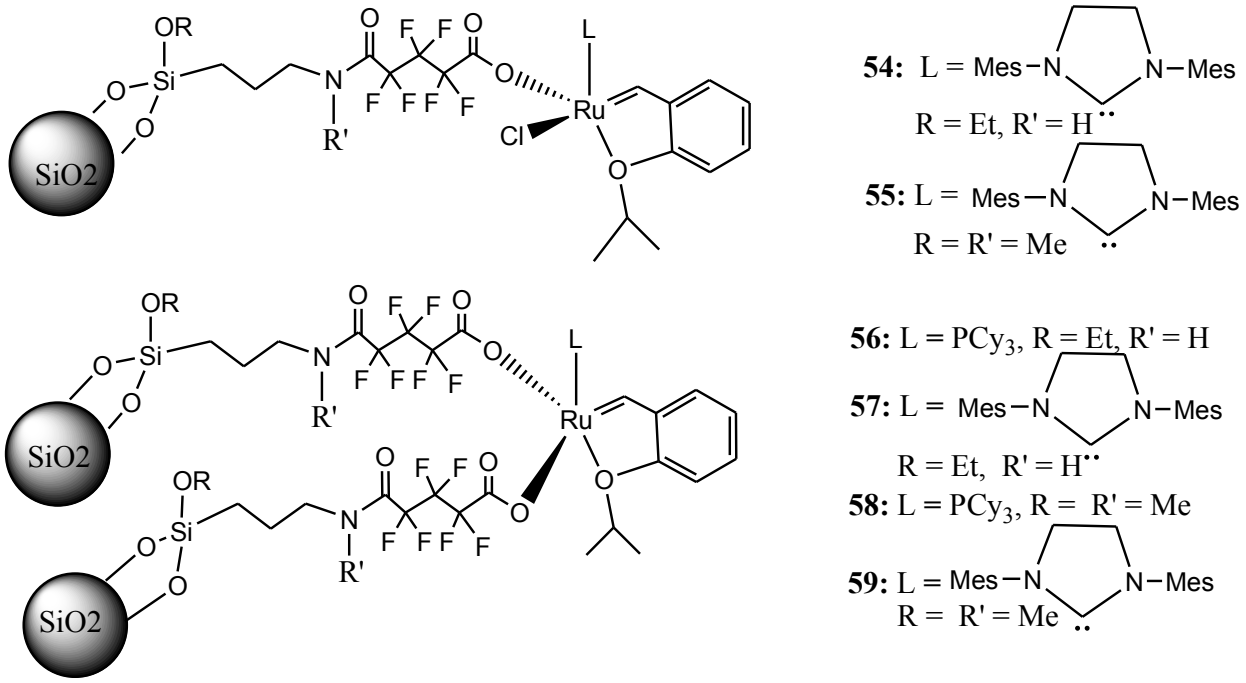

Scheme 23: Mixed anionic ligands catalysts **54**, **55** and disubstituted catalysts **56-59.**

On the other hand, heterogeneous metathesis catalyst **60** was prepared with a ruthenium loading of about 0.78 wt% [40] (Scheme 24). The catalyst demonstrated its activity and high selectivity in ring closing metathesis of 1,7-octadiene and diethyl diallylmalonate, as well as in the ring opening metathesis polymerization of norbornene and cyclooctene, both carried out in a batch

stirred reactor. Almost negligible leaching of ruthenium was observed and successful catalyst reusing was achieved. However, the reaction rate was lower in comparison with its SBA-15 supported analogue.

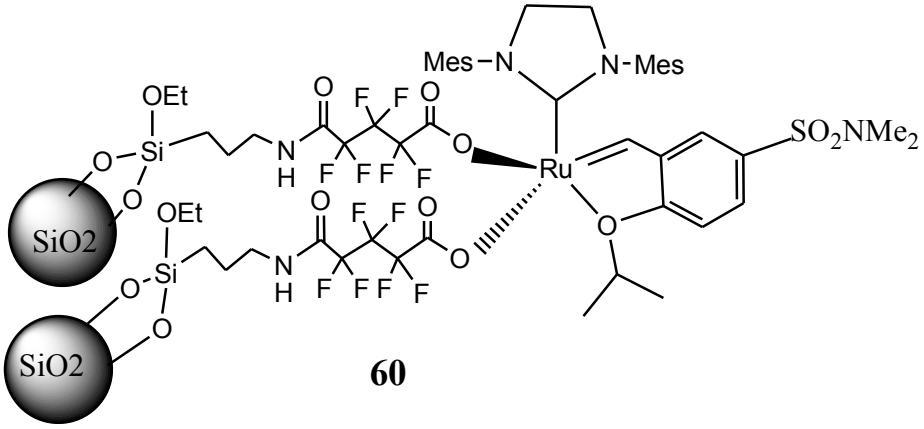

60

Scheme 24: Immobilized ruthenium complex **60**.

Synthesis of a new metathesis initiator **61** by coupling ruthenium-complexes to low generation carbosilane dendrimers, 0th generation (G0–Ru) and first generation (G1–Ru) has been reported by Verpoort *et al.* [41] (Scheme 25). The attachment of the ruthenium complexes to the boundary of the dendrimer is performed by olefin metathesis. With a dendrimeric support the regular occupation of the surface and the good accessibility of all the active catalytic sites for the reactants favor a high activity and selectivity. Besides, product separation is possible via ultra filtration. This dendrimer supported initiator shows a very high activity for the ROMP of norbornene. By using this dendrimeric initiator multi-arm starpolymers can be developed in a controlled manner.

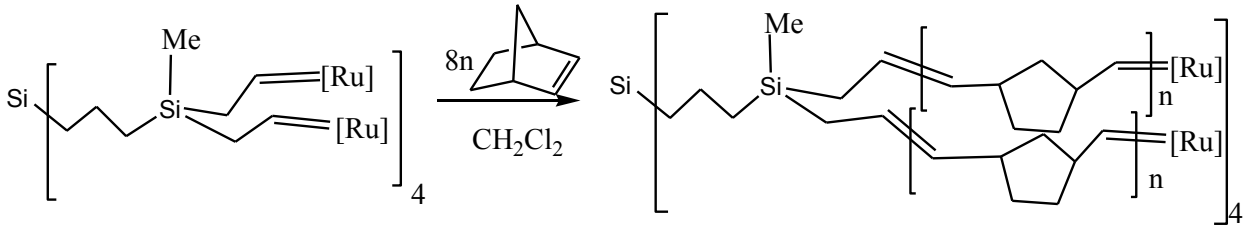

61 *Starpolymer*

Scheme 25: G1-dendrimer ruthenium initiator **61** and its starpolymer.

The Hoveyda-Grubbs catalyst **4** was successfully immobilized on commercial silica in pellet and powder form following a practical and fast synthesis procedure [42]. A solution of 2nd generation

Hoveyda-Grubbs catalyst was brought in contact with a suspension of silica and stirred at 293 K for two hours. A bright greenish powder was acquired with a ruthenium loading of about 0.1 wt%. The activity of the solid system is truly efficient in various metathesis reactions and stable for at least 4000 TONs. Ruthenium contamination of the products was very low (ppb level). The catalyst can be recycled up to four cycles with full conversion in each cycle. The successful use of the robust system has even been demonstrated in a continuous reactor set-up

4.5 Mesoporous Molecular Sieves Supported Ruthenium Metathesis Initiators

In 1992, the preparation of MCM-41 denotes a ground breaking development in hybrid catalysis [43].The creation of a uniform mesoporous skeleton delivers a new mean of immobilization. The large pore size allows large organic and organometallic molecules to pass through the channels and provides optimal contact with the surface. In addition, the regular pore size of MCM-41 can provide shape selectivity not provided by classical inorganic supports. This feature has led to a continuous increase in a number of reports about immobilization of ruthenium metathesis initiators on mesoporous materials.

For instance, heterogeneous catalysts **62** and **63** have been prepared by phosphine exchange between Grubbs' type ruthenium-alkylidene complexes and a phosphinated mesoporous matrix (P-MCM-41) [44] (Scheme 26). The exchange of a phosphine ligand of the homogeneous complex by a P-functionalized spacer molecule was favored due to the increased pKa or donor capacity of the immobilized phosphine ligand. Both catalysts **62** and **63** reveal activity in ROMP of norbornene, however, due to diffusion limitations an enhancement in polydispersity was exhibited for the ROMP of norbornene catalyzed by **62**. Noteworthy is that catalyst **63** even exposes metathesis activity in aquatic environment. The RCM activity of catalysts **62** and **63** is in agreement with that of their homogeneous analogues.

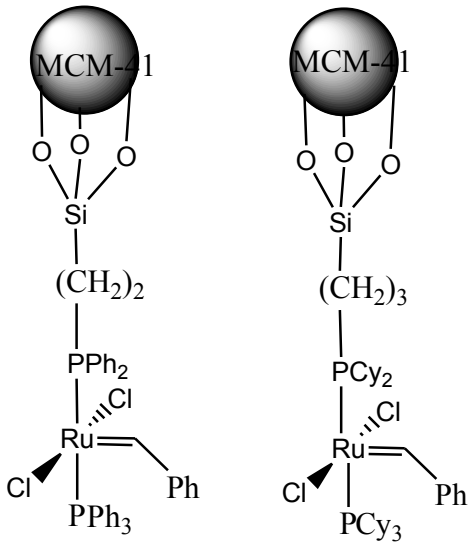

62 **63**

Scheme 26: MCM-41 supported Grubbs' type metathesis catalysts.

Ligand exchange between phosphinated mesoporous silica (SBA-15) and either complex **2** or complex **64** has resulted into catalysts **65** with ruthenium attached to the surface via a PCy_2-linker. On the other hand, catalyst **66** with ruthenium attached via a pyridine ligand has been prepared by ligand exchange between pyridinated mesoporous silica and either complex **2** or complex **64** [45]. Both complexes **2** and **64** generated catalysts with the same structure, however, the usage of complex **64** is preferable since catalysts with high loadings are more easily achieved (Scheme 27).

Hybrid catalysts with ruthenium attached to the surface via PCy_2-linkers exhibited a higher activity and stability in metathesis than those having ruthenium attached via pyridine linkers. The former catalysts displayed a high activity in a series of metathesis reactions (RCM, ROMP and CM), reaching turnover numbers from 200 to 2000 at nearly 100% selectivity and being reusable for several times. Catalysts with pyridine linkers tended to decompose rapidly at incomplete conversions. The filtration tests for all catalysts suggested that the immobilized catalysts were responsible for the catalytic activity during the reactions. Ruthenium leaching in the final reaction mixture was very low for catalysts coordinated to PCy_2-linkers and even negligible for catalyst with pyridine-linkers.

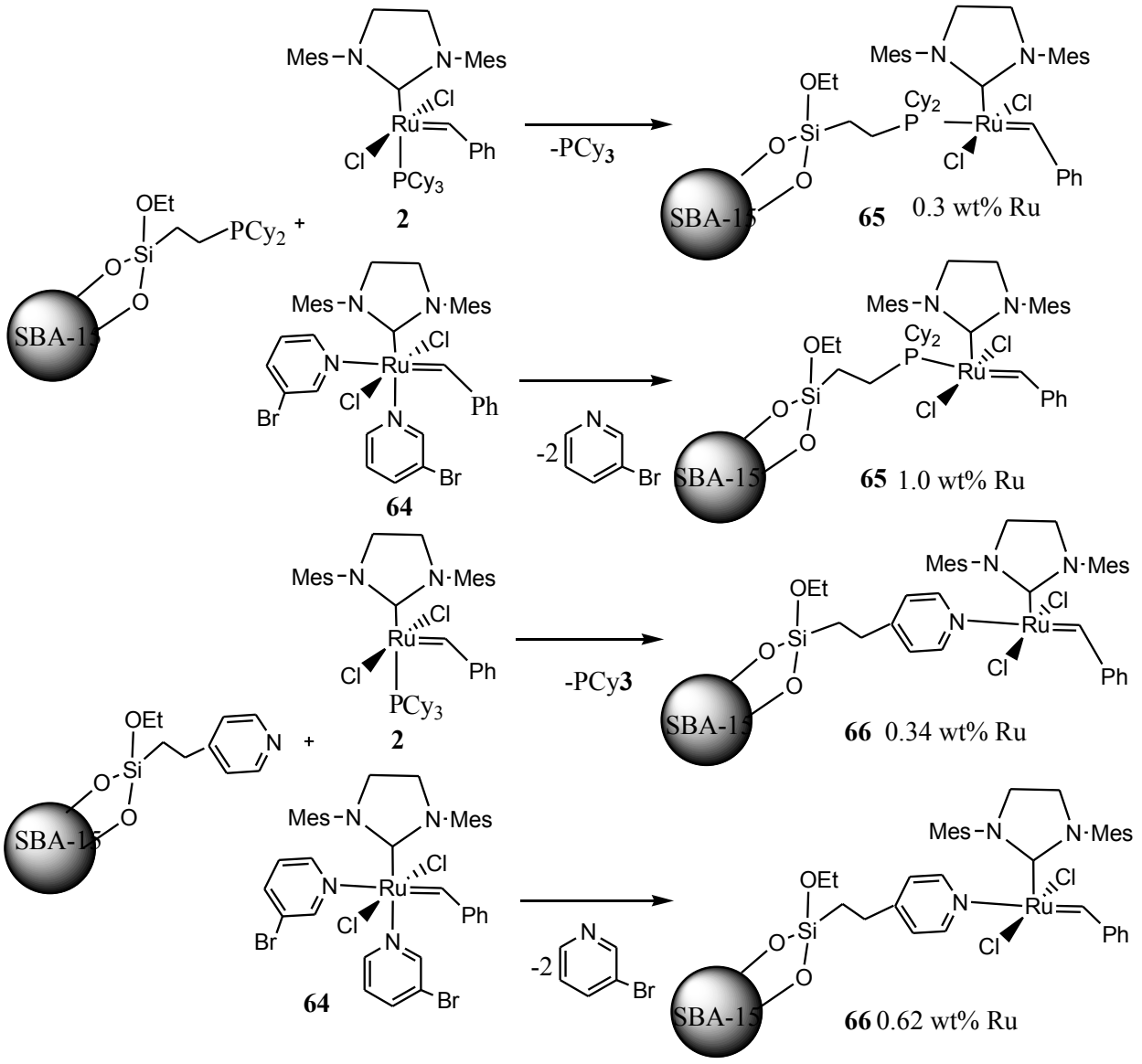

Scheme 27: Synthesis of SBA-15 supported catalysts **65** and **66**.

Shi and coworkers reported catalyst **67,** where the ruthenium catalyst is covalently anchored inside the pore channels of SBA-15 via an NHC-ligand [46] (Scheme 28). The outer surface of SBA-15 was masked with Si-CH_3 groups before being functionalized with the ruthenium complex guaranteeing that the immobilization took place inside the pore and not outside. This approach was made in order to avoid the decomposition of the catalyst. The heterogeneous catalyst **67** displays activities in RCM of DEDAM comparable with its homogeneous analogue proving that the reaction, most probably, is not diffusion-controlled due to the three-dimensional

channels and high porosity of SBA-15. The immobilized catalyst can be repeatedly used without any apparent decrease in catalytic activity along with the cycle times.

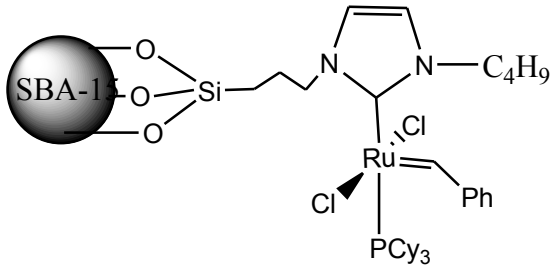

67

Scheme 28: SBA-15 immobilized ruthenium complex **67**.

MCM-41 supported Grubbs-Hoveyda type ruthenium complexes **68** and **69** have been reported by Moreau. These heterogeneous catalysts were realized by anchoring a *bis*-silylated monomer on meso-structured silica MCM-41 followed by the metalation applying standard procedures [47] (Scheme 29). End capping of the residual silanol groups was performed before charging with the metal in order to test if improved materials could be obtained. A ruthenium content of 0.113 mmol Ru/g for catalyst **68** and 0.0494 mmol Ru/g for catalyst **69** was achieved.

These catalysts were evaluated as recyclable catalysts in the RCM reactions of dienes and enynes. For the RCM of *N,N*-diallyl-4-methylbenzene sulfonamide complex **68** offers milder conditions and better results than previous works based on catalysts anchored to insoluble solid supports. RCM of a more challenging substrate, *N,N*-bis(2-methylallyl)-4-methylbenzene-sulfonamide, gave rise to the tetrasubstituted alkene. Moreover, the catalytic material is easy recyclable for the ring-closing enyne metathesis performed on 1-allyloxy-1,1-diphenyl-2-propyne. This is for the first time in the literature that a catalyst is described, which can be recycled in the ring-closing enyne metathesis reaction. However, silylation of residual silanol groups before charging with the metal does not improve the materials. Although the reaction time in the first cycle is lowered, the efficiency upon recycling decreases very rapidly.

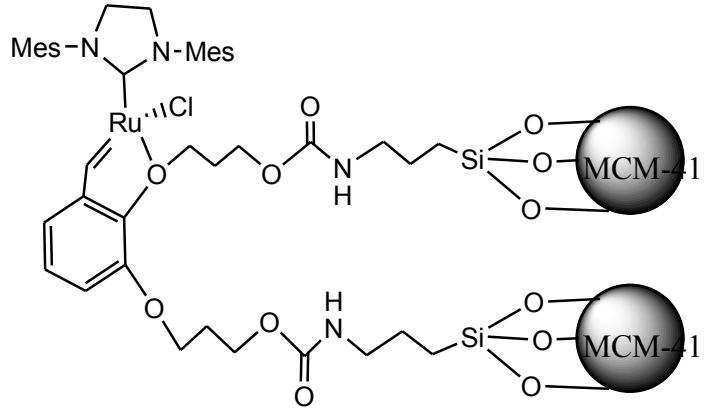

68

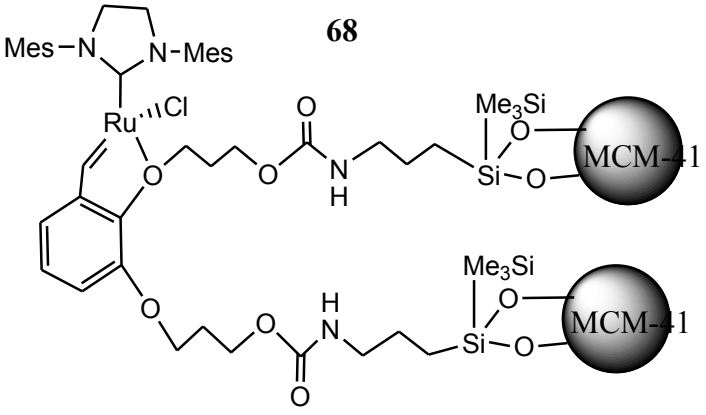

69

Scheme 29: MCM-41 supported catalysts **68** and **69**.

Mesocellular foam (MCF) supported Hoveyda-Grubbs catalysts have been successfully developed by Yinga *et al.* [48]. The ultra large pores and high surface area of MCF allowed the ligands and catalytic complexes to be immobilized without steric hindrance, and facilitated the diffusion of bulky substrates during reaction. The resulting novel heterogeneous catalysts **70a** and **70b** demonstrated excellent activity and reusability for the RCM of various types of substrates (Scheme 30). Although the gradual loss of activity was unavoidable in multiple recycling runs, introducing additional MCF-supported free ligand significantly enhanced the reusability of the heterogeneous catalyst.

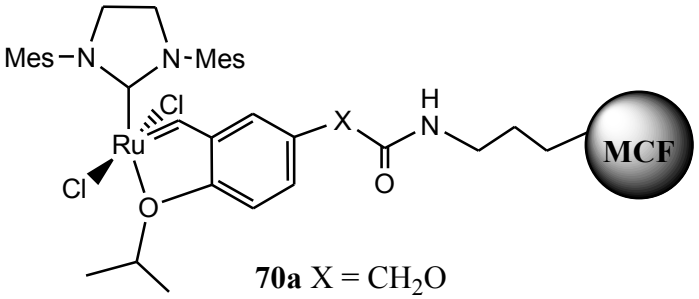

70a X = CH_2O

70b X = O

Scheme 30: MCF immobilized catalyst **70**.

A siliceous mesocellular foam (MCF) immobilized ruthenium metathesis catalyst **71** was efficiently achieved by using click chemistry for linkage with the support [49] (Scheme 31). Aruthenium loading of 0.16 mmol/g was obtained for catalyst **71**, while the ligand density of immobilized ligand was 0.19 mmol/g implying that more than 80% of the immobilized ligand was loaded with ruthenium. The supported catalyst **71** is applicable to a designed reactor system that made use of immobilized catalysts in a continuous process by just circulating the reaction mixture to facilitate the removal of *in situ* generated by-products [50].The catalyst exhibited good activity and recyclability in RCM of various substrates. In most cases, good catalytic activities were maintained for 5 to 10 runs at 50 °C in DCM.

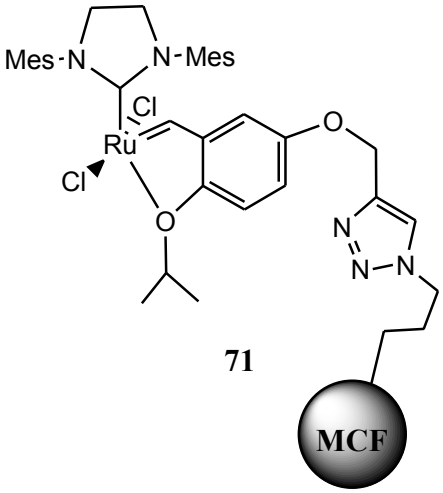

71

Scheme 30: MCF immobilized catalyst **71**.

Heterogeneous metathesis catalysts **72a** and **72b** were prepared by immobilization of commercially available Hoveyda-Grubbs type catalyst on siliceous mesoporous molecular sieves SBA-15 via exchange of chloro-ligands by silver(I) carboxylate [40] (Scheme 32). The catalysts

proved their activity and high selectivity in ring closing metathesis of 1,7-octadiene and DEDAM, as well as in the ring opening metathesis polymerization of norbornene and cylcooctene, both carried out in batch stirred reactor. Almost negligible leaching of ruthenium was observed and successful catalyst reusing was achieved. However, the reaction rate was slower in comparison with the parent Hoveyda-Grubbs alkylidenes under the same reaction conditions. In ROMP, high molecular weight poly(NBE) and poly(COE) were prepared in good or moderate yields.

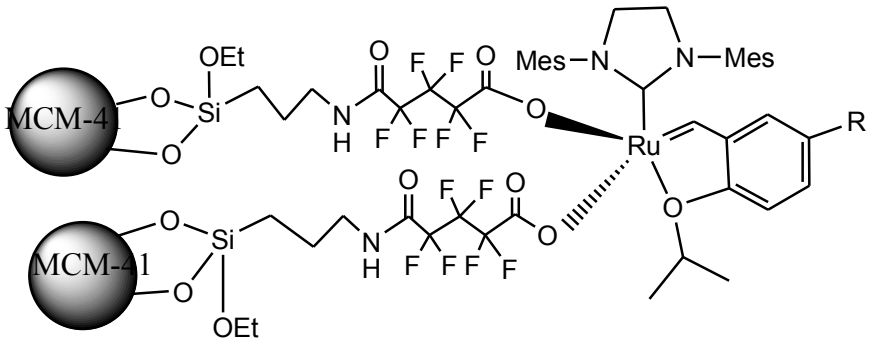

72a: R = H
72b: R = SO_2NMe_2

Scheme 32: SBA-15 immobilized catalyst **72**.

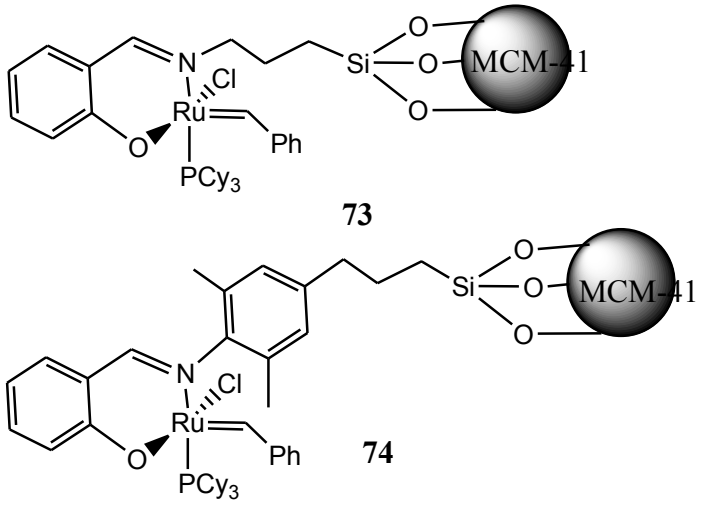

73

74

Scheme 33: MCM-41 supported N,O-bidentate Schiff base complexes **73** and **74**.

Verpoort reported the immobilization of homogeneous N,O-bidentate ruthenium complexes bearing a Schiff base as ancillary ligand onto MCM-41 by treatment of the inorganic support with a tris(alkoxy)silyl functionalized ruthenium complex [51]. They envisaged that the chemical

tethering of organometallic compounds to a solid support to be one of the best strategies with respect to catalyst leaching. Applying this approach two multifunctional Schiff base-containing ruthenium carbene complexes, catalysts **73** and **74** supported on MCM-41 were generated from their homogeneous precursors (Scheme 33).

RCM of various dienes substrates induced by catalysts **73** and **74** allowed cyclization to five-, six- and larger rings, in moderate to high yields, mainly depending on the dienic substrate, catalyst and reaction temperature. Catalyst **74** proved to be more active, however, both catalysts led easily to quantitative conversions of 1,7-octadiene, DEDAM and diallyl ether to give the corresponding cyclic products, when working at 85 °C.

Importantly, work-up of the RCM reaction simply consisted of the removal of the catalyst through filtration and evaporation of the solvent under vacuum.It is noteworthy that both strained and low strained cyclo-olefins (e.g. norbornene or norbornene derivatives and cyclooctene) displayed a high reactivity in ROMP by using both catalytic systems **73** and **74**, under normal reaction conditions. Interestingly, in ROMP, catalyst **73** proved to be more active than catalyst **74**. This result is in sharp contrast to the results obtained from RCM reactions using the same catalytic systems.

4. 6 References

[1] P. Schwab, M. B. France, J. W. Ziller, R. H. Grubbs, *Angew. Chem. Int. Ed*., 1995, ***34**,* 2039. (b) P. Schwab, R. H. Grubbs, J. W. Ziller, *J. Am. Chem. Soc.,*1996, **118***,* 100.(c) E. L. Dias, S. T. Nguyen, R. H. Grubbs, *J. Am. Chem. Soc.*, 1997, **119***,* 3887.

[2] See review articles (a) A. Furstner, Olefin Metathesis and Beyond. *Angew. Chem., Int. Ed*., 2000, **39,** 3013. (b) T. M. Trnka, R. H. Grubbs, *Acc. Chem. Res*., 2001, **34***,* 18. (c) R. H. Grubbs, *Handbook of Metathesis; Wiley-VCH: Weinheim*, 2003. (d) D. Astruc, *New J. Chem.,* 2005, **29***,* 42. (e) P. H. Deshmukh, S. Blechert, *Dalton Trans*., 2007**,** 2479. (f) C. Samojłowicz, M. Bieniek, K. Grela, *Chem. Rev*., 2009, **109***,* 3708. (g) I. Drugutan, V. Dragutan, L. Delaude, A. Demonceau, *ChimicaOggi/Chem. Today*, 2009, **27***,* 13. (h) S. Díez-González, N. Marion, S. P. Nolan, *Chem. Rev.,* 2009, **109***,* 3612. (i) G. C. Vougioukalakis, R. H. Grubbs, *Chem. Rev.,* 2010, **110***,* 1746. (j) A. M. Lozano-Vila, S. Monsaert, A. Bajek, F. Verpoort, *Chem. Rev.,* 2010,**110***,* 4865.

[3] (a) M. Scholl, T. M. Trnka, J. P. Morgan, R. H. Grubbs, *Tetrahedron Lett*. 1999, **40**, 2247. (b) M. Scholl, S. Ding, C. W. Lee, R. H. Grubbs, *Org. Lett.*1999, **1**, 953.

[4] (a) J. S. Kingsbury, J. P. A. Harrity, P. J. Jr. Bonitatebus, A. H. Hoveyda, *J. Am. Chem., Soc*. 1999, **121**, 791.

[5] G. C. Vougioukalakis *Chem. Eur. J.,* 2012, **18**, 8868.

[6] R. Haag, S. Roller, *Topics in Current Chemistry, Springer, Heidelberg,* 2004, 242.

[7] B. M. L. Dioos, I. F. J. Vankelecom, P. A. Jacobs, *Adv. Synth. Catal.,* 2006*,* **348**, 1413.

[8] S. T. Nguyen, R. H. Grubbs, *J. Organometal. Chem.,* 1995,**497**, 195.

[9] S. C. Schürer, S. Gessler, N. Buschmann, S. Blechert, *Angew. Chem. Int. Ed.,* 2000, **39**, 3898.

[10] S. Randl, N. Buschmann, S. J. Connon, S. Blechert, *Synlett.,* 2001**,** 1547.

[11] (a) A. Kirschning, K. Harmrolfs, K. Mennecke, J. Messinger, U. Schon, K. Grela, *Tetrahedron Lett*., 2008, **49**, 3019. (b) N. Kann, *Recent. Mol.,* 2010, **15**, 6306.

[12] A. G. M. Barrett, S. M. Cramp, R. S. Roberts, *Org. Lett.,* 1999, **1**, 1083.

[13] M. Ahmed, A. G. M. Barrett, D. C. Braddock, S. M. Cramp, P. A. A Procopiou, *Tetrahedron Lett.,* 1999**, 40,** 8657.

[14] H. D. Maynard, R. H. Grubbs, *Tetrahedron Lett.,* 1999*,* **40,** 4137.

[15] M. Ahmed, T. Arnauld, A. G. M. Barrett, D. C. Braddock, P. A. Procopioub, *Synlett.,* 2000, 1007.

[16] (a) L. Jafarpour, S. P. Nolan, *Org. let.* 2000, **2***,* 4075. (b) L. Jafarpour, M. P. Heck, C. Baylon, H. M. Lee, C. Mioskowski, S. P.Nolan, *Organometallics,* 2002*,* **21**, 671.

[17] Sherrington, D. C. *Chem. Commun.,* 1998, 2275.

[18] J. Dowden, J. Savovic, *Chem. Commun.,* 2001*,* 37.

[19] K. Grela, M. Tryznowski, M. A. Bieniek, *Tetrahedron Lett.,* 2002, **43**, 9055.

[20] F. Koç, F. Michalek, L. Rumi, W. Bannwarth, R. Haag, *Synthesis,* 2005, 3362.

[21] S. J. Connon, S. Blechert, *Med. Chem. Lett*., 2002, **12,** 1873.

[22] M. T. Zarka, O. Nuyken, R. Weberskirch, *Macromol. Rapid. Commun.,* 2004*,* **25**, 858.

[23] P. Nieczypor, W. Buchowicz, W. J. N. Meester, F. P. J. T. Rutjes, J. C. Mol, *Tetrahedron Lett.,* 2001, **42,** 7103.

[24] J. O.Krause, O. Nuyken, K. Wurst, M. R. Buchmeiser, *Chem. Eur. J.,* 2004*,* **10,** 777.

[25] T. S. Halbach, S. Mix, D. Fischer, S. Maechling, J. O. Krause, C. Sievers, S. Blechert, O. Nuyken, M. R. Buchmeiser, *J.Org. Chem.,* 2005*,* **70,** 4687.

[26] D. C. Braddock, K. Tanaka, D. Chadwick, V. P. W. Böhmc, M. Roeper, *Tetrahedron Lett.,* 2007, **48***,* 5301.

[27] M. R. Buchmeiser, *Macromol. Symp.,* 2010*,* **298**, 17.

[28] M. Mayr, B. Mayr, M. R. Buchmeiser, *Angew. Chem. Int. Ed.,* 2001, **40**, 3839.

[29] Krause, J. O.; Lubbad, S.; Nuyken, O.; Buchmeiser, M. R. *Adv. Synth. Catal.,* 2003*,* **345**, 996.

[30] J. O. Krause, S. H. Lubbad, O. Nuyken, M. R. Buchmeiser, *Macromol. Rapid Commun.,* 2003*,* **24**, 875.

[31] L. Yang, M. Mayr, K. Wurst, M. R. Buchmeiser, *Chem. Eur. J.,* 2004, **10**, 5761.

[32] M. Mayr, D. Wang, R. Kröll, N. Schuler, S. Prühs, A. Fürstner, M. R. Buchmeiser, *Adv. Synth. Catal.,* 2005*,* **347,** 484.

[33] J. S. Kingsbury, S. B. Garber, J. M. Giftos, B. L. Gray, M. M. Okamoto, R. A. Farrer, J. T. Fourkas, A. H. Hoveyda, *Angew. Chem. Int. Ed.,* 2001*,* **40,** 4251.

[34] D. Fischer, S. Blechert, *Adv. Synth. Catal.,* 2005, **347***,* 1329.

[35] X. Elias, R. Pleixats, M. Wong Chi Man, J. J. E. Moreau, *Adv. Synth. Catal.,* 2006, **348***,* 751.

[36] S. Prühs, C. W. Lehmann, A. Fürstner, *Organometallics,* 2004, **23***,* 280.

[37] D. P. Allen, M. M. Van Wingerden, R. H. Grubbs, *Org. Lett.,* 2009, **11***,* 1261.

[38] J. O. Krause, S. Lubbad, O. Nuyken, M. R. Buchmeiser, *Adv. Synth. Catal.,* 2003*,* **345***,* 996.

[39] K. Vehlow, S. Maechling, K. Köhler, S. Blechert, *Journal of Organomet. Chem.,* 2006**, 691**, 5267.

[40] D. Bek, N. Žilková, J. Dědeček, J. Sedláček, H. Balcar, *Top Catal*., 2010, **53***,* 200.

[41] H. Beerens, F. Verpoort, L. Verdonck, *J. Mol. Cat. A: Chem.,* 2000, **151**, 279.

[42] B. Van Berlo, K. Houthoofd, B. F. Sels, P. A. Jacobs, *Adv. Synth. Catal.,* 2008*,* **350**, 1949.

[43] J. Beck, J. Vartuli, W. Roth, M. Leonowicz, C. Kresge, K. Schmitt, C. Chu, D. Olson, E. Sheppard, S. McCullen, J. Higgins, J. Schlenker, *J. Am. Chem. Soc*., 1992,**114***,* 10834.

[44] K. Melis, D. de Vos, P. Jacobs, F. Verpoort, *J. Mol. Cat. A: Chem,*. 2001,**169**, 47.

[45] D. Bek, H. Balcar, N. Žilková, A. Zukal, M. Horáček, J. Čejka, *ACS Catal.,* 2011*,* **1***,* 709.

[46] L. Li, J. A. Shi, *Adv. Synth. Catal.,* 2005*,* **347**, 1745.

[47] X. Elias, R. Pleixats, M. Wong Chi Man, J. J. E. Moreau, *Adv. Synth. Catal.,* 2006*,* **348**, 751.

[48] J. Lim, S. S. Lee, S. N. Riduan, J. Y. Yinga, *Adv. Synth. Catal.,* 2007*,* **349**, 1066.

[49] J. Lim, S. S. Lee, J. Y. Ying, *Chem. Commun.,* 2010**, 46**, 806.

[50] J. Lim, S. S. Lee, J. Y. Ying, *Chem. Commun.*, 2008, 4312.

[51] V. Drăguţan, F. Verpoort, *Revue Roumaine de Chimie,* 2007*,* **52**, 905.

Part II: Results and Discussions

5.1 Introduction

One of the successful developments in the field of ruthenium based olefin metathesis is the introduction of NHCs as ligands. The major advantage of ruthenium catalysts bearing NHCs, such as **1-3** (Scheme 1) is their superior stability relative to the first generation catalysts and their increased activity for olefin metathesis which has been attributed to the ability of NHC ligands to strongly bind a metal center [1].

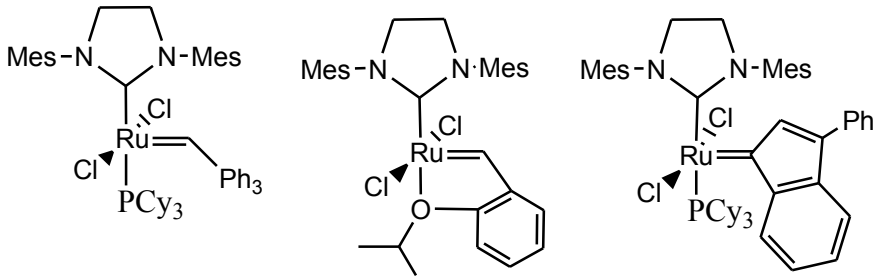

1 **2** **3**

Scheme 1: Ruthenium metathesis catalysts **1-3** bearing NHCs.

Aiming at enhanced catalyst stability, activity and selectivity, a number of modifications have already been performed both at nitrogen and on the carbon backbone of NHC ligands. Among modifications, the introduction of unsymmetrical NHC ligands has resulted in to the catalysts with exceptional selectivity in different metathesis reactions, an application that cannot be performed by some of the catalysts incorporating symmetrical NHC ligands [2]. Of particular interest unsymmetrical NHCs bearing *N*-alkyl, *N*'-aryl NHC have been incorporated to the ruthenium complexes with expectation that, would lead to the catalysts with improved stability and activity since alkyl group is more electrons donor than aromatic group. However, in most cases the activity of this family of catalysts was found to be a function of steric rather than electronic property [2].

Many researchers have investigated the effect of steric bulkiness on metathesis activity of the catalysts bearing *N*-alkyl, *N*'-aryl NHC include our group [3,4]. A series of unsymmetrical NHCs were prepared and coordinated to Grubbs' catalyst to archive complexes **4-8** (Scheme 2). The obtained catalysts were tested for activities in ROMP of 1,5-*cis,cis*-cyclooctadiene and in RCM of diethyl diallyl malonate. While catalysts **4-7** were found to surpass the 1st generation Grubbs' catalyst for the ROMP of 1,5-*cis,cis*-cyclooctadiene, catalyst **8** was considerably less metathesis

active. In RCM on the othe hand, the activity of the catalysts increased inversely with the size of the NHC ligands and catalyst **6** bearing methyl group exceeded Grubbs' complex **2** in activity.

Furthermore, it was found that *N*-alkyl, *N'*-2,6-diisopropylphenyl carbenes always lead to *bis*-coordinated ruthenium complexes [5]. Bis-coordinated complexes **9a,b** (Scheme 2) were prepared and showed substantial olefin metathesis activity at elevated temperature. The exchange of one NHC in **9b** with PCy_3 allowed the isolation of a new complex **10** which displays a fair olefin metathesis activity with a higher initiation rate relative to the Grubbs' catalyst **1**.

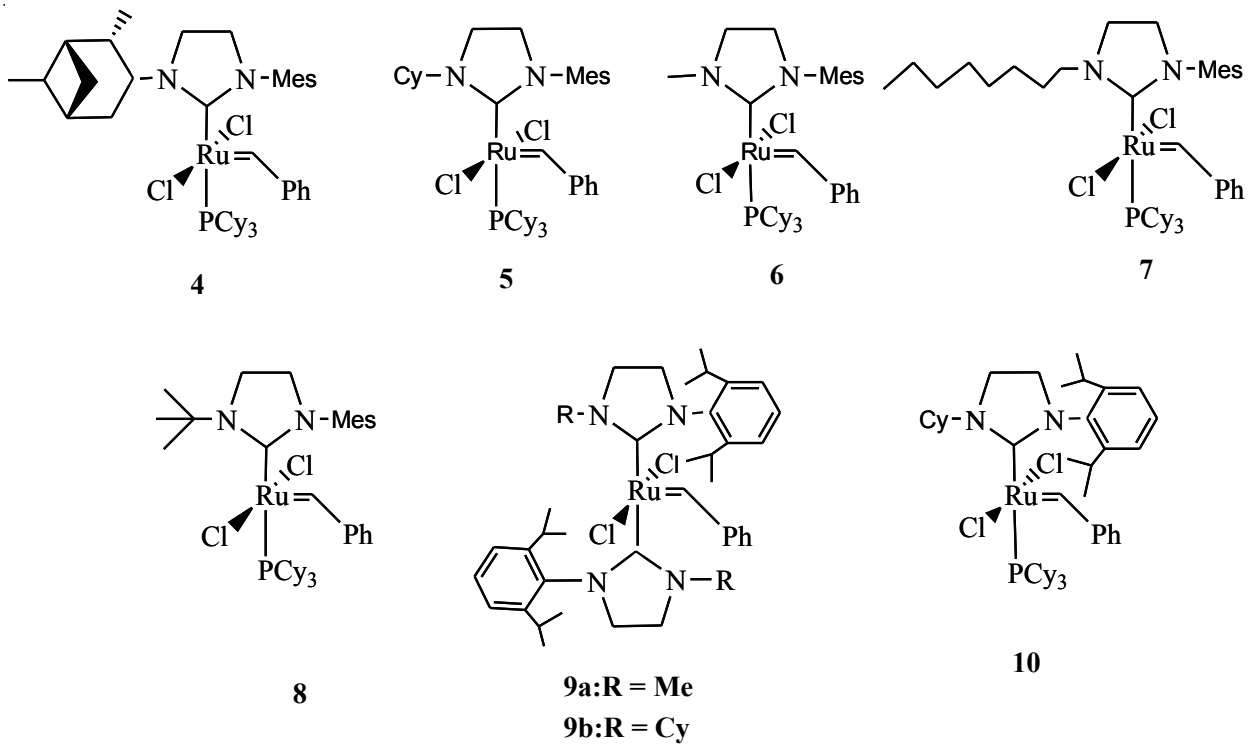

Scheme 2: Unsymmetrical NHC bearing alkyl group in ruthenium initiators **4-10**.

However, together with this achievement, up to this moment there are limited reports about coordination of unsymmetrically modified NHCs on ruthenium indenylidene metathesis initiators [2]. Therefore, as a part of our ongoing study prompted by previous results on Grubbs' catalysts we have coordinated unsymmetrical NHCs bearing *N*-alkyl, *N'*-aryl on ruthenium indenylidene. We envisaged that, this modification would also influence both activity and selectivity of the resulting catalysts.

5.2 Results and Discussion

The main focus of this part of the study was development of second generation ruthenium indenylidene metathesis catalysts **11-13** coordinated with *N*-alkyl, *N'*-aryl heterocylic carbenes.

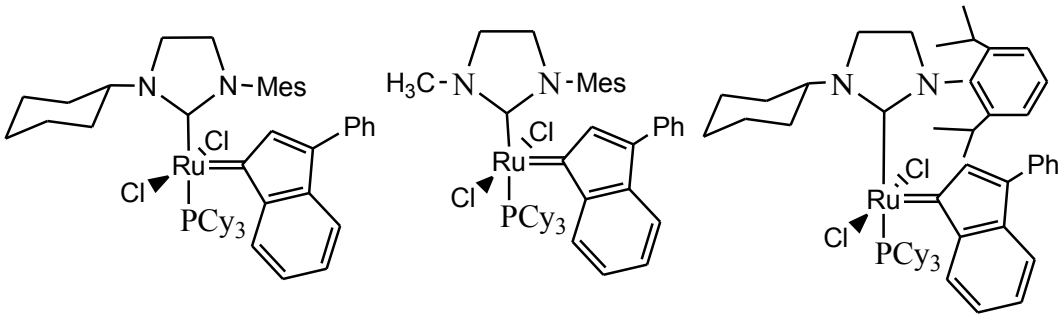

11 **12** **13**

Scheme 3: Ruthenium based indenylidene catalysts **11-13**.

5.2.1 Preparation of *N*-alkyl-*N'*-aryl Imidazolinium Salts.

The preparation of unsymmetrical NHC precursors was straightforward following a standard protocol (Scheme 4) [5]. Condensation of ethyl chlorooxoacetate (**I**) and aniline affords the oxanilic acid ethylester (**II**), which is then treated with the aliphatic amine to produce the corresponding oxalamide (**III**). Reduction and subsequent addition of HCl result in the dihydrochloride salt (**IV**), which then cyclizes to the desired 4,5-dihydroimidazolium chloride (**V**) by the reaction with triethyl orthoformate.

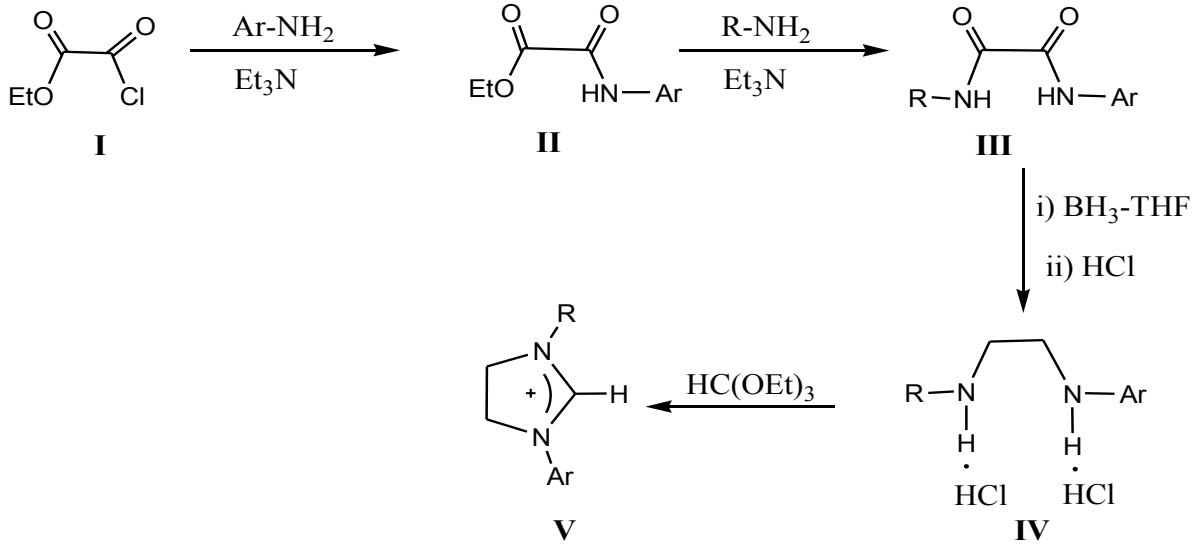

Scheme 4: Synthesis of *N*-alkyl-*N'*-aryl imidazolinium salts**.**

5.2.2 Synthesis of Ruthenium Indenylidene Complexes

5.2.2.1 Synthesis of Complex 15

$(PCy_3)_2Cl_2Ru$(phenylindenylidene) complex (**15)** was used as precursor for the preparation of new complexes. Complex **15** was prepared according to the procedure of Winde *et al.* [6], in which a reaction of appropriate amounts of 1,1-diphenyl-2-propyn-1-ol and $Ru(PPh_3)_3Cl_2$ at 90 °C catalyzed by acetyl chloride produced complex **14**. Subsequent addition of tricyclohexylphosphine followed by precipitation and purification with methanol afforded the desired complex **15** (Scheme 5).

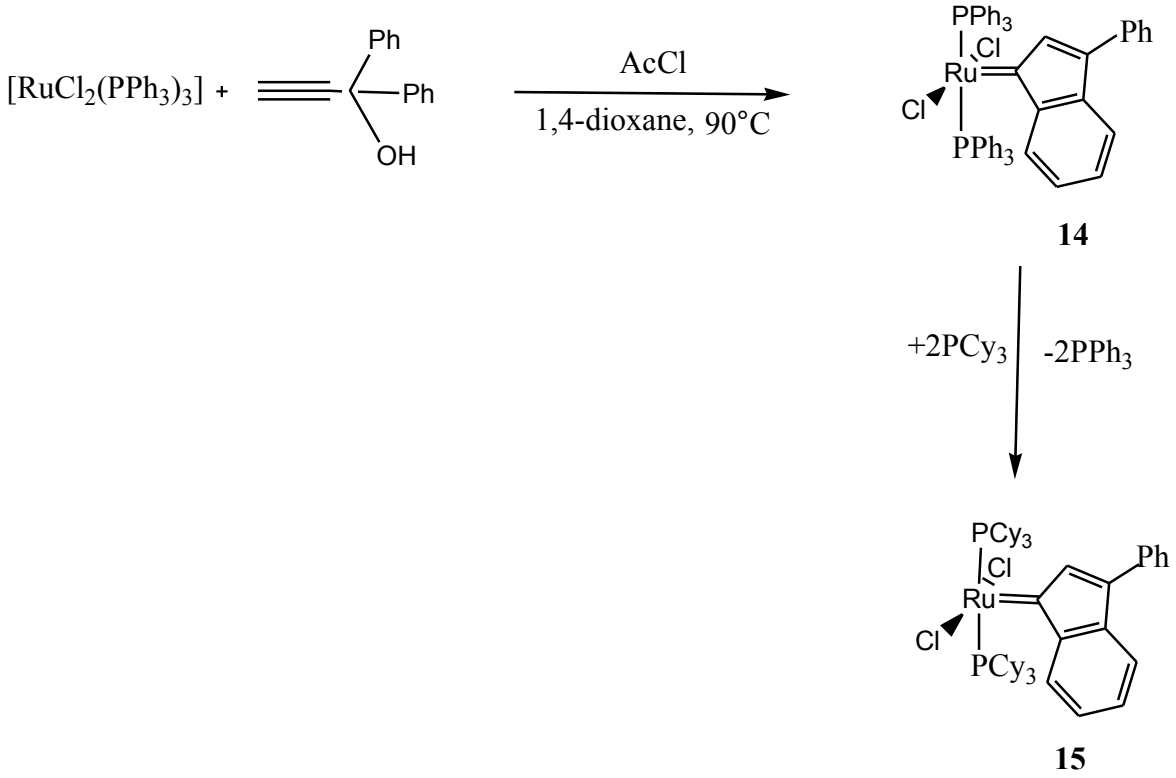

Scheme 5: Preparation of complex **15**.

5.2.2.2 Synthesis of New Ruthenium Indenylidene Complexes

The standard method for the preparation of second generation type of catalysts involves the treatment of the 1st generation complex with unmasked *N*-heterocyclic carbene. Following this protocol, in an attempt to prepare complex **11**, free carbene generated from 1-mesityl-3-cyclohexyl-4,5-dihydroimidazolium chloride with KHMDS solution was allowed to react *in situ* with complex **15** at room temperature while the reaction progress was followed with ^{31}P-NMR. The ^{31}P-NMR spectrum showed full conversion after 6 hours with two signals, a peak at 9.34 ppm was attributed to free PCy_3 and at 20.27 ppm was assigned to complex **11**. However, after solvent evaporation, precipitation in hexane and purification by column chromatography resulted into sticky reddish purple complex which was inactive in ROMP of norbornene. The structure of this complex was analyzed using proton NMR and the spectrum of which is represented in Figure 1. As seen from the figure, apart from decomposition of indenylidene carbene, the coordination of NHC was not successful since all peaks corresponding to immidazolium ligand are not seen.

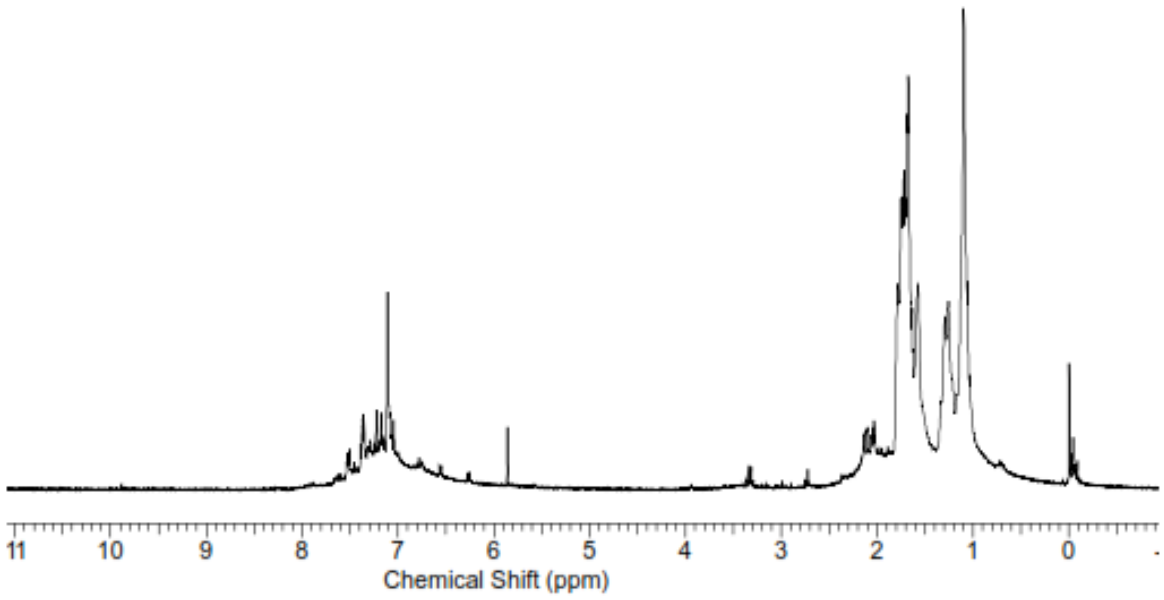

Figure 1: 1D ^{1}H NMR spectrum of isolated reddish purple complex.

Alternatively, the generation of the chloroform NHC adduct (Scheme 6) was attempted, in which addition of an appropriate amount of chloroform to the solution of the free carbene, generated by KHMDS solution, produced oil like solid. All attempts to purify this solid even by column chromatography failed.

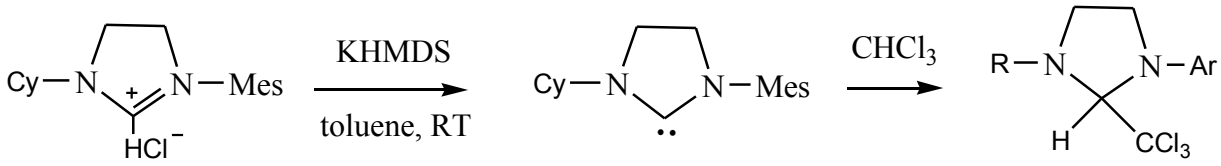

Scheme 6: Prparation of chloroform adduct

Further attempt was made with pyridine substituted 1st generation indenylidene complex (**16**). Complex **16** was prepared according to the procedure of Nolan [7] (Scheme 7), treatment of complex **15** with an excess of pyridine leads to a rapid color change of the reaction mixture from red to black, subsequent precipitation in hexanes and filtration produced the bis(pyridine) adduct as brownish red solid.

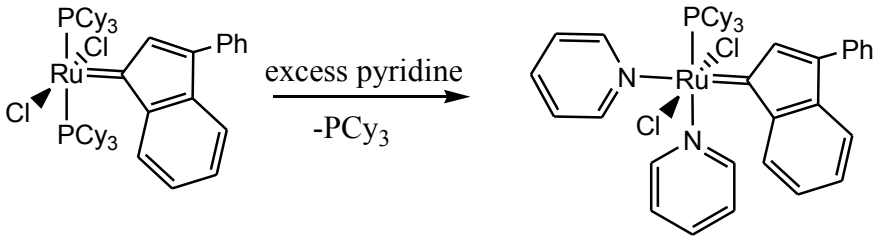

15 **16**

Scheme 7: Synthesis of pyridine substituted complex (**16**).

Reaction of a toluene solution of the prepared complex **16** (1.0 equivalent) with 1.5 equivalent free carbene obtained from 1-mesityl-3-cyclohexyl-4,5-dihydroimidazolium chloride with LiHMDS resulted into reaction mixture with the following ^{31}P-NMR signals. A peak at 20.78 ppm was attributed to complex **11**, the existence of peak at 33.21 ppm suggested that complex **15** was reformed as intermediate during this reaction. The signal for complex **16** was in place at 18.10 ppm and the peak at 9.27 ppm was assigned to free PCy_3. Surprisingly, after precipitation and purification by column chromatography only two complexes were obtained. An orange-red bis(NHC) complex was isolated but also an inactive reddish purple comlplex was produced in high yield.

The observation that reaction of 1-mesityl-3-cyclohexyl-4,5-dihydroimidazole with complex **16** produces bis(NHC) complex prompted us to prepare a variety of this kind of complexes. The general procedure for the preparation of *N*-alkyl, *N'*-aryl *bis*-heterocylic carbene bearing ruthenium complexes from complex **16** is as outlined in Scheme 8. Reaction of 1 equivalent of complex **16** with 3 equivalents free carbene generated *in situ* with LiHMDS afforded ruthenium metathesis initiators **17-19**.

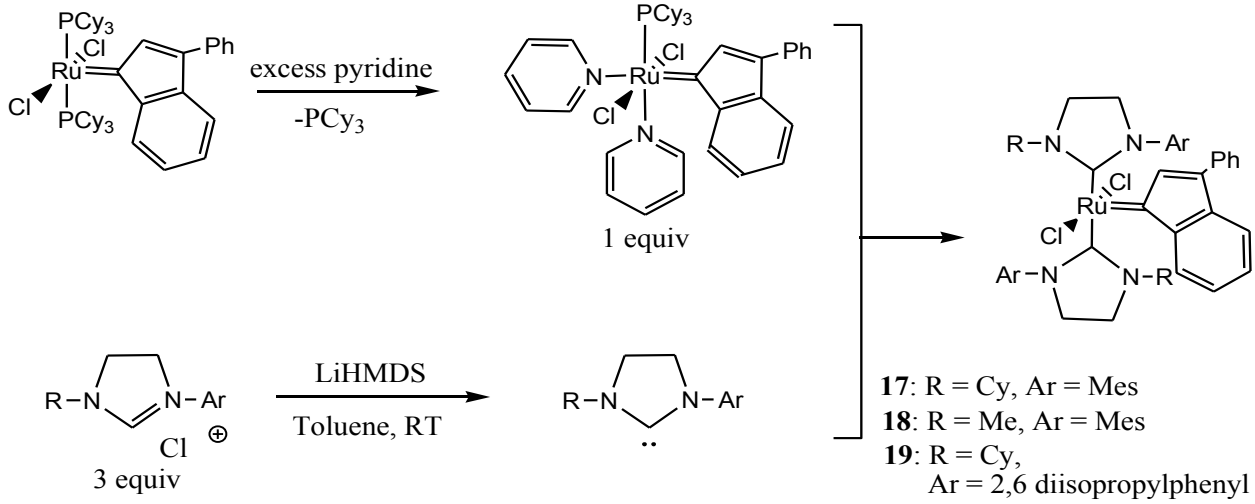

Scheme 8: The general procedure for the preparation of complexes **17-19**.

The ^{31}P-NMR spectrum recorded during the synthesis of complex **17** (after 10 min of reaction) is represented in Figure 2, while Figure 3 represents the rate at which each species containing phosphorous was changing in solution during the synthesis. As seen from the Figures, the peak related to complex **16** (17.10 ppm) disappeared immediately and other three new signals were formed. Peak at 9.38 ppm was associated to free phosphine and the peaks at 20.28 ppm and 33.20 ppm correspond to intermediates formed during the reaction. At the end of reaction, however, only the signal for free phosphine remained (Figure 3 and 4) in the spectrum but it disappeared after purification by column chromatography.

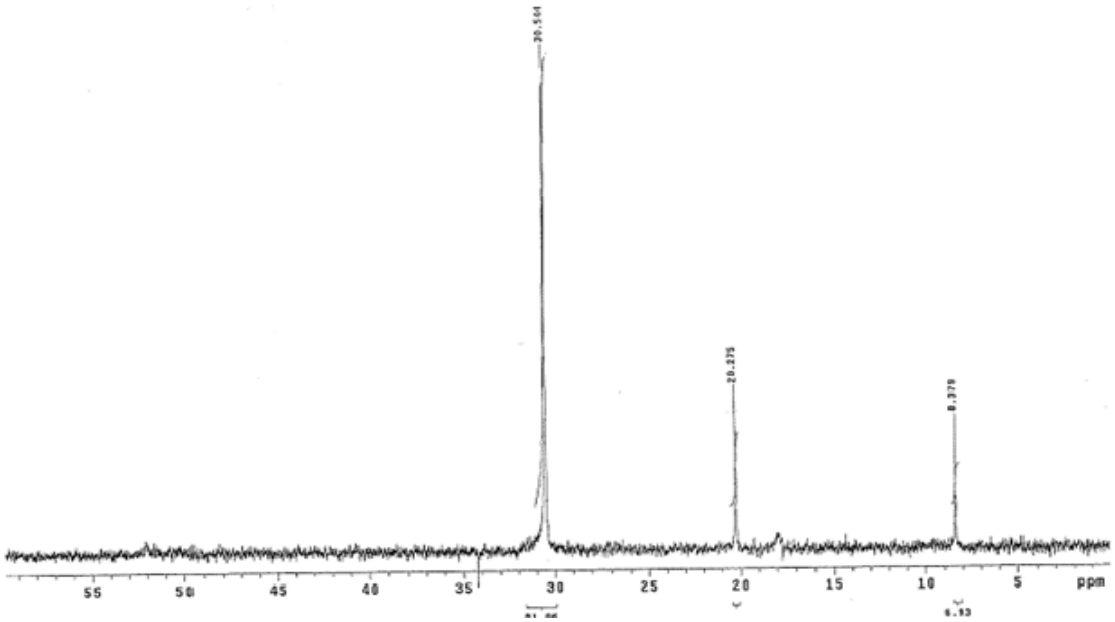

Figure 2: The ^{31}P-NMR spectrum for the synthesis of complex **17**.

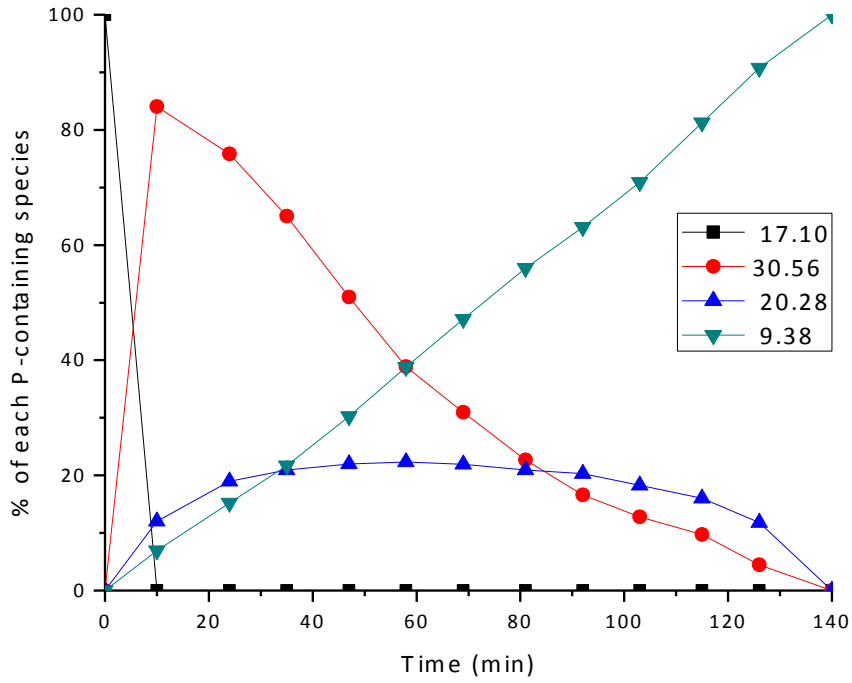

Figure 3: The kinetics for the synthesis of the complex **17**.

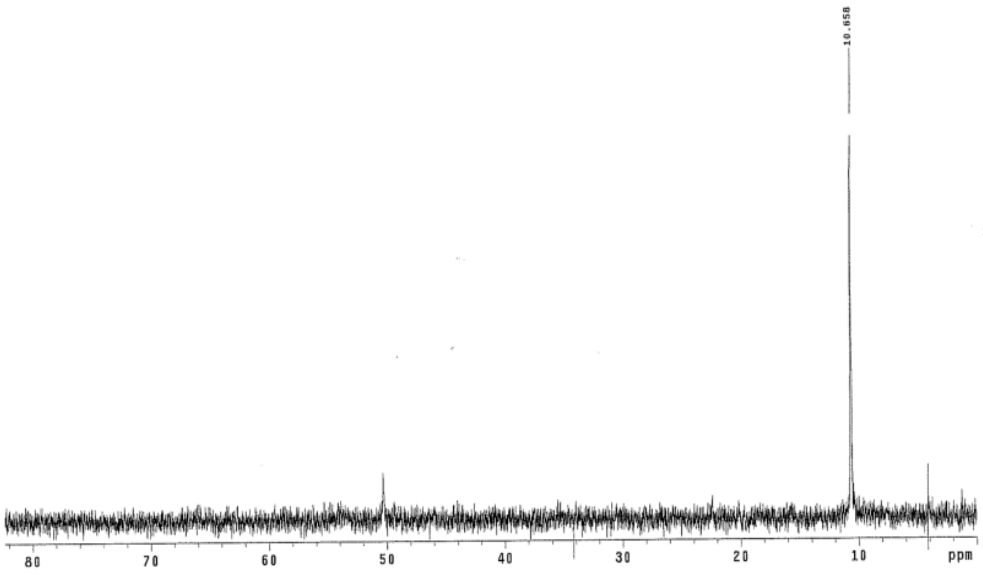

Figure 4: The ^{31}P-NMR spectrum at the end of the synthesis of complex **17.**

The synthesis of complex **19** followed the same trend as in the preparation of complex **17** that is the synthesis was proceeding with production of two intermediates. However, in the synthesis of complex **18** the intermediate associated with the signal at 20.27 ppm in ^{31}P-NMR spectrum was not observed at all. ^{31}P-NMR spectrum recorded during preparation of complex **18** is depicted in Figure 5, while Figure 6 represents the rate at which each species containing phosphorous was changing in solution during the synthesis. The peak related to the starting material (18.30 ppm) disappeared immediately and other two new signals were formed. While peak at 10.13 ppm was associated to free phosphine, signal at 33.21 ppm was attributed to intermediates formed during the reaction which disappeared at the end of reaction.

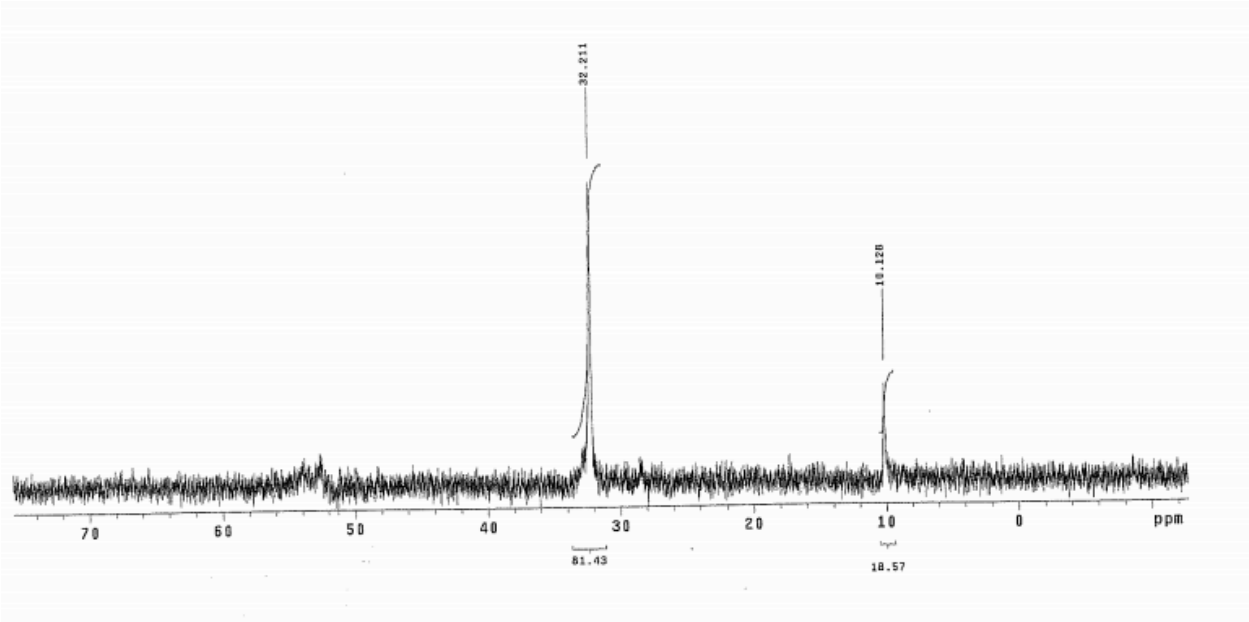

Figure 5: The ^{31}P-NMR spectrum for the synthesis of complex **18** after 10 min.

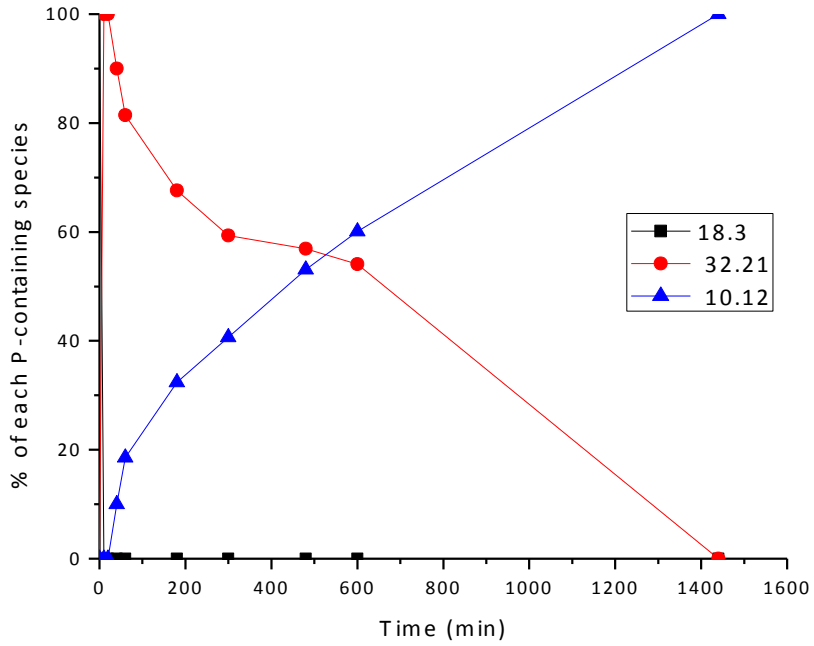

Figure 6: The kinetics for the synthesis of the complex **18**.

The NMR specta are in agreement with the proposed structure of the prepared catalysts. For instance, the ^{1}H NMR spectrum of complex **17** (Figure 7) shows peaks characteristic of the indenylidene unit, doublet around 8.70 ppm [9] and a singlet at around 7.80 ppm for CH–C=Ru [8]. In addition, peaks for the imidazolinylidene ligand are also observed as multiplet at 3.41-3.12 ppm. Analysis of 1D ^{1}H NMR (Figure 7), ^{31}P-NMR (Figure 4) and COSY (Figures 8) spectra and comparison with the spectrum of starting compound (complex **16**) (Figure 9) clearly indicates the coordination of two NHCs to the metal center and the loss of tricyclohexylphosphine as well as pyridine ligands. As seen from 1D ^{1}H NMR (Figure 7) as well from COSY (Figures 8) all signals that are attributed with pyridine (8.18 and 6.09 ppm) characteristic of complex **16** are not apparent. In addition, the existence of single signal corresponding to free phosphine in ^{31}P-NMR spectrum (Figure 4) indicates the decoordination of tricyclohexylphosphine.

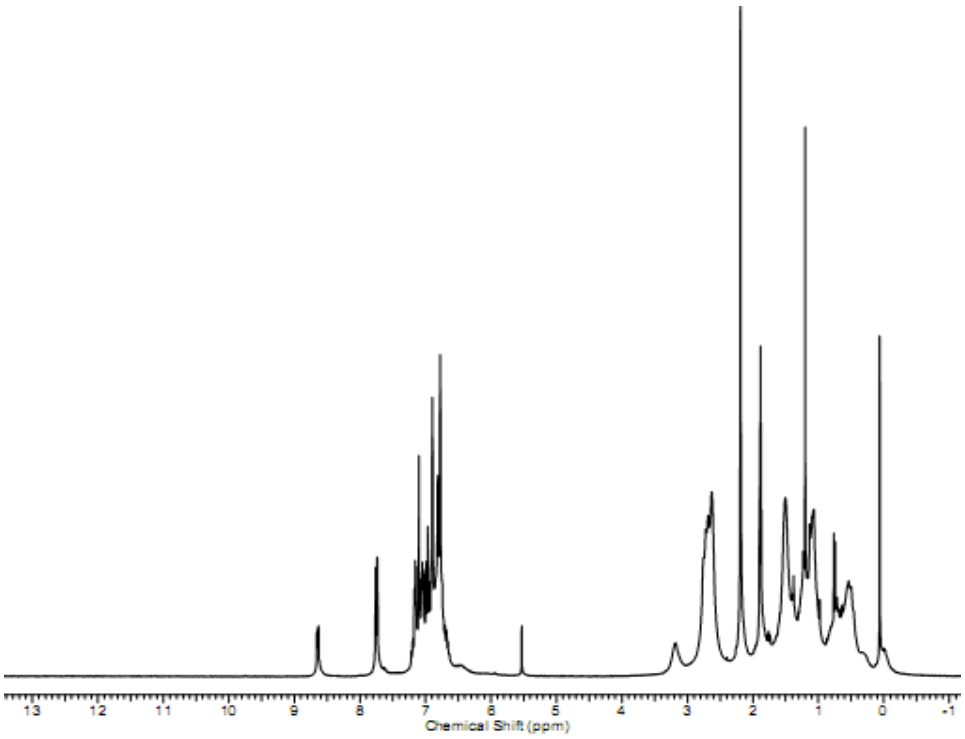

Figure 7: 1D ^{1}H NMR spectrum of catalyst **17**.

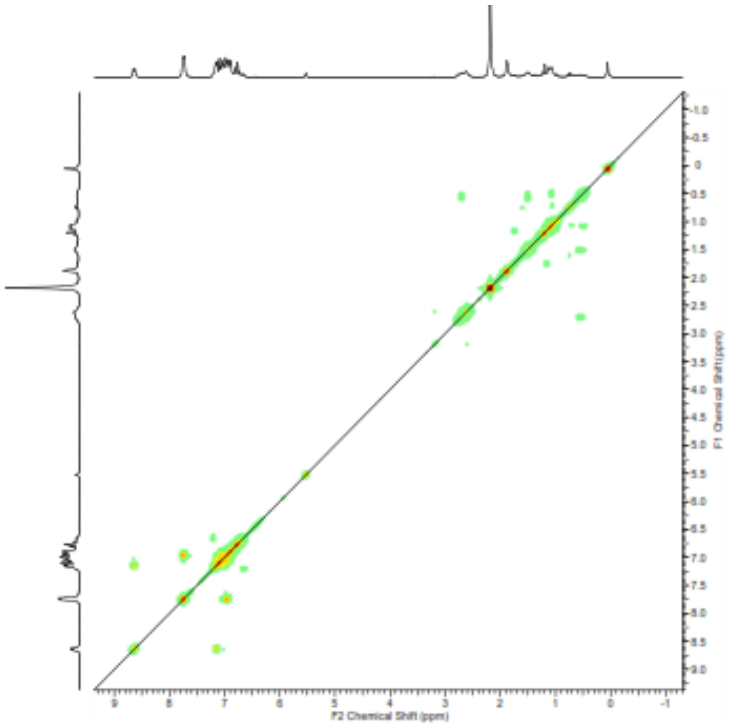

Figure 8: COSY spectrum of catalyst **17**.

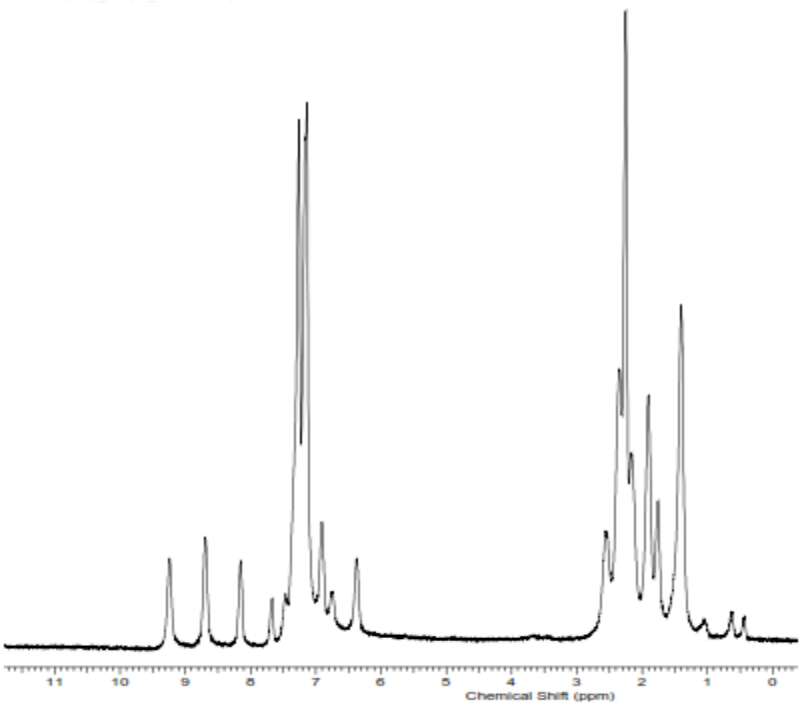

Figure 9: 1D ^{1}H NMR spectrum of complex **16**.

Unfortunately, it was not possible to obtain crystals of sufficient quality to perform single crystal analysis. However, the1D ^{1}H NMR spectrum strongly suggests that only one isomer is isolated from the reaction and NOESY (Figure 9) suggests that only one NHC has the aryl group oriented toward the indenylidene side of the ruthenium center. The ^{13}C NMR specrum on the other hand, shows doublet at around 216.00 ppm which is characteristic for the carbene-carbon.

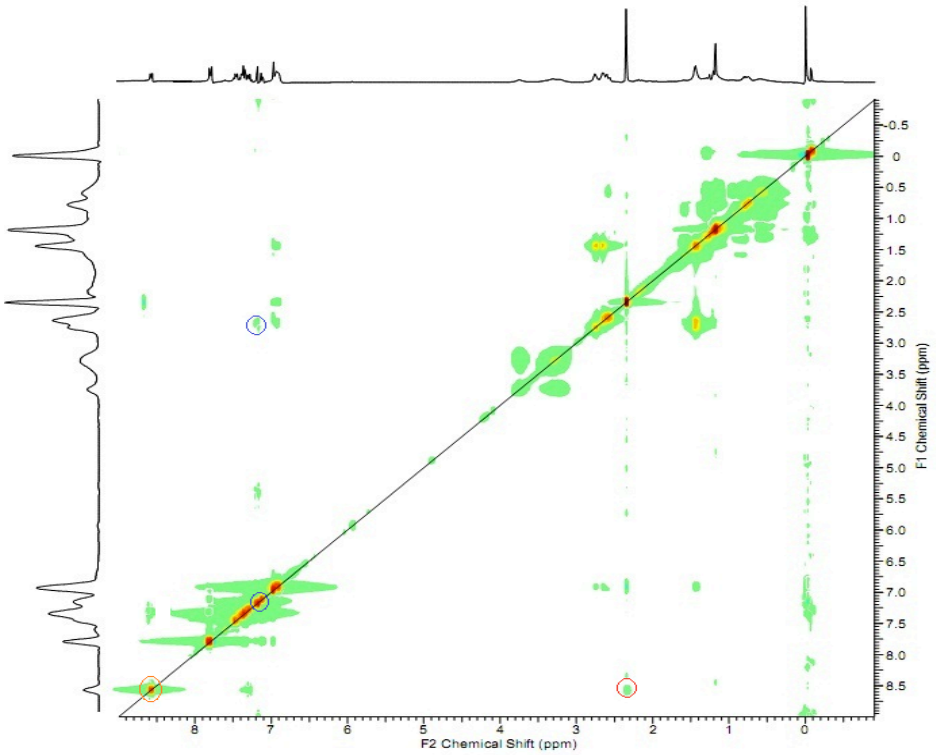

Figure 9: NOESY spectrum of catalyst **17**.

5.3 Screening of the Catalysts

The catalytic activity of complex **17-19** was evaluated for the ROMP of 1,5-*cis,cis*-cyclooctadiene and RCM of diethyl diallyl malonate using different monomer (substrate):catalyst ratios. The obtained results were compared with the activity of bis(NHCs) complexes **9a,b**.

5.3.1 ROMP of 1,5-*cis,cis*-Cyclooctadiene

As a starting point ring-opening metathesis polymerization (ROMP) of cyclooctadiene (COD) (Figure 10) was used.

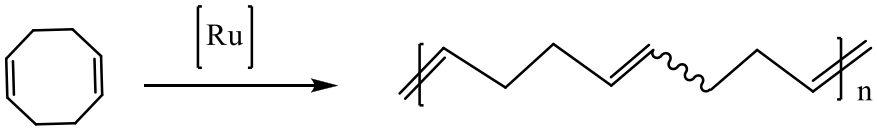

Figure 10: ROMP of COD.

The obtained results are represented in Figures 11-13 and in Table 1. All catalysts **17-19** reveal poor activity in ROMP of COD at room temperature in dichloromethane and in toluene (Table 1, entry 1-3) due to the low degree of lability of the NHCs relative to phosphine ligands. The same observation was reported by Verpoort *et al.* [5] by using complexes **9a,b**. In contrast, rising the temperature to 80 °C improved the activity significantly. Catalysts **17-19** displayed good activity for ROMP of COD at a monomer/catalyst ratio of 300/1, with catalyst **18** showing the best performance. The better performance of catalyst **18** can be attributed to less steric bulk compared with the other catalysts. Increasing the monomer/catalyst ratios to 1000/1 and subsequently to 2000/1 not only decrease the performance but also initiation rate.

Table 1: ROMP of COD

Entry	Catalyst	T [°C]	COD/Catalyst	Time	% Conversion
1	**17**	20	100	24 h	Negligible
2	**18**	20	100	24 h	Negligible
3	**19**	20	100	24 h	Negligible
4	**9a**	20	100	20 h	2
5	**17**	80	300	2 h	100
6	**18**	80	300	1.5 h	100
7	**19**	80	300	2 h	98
8	**9a**	80	300	1	96
9	**9b**	80	300	0.5	100
10	**17**	80	1000	2h	93
11	**18**	80	2000	3h	88
12	**19**	80	1000	3h	100
13	**18**	80	2000	3h	95.5
14	**19**	80	2000	4h	85

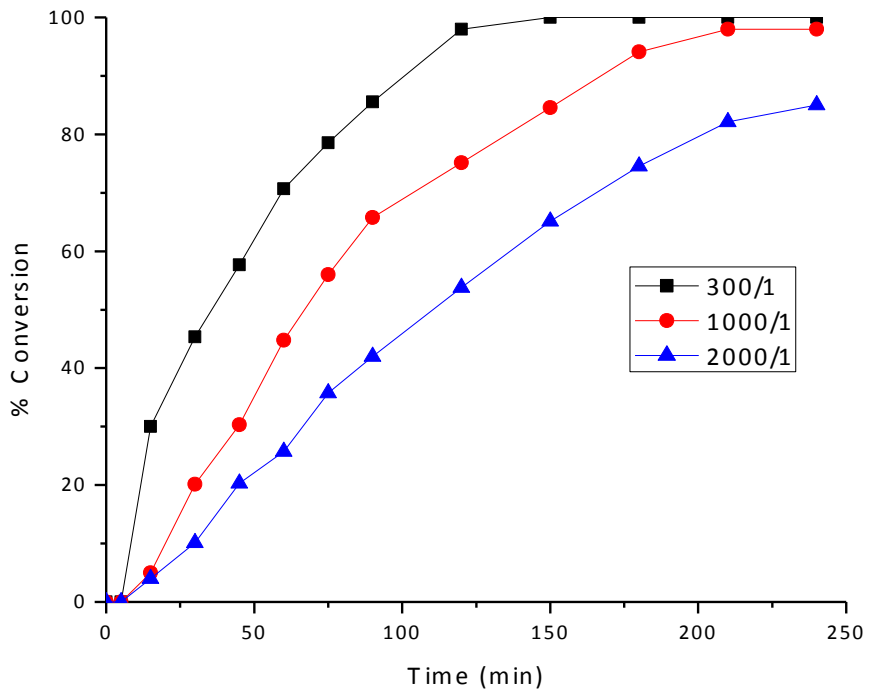

Figure 11: Kinetic plot for catalyst **17** for ROMP of COD in toluene at 80 °C.

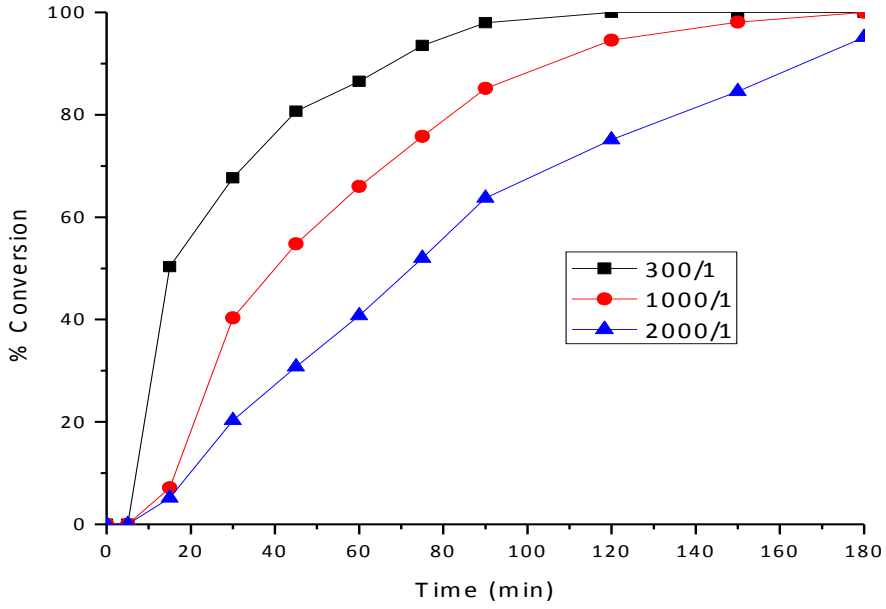

Figure 12: Kinetic plot for catalyst **18** for ROMP of COD in toluene at 80 °C.

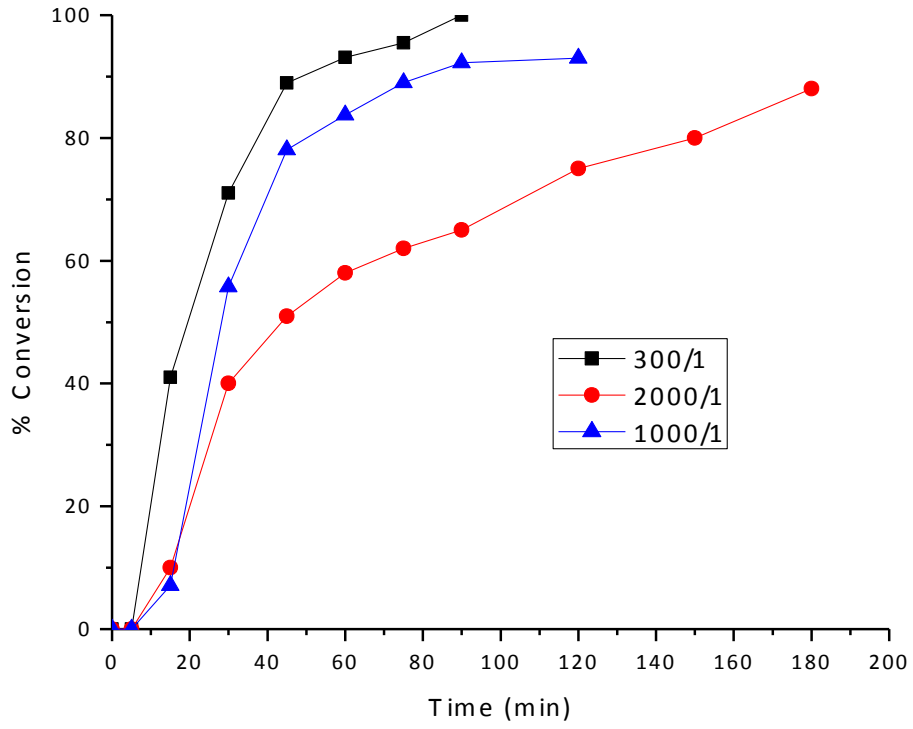

Figure 13: Kinetic plot for catalyst **19** on ROMP of COD in toluene at 80 °C.

5.3.2 RCM of Diethyl Diallyl malonate

To extend the utility of the catalysts we also evaluated the performance for RCM of diethyl diallyl malonate (Figure 14) at different monomer/catalyst ratios. Knowing that the decoordination of NHC from the organometallic complexes is more difficult we performed the reaction in toluene at high temperature (80 °C).

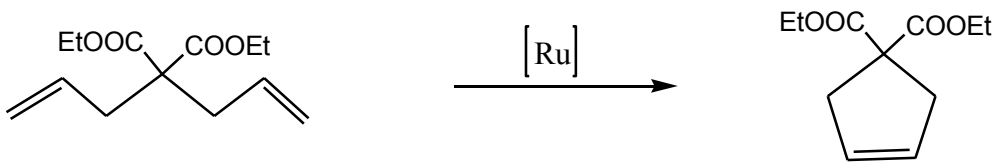

Figure 14: RCM of diethyl diallyl malonate

As seen from Figures 15-17, all prepared catalysts **17-19** proved to be active in this reaction, however, as in ROMP of COD, the activity is found to be a function of the steric bulkiness of the alkyl as well as the aryl groups. Catalyst **17** performed better than catalyst **19** with diisopropylphenyl, in the same way catalyst **18** performed better than **17**. Both **17** and **18** have a cyclohexyl substituent, but the aromatic unit seems to make a difference, with **17** (bearing a mesityl group) performing better than **19**, endowed with diisopropylphenyl group. Using small catalyst ratios (20/1 and 80/1) full conversions easily reached. When the substrate/catalyst ratio is 200/1 catalysts **17** and **19** did not achieve full conversion after 20 hours. The ability of these catalysts to remain in solution at high temperature without noticeable decomposition proved the stability of the catalysts. In solid and dry form the catalysts are highly stable, they can be stored for several months in air without noticeable decomposition.

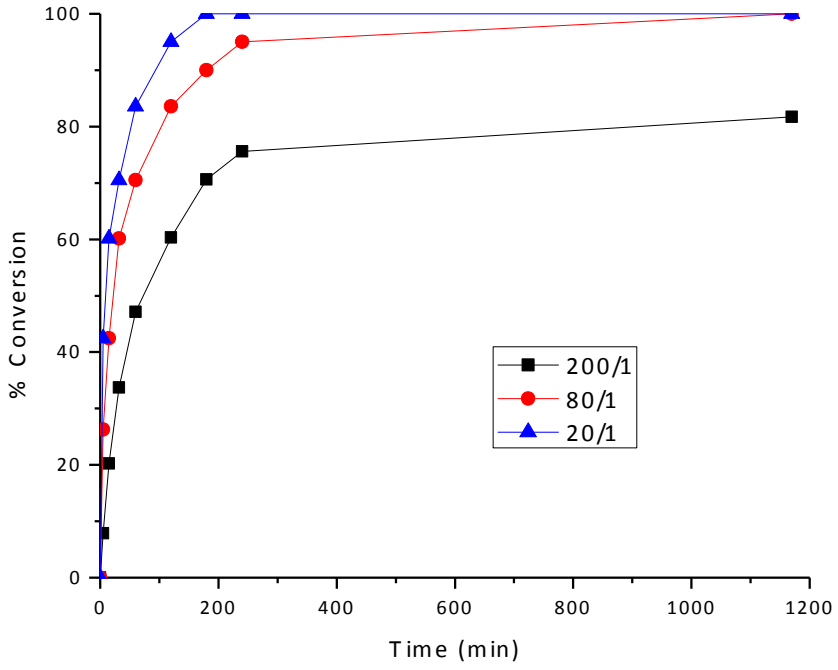

Figure 15: Kinetics plot of catalyst **17** for RCM of diethyl diallyl malonate with different catalyst ratios.

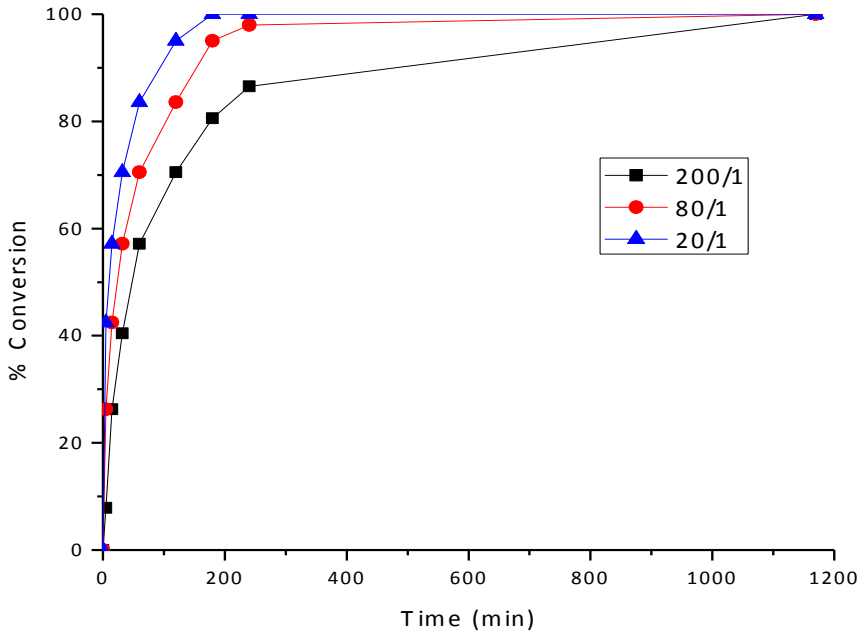

Figure 16: Kinetics plot of catalyst **18** for RCM of diethyl diallyl malonate with different catalyst ratios.

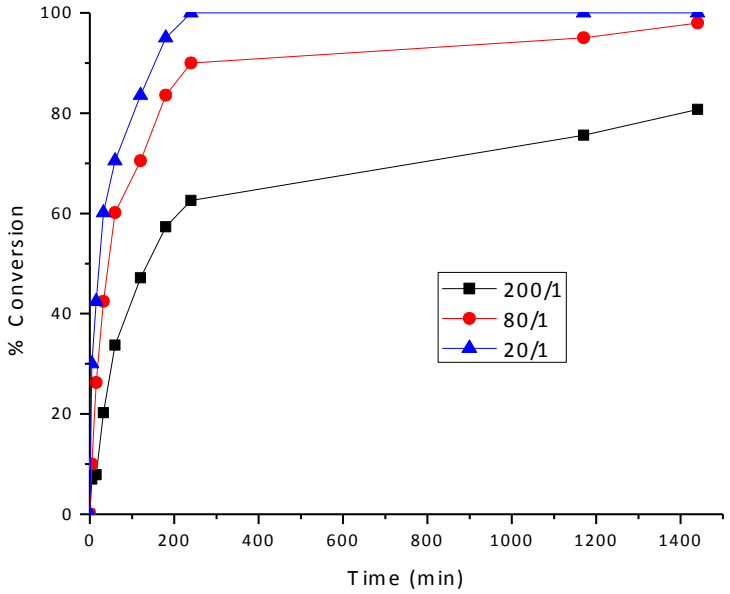

Figure 17: Kinetic plot of catalyst **19** for RCM of diethyl diallylmalonate with different catalyst ratios.

5.4 Experimental

5.4.1 Synthesis of *N*-(mesityl)-oxanilic acid ethyl ester

The synthesis of *N*-(mesityl)-oxanilic acid ethyl ester was done according to the procedure of Grubbs *et al.* [9].

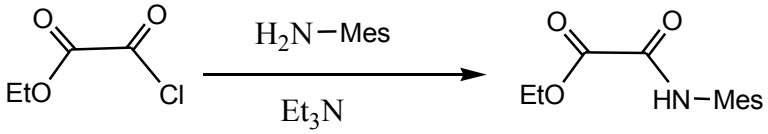

5.4.2 Synthesis of *N*-(2,6-Diisopropylphenyl)-oxanilic acid ethyl ester

The synthesis of *N*-(2,6-Diisopropylphenyl)-oxanilic acid ethyl ester was done according to the procedure of Grubbs *et al*. [9].

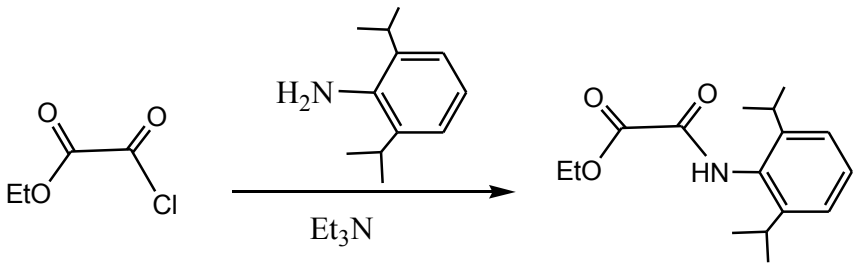

5.4.3 Synthesis of *N*-Mesityl-*N'*-cyclohexyl oxalamide.

The synthesis of *N*-Mesityl-*N*'-cyclohexyl-oxalamide was done according to the procedure of Verpoort *et al.* [3].

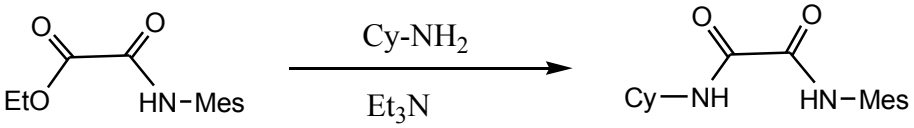

5.4.4 Synthesis of *N*-Mesityl-*N'*-methyl-oxalamide

The synthesis of *N*-Mesityl-*N'*-methyl-oxalamide was done according to the procedure of Verpoort *et al.* [3].

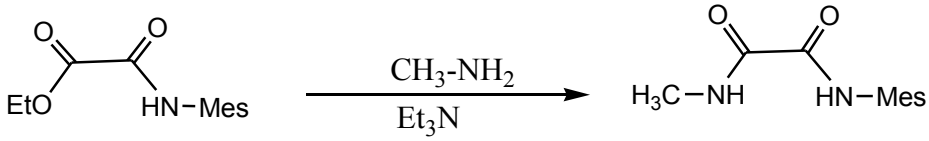

5.4.5 Synthesis of *N*-(2,6-Diisopropylphenyl)-*N'*-cyclohexyl-oxalamide.

The synthesis of *N*-(2,6-Diisopropylphenyl)-*N*'-cyclohexyl-oxalamide was done according to the procedure of Verpoort *et al.* [4].

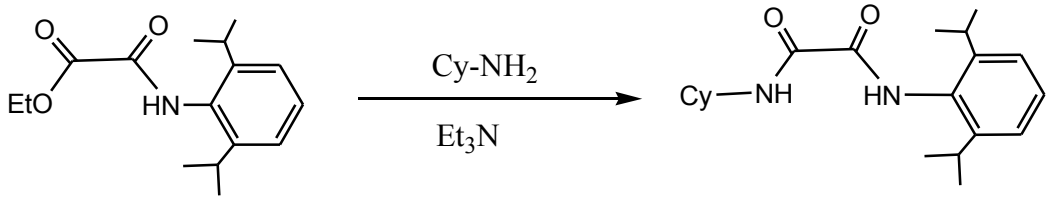

5.4.6 Synthesis of 1-Mesityl-3-cyclohexyl-4, 5-dihydroimidazolium chloride

The synthesis of 1-Mesityl-3-cyclohexyl-4, 5-dihydroimidazolium chloride was done according to the procedure of Verpoort *et al.* [3].

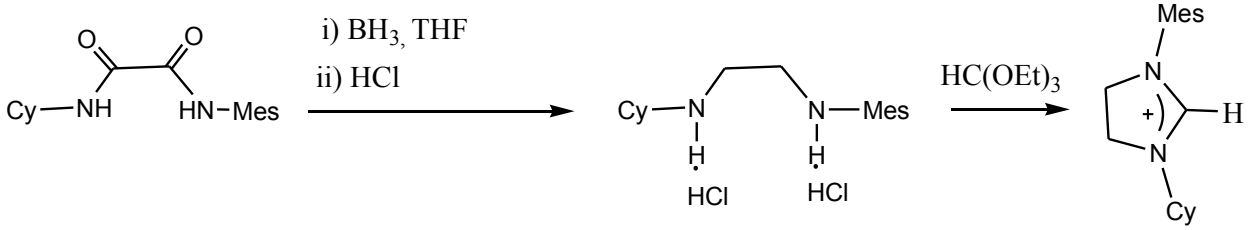

5.4.7 Synthesis of 1-Mesityl-3-methyl-4,5-dihydroimidazolium chloride

The synthesis of 1-Mesityl-3-methyl-4,5-dihydroimidazolium chloride was done according to the procedure of Verpoort *et al.* [3].

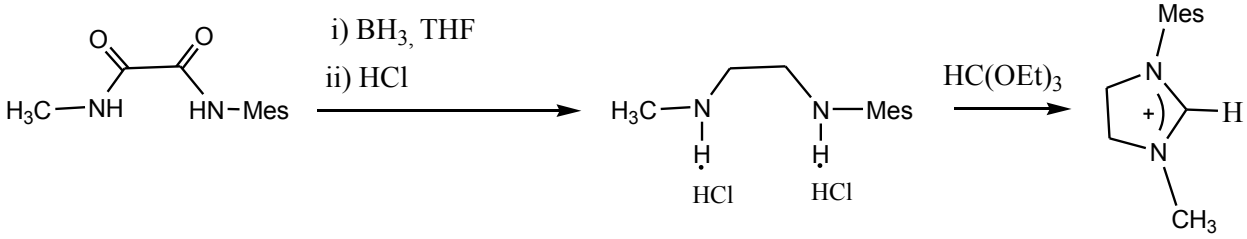

5.4.8 Synthesis of 1-(2,6-Diisopropylphenyl)-3-cyclohexyl-4,5-dihydroimidazolium chloride

The Synthesis of 1-(2,6-Diisopropylphenyl)-3-cyclohexyl-4,5-dihydroimidazolium chloride according to the procedure of Verpoort *et al.* [4].

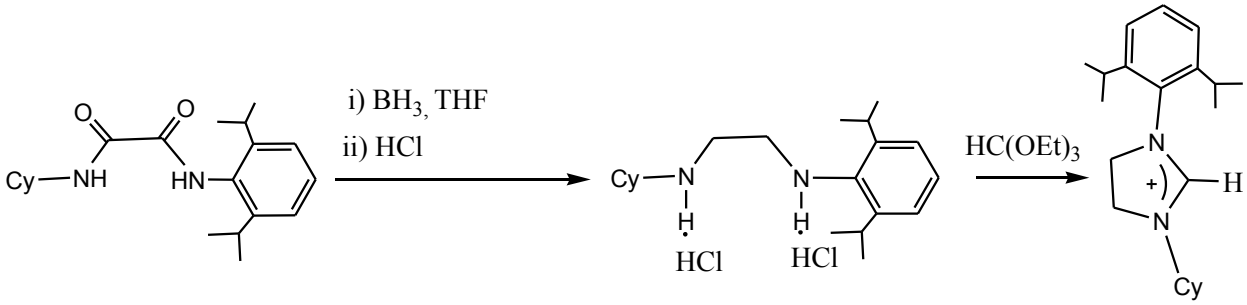

5.4.9 Synthesis of $(PCy_3)_2Cl_2Ru$(phenyl-indenylidene) (15).

The synthesis of $(PCy_3)_2Cl_2Ru$(phenyl-indenylidene) (**15**) was done according to the procedure of Winde *et al.* [6].

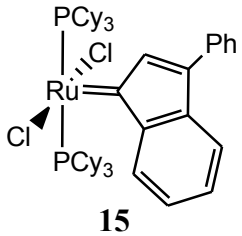

15

5.4.10 Synthesis of $Cl_2Ru(PCy_3)(Py)_2$(3-phenyl-indenylidene (16)

The synthesis of $Cl_2Ru(PCy_3)(Py)_2$(3-phenyl-indenylidene was done according to the procedure of Nolan [7].

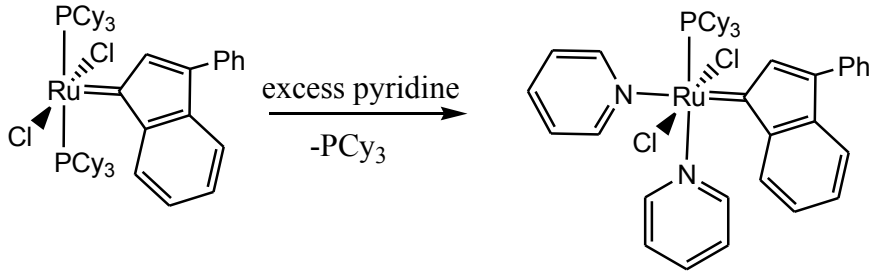

16

5.4.11 Synthesis of Complex 17

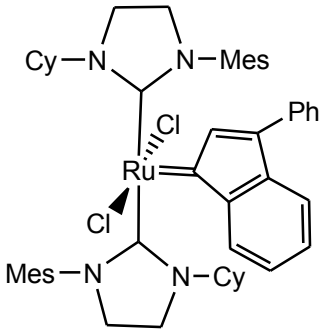

17

N-cyclohexyl, *N*'-mesityl-4,5-dihydroimidazolium chloride (250 mg, 0.815 mmol) was mixed with 5 ml dry toluene under inert atmosphere, and 1 ml (1 mmol) of LiHMDS (lithium bis(trimethylsilyl) amide solution 1 M in toluene) was then added. The mixture was stirred 45 minutes at 25 °C. Thereafter, 0.272 mmol (220 mg) of pyridine complex {Cl_2 Ru (PCy_3)Py_2(3-phenyl-indenylidene)} was dissolved in 5 ml of dry toluene under inert atmosphere and free carbene solution was added *via* syringe. The resulting mixture was stirred for 2 h between 25 °C -35 °C and the conversion was determined by ^{31}P-NMR. The solvent was evaporated at low pressure at 20 °C. Hexane was added stirred for 2 h and a light-brown precipitate was formed. After filtration, the compound was purified by column chromatography (silica gel 60, hexane/ether 9/1 v/v) resulting an orange-red solid (209 mg, 85% yield).

^{31}P NMR (300.18 MHz, 22° C: C_6D_6) showed no peak. ^{1}HNMR (500.13 MHz; 22° C C_6D_6; Me_4Si) δ(ppm) 8.9 (d, 1H); 7.699 (s, 1H, phenyl), 7.674 (s, 1H); 7.670 (s, 1H); 7.31(t, 1H, phenyl); 7,23 (t, 2H, phenyl); 7.16 (td, 1H), 7.10 (td, 2H); 7.06 (dd,1H); 6.985 (s, 1H, Mes-m-CH); 6.831 (s,1H, Mes-m-CH), 6.743 (s,1H, Mes-m-CH), 6.709 (s,1H, Mes-m-CH), 3.41-3.32 (m,2H, N-CH); 3.28-3.22 (m,2H, N-CH); 3.22-3.17 (m,2H, N-CH); 3.18-3.12 (m,2H, N-CH); 2.85 (s, 3H, Mes-CH_3); 2.83 (s, 3H, Mes-CH_3); 2.65(q, 2H, NCy); 2.56 (s, 3H, Mes-CH_3); 2.22 (s, 3H, Mes-CH_3); 2.21(s, 3H, Mes-CH_3); 1.82 (m, 2H, Cy); 1.78 (s, 3H, Mes-CH3); 1.71 (m, 2H, Cy); 1.57 (m, 2H, Cy); 1.52 (m, 2H, Cy); 1.36-1.09 (m,12H, Cy). 13C NMR (300.18 MHz; 22° C; C_6D_6; Me_4Si), δ(ppm), 291.4 (d 1C, C1); 216.3 (d,1C, C_2); 142.95; 140.49; 139.98; 138.01; 137.09; 136.55; 136.10; 134.89; 131.09; 128.81; 128.12; 127.97; 127.80; 127.49; 127.27; 127.17; 126.90; 126.58; 126.26; 124.94; 124.07; 123.75; 123.43; 122.10; 121.35; 120.07; 116.25; 54.72; 50.33; 42.58; 41.99; 31.06; 30.28; 28.98; 25.90; 24.73; 19.94; 19.56; 19.31; 19.05; 18.80; 18.54; 18.29.

5.4.12 Synthesis of Complex 18

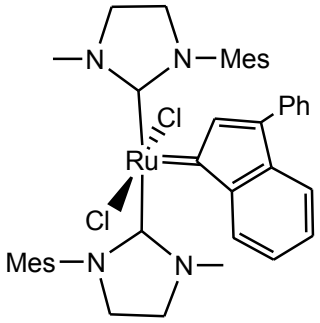

18

N-methyl, *N*'-mesityl-4,5-dihidroimidazolium chloride (150 mg, 0.628 mmol) was mixed with 5 ml dry toluene under inert atmosphere, and 0.65 ml (0.65 mmol) of LiHMDS (lithium bis(trimethylsilyl) amide solution 1 M in toluene) was then added. The mixture was stirred 45 mininutes at 25 °C and thereafter 0.21 mmol (168 mg) of pyridine complex {Cl_2 Ru(PCy_3)Py_2(3-phenyl-indenylidene)} was dissolved in 5 ml dry toluene under inert atmosphere and free carbene solution was added *via* syringe. The resulting mixture was stirred for 5 h at 45 °C and conversion determined by ^{31}P-NMR. The solvent was evaporated at low pressure at 20 °C. Pentane was added stirred for 2 h and a light-green precipitate was formed. After filtration, the

compound was purified by column chromatography (silica gel 60, hexane/ethyl acetate 8/2 v/v) resulting into greenish solid (69.37 mg, 43% yield).

^{31}P NMR (300.18 MHz, 22° C: C_6D_6) no peak detected. ^{1}HNMR (500.13 MHz; 22° C C_6D_6; Me_4Si) δ(ppm) 8.59 (d, 1H); 7.54 (s, 1H, phenyl), 7.52 (s, 1H); 7.650 (s, 1H); 7.35(t, 1H, phenyl); 7.23 (t, 2H, phenyl); 7.11 (td, 1H), 7.09 (td, H); 7.05 (dd,1H); 6.78 (s, 1H, Mes-m-CH); 6.76 (s,1H, Mes-m-CH), 6.57 (s,1H, Mes-m-CH), 6.55 (s,1H, Mes-m-CH), 3.91 (m,2H, N-CH); 3.82 (m,2H, N-CH); 3.36 (s 3H NCH_3); 3.32 (s 3H NCH_3); 3.19 (m,2H, N-CH); 3.14 (m,2H, N-CH); 2.86 (s, 3H, Mes-CH_3); 2.65 (s, 3H, Mes-CH_3); 2.20 (s, 3H, Mes-CH_3); 1.89 (s, 3H, Mes-CH_3); 1.48(s, 3H, Mes-CH_3);1.09 (s, 3H, Mes-CH3); 0.73; 0.70. ^{13}C NMR (300.18 MHz; 22° C; C_6D_6; Me_4Si), δ(ppm), 291.4 (d 1C, C1); 216.3 (d,1C, C_2); 143.1; 140.49; 139.1; 138.01; 137.44; 136.55; 132.42; 130.13; 129.15; 128.83; 128.52; 128.25; 127.97; 127.80; 127.93; 127.60 ;126.74; 125.41; 125.09; 124.94; 124.77; 123.75; 123.43; 122.69; 121.40; 120.07; 116.25; 54.62; 50.23; 42.48; 41.90; 31.06; 30.38; 19.98; 18.90; 18.73.

5.4.13 Synthesis of Complex 19

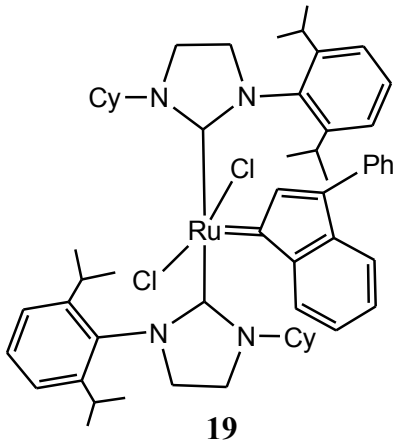

19

N-cyclohexyl, *N*'-2,6-diisopropylphenyl-4,5-dihidroimidazolium chloride (260 mg, 0.743 mmol) was mixed with dry toluene under inert atmosphere, and then 1 ml (1 mmol) of LiHMDS (lithium bis(trimethylsilyl) amide solution 1 M in toluene) was added. The mixture was stirred 45 minutes at 25 °C, thereafter, 0.248 mmol (198 mg) of pyridine complex was dissolved in dry toluene under inert atmosphere and free carbene solution was added *via* syringe. The resulting mixture was stirred 3 h at room temperature with conversion checked by ^{31}P-NMR. The solvent

was evaporated at low pressure at 20 °C. Hexane was added and stirred for 2 h and a light-brown precipitate was formed. After filtration, the compound was purified by column chromatography (silica gel 60, pentane/ethyl acetate 7/3 v/v) resulting into brown solid (193.9 mg, 79% yield).

^{31}P NMR (300.18 MHz, 22° C: C_6D_6) showed no peak. ^{1}HNMR (500.13 MHz; 22° C C_6D_6; Me_4Si) δ(ppm) 8.87 (d, 1H); 7.62 (s, 1H, phenyl), 7.59 (s, 1H); 7.59 (s, 1H); 7.24(t, 1H, phenyl); 7.23 (t, 2H, phenyl); 7.21 (td, 1H), 7.12 (td, H); 7.04 (dd,1H); 6.92 (s, 2H); 6.82 (s, 2H), 6.75(br s, 2H) 3.81 (m, 2H, N-CH); 3.68 (m, 2H, N-CH); 3.62 (m,2H, N-CH); 3.58 (m,2H, N-CH); 3.46 (m 1H); 3.14 (m 1H); 2.84 (m 1H); 2.65 (m 1H); 2.55 (s, 3H, CH_3); 2.53 (s, 3H, CH_3); 2.35(q, 2H, NCy); 2.26 (s, 3H, CH_3); 2.02 (s, 3H, CH_3); 2.01(s, 3H, CH_3); 1.88 (s, 3H, CH3);1.82 (m, 2H, Cy); 1.78 (s, 3H, CH3); 1.58 (s, 3H, CH3);1.46-1.09 (m, 20H, Cy). ^{13}C NMR (300.18 MHz; 22° C; C_6D_6; Me_4Si), δ(ppm), 291.5 (d 1C, C1); 216.3 (d,1C, C_2); 144.03; 141.95; 140.49; 138.98; 138.01; 136.93; 136.52; 136.20; 134.89; 132.42; 131.27; 128.81; 128.42 127.49; 127.17; 126.59; 126.26; 124.95; 124.07; 123.65; 123.43; 123.2; 122. 76; 122.10; 121.35; 120.07; 116.25; 55.4; 54.70; 50.03; 42.56; 42.1; 41.90; 32.1; 31.06; 30.28; 29.6; 28.98; 27.9; 26.0; 25.1; 24.8; 23.0; 22.0; 21.94; 21.56; 20.05; 18.75; 18.32.

5.4.14 General Procedure for the ROMP of 1, 5-*cis,cis*-Cyclooctadiene

An NMR-tube was charged with the appropriate amount of catalyst and dissolved in 0.35 ml of toluene-*d8*. Thereafter, 0.1 ml (0.82 mmol) 1,5-*cis,cis*-cyclooctadiene was added, the NMR-tube was closed and temperature was raised to 80 °C. The conversion was determined by integration of the olefinic ^{1}H NMR peaks of the formed polybutadiene (5.31 ppm) and of the consumed 1,5-*cis,cis*-cyclooctadiene (5.52 ppm).

5.4.15 General Procedure for the Ring-Closing Metathesis of Diethyl diallyl malonate

The appropriate amount of catalyst in NMR tube was dissolved in 0.3 ml of toluene-*d8* and left for 2 minutes before addition of 0.13 ml of diethyl diallyl malonate. The NMR tube was then closed and the temperature was raised to 80 °C. Conversion was monitored by integration of the allylic methylene peaks in the ^{1}H NMR spectrum of the diethyl diallyl malonate and of the product.

5.5 References

[1] S.T. Nguyen, L.K. Johnson, R.H. Grubbs, W. Z. Joseph, *J. Am. Chem. Soc.,* 1992, **114**, 3974.

[2] F. B. Hamad, T. Sun, S. Xiao, F. Verpoort, *Coord. Chem. Rev.,* 2013, **257**, 2274.

[3] N. Ledoux, B. Allaert, S. Pattyn, H. V. Mierde, C. Vercaemst, F. Verpoort, *Chem. Eur. J.,* 2006, **12**, 4654.

[4] N. Ledoux, B. Allaert, A. Linden, P. Van Der Voort, F. Verpoort, *Organometallics,* 2007, **26**, 1052.

[5] A. W. Waltman, R. H. Grubbs, *Organometallics,* 2004, **23**, 3105.

[6] R. Winde, R. Karch, A. Rivas-Nass, A. Doppiu, G. Peter, E. Woerner, WO 2010/037550.

[7] H. Clavier, J. L. Petersen, S. P. Nolan, *J. Organometallic Chem.,* 2006, **691**, 5444.

[8] T. Opstal and F. Verpoort, *Angew. Chem., Int. Ed.,* 2003, **42(25),** 2876.

[9] A. W. Waltman, R. H. Grubbs, *Organometallics,* 2004, **23**, 3105.

6.1 Introduction

A success of alkylidene complexes in olefin metathesis reactions has tremendously stimulated the field of ruthenium-catalyzed organic synthesis [1-10]. Indeed, several ruthenium carbenes initially used for metathesis reaction, turn out to be active catalysts for other kind of reactions such as hydrogenation, isomerisation, Kharasch reaction, oxidation, etc [11]. Ruthenium indenylidene complexes, another class of robust and efficient olefin metathesis pre-catalysts can be used as attractive alternative to benzylidene-based olefin metathesis catalysts. In a previous chapter, we reported the preparation and application of ruthenium indenylidene catalysts **1-3** bearing bis (*N*-alkyl, *N'*-aryl heterocyclic carbene) in olefin metathesis reactions. These catalysts proved to be efficient for ROMP of 1,5-*cis,cis*-cyclootadiene as well as for RCM of diethyl diallyl malonate at higher temperature. In this chapter, we report the activity of catalysts **1-3** (Scheme 1) in non-metathesis reactions, particularly isomerization and Kharasch addition.

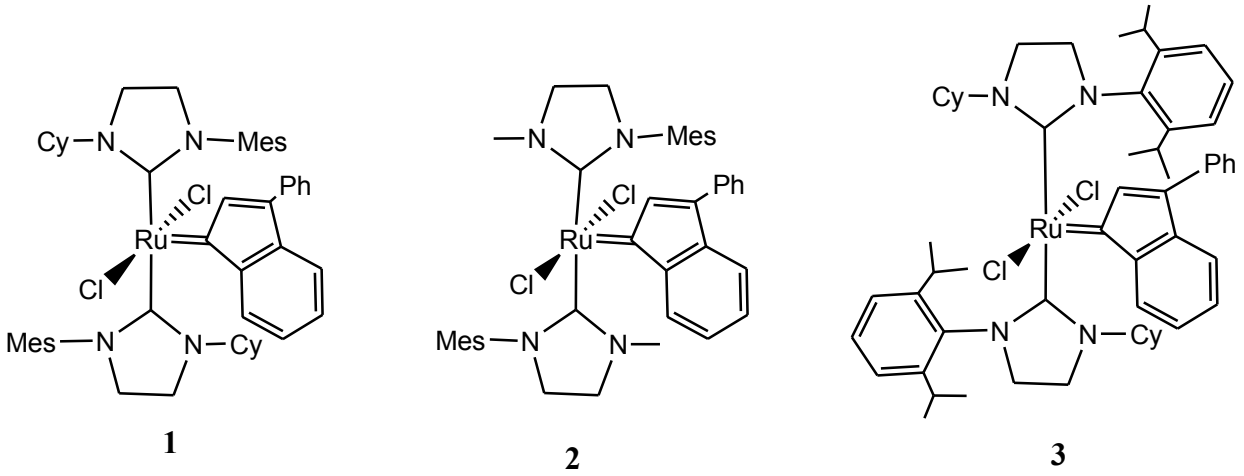

Scheme 1: Ruthenium indenylidene catalysts **1-3**.

6.2 Results and Discussion

6.2.1 Isomerization of Allylic Alcohols

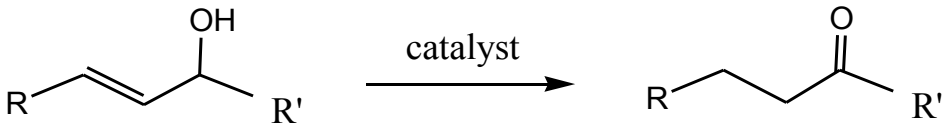

Initial efforts focused on the isomerization of penten-3-ol, hepten-3-ol and 2-cyclohexen-1-ol to their corresponding carbonyl compounds at room temperature. However, by applying 5 mol% of either catalyst no noticeable conversion was observed after 72 h of reaction for all substrates.

From mechanistic point of view allylic alcohol can coordinate to ruthenium either with its olefin moiety or via its alcoholate functionality. In order for isomerization towards the aldehyde (or ketone) to occur, NHC ligand needs to dissociate with coordination of the olefin moiety [12].

The failure of our catalysts to initiate isomerization at room temperature can be explained in terms of difficulty in de-coordination of the heterocyclic carbene from the metal center to form vacancy for the coordination of the allylic alcohol. However, upon addition of 5 mol% of KO*t*Bu the isomerization of penten-3-ol and hepten-3-ol was quantitative after 72 h (Figure 1 and 2). The relative poor performance of catalyst **3** might be caused by steric hindrance. Nevertheless, even in the optimized conditions isomerization of 2-cyclohexen-1-ol was not possible applying these catalysts.

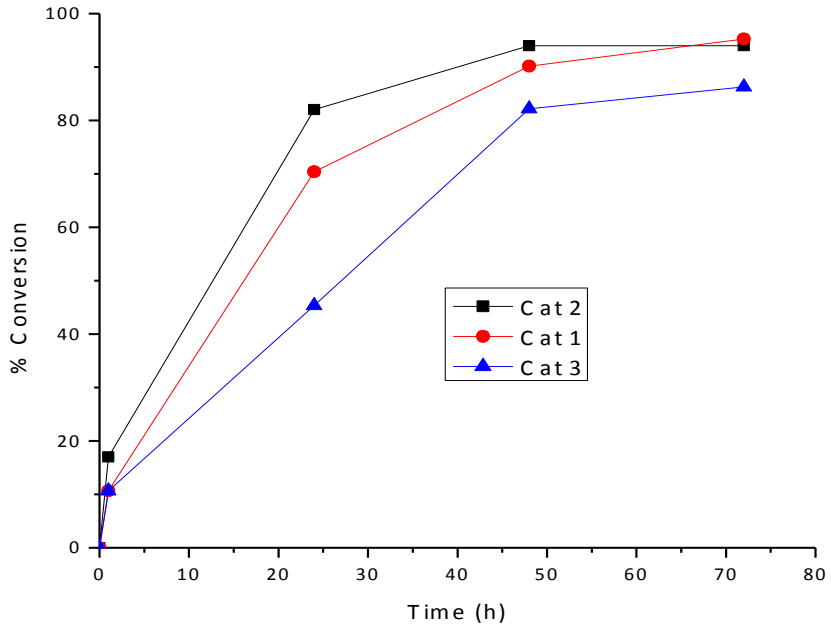

Figure 1: Isomerization of hepten-3-ol at room temperature using 5 mol% catalyst and 5 mol% KO*t*Bu.

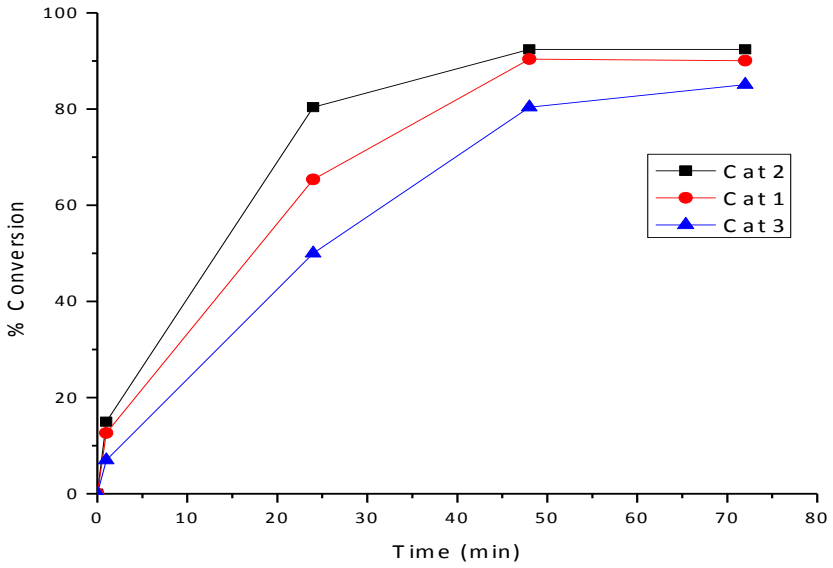

Figure 2: Isomerization of penten-3-ol at room temperature with 5 mol% catalyst and 5 mol% KO*t*Bu.

Effort to determine the mechanism by which catalysts **1-3** work was done by closely monitoring the change in NMR spectrum with time for isomerization of penten-3-ol using catalyst **1**. Figure 3 represents a spectrum of the blank with the assignment of the signals relative to the structure of the substrate.

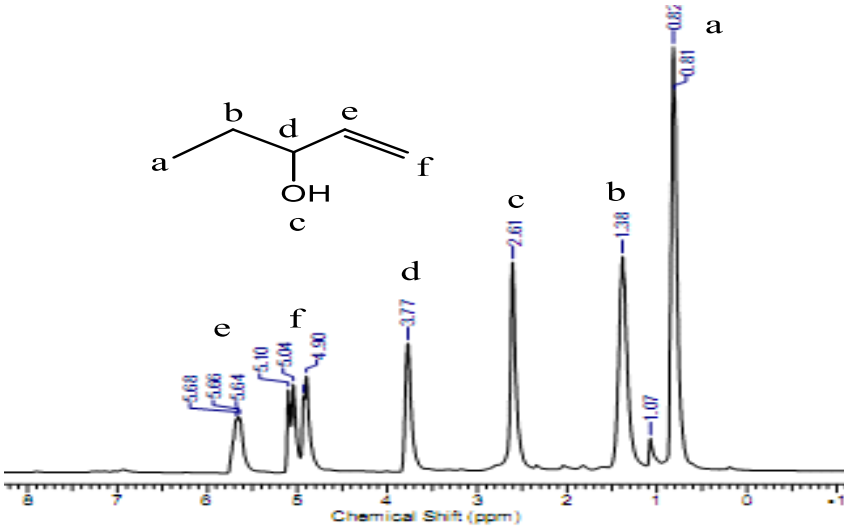

Figure 3: ^{1}H NMR spectrum of pent-3-ol in deuterated toluene in the presence of 5 mol% KO*t*Bu.

The structure of the spectrum changed completely just 60 minutes after addition of catalyst **1** to the reaction mixture (Figure 4). The important observation is disappearance of hydroxyl proton '**c**' signal indicating the coordination of metal center to the allylic alcohol generating a metal alkoxide intermediate **II**. The easy formation of the metal alkoxide intermediate can explain the positive effect of a base. An additional effect might be caused by creation of a vacant site on the ruthenium center by removing chloride ion through precipitation of solid KCl [13]. After 72 h all peaks that belong to the original substrates and intermediates disappeared and only signals for final product **III** remained in the spectrum (Figure 5).

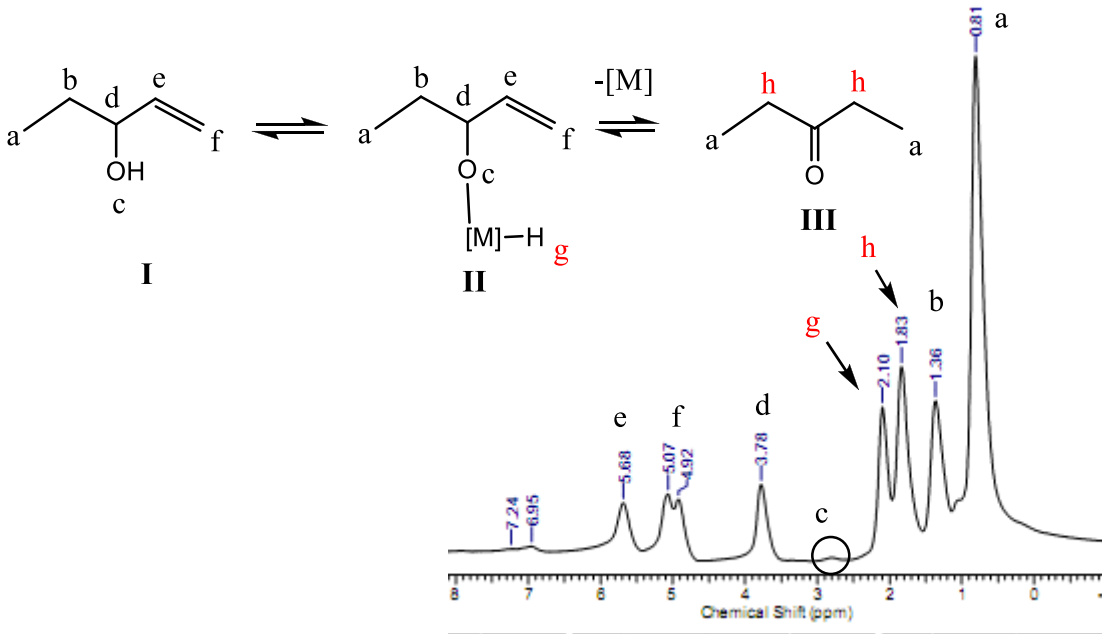

Figure 4: ^{1}H-NMR spectrum showing intermediates and final product of the isomerization of pent-3-ol by 5 mol% catalyst **1** and 5 mol% KO*t*Bu.

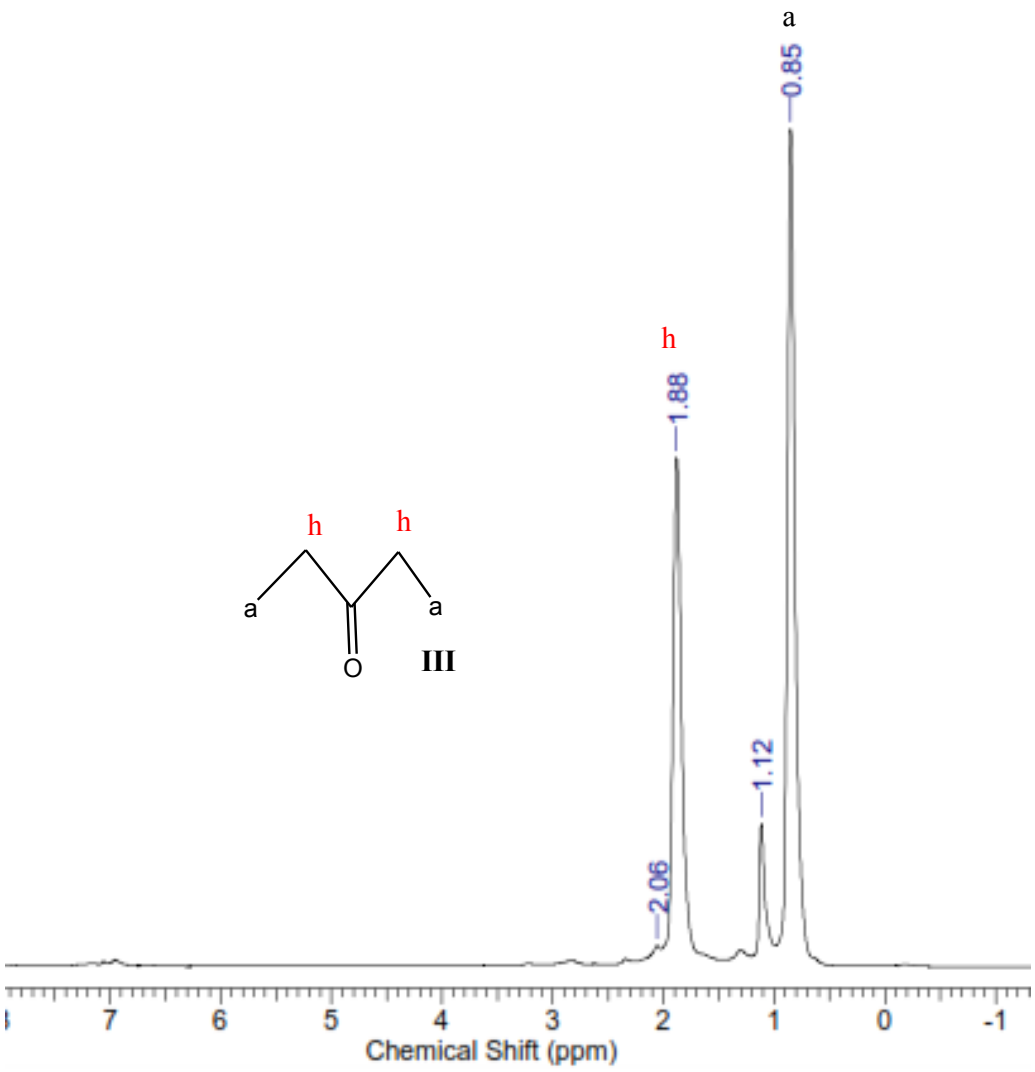

Figure 5: ^{1}H-NMR spectrum showing the final product after the isomerization of pent-3-ol by 5 mol% catalyst **1** with 5 mol% KO*t*Bu.

By rising the temperature to 80 °C, a significant increase of the reaction rate was observed. For the isomerization of hept-3-ol, the reaction rate improved with a factor of 18, 24 and 12 for catalyst **1, 2** and **3** respectively (Figure 6) while for the isomerization of penten-3-ol, the reaction rate enhanced with a factor of 14, 18 and 9 for catalyst **1, 2** and **3** respectively (Figure 7). Together with the effect of temperature on the activation energy, at higher temperature the de-coordination of one of the NHC ligands from metal center has taken place and providing a vacancy suitable for the coordination of allylic alcohol and thus enhancing the reaction rate dramatically.

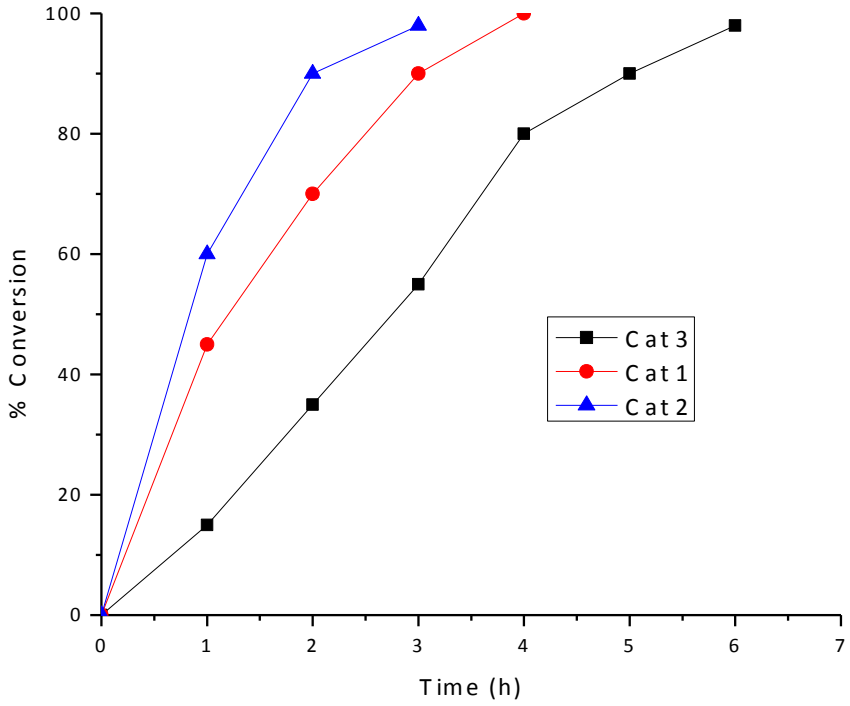

Figure 6: Isomerization of hepten-3-ol at 80 °C using 5 mol% catalyst and 5% KO*t*Bu.

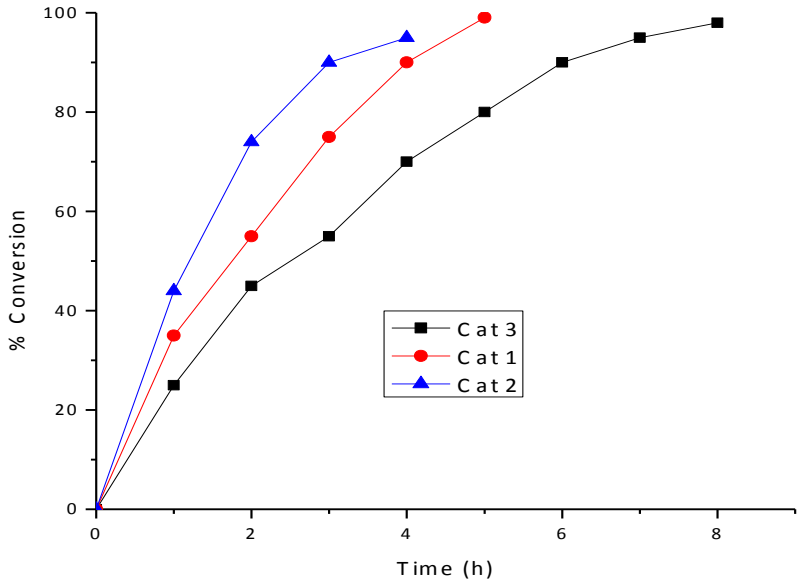

Figure 7: Isomerization of penten-3-ol at 80 °C using 5 mol% catalyst and 5% KO*t*Bu.

Using only 5 mol% catalyst without base no conversion were observed from all substrate after 24 h of reactions at 80 °C. However, by increasing the amount of catalysts to10 mol% under the same conditions all catalysts isomerized the substrates without addition of base (Table 1). In all cases, the performance of the catalysts under this condition resembles those when 5 mol% of base was used, in addition to 5 mol% of catalyst at 80 °C (Figure 6 and 7). The fact that 5 mol% of the catalysts can be replaced by 5 mol% of base in this reaction is worth noting since the cost of catalyst is not comparable to that of the base.

Table 1: Isomerization of allylic alcohols using 10 mol% catalysts **1-3** at 80 °C.

Substrate	catalyst	Time (h)	% Conversion
hepten-3-ol	**1**	4	100
hepten-3-ol	**2**	2.5	98
hepten-3-ol	**3**	6	95
penten-3-ol	**1**	5	95
penten-3-ol	**2**	4	90
penten-3-ol	**3**	8	90

6.2.2 Atom Transfer Radical Addition (Kharasch addition)

Being successful in isomerization of allylic alcohol we aimed at investigating the scope of catalysts **1-3** on Kharasch addition to olefins (Scheme 2). In this regard the plan was addition of chloroform and carbon tetrachloride to *n*-octene, *n*-hexene and styrene.

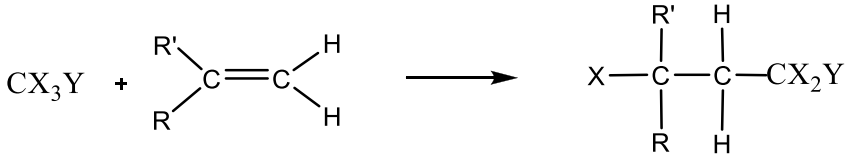

X = halogen, Y = H, halogen

Scheme 2: Kharasch addition.

6.2.2.1 Addition of Chloroform and/or Carbon tetrachloride to *n*-Octene-1, *n*-hexene and styrene

$$C_6H_{13}CH{=}CH_2 + CCl_4 \longrightarrow C_6H_{13}CHClCH_2CCl_3$$

$$C_6H_{13}CH{=}CH_2 + CHCl_3 \longrightarrow C_6H_{13}CH_2CH_2CCl_3$$

In an attempt to perform Kharasch addition of chloroform to *n*-octene-1, a 3:1 mixture of chloroform and 1-octene was allowed to react at 80 °C in the presence of 2.5 mol% of catalyst (**1-3**) and the conversion monitored by NMR. Proton NMR spectrum of *n*-octene-1 solution in chloroform is represented in Figure 8. To our surprise the expected Kharasch addition that is chlorononane product was not attained no matter which catalyst was used instead structure corresponding to an isomerization product (*n*-octene-2) was revealed (Figure 9). The same structure was also obtained (with exclusion of the peak for chloroform) when deuterated chloroform was used as both solvent and reagent.

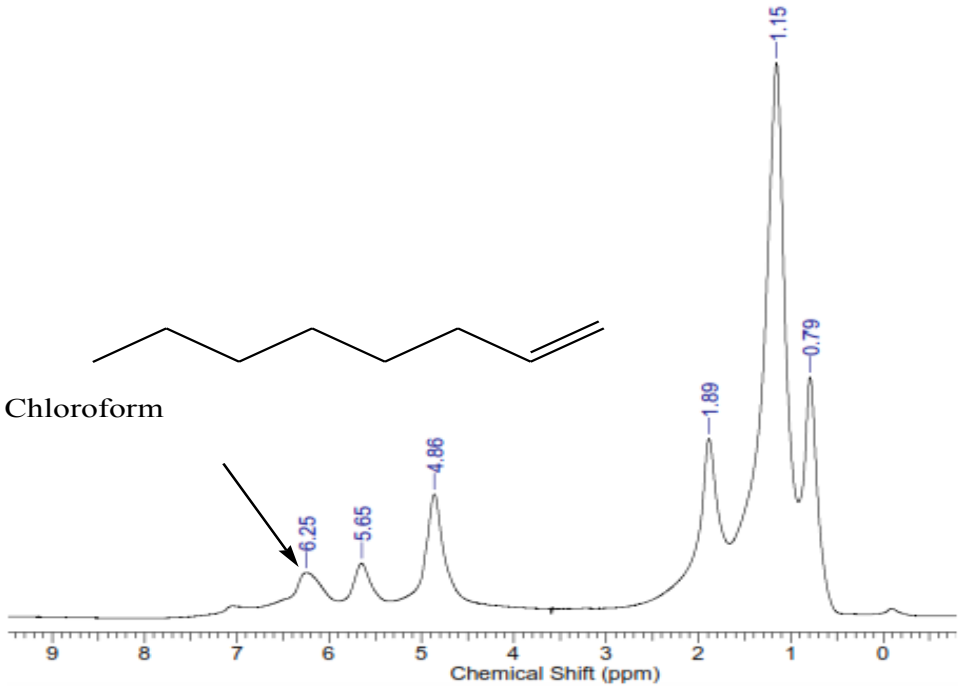

Figure 8: NMR spectrum of *n*-octene-1.

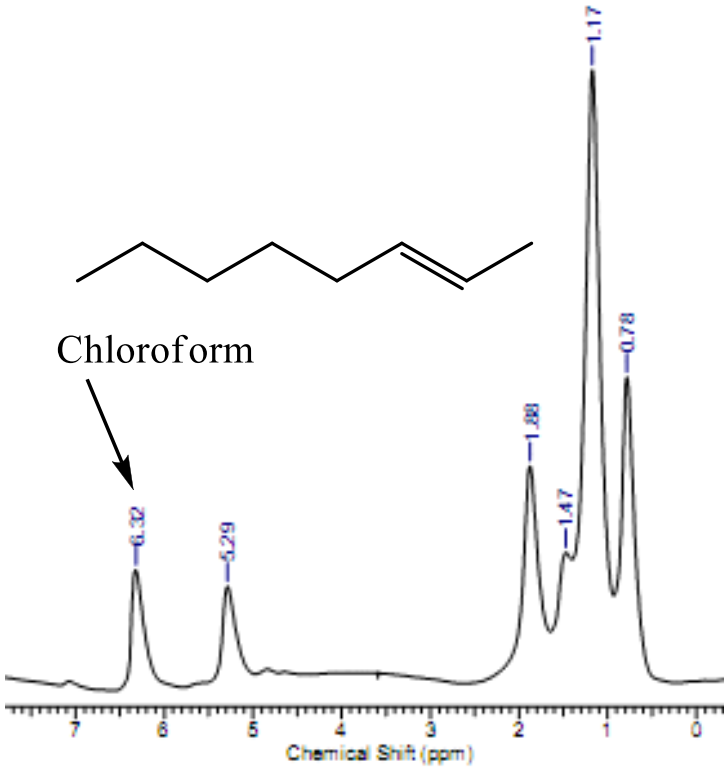

Figure 9: NMR spectrum of *n*-octene-2.

Many researchers have reported the use of different catalytic system for the Kharasch addition of chloroform or carbon tetrachloride to *n*-octene-1 of which Kharasch is the first one [14]. He successfully performed the addition of chloroform and carbon tetrachloride to *n*-octene-1 in the presence of small amount of diacetyl or dibenzoyl peroxide as radical generator with a yield superior to 60%. Using 1 mol% of either $RuCl_2(PPh_3)_3$ or $RuCl_2(PPh_3)_4$ catalyst at 140 °C isomerization of octene-1 to octene-2 was observed to occur although to a small extent in addition to the expected 1,1,1,3-tetrachlorononane. In this reaction, l,l-dichlorononane was also produced [15].

It has been demonstrated also that the ability of the Grubbs' ruthenium complexes, $RuCl_2(=CHPh)(PR_3)_2$ (R = phenyl, cyclopentyl, and cyclohexyl), to mediate the Kharasch addition on olefins markedly depends on the size of phosphine ligands, nature of the chlorinated reagent and substrate [16,17]. In the Kharasch addition of $CC1_4$, the highest activity was obtained with $RuCl_2(=CHPh)(PPh_3)_2$, the complex $RuCl_2(=CHPh)(PCy_3)_2$, bearing tricyclohexylphosphine, a basic and bulky ligand, led to a significantly less active catalytic

system [16]. Kharasch addition of $CC1_4$ and chloroform to octene-1 was proved to be less efficient accompanied with some olefin metathesis [17].

Failure of our catalysts to mediate Kharasch addition of chloroform to octene-1 can be associated with the presence of NHCs ligands which are more basic and bulkier than phosphine ligands found in Grubbs' catalysts $[RuCI_2(=CHPh)(PR_3)_2]$ and on the other hand, with proved difficulty in Kharasch addition of haloalkane to octene-1

Knowing that the proceeding reaction is isomerization, we monitored its progress in time and the results are represented graphically in Figure 10. The effect of stericity factor is clearly seen from the obtained results, the least sterically hindered catalyst **2** is effective.

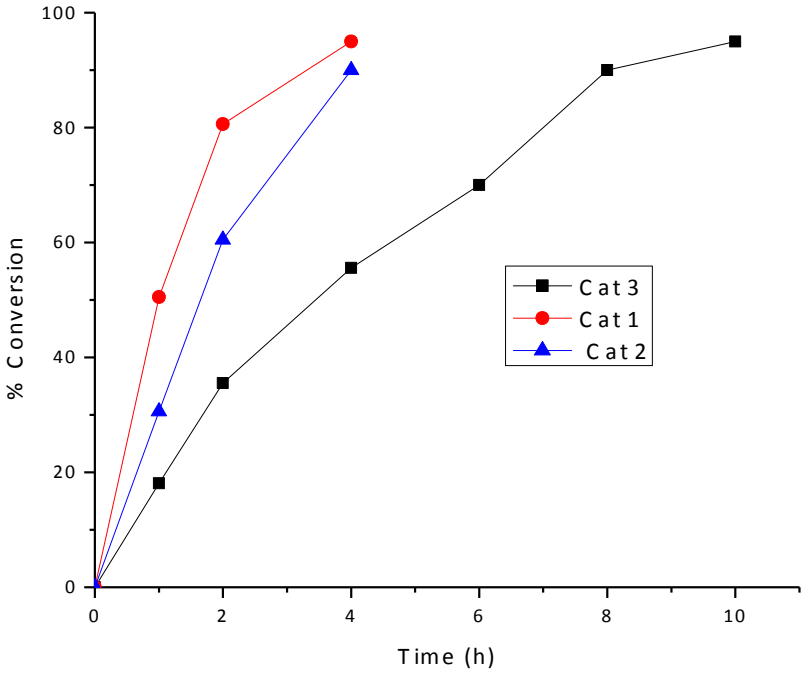

Figure 10: Isomerization of octene-1 in chloroform at 80 °C with 2.5 mol% catalyst.

Kharasch addition of CCl_4 to *n*-octene-1 was also attempted using catalysts **1-3** in toluene, however, as in addition of $CHCl_3$ the isomerization products were observed. The non-polar CCl_4 showed significant effect in the isomerization of octene-1. For instance, by using catalyst **2** in the

same reaction condition as for $CHCl_3$ that is, 2.5 mol% catalyst at 80 °C, maximum conversion of 45% was attained after 24 h (Table 2).

It is known that a polar solvent accelerates the isomerization reactions [18] and also metathesis reactions. Optimum conditions for the metathesis of internal linear alkenes, in the presence of $Ru(=CHPh)Cl_2(PCy_3)_2$ as the catalyst, were found in dichloromethane and dichloroethane at temperatures of 20-70 °C [19].

Table 2: Conversion (%) of octene-1 and hexene-1 in isomerized product after 24 h using catalysts **1-3** (2.5 mol%) in CCl_4.

Entry	Substrate	Catalyst	% Conversion
1	Octene-1	**1**	35
2	Octene-1	**2**	45
3	Octene-1	**3**	20
4	Hexene-1	**1**	20
5	Hexene-1	**2**	35
6	Hexene-1	**3**	20

6.2.2.2 Addition of Chloroform and Carbon tetrachloride to *n*-Hexene-1 and Styrene

As widely recognized, octene-1 is a poor substrate for Kharasch addition of chloroform and carbon tetrachloride and this could partially explain our failure with this reaction. In that respect we planned to perform the same reaction with *n*-hexene-1 and styrene under the same condition in order to see if there would be any different behavior. In the reaction of either chloroform or carbon tetrachloride with styrene at 80 °C using 2.5 mol% of catalyst no conversion whatsoever observed after 24 h of reaction. However, in case *n*-hexene-1 isomerization product was also revealed. The results of isomerization of *n*-hexene-1 in chloroform are shown in Figure 11 while those in carbon tetrachloride are given in table 2. In all cases the results follow the same trend as the isomerization of *n*-octene-1 best result are obtained using catalyst **2** in chloroform.

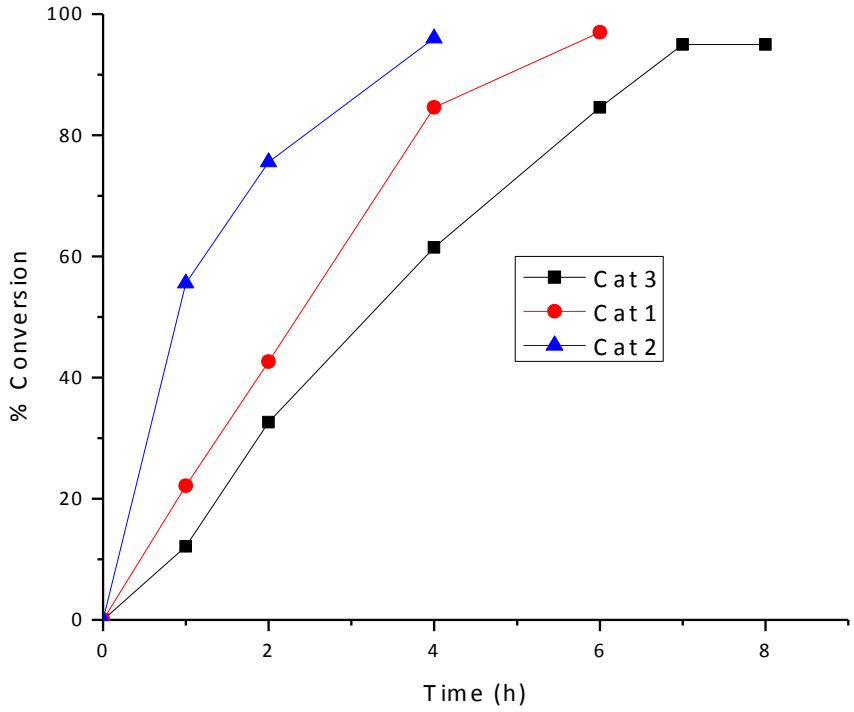

Figure 11: Isomerization of hexene-1 in chloroform at 80 °C with catalysts **1-3 (**2.5 mol%).

6.3 Experimental

6.3.1 General Procedure for Isomerization of Allylic Alcohols

6.3.1.1 Isomerization of Allylic Alcohols at Room Temperature

An NMR-tube was charged with 2.5 µmol (5 mol%) of catalyst and dissolved in 0.5 ml deuterated chloroform. After that 0.05 mmol of substrate and 2.5 µmol (5 mol%) of KO*t*Bu were added. The NMR-tube was closed and the temperature was kept at room temperature (20 °C). The conversion was determined by integration of the ^{1}H NMR signals of the consumed alcohol (5.68 ppm) and of the formed carbonyl compound (1.86 ppm).

6.3.1.2 Isomerization of Allylic Alcohols at 80 °C

The reaction was performed at 80 °C in toluene-*d8* applying procedure described in 6.3.1.1, in some cases 10 mol% of catalyst was used without base.

6.3.2 General Procedure for Isomerization of Olefin

An NMR-tube was charged with the 1.0 μmol (2.5 mol%) of catalyst and dissolved in 3:1 mixture of either deuterated chloroform or carbon tetrachloride and substrate respectively. The NMR-tube was closed and the temperature was raised to 80 °C. The conversion was determined by integration of the ^{1}H NMR olefinic peaks of the starting material (4.86 ppm) and of the product (5.29 ppm).

6.4 References

[1] A. Fürstner, *Angew. Chem., Int. Ed.,* 2000, **39**, 3013.

[2] T. M. Trnka, R. H. Grubbs, *Acc. Chem. Res.,* 2001, **34**, 18.

[3] Handbook of Metathesis; Grubbs, R. H., Ed., Wiley-VCH: Weinheim, 2003, 1204.

[4] D. Astruc, *New J. Chem.* 2005, **29**, 42.

[5] P. H. Deshmukh, S. Blechert, *Dalton Trans.,* 2007, 2479.

[6] C. Samojłowicz, M. Bieniek, K. Grela, *Chem. Rev.,* 2009, **109**, 3708.

[7] I. Drugutan, V. Dragutan, L. Delaude, A. Demonceau, *Chimica Oggi / Chem. Today* 2009, **27**, 13.

[8] S. Díez-González, N. Marion, and S. P. Nolan, *Chem. Rev.,* 2009, **109**, 3612.

[9] G. C. Vougioukalakis, R. H. Grubbs, *Chem. Rev.,* 2010, **110**, 1746.

[10] A. M. Lozano-Vila, S. Monsaert, A. Bajek, F. Verpoort, *Chem. Rev.,* 2010, **110**, 4865.

[11] B. Alcaide, P. Almendros, *Chem. Eur. J.,* 2003, **9,** 1259**.**

[12] R. C. van der Drift, E. Bouwman, E. Drent, *J. Organomet. Chem.,* 2002, **650**, 1.

[13] J. E. Bäckvall, U. Andreasson, *Tetrahedron Lett.,* 1993, **34**, 5459.

[14] M.S. Kharasch, E.V. Jensen, W.H. Urry, *Science,* 1945,**102**, 128.

[15] H. Matsumoto, T. Nakano, Y. Nagai, *Tetrahedron Lett.,* 1973, **51**, 5147.

[16] F. Simal, A. Demonceau, A. F. Noels, *Tetrahedron Lett*., 1999, **40**, 5689.

[17] J. A. Tallarico, L. M. Malnick, M. L. Snapper, *J. Org. Chem.* 1999, **64**, 344.

[18] M. P. Wolfgang. A. Herrmann, *Applied Homogeneous Catalysis with Organometallic Compounds* VCH Weinhein, 2002**, 3,** 980**.**

[19] W. Buchowicz and J. C. Mol, *J. Mol. Catal. A: Chem.,* 1999, **148**, 97.

7.1 Introduction

Olefin metathesis has become a powerful tool for carbon–carbon bond formation in organic chemistry. Since the discovery of well-defined ruthenium benzylidene complexes several research groups have dedicated their efforts to synthesize related catalytic derivatives, with improved properties [1-9]. Among these developments ruthenium indenylidene catalysts bearing different ancillary ligands proved to have higher thermal stability and activity than their benzylidene counterparts [10-17].

Immobilization of ruthenium metathesis catalysts on solid supports has attracted much attention, because it opens up the possibility for easy catalyst-product separation and reuse as well as reduction of the residual ruthenium content in the organic products [18-20]. The immobilization of the ruthenium metathesis catalysts has been achieved via exchange of phosphine [21, 22], N-heterocyclic carbene (NHC) [23-27], alkylidene ligand [28-32] or exchange of halogen [33-36]. Various support materials have been utilized, which include inorganic materials, insoluble polymers, soluble polymers and ionic liquid functionalities [37]. However, Jeremias *et al*. [38] reported that, Grubbs' 1st generation catalyst loses its stability and quickly rearranges to a variety of unexpected products when introduced into a mesoporous silica matrix. This deactivation is associated with combination of confinement and surface effects. The problem can be solved by masking the surface silanol groups prior to the introduction of the Grubbs' catalyst.

We are interested on investigating the stability of the ruthenium indenylidene catalysts **1** and **2** immobilized on silica supported niobic acid. Niobic acid ($Nb_2O_5.nH_2O$), is an unusual solid acid possessing both Lewis and Brønsted acidic sites. The acid strength of the niobic acid is high (pKa = -2.12), corresponds to 70% H_2SO_4 in spite of its water content [39]. Both Lewis acidic sites and Brønsted acidic sites are retained in niobic acid supported on silica [40].

In the support used in this study, the niobia species and thus ruthenium indenylidene catalyst were only dispersed on surface of the silica and not inside the pores since the size of the molecule of niobium pentoxide precusor is larger relative to the pore size of the silica gel used, therefore, the niobium species could not possibly enter the pores of the silica. In this case the metathesis also took place on the surface different from the work of Jeremias *et al*. [38] in which the reactions proceed exclusively inside the pores.

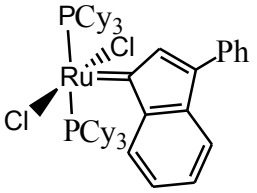

1

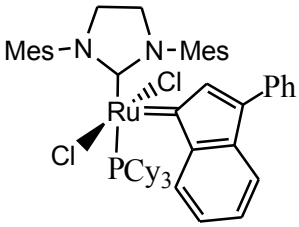

2

Scheme 1: Ruthenium indenylidene metathesis initiators.

To the best of our knowledge, up to this moment only one report is available about immobilization of ruthenium indenylidene catalysts. Ruthenium indenylidene metathesis initiators have been immobilized on macroporous poly-DVB through carbene to afford boomerang catalysts (Scheme 2) [41].These catalysts become homogeneous in the course of metathesis reactions and then return to heterogeneous after completion of the reactions in solution. Although these catalysts have not been tested on ring opening metathesis polymerization, in ring-closing metathesis they showed activities comparable or better than their homogeneous counterparts. Relative to poly-DVB, niobic acid as a support for catalysts has got an advantage in that, the immobilization of catalysts is very simple.

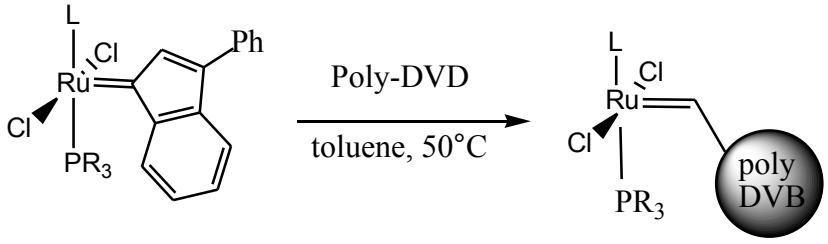

R = Cy, CyP

L =

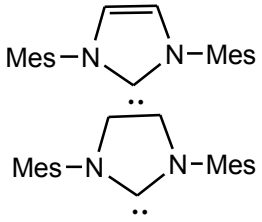

Scheme 2: Immobilization of ruthenium indenylidene catalysts on poly-DVB

7.2 Results and Discussion

7.2.1 Silica Gel as a Supporting Material

The right choice of supporting materials as well as the choice of suitable properties such as pore size, specific surface and chemical surface compositions is important factor influencing the immobilization of the catalysts. Amorphous and porous silica at present constitute the best catalyst support because they possess high surface area and porosity. In addition they have good mechanical properties, are stable and inert under reaction most conditions.

The chemical properties of amorphous silica are mostly governed by the chemistry of its surface, especially by the presence of silanol groups. Therefore, a change in structure due to thermal or subsequent chemical treatment can strongly alter the properties [42-44]. Concentration of silanol groups on the surface of silica is at a maximum on the pure silica gel and is about 8 Brønsted acid OH groups per nm^2. These are classified as isolated (or single), geminal and hydrogen-bonded (vicinal) hydroxyl groups (Scheme 3).

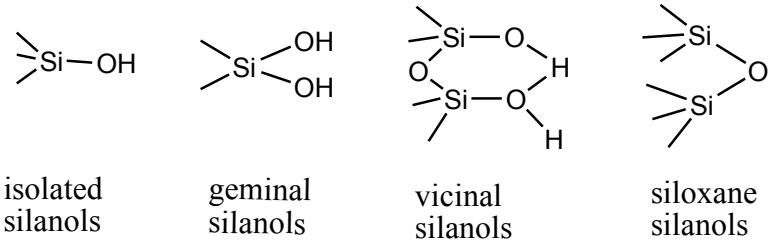

Scheme 3: Types of silanol groups.

By heating silica gel at a temperature between 100-200 °C a partial dehydroxylation of the silica gel takes place, reducing the number of OH groups to approximately 5.5 per nm^2. One-half of these OH groups are geminal pairs and the other half are vicinal ones. The number of hydroxyl groups decreases continuously as the temperature is raised, until at a temperature of 600-800 °C almost completely dehydroxylated silica with approximately 1 OH group per nm^2 is left [45].

The silica gel suitable for supporting niobic acid which can lead to evenly dispersion of niobic acid is one bearing only the isolated silanol groups (Scheme 4). In this study the silica support was prepared by heating the silica gel at 600 °C for 12 h in an oven followed by degassing at 200 °C.

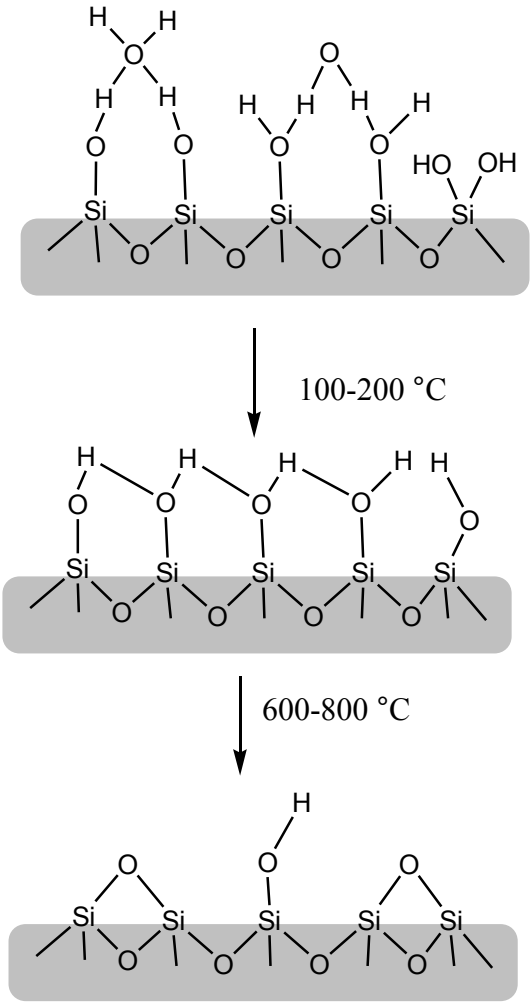

Scheme 4: Dehydration of a silica gel surface.

7.2.2 Dispersion of Niobic Acid Monolayer on Silica (NbO_x/SiO_2)

The dispersion of niobic acid monolayer on silica was carried out according to Verpoort *et al*. [46] with slight modification. The suspension of silica gel in hexane solution of niobium ethoxide was refluxed in argon atmosphere. The solid was recovered by filtration, washed with dry hexane and dried under vacuum. The hydrolysis was done by treating the obtained solid with NH_4OH (Scheme 5). Different concentrations of niobium ethoxide were used to achieve NbO_x/SiO_2 with different Si:Nb ratios.

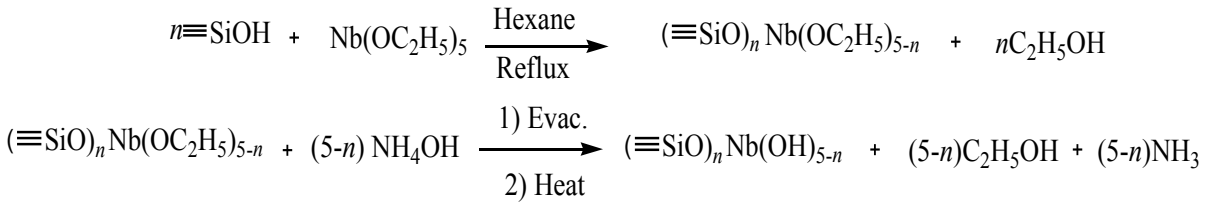

Scheme 5: Dispersion of niobic acid monolayer on silica.

The acidity of the resulting NbO_x/SiO_2 was improved by treating the materials with inorganic acids. This was done by immersing the supported niobic acid in either concentrated H_2SO_4 or H_3PO_4 solutions to obtain $SNbO_x/SiO_2$ and $PNbO_x/SiO_2$ respectively. It has been reported that adsorbed phosphate and sulphate is responsible for modifying the acidic character by decreasing the thermal mobility of niobium oxide and increasing its crystallization temperature [47]. The reaction between acids and moieties found on the surface of niobic acid can be described as shown in Scheme 6 [48,49].

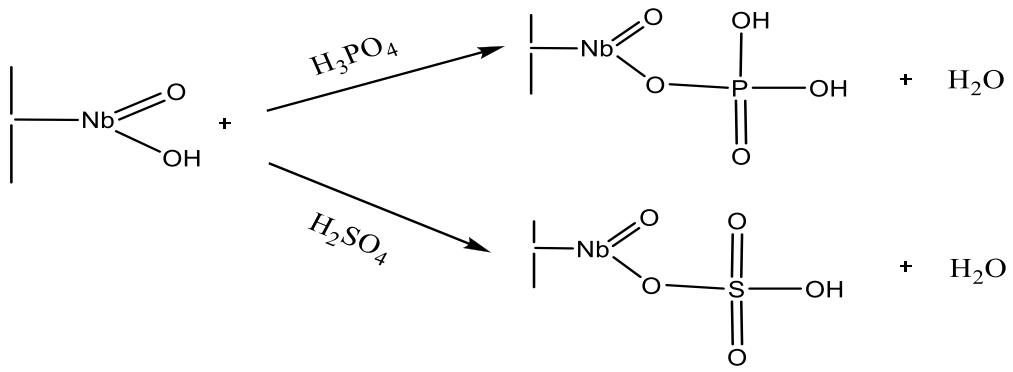

Scheme 6: Absorption of acids on niobic acid surface.

7.2.3 Immobilization of Ruthenium Catalysts on Prepared Support

The immobilization of catalysts was simple and straightforward. It was performed by adding to a stirred solution of known concentration of homogeneous catalyst in dichloromethane to the appropriate amount of support. In this way the supported catalysts were recovered by filtration, washing and drying in vacuum.

7.2.4 Determination of the Structures of the Supported Catalysts

The structure of supported catalysts was determined by monitoring HCl gas evolved during immobilization process. This was done by allowing the evolved HCl to react with known concentration of NaOH by passage of argon. Thereafter the NaOH solution was titrated with HCl to determine the amount consumed which is equivalent to the amount of HCl evolved during immobilization and thus number of chlorides decoordinated from the metal center (Figure 1). The result of titration reveals that all chlorides from the homogeneous indenylidene were replaced by oxygen from niobic acid support.

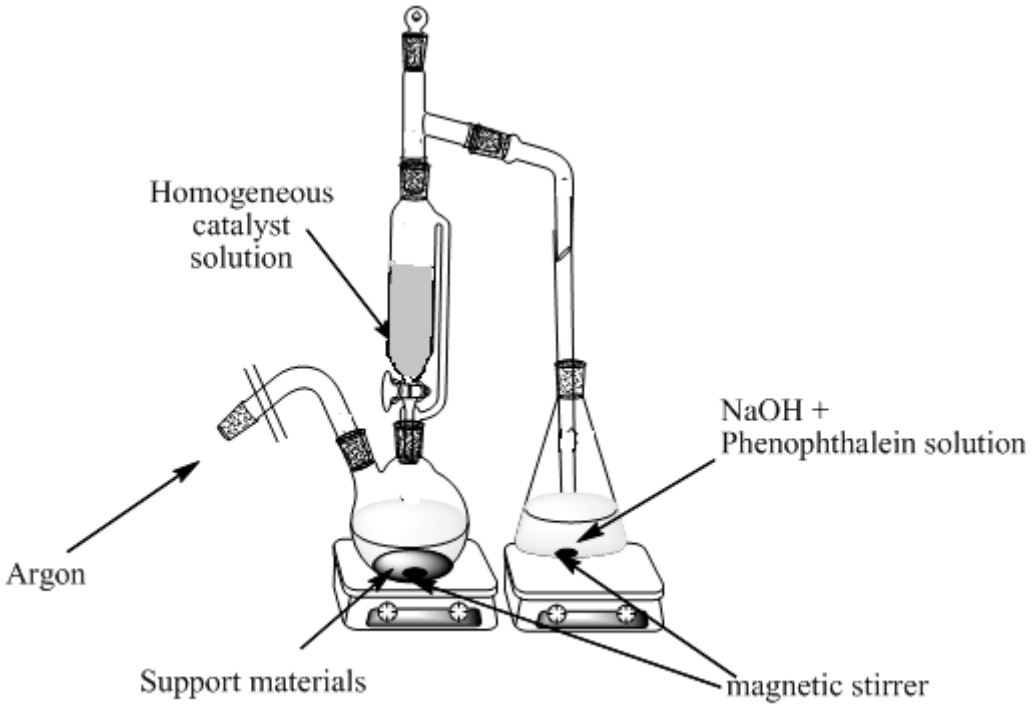

Figure 1: Determination of HCl produced during the immobilization of the catalysts.

On the other hand, as stated from theoretical point of view the pore size of the silica used in this study is smaller relative to the molecular size of the niobium ethoxide precursor. Therefore, the niobium species could not possibly enter the pore of the silica and is only dispersed on the surface of the silica and thus, also the catalyst is also immobilized only on the surface of the support. The fact that the immobilization takes place on the surface of the support and all

chlorides from the ruthenium indenylidene catalyst were replaced by oxygen from niobic acid enabled us to propose structures **3-8** for the supported catalysts (Scheme 7).

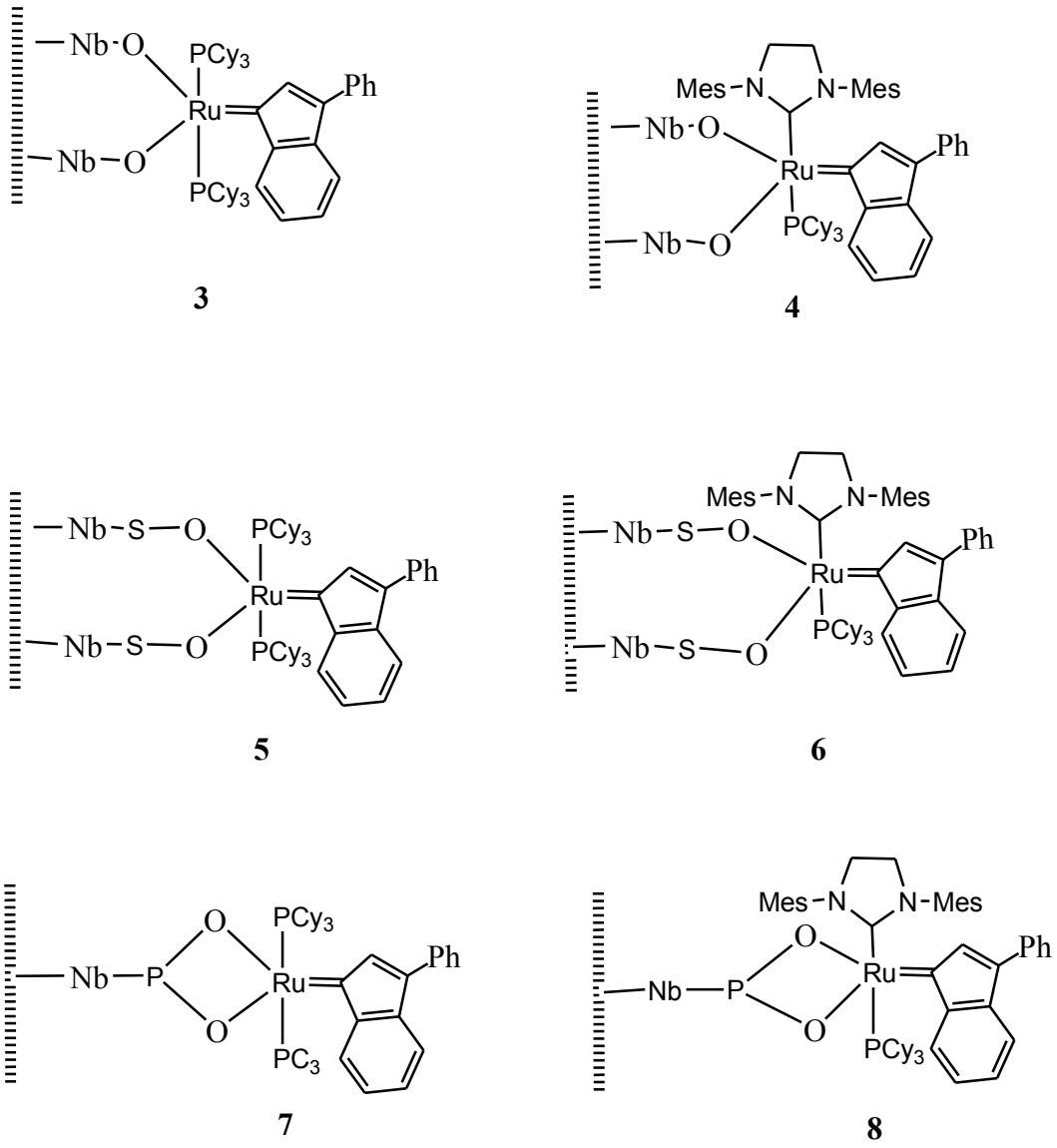

Scheme 7: Proposed structure of the prepared catalysts.

7.2.5 Characterization of Support and Supported Catalysts

The support and the supported catalysts were characterized by various techniques. The techniques include: Fourier Transform Infrared Spectroscopy (FTIR), pyridine adsorption, nitrogen adsorption and NMR.

7.2.5.1 Fourier Transform Infrared Spectroscopy (FTIR)

The quality of the prepared materials was proved by fourier transform infrared spectroscopy. Figure 2 represents the FTIR spectra of (a) SiO_2 preheated at 200 °C and (b) SiO_2 preheated at 600 °C. As seen from the figure, the spectrum of SiO_2 preheated at 200 °C shows the broad peak between 3000 $cm^{-1}$and 3800 cm^{-1}. This is due to stretching vibrations of different types of silanol groups combined together. In addition to the hydroxyl group vibration, the spectrum also shows the typical Si-O lattice vibrations that are, two broad bands between 2100 cm^{-1} and 1800 cm^{-1}, with medium intensity, a strong and broad band with two peaks in the region 1450 cm^{-1} to 900 cm^{-1} [50]. Nevertheless, the spectrum of SiO_2 preheated at 600 °C shows sharp a peaks at 3742 cm^{-1} which is attributed to free (non hydrogen bonded) surface hydroxyl groups in addition to other peaks related to Si-O lattice vibrations [50].

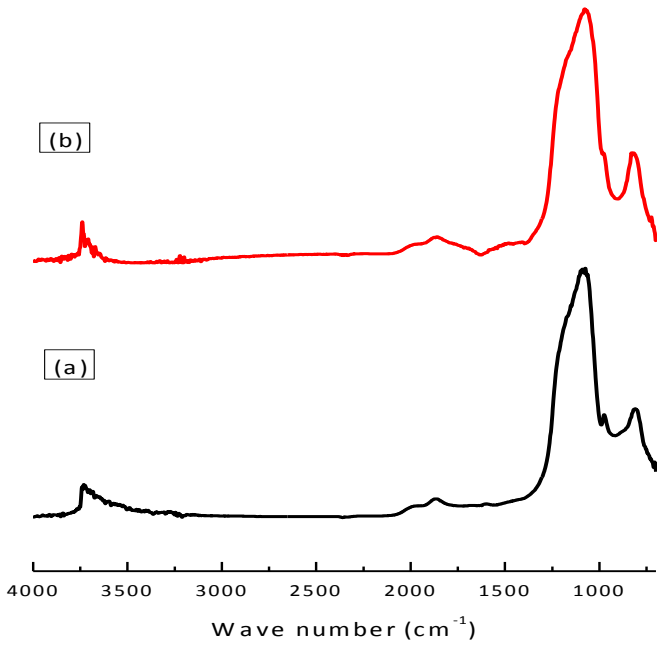

Figure 2: FTIR spectra of (a) SiO_2 preheated at 200 °C and (b) SiO_2 preheated at 600°C.

The silica gel preheated at 600 °C was modified to achieve niobic acid monolayer on silica and the spectrum is represented in Figure 3a. The spectrum has some changes with respect to that of the parent silica in the hydroxyl group vibration region. The spectrum exhibits sharp peak at 3729 cm^{-1} connected with a broad peak centered at 3546 cm^{-1}, which is assigned to the hydroxyl stretching mode of free Nb-O-H groups and hydrogen bonded hydroxyl groups respectively [51]. However, in the wave number area between 2000 cm^{-1} and 700 cm^{-1}, there is no significant difference between the spectrum of parent silica and that of the niobia modified one. This is because the infrared technique was not able to detect the presence of niobium due to the low vibration intensity compared to that of silica. Didik *et al.* reported similar observation [51].

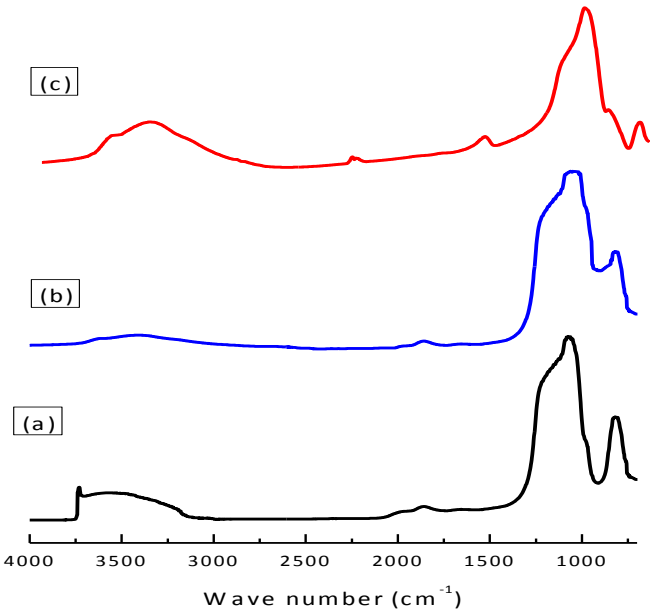

Figure 3: FTIR spectra of (a) NbO_x/SiO_2 (b) $SNbO_x/SiO_2$ (c) $PNbO_x/SiO_2$.

In the spectrum of $SNbO_x/SiO_2$ (3b), the expected peaks at 854, 1050 and 1206 cm^{-1} attributed to S-O and S=O bonds [52] are not observed due to the relatively high vibration intensity of Si-O. Likewise in the spectrum of $PNbO_x/SiO_2$ (3c) peaks at 1010 and 992 cm^{-1}, due the asymmetrical stretching oscillations of the P=O and P-O bonds are also masked by Si-O lattice vibrations [52].

The treatment of NbO_x/SiO_2 with sulfuric or phosphoric acid also caused disappearance of the signal previously located at 3729 cm^{-1} which was assigned to hydroxyl stretching mode of free Nb-O-H groups. Furthermore, the broad peak centered at 3546 cm^{-1}, due to hydrogen bonded hydroxyl groups in the starting material has shifted to 3410 cm^{-1} (in $SNbO_x/SiO_2$) and to 3385 cm^{-1} (in $PNbO_x/SiO_2$), because of the additional S–OH and P–OH groups introduced in the new materials [52].

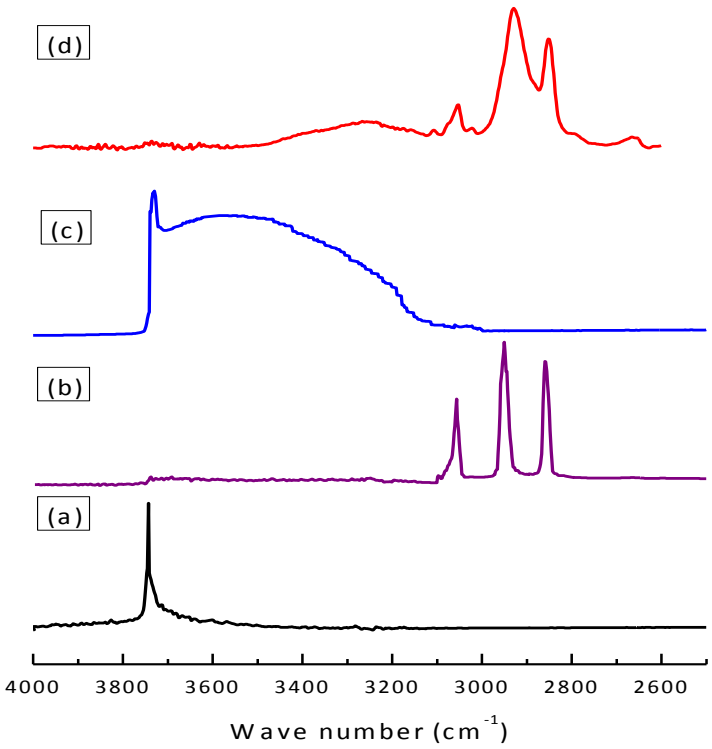

Figure 4: FTIR spectra of the (a) SiO_2, (b) free complex **1** (c) NbO_x/SiO_2 (d) catalyst **3** in the hydroxyl vibration region.

Immobilization of catalysts on the prepared supports was done and the spectra of the representative samples in the hydroxyl vibration region are shown in Figures 4 and 5. The spectrum of the supported catalysts (Figure 4d and 5) are different from that of NbO_x/SiO_2 (4c) as well as from that of SiO_2 (4a) but resembles that of free **1** (4b) in that the presence of peak due

to =C–H aromatic stretching vibration at 3056 cm^{-1} is still present implying the presence of the indenylidene carbene. In addition, two new peaks, at 2950 cm^{-1} and at 2860 cm^{-1} are also visible. These peaks are associated with the aliphatic C-H stretching mode deriving from the cyclohexyl groups.

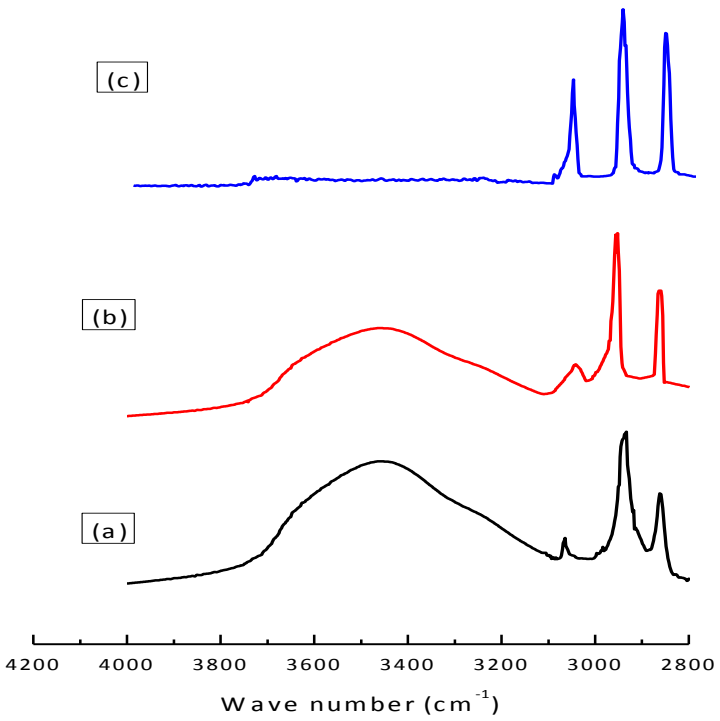

Figure 5: FTIR spectra of the (a) catalyst **7** (b) catalyst **5** (c) catalyst **4** in the hydroxyl vibration region.

In Figure 6 comparison is made between the spectrum of the catalyst **3** from 2000 cm^{-1} to 700 cm^{-1} with that of SiO_2 and NbO_x/SiO_2. The spectrum of catalyst **3** (c) shows new bands at 1545 cm^{-1} and 1560 cm^{-1} which are not seen in the spectra of SiO_2 (a) and NbO_x/SiO_2 (b). These signals which are corresponding to the aromatic ring-breathing mode [50] confirm that the immobilization was successful.

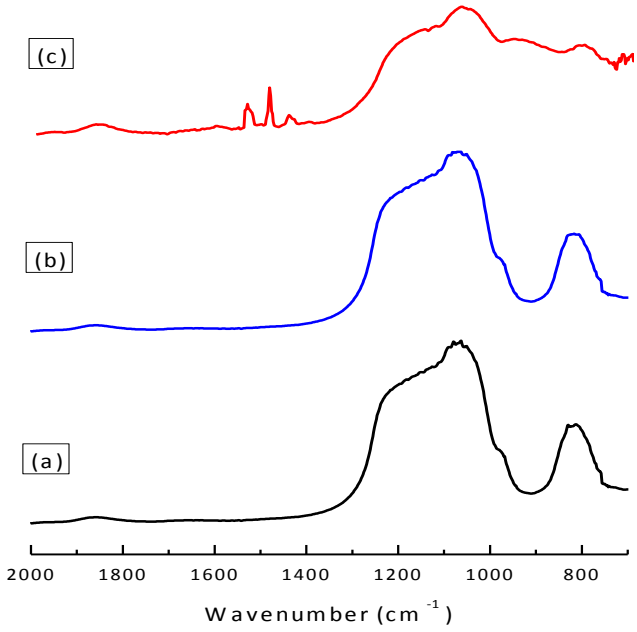

Figure 6: FTIR spectra of the (a) SiO_2, (b) NbO_x/SiO_2 (c) catalyst **3**.

7.2.5.2 Acidity Study

The acidity of the materials under investigation was monitored by FTIR using pyridine as a probe molecule. The bands at 1490 cm^{-1} and 1450 cm^{-1} were employed for the determination of the amount of Brønsted and Lewis acid sites respectively. The extinction coefficient (ε) of these bands is available in the literature [53]. For the extinction coefficient values related to the absorption bands at 1545 cm^{-1} (Brønsted sites) and at 1455 cm^{-1} (Lewis sites) the value1.67 cm μmol^{-1} and 2.22 cm μmol^{-1} were used respectively. Concentration of the acid was evaluated from the difference spectra relative to all samples after baseline correction.

Figure 7 represents spectra of the characteristic samples in the pyridine region. As seen from the figure SiO_2 (a) displays no vibration peaks between 1450 cm^{-1} and 1600 cm^{-1} which are due to adsorbed pyridine molecules. This means that there are no acidic sites present in the silica gel. The spectrum of silica supported niobic acid (b) exhibits peaks at 1450 cm^{-1}, 1490 cm^{-1}, 1540

cm^{-1} and 1600 cm^{-1}. The peak around 1450 cm^{-1} is due to Lewis acidic site while the vibration peak at around 1540 cm^{-1} is due to Brønsted acidic sites. The physically adsorbed pyridine molecule is observed at around 1600 cm^{-1}. The band at 1490 cm^{-1} is assigned to the pyridine molecule vibration band, which is independent of the acid site [51].

On the other hand, spectra of supported catalysts **3** and **4** (c and d respectively) in the pyridine regions show bands shown by their parent support except the band due to Brønsted acidic sites. This band has diminished in great percentage (Table 1), implying that immobilization is the result of interaction between niobium-Brønsted acidic sites and ruthenium complex.

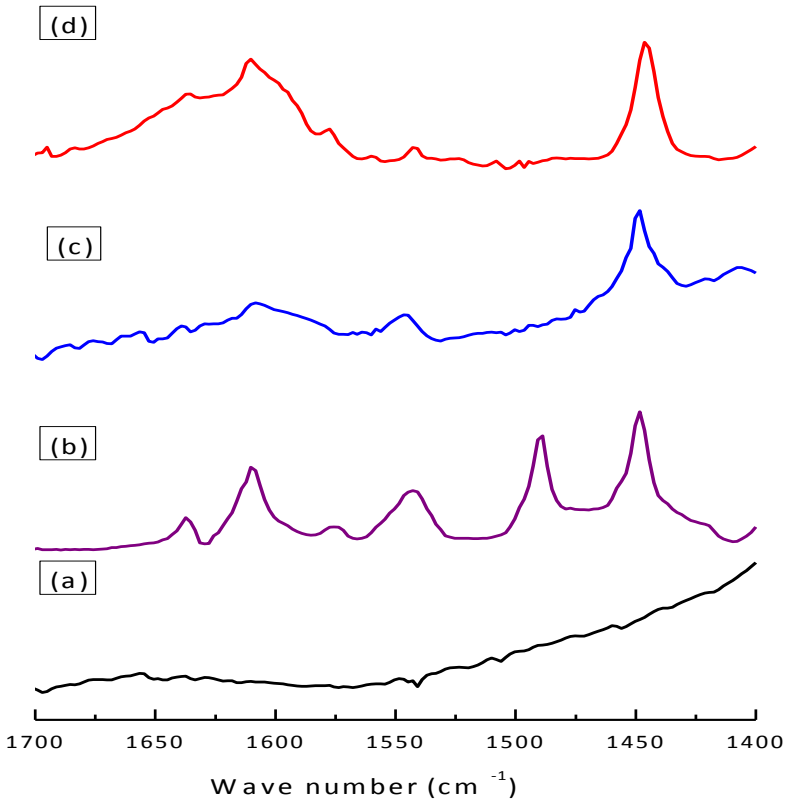

Figure 7: FTIR Spectrum of the (a) SiO_2 (b) Nb/SiO_2 (c) catalyst **3** (d) catalyst **4** in the pyridine region.

FTIR Spectra of the different supports in the pyridine region are compared in Figure 8. As seen from the figure, all support materials that are Nb/SiO_2, $SNbO_x/SiO_2$ and $PNbO_x/SiO_2$ display vibration peaks characteristics of adsorbed pyridine molecules. However, the quantitative amounts of acids sites are dissimilar for different materials (Table 1). The amount of Lewis acids and thus the total acidity in the $SNbO_x/SiO_2$ and $PNbO_x/SiO_2$ supports are higher than in the parent NbO_x/SiO_2 support due to the adsorbed phosphate and sulphate which improve the acidic character by decreasing the thermal mobility of niobium oxide and increasing its crystallization temperature [47]. On the other hand, the acidity of $PNbO_x/SiO_2$ has increased more compared to $SNbO_x/SiO_2$ which is most probably because of extra hydroxyl group available in $PNbO_x/SiO_2$. The assignment of the infrared peaks and bands to supports and supported catalysts are summarized in Table 2.

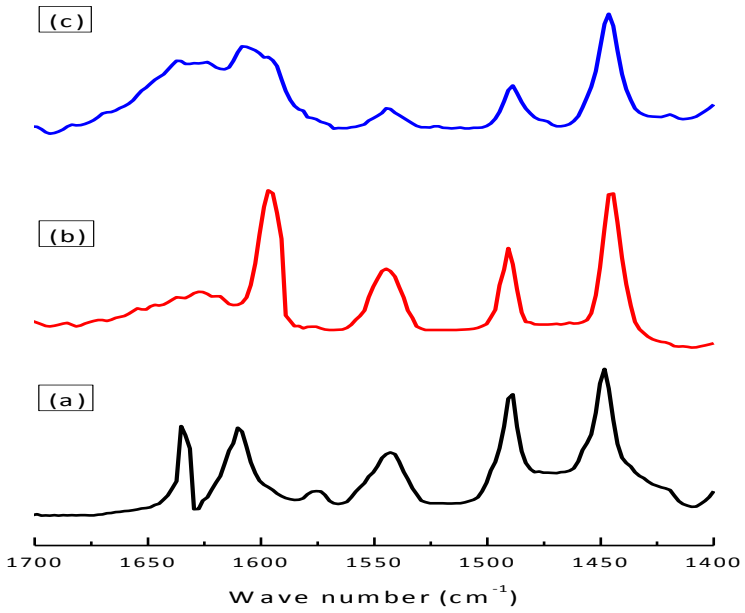

Figure 8: FTIR Spectrum of the (a) Nb/SiO_2 (b) $PNbO_x/SiO_2$ and (c) $SNbO_x/SiO_2$ in the pyridine region.

Table 1: Amount of acid of the samples

	Acidity in µmol /g		
Sample	**Brønsted acidity**	**Lewis acidity**	**Total acidity**
SiO_2	-	-	-
NbO_x/SiO_2	47	67	114
$SNbO_x/SiO_2$	43	72	115
$PNbO_x/SiO_2$	58	73	131
Catalyst **3**	2.35	65	67.35
Catalyst **4**	9.4	68	77.4
Catalyst **5**	10	70	80
Catalyst **6**	7.35	70	77.35
Catalyst **7**	6.50	60	66.50
Catalyst **8**	5.5	71	76.5

Table 2: Assignment of the infrared peaks and bands to the materials under investigation

Wave number, cm^{-1}	**Assignment**
2100, 1800,1450-900	Si-O vibration
3000, 3742, 3000	O-H stretching
1500-1630	O-H vibration
3729, 3546	Nb-O-H stretching
3410	S-OH
3385	P-OH
1545, 1560	Aromatic ring breathing mode
3056	=C-H aromatic stretching vibration
2950, 2860	C-H stretching
1450	Lewis acidic site
1490	Pyridine molecule vibration band
1540	Brønsted acidic site
1600	Physisorbed pyridine

7.2.5.3 Nitrogen Adsorption

Nitrogen adsorption was used for porosity characterization of prepared materials and the obtained results are summarized in Table 3. The results clearly indicate that there is no significant difference between the porosity characteristics of the support and supported catalysts. This implies that, the immobilization does not affect the morphology of the support and that the process takes place on the surface.

Table 3: Results of nitrogen adsorption studies on the representative samples.

Material	**Surface Area (BET) m^2/g**	**Pore Volume (BJH) cm^3/g**
NbO_x/SiO_2	244	0.6338
Catalyst **3**	243	0.6147
Catalyst **4**	241	0.6562
Catalyst **5**	240	0.6342
Catalyst **6**	242	0.6452
Catalyst **7**	239	0.6130
Catalyst **8**	230	0.6772

7.2.5.3.1 Adsorption-Desorption Isotherms of the Supports and Supported Catalysts

The adsorption-desorption isotherms of NbO_x/SiO_2 support and its respective supported catalysts **3** and **4** are depicted in Figure 9. All obtained isotherms exhibit a type IV behavior according to IUPAC classification [54]. The isotherms exhibit three rapid nitrogen uptake steps. The first rapid nitrogen uptake at low relative pressure (< 0.1) is attributed to a gradual microporous filling by the nitrogen. This is followed by a monolayer adsorption at relative pressure greater than 0.1. At relative pressure greater than 0.5, initial multilayer adsorption is observed causing capillary condensation. The isotherms show hysteresis loops at relative pressure greater than 0.6, which can be classified as type H1 according to IUPAC classification [54]. On the other hand, there is no significant difference in structure of isotherms among catalysts immobilized on different support materials as all isotherms resulting from different catalysts exhibit the type IV behavior according to IUPAC classification (Figure10).

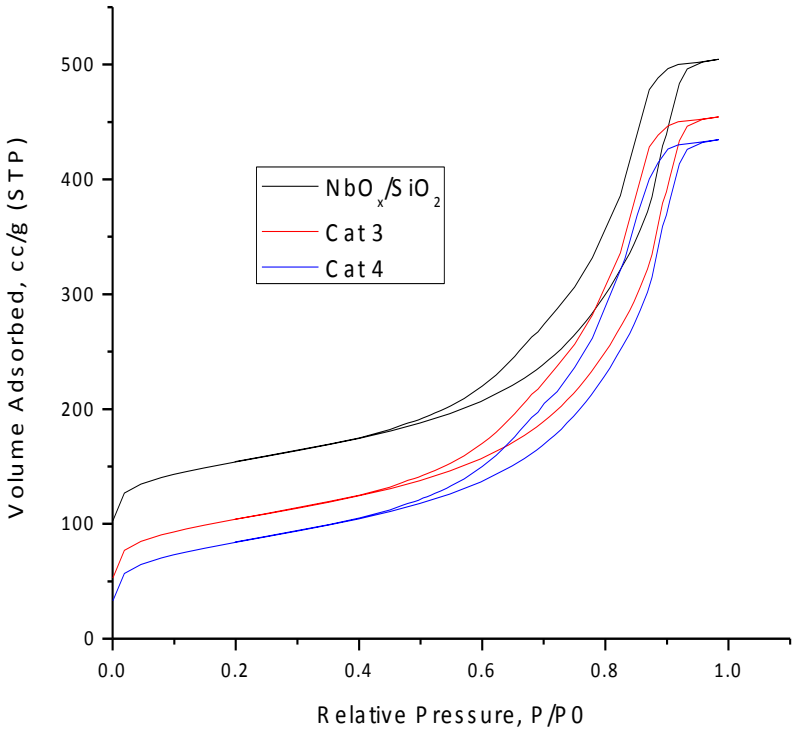

Figure 9: Adsorption-desorption isotherms of NbO_x/SiO_2, catalysts **3** and **4**.

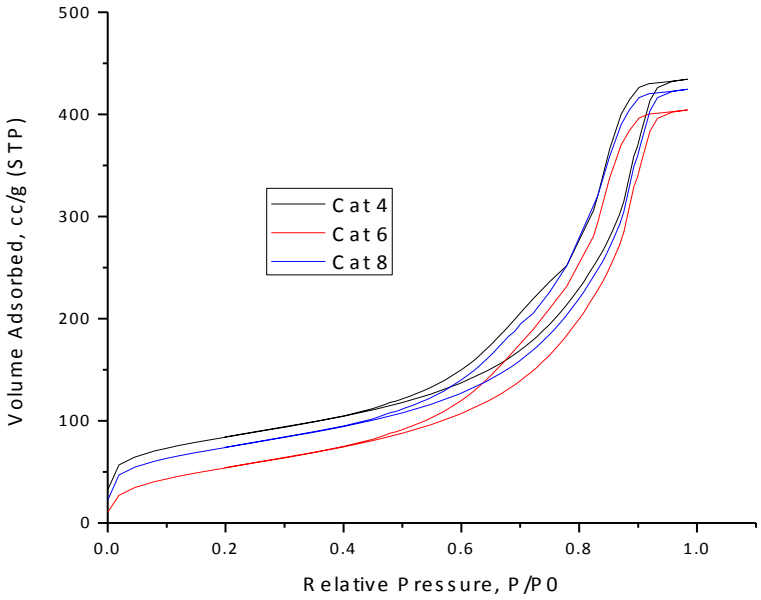

Figure 10: Adsorption-desorption isotherms of catalysts **4, 6** and **8**.

7.2.6 Catalytic Test

The supported catalysts **3-8** were tested on their activity in ring opening metathesis polymerization (ROMP) of norbornene and 1,5-*cis,cis*-cyclooctadiene (COD). As explained in the introductory part of this chapter only one report about immobilization of indenylidene catalyst is available up to this moment. In this report ruthenium indenylidene catalysts were supported on poly-DVB to afford boomerang catalysts. The afforded boomerang catalysts were tested in RCM but not in ROMP, therefore, they are not suitable benchmark for the performance of our catalysts.

7.2.6.1 ROMP of COD

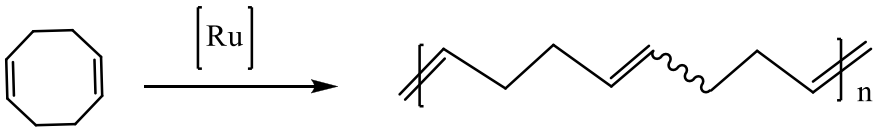

Figure 11 provides the reaction kinetics of catalysts **3** and **4** in ROMP of 800 equivalent COD at 90 °C while the activity of catalysts **5-8** in that reaction is represented in Table **4**. As seen from the figure and the table all catalysts which are the result of immobilized complex **2** have better perfomance than their corresponding catalysts which are the results of immobilized complex **1** which can be explained due to the presence of the strong electron donating NHC ligand. In addition, there is no significant difference in activity between the catalysts immobilized on Nb/SiO_2 and those immobilized $PNbO_x/SiO_2$ and $SNbO_x/SiO_2$. In all cases the supported catalysts **3-8** turned out to be less suited for polymerization relative to their homogeneous counter parts [55], not only in terms of activity but also stability as these catalysts decomposed after some time.

Table 4: Activity of catalysts **5-8** on ROMP of 800 equiv. COD at 90 °C after 1.5 hours of reactions.

Catalyst	% Conversion
5	90
6	100
7	95
8	100

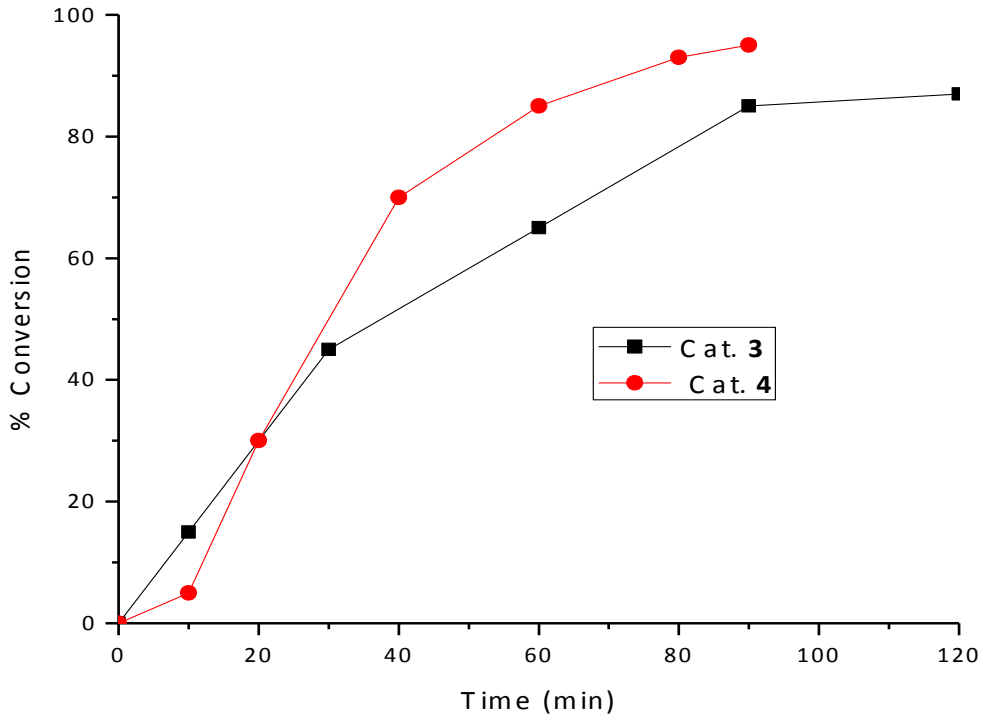

Figure 11: Kinetic plots for ROMP of 800 equiv. at 90 °C COD using catalyst **3** and catalyst **4**.

7.2.6.2 ROMP of Norbornene

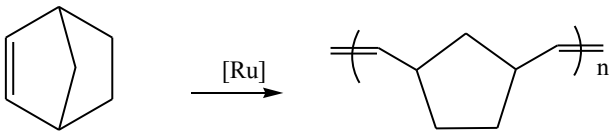

Figures 12 and 13 present the reaction kinetics of catalysts **3** and **4** respectively for ROMP of norbonene using 5000 and 10000 equivalents at room temperature. The activity of catalysts **4-8** on ROMP of norbonene with 10000 equivalents at room temperature is shown in Table 5. All supported catalysts initiated the polymerization reaction immediately, which is in contrast with the homogeneous benzylidene analogues (1st and 2nd generation Grubbs' catalysts). As in ROMP of COD, the catalysts resulted from complex **2** have better activity than the corresponding catalysts resulted from immobilized complex **1** and influence of acid treatment on activity of the catalysts is not significant.

Table 5: Activity of catalysts **5-8** on ROMP of 10000 equivalent norbornene at room temperature after 1.5 h of reactions.

Catalyst	% Conversion
5	95
6	100
7	95
8	100

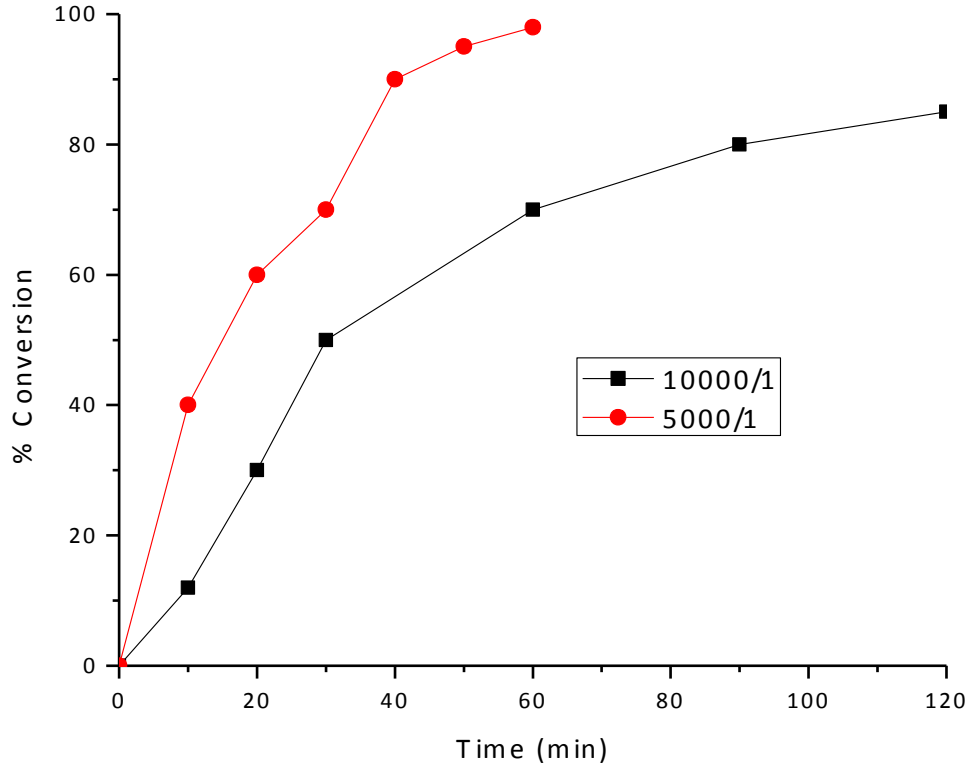

Figure 12: ROMP of norbornene by catalyst **4** at room temperature with different monomer: catalyst ratios.

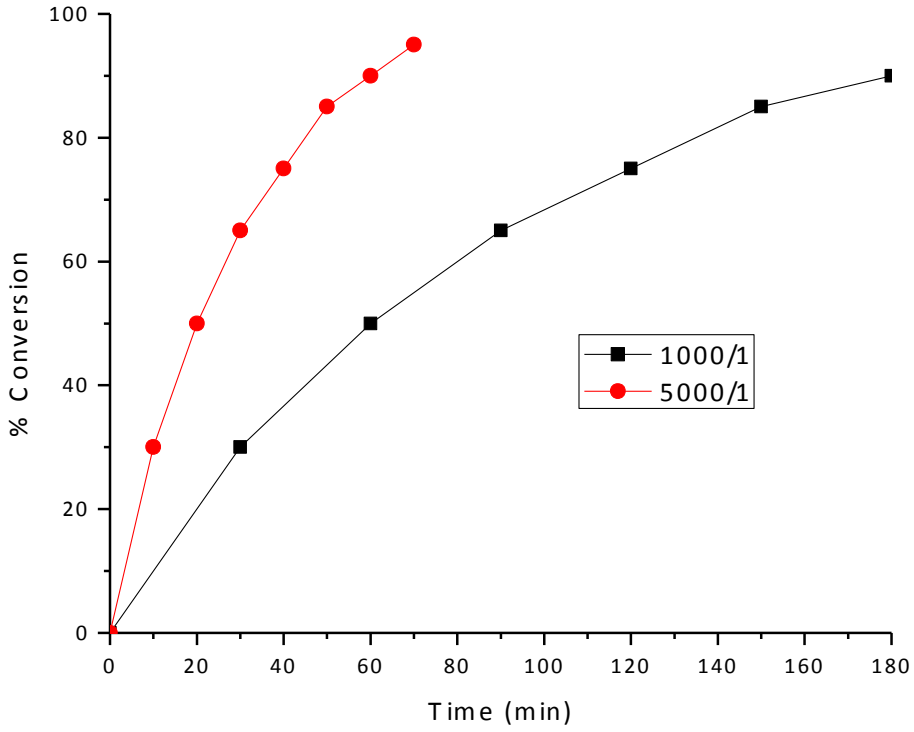

Figure 13: ROMP of norbornene by catalyst **3** at room temperature with different monomer: catalyst ratios.

7.2.7 Deactivation of the Catalysts

The metathesis activity of all immobilized catalysts diminishes slowly and was lost completely after a weak. The rate of decomposition of catalysts **3** and **4** was monitored in ROMP of COD using 300 equivalents of COD (Figure 14). The samples of the catalyst were taken after every 24 hours from the same batch and all reactions were stopped after 30 minutes. The average rate of decrease in the polymerization yield was found to be about 0.67% per hour for catalyst **3** and about 0.57% per hour for catalyst **4**. Nevertheless, all catalysts immobilized on $PNbO_x/SiO_2$ and $SNbO_x/SiO_2$ turn out to be less stable than their corresponding ones immobilized on NbO_x/SiO_2 as these catalysts decomposed completely after only two days of their preparation (Table 6).

Table 3: Time for complete decomposition of the catalysts

Catalyst	Time (hour)
3	150
4	170
5	48
6	48
7	48
8	48

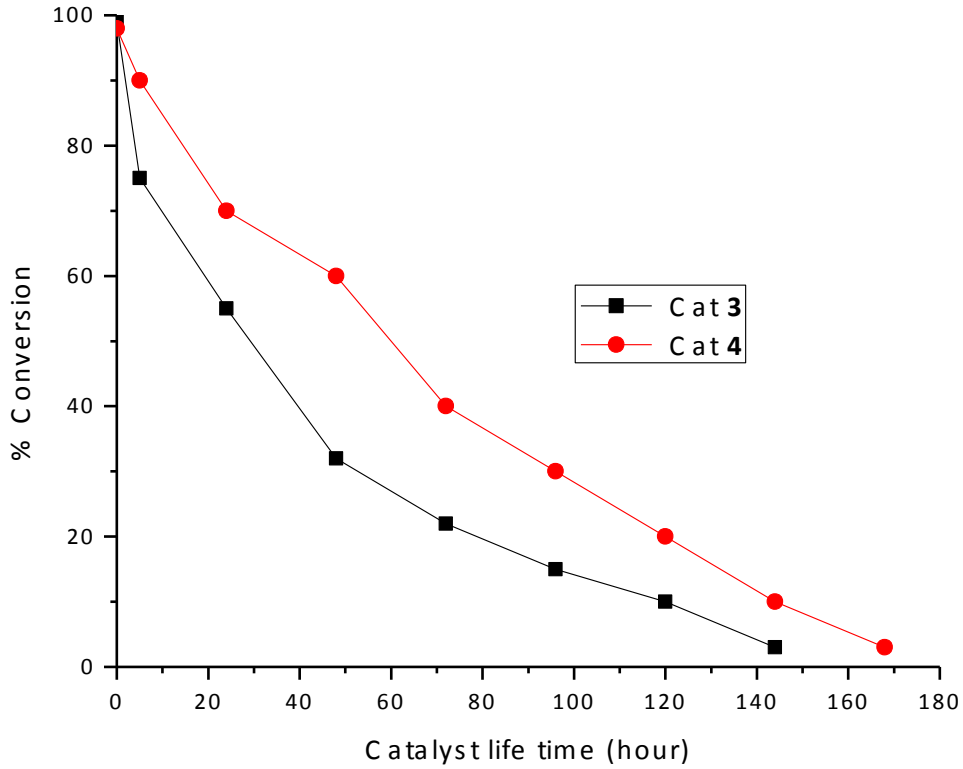

Figure 14: Deactivation of catalyst **4** and catalyst **3** in ROMP of 300 equiv. COD.

Infrared measurements were performed to investigate the structure of the decomposed catalysts. The result of the representative catalyst **4** is shown in Figure 15. As seen from the figure the peak at 3056 cm^{-1} which is associated with =C–H aromatic stretching vibration of the indenylidene

carbene disappeared, indicating that the active site of the catalysts is totally lost. Since precautions were made for save keeping the immobilized catalysts, we propose that the water molecules found in hydrated niobium oxide slowly migrate to the active site of the catalyst and cause changes in molecular structure of the catalyst.

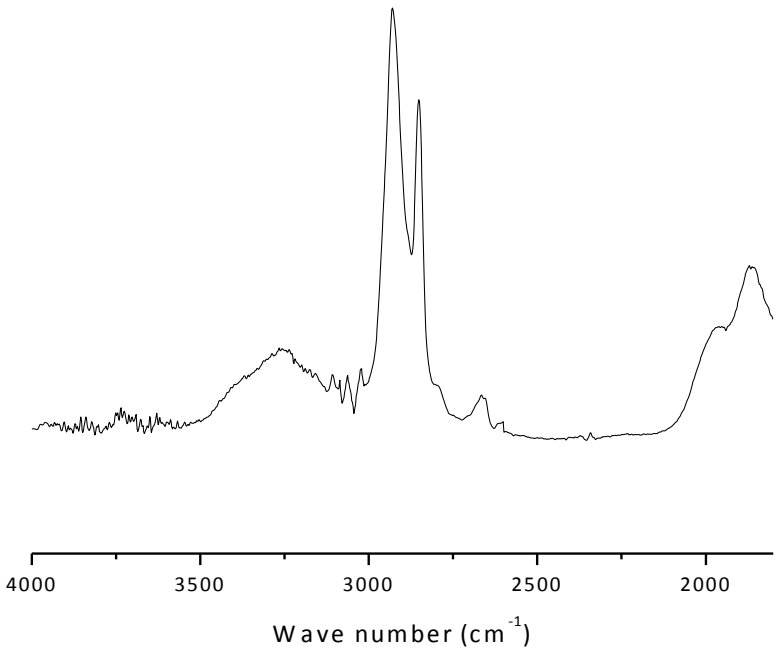

Figure 15: FTIR spectrum for deactivated catalyst **4**.

The detail mechanism for the decomposition of catalysts is still under investigation, however, the following reaction is proposed (Scheme 8).

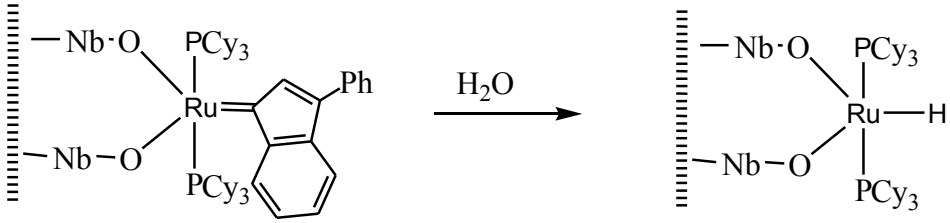

Scheme 8: Proposed decomposition of catalyst **3** due to water molecule from niobic acid.

7.3 Experimental

7.3.1 Dispersion of Niobic Acid Monolayer on Silica (NbO_x/SiO_2)

About 6.0 g of silica gel was dried at 500 °C for 12 h in oven followed by degassing the dried silica at 200 °C under vacuum for 1 h. The dried silica was immediately added to a stirred solution of 4.1 mmol of niobium ethoxide in dry hexane (60 ml) and refluxed for 1h under argon. After an hour the solid was filtered under argon atmosphere, washed with dry hexane and dried for an hour under vacuum at 200 °C. Thereafter, the solid was treated with 50 ml of NH_4OH (1 M) for about an hour followed by filtration and drying for 2 h at 200 °C under vacuum which yielded 5.0 g the niobic acid monolayer on silica (NbO_x/SiO_2).

7.3.2 Treatment of $NbOx/SiO_2$ with mineral acids

About 2.0 g of NbO_x/SiO_2 was added to 50.00 ml of either concentrated H_2SO_4 or 1.5 M of phosphoric acid solution, and the mixture was refluxed for 4 h at 70 °C. The solids obtained from these treatments were exhaustively washed with distilled water until all excess acid was removed, and dried at 200 °C for 3 h under vacuum. The final materials were designated as $PNbO_x/SiO_2$ (yield 2.0 g) and $SNbO_x/SiO_2$ (yield 2.0 g).

7.3.3 Immobilization of Ruthenium Catalysts on Prepared Support

The immobilization of catalysts was simple and straightforward. It was performed by adding to a stirred solution of homogeneous catalyst in dichloromethane (20 ml, 0.5 mM), 1.0 g of support. The mixture was stirred for about an hour under argon atmosphere. After that, the supported catalyst was filtered, washed with dichloromethane and dried in vacuum (yield 1.0 g).

7.3.4 Study of Acidity

Acidity of the samples under investigation was monitored by FTIR spectroscopy using pyridine as a probe molecule. Pyridine was dried on molecular sieves for one week before being used. A typical experiment was carried out according to the following procedure: The dry samples were outgassed at 200 °C for about an hour in the environmental chamber of the spectrometer before pyridine adsorption. Pyridine was adsorbed at room temperature (20 °C) for a minute followed by desorption at 150 °C for 30 minutes before spectrum collection. The bands at 1540 cm^{-1} and

1450 cm^{-1} were employed for the determination of the amount of Brønsted and Lewis acid sites respectively. The extinction coefficient (ε) of these bands is available in the literature[17]. The used extinction coefficient values related to the absorption bands at 1545 cm^{-1} (Brønsted sites) and at 1455 cm^{-1} (Lewis sites) are 1.67 and 2.22 μmol^{-1} respectively. Acid concentrations were evaluated from the difference spectra after baseline correction.

7.3.5 Determination of the Structure of the Supported Catalysts

The structure of supported catalysts was indirectly determined by monitoring HCl gas evolved during immobilization process as follows: The known concentration (20 ml, 0.5 mM) of homogeneous catalyst in dichloromethane was dropped in a two neck round bottomed Schlenk flask contain 1.0 g of dry support. The evolved HCl gas was carried out by passage of dry argon and allowed to react with 0.002 M (20 ml) of NaOH. The amount of NaOH consumed was determined and found to be equivalent to the amount of HCl evolved during immobilization and thus with the number of substituted chloride.

7.3.6 Characterization of Supports and Supported Catalysts

The supports and the supported catalysts were characterized by fouier transform infrared spectroscopy and nitrogen adsorption.

7.3.6.1 Nitrogen Physisorption Study

Before analysis about 0.02 g of the sample in a sample cell was degassed in a degassing station at 120 ºC for 3 hours. The sample cell was then connected to the analysis pot, where the sample was analysed for both adsorption and desorption process. In the analysis pot, the sample cell with sample was cooled using liquid nitrogen at a temperature of 77.2 K. After completion of the analysis, the analyzed sample was accurately re-weighed and the new sample weight was used for data analysis. The BET method was used to analyze the surface area, whereas the BJH method was employed for pore size distributions determination.

7.3.6.2 Fourier Transform Infrared Spectroscopy

Potassium bromide (KBr) was used as the diluents (matrixes) for sample measurements. About 1.0 mg of the dried sample and amount 30 mg of KBr were finely ground. The powder mixture was then mounted in a sample holder through which the light beam of the spectrometer was

passed. The spectra were recorded at room temperature and background spectrum of finely ground anhydrous KBr was subtracted from the spectra. The spectrum obtained was used for qualitative determination of functional groups

7.3.7 Catalytic Tests

The supported catalysts were tested on their activity and stability for ROMP of norbornene and of cyclootadiene.

7.3.7.1 ROMP of Norbornene

The catalyst (1.0 μmol) was mixed with an appropriate amount of norbornene solution in dichloromethane in 15 ml vial. The reaction mixture was stirred and the reaction was stopped at different time intervals and the polymerization was stopped by addition of 2-3 ml of an ethylvinylether/BHT. The solution was stirred till the deactivation of the catalytically active species was completed. To remove the heterogeneous catalyst from the reaction mixture, the formed gel was dissolved in 50 ml THF and the catalyst was filtered off. The polymer was re-precipitated by pouring the filtrate into 50 ml methanol (containing 0.1% BHT). The obtained white polymers were then filtered off and dried in vacuum overnight.

7.3.7.2 ROMP of Cyclooctadiene

The catalyst (1.0 μmol) and appropriate amount of cyclooctadiene solution in toluene were mixed in 15 ml vial and the temperature was raised to 90 °C. The reaction mixture was stirred and the reaction was stopped at different time intervals and the polymerization was stopped by addition of 2-3 ml of an ethylvinylether/BHT. The solution was stirred till the deactivation of the catalytically active species was completed. To remove the heterogeneous catalyst from the reaction mixture, the formed gel was dissolved in 50 ml THF and the catalyst was filtered off. The polymer was re-precipitated by pouring the filtrate into 50 ml methanol (containing 0.1% BHT). The obtained white polymers were then filtered off and dried in vacuum overnight.

7.3.7.3 ROMP of Cyclooctadiene for Decomposition Study

The sample of catalyst (1.0 μmol) was taken from the same batch after every 24 hours and the first sample was taken immediately after catalyst preparation. The catalyst sample and 0.3 mmol

cyclooctadiene in toluene were mixed in 15 ml vial and the temperature was raised to 90 °C. The reaction mixture was stirred and all reactions were stopped after 30 minutes. The polymerization was stopped by addition of 2-3 ml of an ethylvinylether/BHT. The solution was stirred till the deactivation of the catalytically active species was completed. To remove the heterogeneous catalyst from the reaction mixture, the formed gel was dissolved in 50 ml THF and the catalyst was filtered off. The polymer was re-precipitated by pouring the filtrate into 50 ml methanol (containing 0.1% BHT). The obtained white polymers were then filtered off and dried in vacuum overnight.

7.4 References

[1] A. Fürstner, Angew. *Chem., Int. Ed.,* 2000, **39**, 3013.

[2] T. M. Trnka, R. H. Grubbs, *Acc. Chem. Res.,* 2001, **34**, 18.

[3] Handbook of Metathesis; R. H., Grubbs, Ed.; Wiley-VCH: Weinheim, 2003, 1204.

[4] D. Astruc, *New J. Chem.,* 2005, **29**, 42; (e) P. H. Deshmukh, S. Blechert, *Dalton Trans.,* 2007, 2479.

[5] C. Samojłowicz, M. Bieniek, K. Grela, *Chem. Rev.,* 2009, **109**, 3708.

[6] I. Drugutan, V. Dragutan, L. Delaude, A. Demonceau, *Chimica Oggi/Chem. Today,* 2009, **27**, 13.

[7] S. Díez-González, N. Marion, and S. P. Nolan, *Chem. Rev.,* 2009, **109**, 3612.

[8] G. C. Vougioukalakis, R. H. Grubbs, *Chem. Rev.,* 2010, **110**, 1746.

[9] A. M. Lozano-Vila, S. Monsaert, A. Bajek, F. Verpoort, *Chem. Rev.,* 2010, **110**, 4865.

[10] L. Jafarpour, H. J. Schanz, E. D. Stevens, S. P. Nolan, *Organometallics,* 1999, **18**, 5416.

[11] V. Dragutan, I. Dragutan, F. Verpoort, *Platinum Met. Rev.,* 2005, **49**, 33.

[12] T. Opstal, F. Verpoort, Angew. *Chem. Int. Ed.,* 2003, **42**, 2876.

[13] R. Castarlenas, P. H. Dixneuf, *Angew. Chem. Int. Ed.,* 2003, **42**, 4524.

[14] T. Opstal, F. Verpoort, *Synlett.,* 2002, **6**, 935.

[15] T. Opstal, F. Verpoort, *New J. Chem.,* 2003, **27**, 257.

[16] A. M. Lozano Vila, S. Monsaert, R. Drozdzak, S. Wolowiec, Verpoort, F. *Adv. Synth. Catal*., 2009, **351**, 2689.

[17] P. M. S. Hendrickx, R. Drozdzak, F. Verpoort, J. C. Martins, *Magn. Reson. Chem.,* 2010, **48**, 443.

[18] M. R. Buchmeiser, *New J. Chem.,* 2004, **28**, 549.

[19] M. R. Buchmeiser, *Chem. Rev.,* 2009, **109**, 303.

[20] C. Copéret, J.-M. Basset, *Adv. Synth. Catal.,* 2007, **349**,78.

[21] S. T. Nguyen, R. H. Grubbs; *J. Organomet. Chem*., 1995, **497**, 195.

[22] F. Verpoort, P. Jacobs, D. De Vos, K. Melis, *J. Mol. Cat., A,* 2001, **169**, 47.

[23] (a) S. C. Schurer, S. Gessler, N. Buschmann, S. Blechert, *Angew. Chem. Int. Ed.,* 2000, **39**, 3898. (b) Monge-Marcet, R. Pleixats, X. Cattoën, M. W. Chi Man, *Tetrahedron,*

2013, **69**, 341. (c)A. Monge-Marcet, R. Pleixats, X. Cattoën, M. W. Chi Man, *J. Mol. Cat., A,* 2012, **357**, 59.

[24] S. Randl, N. Buschmann, S. J. Connon, S. Blechert, *Synlett.,*2001, **10**, 1547.

[25] M. Mayr, B. Mayr, M. R. Buchmeiser, *Angew. Chem. Int. Ed*., 2001, **40**, 3839.

[26] M. Mayr, M. R. Buchmeiser, K. Wurst, *Adv. Synth. Catal.,* 2002, **344**, 712**.**

[27] S. Pruhs, C. W. Lehmann, A. Furstner, *Organometallics*, 2004, **23**, 280.

[28] M. Ahmed, A. G. M. Barrett, D. C. Braddock, S. M. Cramp, P. A. Procopiou, *Tetrahedron Lett.,* 1999, **40**, 8657.

[29] A. G. M. Barrett, S. M. Cramp, R. S. Roberts, *Org. Lett*., 1999, **1**, 1083.

[30] M. Ahmed, T. Arnauld, A. G. M. Barrett, D. C. Braddock, P. A. Procopiou, *Synlett*, 2000, 1007.

[31] L. Jafarpour, S. P. Nolan, *Org. Lett.,* 2000, **2**, 4075.

[32] L. Jafarpour, M. P. Heck, C. Baylon, H. Man Lee, C. Mioskowski, S. P. Nolan, *Organometallics,* 2002, **21**, 671.

[33] P. Nieczypor, W. Buchowicz, W. J. N. Meester, F. P. J. T. Rutjes, J. C. Mol, *Tetrahedron Lett.,* 2001, **42**, 7103.

[34] J. O. Krause, S. H. Lubbad, O. Nuyken, M. R. Buchmeiser, *Adv. Synth. Catal.,* 2003, **345**, 996.

[35] J. O. Krause, K. Wurst, O. Nuyken, M. R. Buchmeiser, *Chem. Eur. J.,* 2004, **10**, 778.

[36] J. O. Krause, S. H. Lubbad, O. Nuyken, M. R. Buchmeiser, *Macromol. Rapid Commun.,* 2003, **24**, 875.

[37] (a) P. Śledź, M. Mauduit, K. Grela, *Chem. Soc. Rev.,* 2008, **37**, 2433. (b) M. Bru, R. Dehn, J. H. Teles, S. Deuerlein, M. Danz, I. B. Müller, M. Limbach, *Chem. Eur. J.* 2013, **19**, 11661. (c) A. Monge-Marcet, R. Pleixats, X. Cattoën, M. W. Chi Man, *J. Sol-Gel Sci. Technol.,* 2013, **65**, 93.

[38] S. Polarz, B. Völker and F. Jeremias, *Dalton Trans.,* 2010, **39**, 577.

[39] L. Jafarpour, M. P. Heck, C. Baylon, H. M. Lee, C. Mioskowski, S. P. Nolan, *Organometallics,* 2002*,* **21**, 671.

[40] K. Tanabe, *Mater. Chem. Phys.,* 1987, **17**, 217.

[41] L. Jafarpour, M. P. Heck, C. Baylon, H. M. Lee, C. Mioskowski, S. P. Nolan, *Organometallics,* 2002*,* **21**, 671.

[42] M. Ziolek, *Catal. Today*, 2003, **78**, 47.

[43] S. Collins, W. M. Kelly, D. A. Holden, *Macromolecules,* 1992, **25**, 1780.

[44] J. C. W. Chien, D. He, *J. Polym. Sci., Part A: Polym. Chem.,*1991, **29**, 1603.

[45] C. Janiak, B. Rieger, *Angew. Makromol. Chem.,* 1994, **215**, 47.

[46] J. C. W. Chien, *Top. Catal.,* 1999, **7**, 23.

[47] F. Verpoort, G. De Doncker, A. R. Bossuyt, L. Fiermans, L. Verdonck, *J. Electron. Spectrosc. Relat. Phenom.,* 1995, **73**, 271.

[48] K. Tanabe *Catal. Today,* 2003, **78**, 65.

[49] M.S.P. Francisco, W.S. Cardoso, Y. Gushikem, R. Landers, Y.V. Kholin, *Langmuir*, 2004, **20**, 8707.

[50] M. K. de Pietre, L. C. P. Almeida, R. Landers, R. C. G. Vinhas, F. J. Luna, *Reac. Kinet. Mech. Cat.*, 2010, **99**, 269**.**

[51] T. Takei, K. Kato, A. Meguro, and M. Chikazawa, *Colloids Surf. A: Physicochem. Eng. Asp.*, 1999, **77**, 1590.

[52] P. Didik, R. Zainab, E. Salasiah and N. Hadi, *Akta Kimindo,* 2005, **1**, 11.

[53] F. Jardim W. Jardim M. R. Alberici C. M. Canela, J. *Photochem. Photobiol. A,* 1998, **112**, 73.

[54] C. A. Emis, *J. Catal.,* 1993, **141**, 347.

[55] K. S. W. Sing, D. H. Everet, R. A. W. Haul, L. Moscou, R. A. Pierotti, J. Rouquerol, and T. Siemieniewska, *Pure Appl. Chem.,* 1985, **57**, 603.

8.0 Immobilization of Indenylidene Ruthenium Catalysts on Silica Supported Methylaluminoxane

8.1 Introduction

In previous chapter we reported the immobilization of the ruthenium indenylidene metathesis catalysts **1** and **2** on the niobic acid on silica through the exchange of the chloride ligands of the indenylidene initiators with the oxygen of the supported niobic acid. Although the supported catalysts **3**-**8** (Figure 1) were not stable, they showed moderate activity on the ring-opening metathesis polymerization of norbornene and 1,5-*cis,cis*-cyclooctadiene. During the immobilization of ruthenium indenylidene catalysts in the niobic acid only Brønsted acidic sites were used and Lewis acidic sites stayed nearly untouched. We are interested on investigating what will happen when a solid with only Lewis acidic sites is used as a support. In this chapter we report on the immobilization of the ruthenium indenylidene catalysts (**1** and **2**) on a strong Lewis acidic-silica supported methylaluminoxane (MAO). The immobilized MAO has been successfully used in heterogenization of polymerization catalysts in which it served as weekly coordinating anion and provided vacant reaction sites around the transition metal center [1,2]. We hope that, silica supported MAO can also serve as suitable support for immobilization of ruthenium indenylidene metathesis catalysts **1** and **2**.

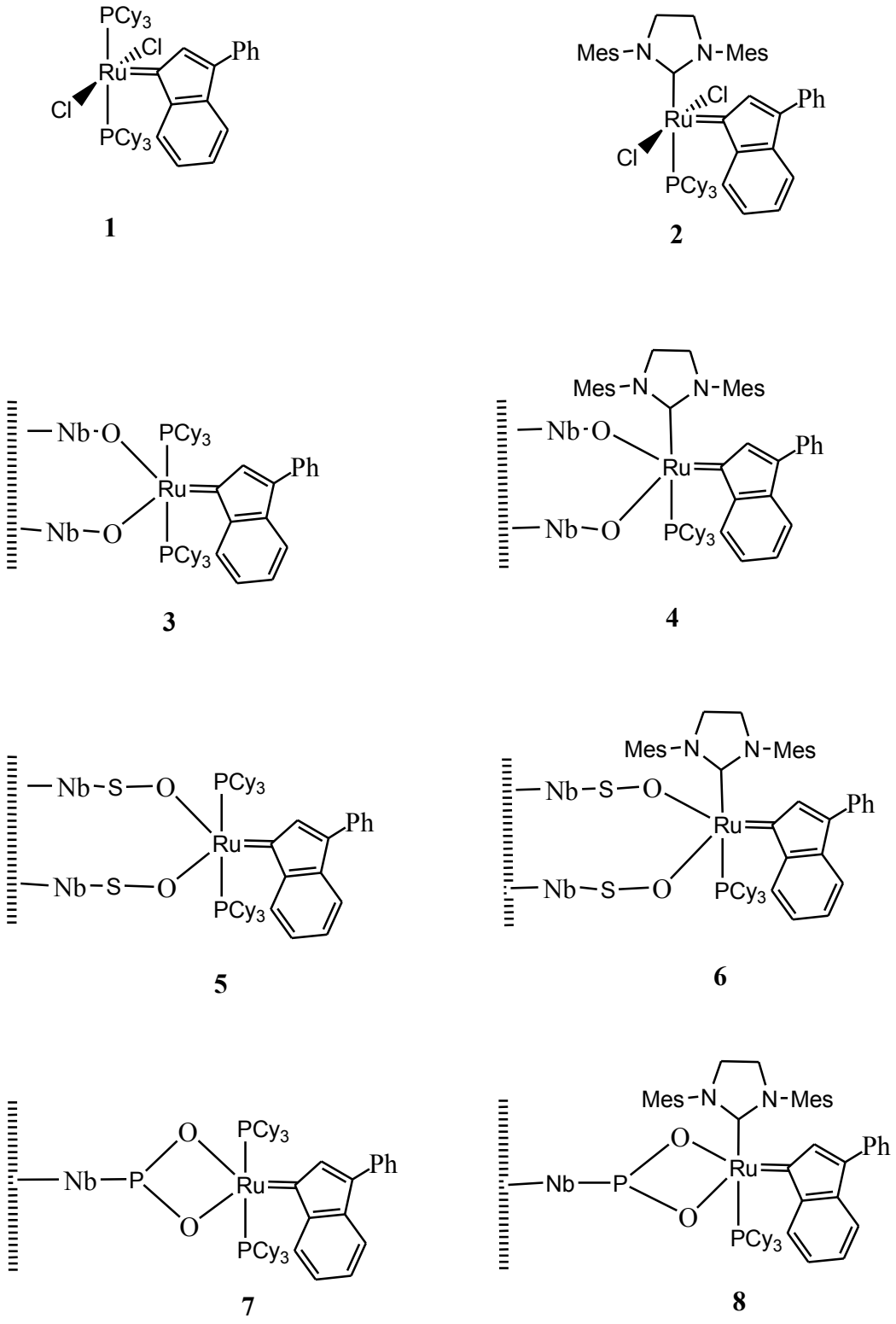

Figure 1: Ruthenium indenylidene catalysts.

8.2 Results and Discussion

8.2.1 Preparation of Silica Supported MAO

As in previous chapter we have chosen to use silica gel as support for MAO due to its suitable properties like stability and inertness under reaction conditions. Silica supported MAO can be prepared either *in situ* by controlled hydrolysis of trimethylaluminium (TMA) with the silanol groups and physisorbed water of the silica support [3] or by adsorption of pre-synthesized MAO on support [4]. The immobilized MAO prepared *in situ* has an advantage over that prepared by the grafting approach in that alumoxane is distributed uniformly on the support. In this respect the immobilized MAO used in this work is the one prepared *in situ* according to the procedure of Chang with little modification [5].

Pretreatment of the support was done by treating the silica gel with enough water to form a slurry mixture which was then air dried at room temperature to a free state to form water-impregnated silica gel. The water content of this kind of material measured at ignition at 1000° C was found to be about 37 wt% [5].

The water-impregnated silica gel was then added to a hexane solution of trimethylaluminium (TMA) in glove box and stirred at 0 °C for about 1 hour. During this reaction methane gas was evolved instantly and stopped after complete addition. Filtration and thorough wash with hexane afforded a multilayer of MAO on silica as white powders (Figure 2). Excess of TMA was used to make sure all active sites that are isolated and hydrogen-bonded silanol groups as well as siloxane groups have been consumed. Unlike pure TMA, the resulting supported MAO does not inflame spontaneously when exposed to air however, it changes color to dark brown.

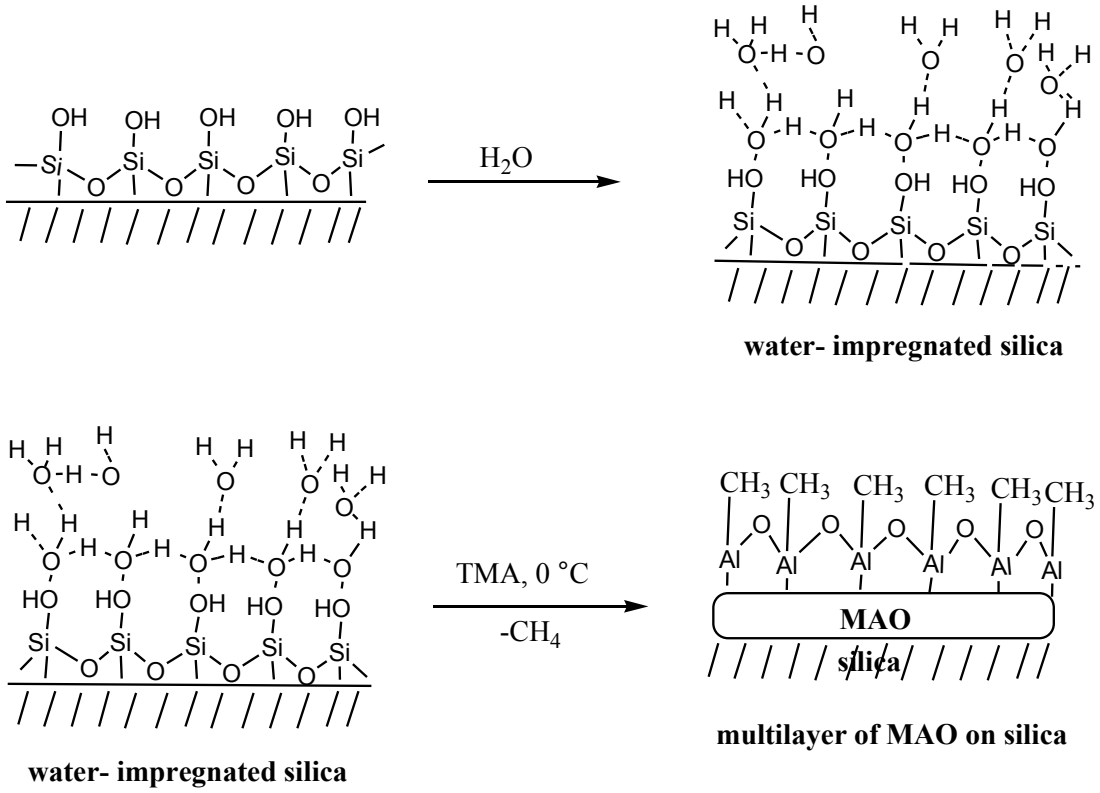

Scheme 1: Immobilization of MAO on silica gel.

8.2.2 Grafting of Complexes 1 and 2 on Silica Supported MAO

The immobilization of catalysts was performed by adding to a stirred solution of known concentration of the homogeneous catalyst in dichloromethane the appropriate amount of modified support. Immediately a color change of the support from white to light brown was noticed implying that the immobilization was successful. The supported catalysts were recovered by filtration, washing and drying in vacuum.

In previous chapter we managed to prove that the immobilization of catalysts on niobic acid on silica was through the exchange of the chloride ligands of catalysts by oxygen of the support through the evolution of HCl. Based on this finding, we propose that the same mechanism can apply to the immobilization on Lewis acidic supported MAO, however, this time Cl_2 is evolved instead of HCl and the following structures are proposed (Scheme 2).

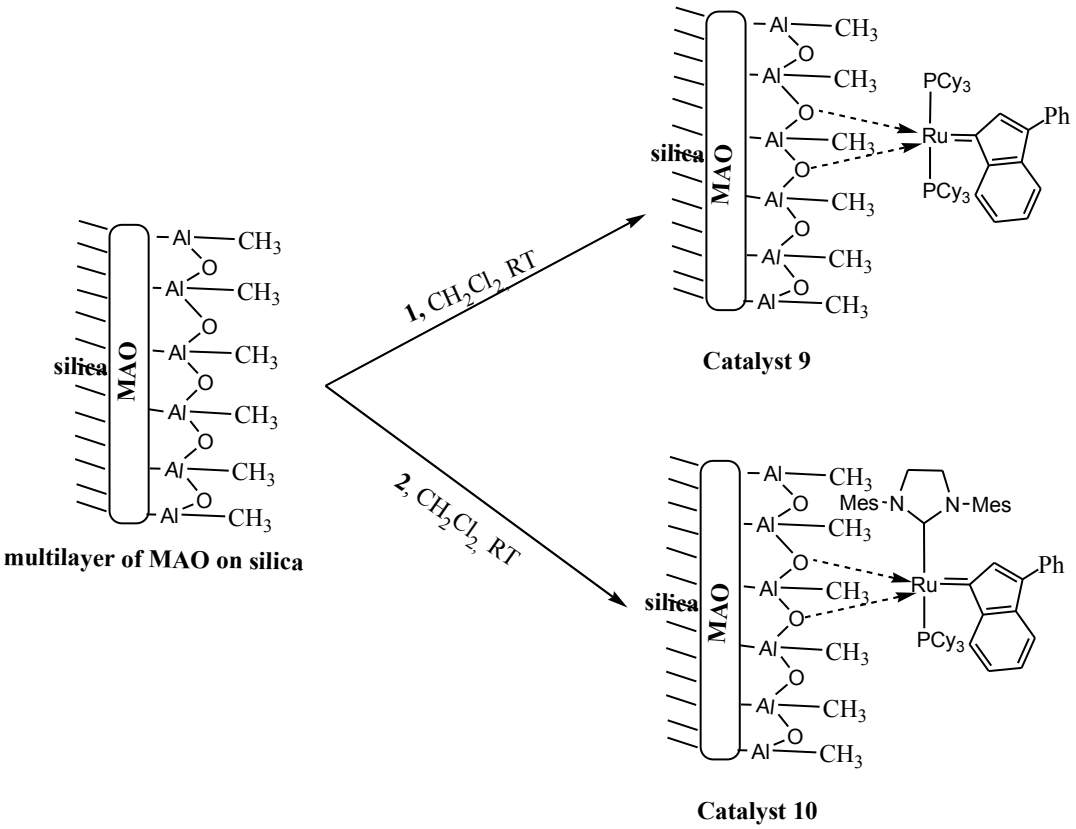

Scheme 2: Grafting of complexes **1** and **2** on silica supported MAO.

8.2.3 Characterization of Support and Supported Catalysts

The support and the supported catalysts were characterized by Fourier Transform Infrared Spectroscopy (FTIR) and nitrogen adsorption.

8.2.3.1 Fourier Transform Infrared Spectroscopy

The quality of the prepared materials was determined by Fourier transform infrared spectroscopy. Figure 2 represents the FTIR spectra of (a) water-impregnated SiO_2 (b) MAO-SiO_2 (c) Catalyst **9**. As seen from the figure, the spectrum of water-impregnated SiO_2 shows a sharp peak at 3750 cm^{-1} and a broad band around 3450 cm^{-1}, corresponding to the isolated and hydrogen-perturbated silanol groups respectively. In addition to the hydroxyl group vibration, the spectrum also shows the typical Si–O lattice vibrations that are two broad bands between

2100 cm^{-1} and 1800 cm^{-1} with medium intensity. The bending vibration of the adsorbed water is visible at 1630 cm^{-1} [6].

The water-impregnated silica gel was treated with TMA to afford a multilayer of MAO-SiO_2. The spectrum of MAO-SiO_2 (b) reveals some changes relative to that of the parent silica. While the bending vibration of the adsorbed water shows reduced intensity, peak that correspond to the silanol groups has been replaced by that of Al-OH groups around 3660 cm^{-1} and that of C-H stretching between 2800 and 3000 cm^{-1}. All peaks that are typical of Si–O lattice vibrations are still visible.

On the other hand, the spectrum of catalyst **9** (c) shows bands for the aromatic ring breathing mode at 1545 cm^{-1} and 1560 cm^{-1} as well as that of =C–H aromatic stretching vibrations at 3056 cm^{-1} [6]. The assignment of the infrared peaks and bands to supports and supported catalysts are summarized in Table 1.

Table 1: Assignment of the pnfrared peaks and bands to the supports and the supported catalysts

Wave number, cm^{-1}	**Assignment**
2100, 1800,1450-900	Si-O vibration
3750, 3450	O-H stretching
1500-1630	O-H vibration
3660	Al-O-H stretching
2800, 3000	C-H stretching
1545, 1560	Aromatic ring breathing mode
3056	=C-H aromatic stretching vibration

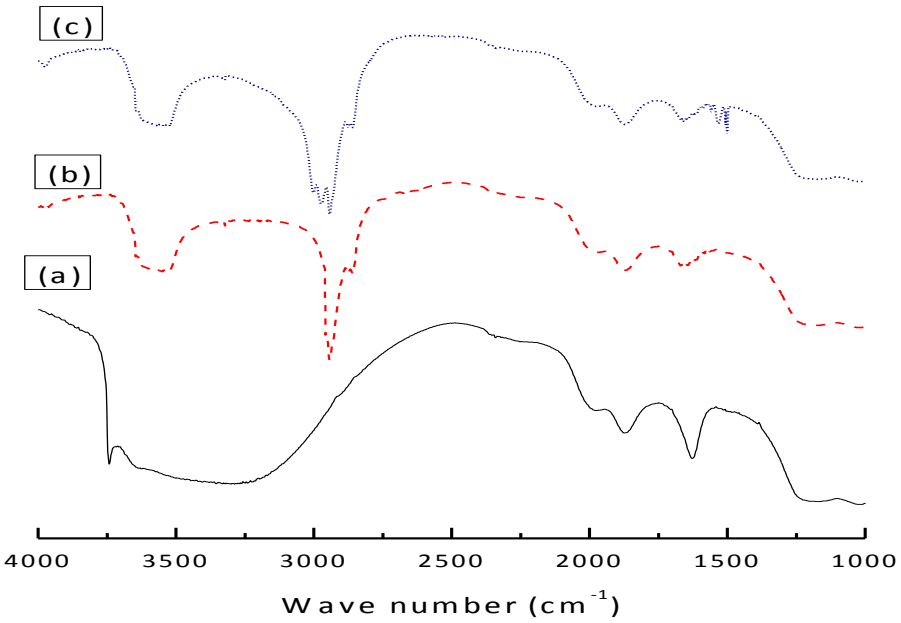

Figure 2: FTIR spectra of (a) water-impregnated SiO_2 (b) MAO-SiO_2 (c) Cat **9**.

8.2.3.2 Nitrogen Adsorption

Nitrogen adsorption was used for porosity characterization of prepared materials and the results obtained are summarized in Table 2. The results show the decrease in surface areas after each step of catalyst immobilization implying that the anchored materials occupy some space of silica's pore volume. In all cases the catalysts resulted from immobilization of second generation ruthenium indenylidene (e.g catalysts **4** and **10**) showed greater decrease in surface area than those resulted from first generation analogs (e.g catalysts **3** and **9**). This might be due to the fact that the size of immidozolinium ligand is bigger as compared to that of tricyclohexylphosphine. On the other hand, catalysts immobilized on silica supported MAO exhibited smaller surface area realative to those immobilized on silica supported niobic acid. Likewise, the dissimilarity

can be explained in term of their difference in size, that is the bulk supported MAO can occupy more volume.

Table 2: Results of nitrogen adsorption studies on the representative samples

Material	**Surface Area (BET) m^2/g**	**Pore Volume (BJH) cm^3/g**
SiO_2	480	0.75
MAO-SiO_2	158	0.69
Catalyst **3**	243	0.61
Catalyst **4**	241	0.66
Catalyst **9**	153	0.63
Catalyst **10**	142	0.62

8.2.3.2.1 Nitrogen Adsorption-Desorption Isotherms of the Supports and Supported Catalysts

The adsorption-desorption isotherms of the parent silica gel, MAO-SiO_2 support and its respective supported catalyst **9** are shown in Figure 3. The isotherms obtained exhibit a type IV behavior according to IUPAC classification [7]. The isotherms reveal three rapid nitrogen uptake steps. The first rapid nitrogen uptake at low relative pressure (< 0.1) is attributed to a gradual microporous filling by the nitrogen. This is followed by monolayer adsorption at relative pressure greater than 0.1. At relative pressure greater than 0.5, initial multilayer adsorption is observed causing capillary condensation. The isotherms show hysteresis loops at relative pressure greater than 0.6, which can be classified as type H1 according to IUPAC classification [7].

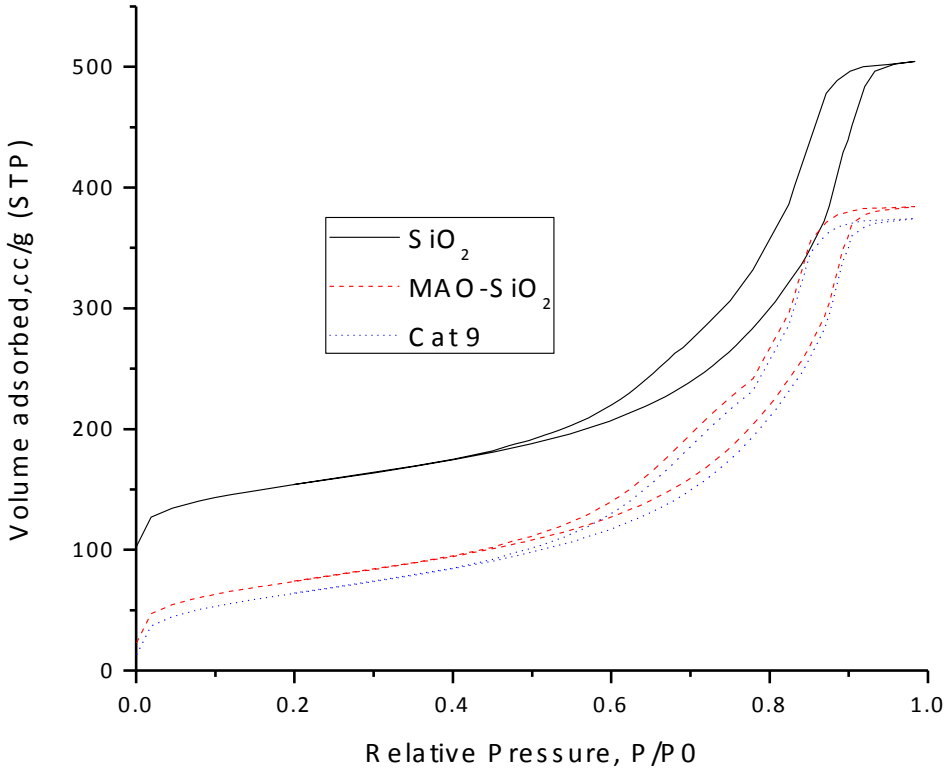

Figure 3: Adsorption-desorption isotherms of (a) SiO_2, (b) MAO-SiO_2 and (c) catalyst **9**.

8.2.4 Catalytic Test

The supported catalysts **9** and **10** were tested towards their activity for ring opening metathesis polymerization (ROMP) of norbornene and 1,5-*cis,cis*-cylooctadiene (COD) and the obtained results were compared with those of their corresponding catalysts immobilized on niobic acid.

8.2.4.1 ROMP of COD

Figure 4 shows reaction kinetics of catalysts **3**, **4, 9** and **10** for ROMP of 800 equivalent COD at 90 °C. As seen from the figure catalysts **9** and **10** have demonstrated activity which are comparable to that of their corresponding catalysts immobilized on niobic acid. As expected catalyst **10** shows better activity relative to catalyst **9** which is due to the presence of strong electron donating NHC ligand.

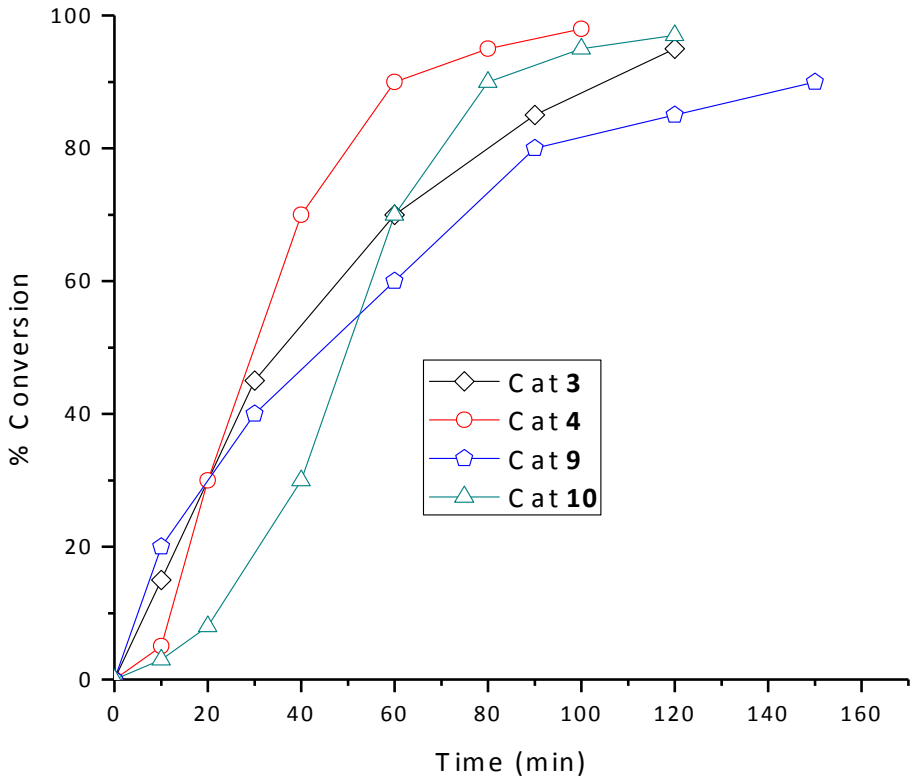

Figure 4: Activity of catalysts **3**, **4, 9** and **10** in ROMP of 800 equivalent COD at 90 °C.

8.2.4.2 ROMP of Norbornene

The activity of catalysts **3**, **4, 9** and **10** for ROMP of 10000 equivalents norbornene at room temperature is shown in Figure 5. As in ROMP of COD, catalysts **9** and **10** have demonstrated activities which are comparable with those of corresponding catalysts supported on niobic acid and catalyst **10** reveals better catalytic performance than catalyst **9**.

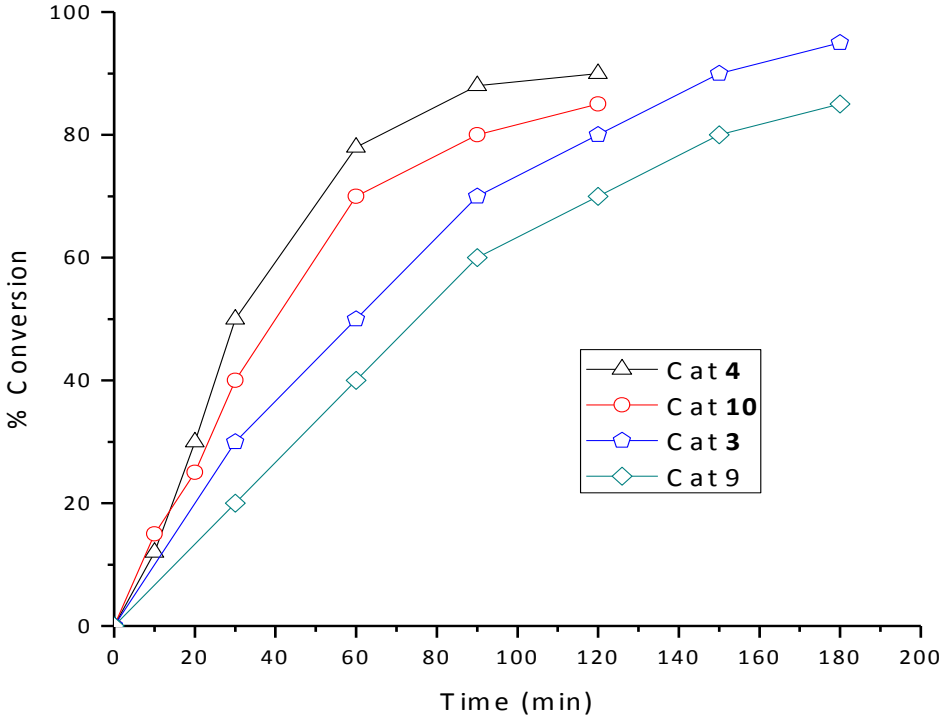

Figure 5: ROMP of 10000 equivalents norbornene applying catalysts **3**, **4, 9** and **10** at room temperature.

8.2.5 Stability of Catalysts

As stated in the introductory part of this chapter the silica supported MAO has been prepared as alternative support for ruthenium indenylidene after proved failure of niobic acid on silica. The activity of niobic acid supported catalysts on metathesis was found to slowly diminish to completely inactive which was associated with decomposition of the catalysts caused by the water molecules found in hydrated niobium oxide. We hoped that supported MAO could solve the problem. Like previous chapter the rate of decomposition of the catalysts was monitored in ROMP of 300 equivalents COD at 90 °C. The results revealed that catalysts **9** and **10** are less stable relative to the niobic acid supported analogs (catalyst **3** and **4**) as they decomposed within 24 hours after their preparation (Table 3).

Table 3: Time for complete decomposition of the catalysts

Catalyst	Time (hour)
9	24
10	24
3	150
4	170

The exact reason for this drawback is still not known, however, we propose that some physisorbed water, still available in the supported catalysts, can react with the carbene to form ruthenium hydride (Scheme 3). As seen from the infrared spectrum of the catalysts **9** (Figure 2c) the bending vibration of the adsorbed water is still visible at 1630 cm^{-1}.

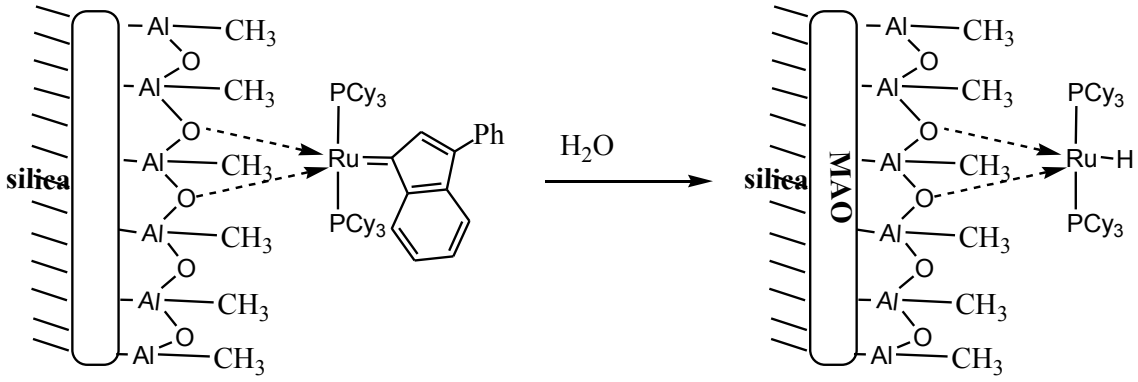

Scheme 3: Decomposition of catalysts due to the physisorbed water.

8.3 Experimental

8.3.1 Preparation of Silica Supported MAO

1.0 g of silica gel (Davisil 633) was treated with enough water to form a slurry mixture. The formed slurry was then air dried at room temperature to a free flowing state to form water-impregnated silica gel. A dried 100 ml Schlenk flask was then charged with 50 ml of dry hexane, cooled to 0 °C and flushed with N_2 for about 30 minutes before addition of 2 ml of TMA (2 M in hexane). Thereafter, 1.0 g of the prepared water-impregnated silica gel was added and further

stirred for 30 minutes at 0 °C followed by filtration, washing with hexane and drying for 2 h at 120 °C under vacuum to afford 0.8 g multilayer of MAO on silica.

8.3.2 Grafting of Complexes 1 and 2 on Silica Supported MAO

The immobilization of catalysts was performed by adding to a stirred solution of known concentration (20 ml, 0.5 mM) of homogeneous catalyst in dichloromethane the 1.0 g of support and stirred for about an hour under argon atmosphere. Thereafter, the supported (1.0 g) catalyst was filtered, washed with dichloromethane and dried in vacuum.

8.3.3 Characterization of Supports and Supported Catalysts

The supports and the supported catalysts were characterized by fouier transform infrared spectroscopy and nitrogen adsorption.

8.3.3.1 Nitrogen Physisorption Study

Before analysis about 0.02 g of the sample in a sample cell was degassed in a degassing station at 120 ºC for 3 hours. The sample cell was then connected to the analysis pot, where the sample was analysed for both adsorption and desorption process. In the analysis pot, the sample cell with sample was cooled using liquid nitrogen at a temperature of 77.2 K. After completion of the analysis, the analyzed sample was accurately re-weighed and the new sample weight was used for data analysis. The BET method was used to analyze the surface area, whereas the BJH method was employed for pore size distributions determination.

8.3.3.2 Fourier Transform Infrared Spectroscopy

Potassium bromide (KBr) was used as the diluents (matrixes) for sample measurements. About 1.0 mg of the dried sample and amount 30 mg of KBr were finely ground. The powder mixture was then mounted in a sample holder through which the light beam of the spectrometer was passed. The spectra were recorded at room temperature and background spectrum of finely ground anhydrous KBr was subtracted from the spectra. The spectrum obtained was used for qualitative determination of functional groups

8.3.4 Catalytic Test

The supported catalysts were tested on their activity and stability for ROMP of norbornene and cyclooctadiene.

8.3.4.1 ROMP of Norbornene

The catalyst (1.0 μmol) and 0.01 mol norbornene solution in dichloromethane were mixed in 15 ml vial. The reaction mixture was stirred and the reaction was stopped at different time intervals and the polymerization was stopped by addition of 2-3 ml of an ethylvinylether/BHT. The solution was stirred till the deactivation of the catalytically active species was completed. To remove the heterogeneous catalyst from the reaction mixture, the formed gel was dissolved in 50 ml THF and the catalyst was filtered off. The polymer was re-precipitated by pouring the filtrate into 50 ml methanol (containing 0.1% BHT). The obtained white polymers were then filtered off and dried in vacuum overnight.

8.3.4.2 ROMP of Cyclooctadiene

The catalyst (1.0 μmol) and 0.8 mmol cyclooctadiene solution in toluene were mixed in 15 ml vial and the temperature was raised to 90 °C. The reaction mixture was stirred and the reaction was stopped at different time intervals and the polymerization was stopped by addition of 2-3 ml of an ethylvinylether/BHT. The solution was stirred till the deactivation of the catalytically active species was completed. To remove the heterogeneous catalyst from the reaction mixture, the formed gel was dissolved in 50 ml THF and the catalyst was filtered off. The polymer was re-precipitated by pouring the filtrate into 50 ml methanol (containing 0.1% BHT). The obtained white polymers were then filtered off and dried in vacuum overnight.

8.3.4.3 ROMP of Cyclooctadiene for Decomposition Study

The sample of catalyst (1.0 μmol) was taken from the same batch after every 24 hours and the first sample was taken immediately after catalyst preparation. The catalyst sample and 0.3 mmol cyclooctadiene in toluene were mixed in 15 ml vial and the temperature was raised to 90 °C. The reaction mixture was stirred and all reactions were stopped after 30 minutes. The polymerization was stopped by addition of 2-3 ml of an ethylvinylether/BHT. The solution was stirred till the

deactivation of the catalytically active species was completed. To remove the heterogeneous catalyst from the reaction mixture, the formed gel was dissolved in 50 ml THF and the catalyst was filtered off. The polymer was re-precipitated by pouring the filtrate into 50 ml methanol (containing 0.1% BHT). The obtained white polymers were then filtered off and dried in vacuum overnight.

8.4 References

[1] M. Chang, U. S. Patent, 5006500 (1991).

[2] D. H. Lee, S.Y. Shin, *Macromol. Symp.,* 1997, **97**, 195.

[3] L. K. Van Looveren, D. E. De Vos, K. A. Vercruysse, D. F. Geysen, B. Janssen, P. A. Jacobs, *Catal. Lett,*. 1998, **56**, 53.

[4] J. C. W. Chien, D. J. He, *Polym. Sci. A: Polym. Chem.,* 1991, **29**, 1603.

[5] M. Chang, U. S. Patent, 5086025, (1992).

[6] T. Takei, K. Kato, A. Meguro, M. Chikazawa, *Colloids Surf. A: Physicochem. Eng. Asp.,* 1999, **77**, 1590.

[7] K. S. W. Sing, D. H. Everet, R. A. W. Haul, L. Moscou, R. A. Pierotti, J. Rouquerol, T. Siemieniewska, *Pure Appl. Chem.,* 1985, **57**, 603.

Part III: Summary Conclution and Outlook

9.1 Summary

In organic chemistry, methods for carbon-carbon bonds formation are extremely important. Olefin metathesis has been used for several decades as among method for carbon-carbon bonds formation and now has become a standard method.

Yves Chauvin's metathesis reaction mechanism represents a great step forward since it shows how the catalysts work. This mechanism made the development of well-defined single species possible. A number of reseachers made major contributions to the development of metathesis catalysts and their applications, but a major breakthrough in this area was made by R. H. Grubbs and R. R. Schrock. While Schrock developed molybdenum and tungsten based alkylidene catalysts, Grubbs developed ruthenium alkylidene catalysts which display not only functional groups tolerance but also improved activity.

Along these lines, numerous ruthenium complexes have been prepared and used successfully as efficient metathesis catalyst precursors in wide range of well-established synthetic procedures such as ring-closing metathesis, cross-metathesis, ring-opening metathesis polymerization and acyclic diene metathesis. Interesting feature of these carbenes is that, they can be applied in other kind of reaction apart from olefin metathesis. These reactions include: Kharasch addition, atom transfer radical polymerization, hydrogenation of olefins, oxidation of alcohols, isomerization reactions *etc*.

In addition, ruthenium carbenes can be immobilized on various support materials to yield heterogeneous catalysts that combine the advantages of conventional heterogeneous catalysts with the versatility of homogeneous ones. Heterogeneous catalysts not only allow for easy of separation and recovery from the reaction medium but also show repeated recycling potential, good stability and easy of handling.

It is known that, fine-tuning the ancillary ligands around the metal coordination sphere influences activity and selectivity of the resulting catalysts. In this respect, the first part of this thesis aimed at developing the second generation ruthenium indenylidene metathesis catalysts **1-3** (Scheme 1) coordinated with *N*-alkyl, *N'*-aryl heterocyclic carbenes.

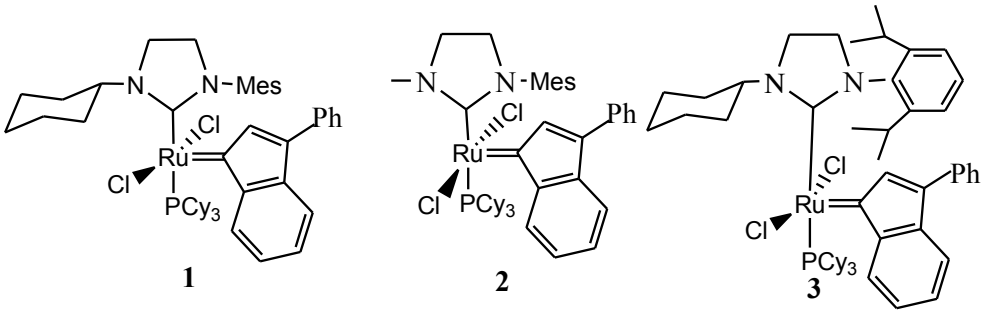

Scheme 1: Ruthenium based indenylidene catalysts **1-3**.

In achieving this objective different techniques were applied, these include treatment of the 1st generation complex with generated free *N*-heterocyclic carbene, use of chloroform and pyridine adducts. However, in all cases the desired complexes (**1-3**) were not obtained instead bis(NHC) complexes **4-6** were afforded in reaction of unsymmetrical heterocyclic carbene with pyridine adduct according to Scheme 2.

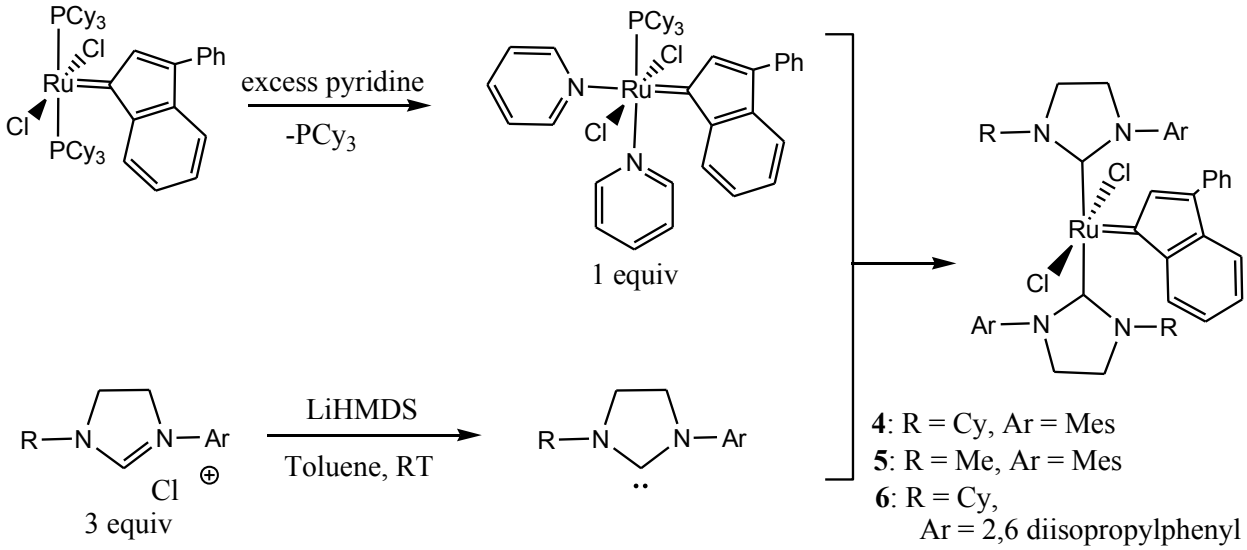

Scheme 2: The general procedure for the preparation of complexes **4-6**.

The catalytic activity of complexes **4-6** was evaluated in both metathesis and non-metathesis reactions. In metathesis reactions the catalysts were tested in the ROMP of 1,5-*cis,cis*-cyclooctadiene and RCM of diethyl diallyl malonate using different monomer:catalyst ratios. All catalysts **4-6** reveal poor activity in these reactions at room temperature due to low lability of

NHCs relative to phosphine ligands. In contrast, rising temperature to 80 °C improved the activity significantly.

In non-metathesis reaction, our initial efforts focused on isomerization of allylic alcohols and Kharasch addition. We were successful in isomerization of penten-3-ol, hepten-3-ol to their corresponding carbonyl compounds. In this reaction the effect of temperature was clearly seen as by applying 5 mol% of either catalyst at room temperature no noticeable conversion was observed after 72 h of reaction in all substrates. Upon addition of 5 mol% of KO*t*Bu the reaction was quantitative after 72 h, rising temperature to 80 °C, however, significantly increases the rate of conversion.

Interestingly, 5 mol% of catalysts alone did not work in this reaction even at higher temperature. To get the catalysts work well either 10 mol% of catalyst or combination of 5 mol% of catalysts with 5 mol% of KO*t*Bu should be used at 80 °C. Nevertheless, together with these conditions isomerization of 2-cyclohexen-1-ol was not possible by these catalysts.

In case of Kharasch addition, the plan was addition of chloroform and carbon tetrachloride to *n*-octene, *n*-hexene and styrene. To our surprise by applying 2.5 mol% of the either catalyst at 80 °C the expected Kharasch addition results were not obtained instead results which are corresponding to isomerization products were revealed in case of *n*-octene, *n*-hexene. In the reaction of either chloroform or carbon tetrachloride with styrene under these reaction conditions no conversion whatsoever observed after 24 h of reaction. Failure of our catalysts to mediate Kharasch addition can be associated with the presence of NHC ligands which are more basic and bulkier than phosphine ligands.

The next part of this study dealt with the development heterogeneous catalysts in which ruthenium indenylidene catalysts **7** and **8** (Scheme 3) were immobilized on silica supported niobic acid as well as on silica supported methylaluminoxane (MAO).

The dispersion of niobic acid monolayer on silica was done by refluxing a suspension of silica gel in a hexane solution of niobium ethoxide under argon atmosphere. The acidity of the resulting NbO_x/SiO_2 was manipulated by treating the materials with either concentrated H_2SO_4 or H_3PO_4 solutions to obtain $SNbO_x/SiO_2$ and $PNbO_x/SiO_2$ respectively. Upon stirring a suspension

of the obtained support with the homogeneous catalyst in dichloromethane, the supported catalysts **9-14** (Scheme 3) were afforded.

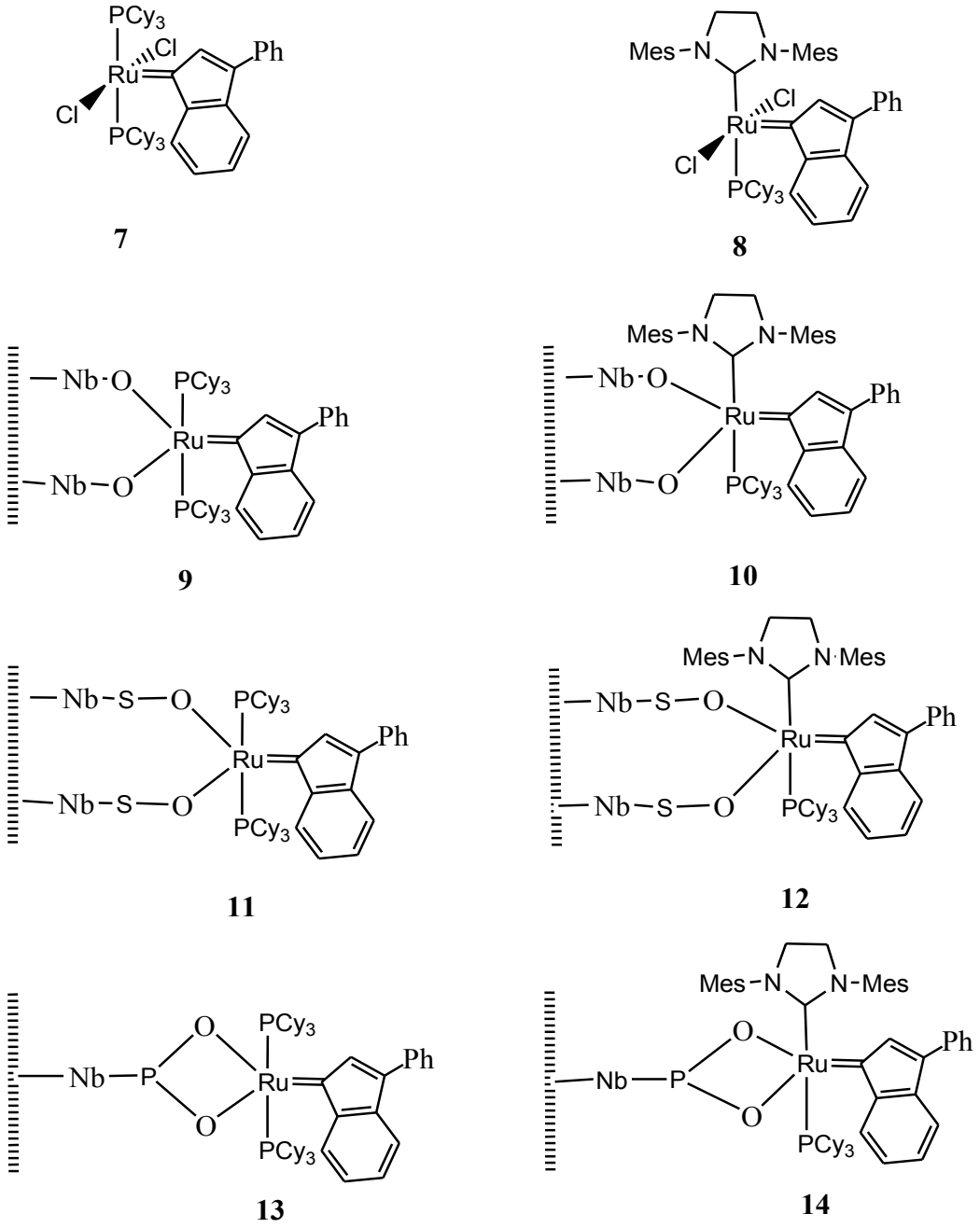

Scheme 3: Homogeneous ruthenium indenylidene catalysts (**7** and **8**) and niobic acid supported catalysts (**9-14**).

The support and the supported catalysts were characterized by various techniques. The techniques include: Fourier Transform Infrared Spectroscopy (FTIR), pyridine adsorption, and nitrogen adsorption. While FTIR proved the immobilization was successful, pyridine adsorption revealed that immobilization is the result of interaction between niobium-Brønsted acidic sites and the ruthenium complex. On the other hand, nitrogen adsorption reveals that the texture of the support was not deformed as a result of catalyst immobilization. The supported catalysts show moderate activity for the ring-opening metathesis polymerization (ROMP) of norbornene and 1,5-*cis*-*cis*-cyclooctadiene (COD). Unfortunately, the catalysts slowly loose activity to become completely inactive after one week due the decomposition. We propose that this undesirable deactivation is due to water molecules which are released from the support. The rate of decomposition was monitored in ROMP of COD and the average rate of decrease in the polymerization yield was found to be about 0.67% per hour for catalyst **9** and about 0.57% per hour for catalyst **10**.

The results obtained for the immobilized catalysts on silica supported niobic acid prompted us to investigate the suitability of a strong Lewis acidic-silica supported methylaluminoxane (MAO) as support for ruthenium indenylidene catalysts **7** and **8** (Scheme 3). Silica supported MAO was prepared *in situ* by controlled hydrolysis of trimethylaluminium (TMA) with the silanol groups and physisorbed water of the silica support.

As proved by FTIR and nitrogen adsorption, the ruthenium indenylidene catalysts **15** and **16** (Scheme 4) have been successful immobilized on silica supported MAO without deforming the texture of the support. As in case of niobic acid supported catalysts, the MAO supported catalysts show moderate activity for the ring-opening metathesis polymerization (ROMP) of norbornene and 1,5-*cis*-*cis*-cyclooctadiene (COD) and found to be less stable relative to their niobic acid supported analogs.

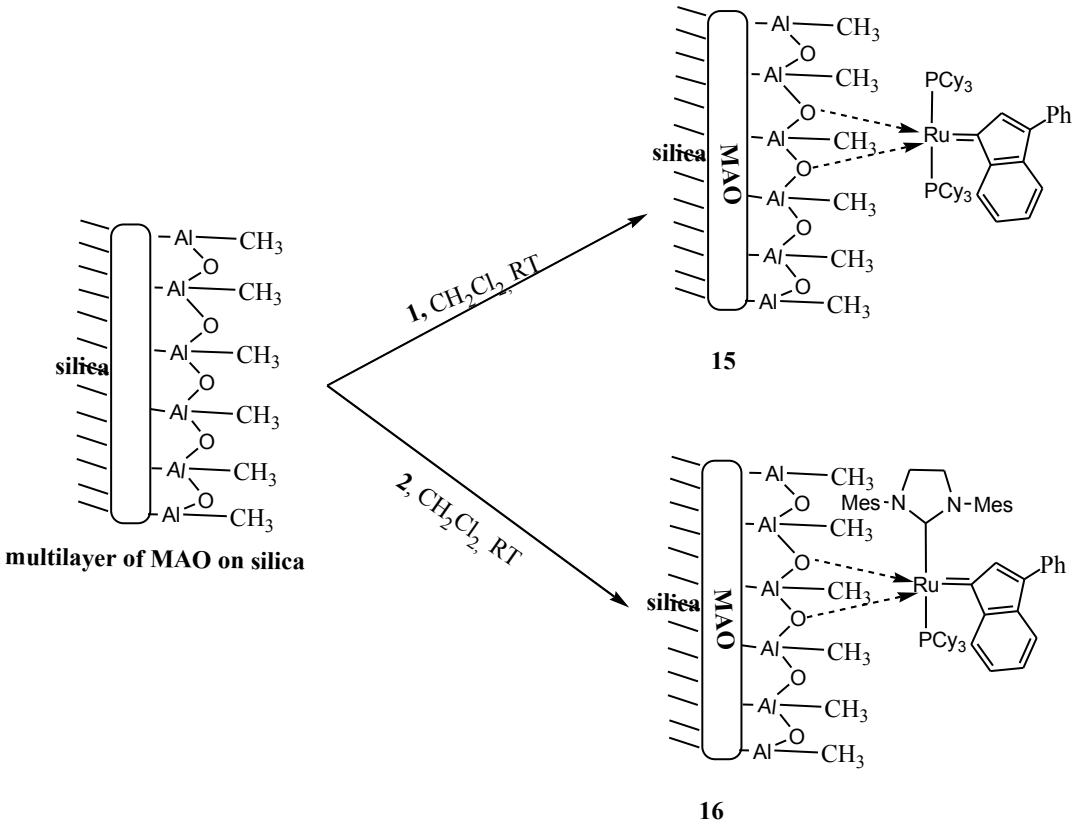

Scheme 4: Grafting of complexes **7** and **8** on silica supported MAO.

9.2 Outlook

Nowadays a number of ruthenium metathesis catalysts have been developed owing to their accessibility, remarkable activity and selectivity, connected with good tolerance towards functional groups, air and moisture. Innovative development in the class of ruthenium metathesis catalysts coordinated with NHC has been experienced which mainly directed toward tuning their catalytic activity and selectivity through altering both steric and electronic properties. The unsymmetrical NHC ligands in particular, have been introduced to induce dissymmetry, a key for achieving higher level of selectivity in different reactions. A great number of the ruthenium complexes bearing unsymmetrical NHC ligands have been developed up to this moment. The bis-coordinated ruthenium indenylidene developed in this work showed moderate activity at higher temperature in RCM, ROMP and other kind of reactions such as isomerization of allylic alcohols and isomerization of alkenes. Failure of these catalysts to work at room temperature has been attributed to the lack of labile ligand.

This call for further research which will focus on tuning of unsymmetrical NHC ligands to achieve more active and selective ruthenium complexes coordinated with non-labile NHC ligand with the labile one. The research should go in hand with design and synthesis of heterogeneous catalysts that can be recovered from the reaction mixture and be recycled. Although the support materials used in this study proved to be not suitable for metathesis, the obtained results can be considered as a challenge in the journey toward designing stable and active heterogeneous ruthenium indenylidene catalysts. Up to now a number of solid materials have been developed and successfully utilized in the immobilization of ruthenium benzylidene complexes. It is expected that the same materials can act as the suitable supports for ruthenium indenylidene and therefore, a study about development heterogeneous ruthenium indenylidene analogs would be of great interest.

10.1 Samenvatting

In de organische scheikunde zijn methoden om koolstof-koolstof bindingen te vormen uiterst belangrijk. Olefine metathese is reeds enkele decennia gebruikt op industriële schaal als een methode om koolstof-koolst of bindingen te vormen en nu is uitgegroeid tot een standaard methode.

Het metathese reactiemechanisme, ontdekt door Yves Chauvin, betekende een grote stap voorwaarts, daar het laat zien hoe de katalysatoren werken. Dank zij dit mechanisme werd de ontwikkeling van goed gedefinieerde katalysatoren mogelijk. Tal van chemici hebben belangrijke bijdragen geleverd aan de ontwikkeling van metathese katalysatoren en hun toepassingen, maar de grote doorbraak op dit gebied werd gemaakt door R.H. Grubbs en R. R. Schrock. Terwijl Schrock molybdeen en wolfraam gebaseerde alkylideen katalysatoren ontwikkelde, ontwikkelde Grubbs ruthenium alkylideen katalysatoren die niet alleen een verbeterde functionele groep tolerantie maar ook verbeterde activiteit vertonen.

Tal van rutheniumcomplexen werden bereid en met succes gebruikt als efficiënte metathesekatalysator in tal van synthetische procedures zoals ringsluitingsmetathese, ringopeningmetathese, cross-metathese, ring-opening metathese polymerisatie en acyclisch dieënmetathese. Een interessant kenmerk van deze ruthenium carbenen is dat zij kunnen worden toegepast in andere reacties naast de olefine metathese. Deze reacties zijn onder andere de Kharasch reactie, atoomtransfer radicalaire polymerisatie, hydrogenatie van alkenen, oxidatie van alcoholen, en isomerisatiereacties. Daarnaast kunnen ruthenium carbenen worden geïmmobiliseerd op verschillende dragermaterialen ter vorming van heterogene katalysatoren die de voordelen van conventionele heterogene katalysatoren combineren met de veelzijdigheid van homogene katalysatoren.

Heterogene katalysatoren zorgen niet alleenvoor een gemakkelijke scheiding en terugwinning uit het reactiemedium maar bezitten ook hethergebruikspotentieel en een goede stabiliteit.
Het is bekend dat het afstemmen van de liganden rond de metaalcoördinatiesfeer de activiteit en selectiviteit van de verkregen katalysatoren beïnvloed. In dit opzicht, is het eerste deel van dit proefschrift gericht op de ontwikkeling van tweede generatie ruthenium indenylidene metathese katalysatoren **1-3** (Schema 1) gecoördineerd met *N*-alkyl, *N'*-aryl heterocyclische carbenen.

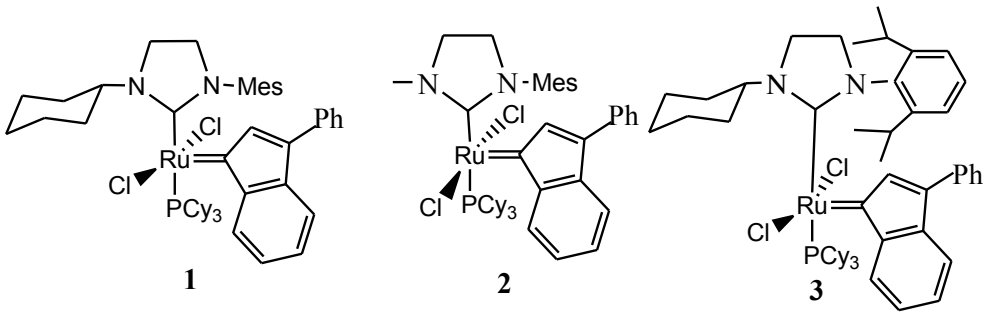

Schema 1: Ruthenium indenylideen katalysatoren **1-3**.

Om dit doel te bereiken werden verschillende technieken toegepast, deze omvatten de behandeling van het 1^{e}generatie ruthenium indenylideen complex met een vrij N-heterocyclisch carbeen, het gebruik van chloroformadducten en pyridine gesubstitueerde indenylideen complexen. Echter, in alle gevallen waren we niet succesvol in het verkrijgen van de gewenste complexen **1-3**. In plaats daarvan werden bis (NHC)-complexen **4-6** bekomen in reactie van een asymmetrische heterocyclisch carbeen met pyridine gesubstitueerde indenylideen complexen zoals weergegeven in Schema 2.

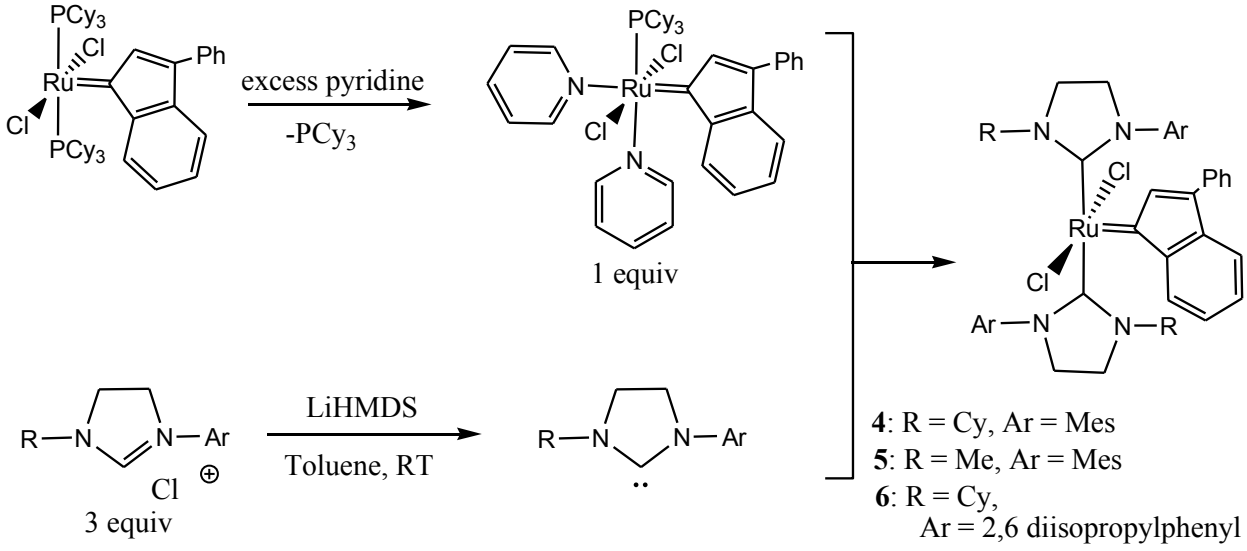

Schema 2: De algemene procedure voor de bereiding van complexen **4-6**.

De katalytische activiteit van complexen **4-6** werd geëvalueerd in zowel metathese als in niet-metathese reacties. In olefine metathese reacties werden de katalysatoren getest op de ROMP van 1,5-*cis*,*cis*-cyclooctadieën en de RCM van diethyldiallylmalonaat met verschillende katalysator/monomeer- of substraatverhoudingen.

Alle katalysatoren (**4-6**) vertonen een minder goede activiteit voor deze reacties bij kamertemperatuur, te wijten aan de lage labiliteit van NHCs ten opzichte van fosfineliganden. Daarentegen, bij verhoogde temperatuur (80 °C), verbetert de activiteit aanzienlijk.

Wat de niet-metathese reacties betreft, ging onze aandacht uit naar de isomerisatie van allylalkohol en de Kharasch additie reactie. We waren succesvol in isomerisatie van penten-3-ol en hepten-3-ol tot hun overeenkomstige carbonyl-verbindingen. In deze reactie,gebruikmakende van 5 mol% katalysator, werd het effect van de temperatuur duidelijk aangetoond daar bij kamertemperatuur geen merkbare omzetting werd waargenomen voor alle substraten, zelfs na 72 h reactie. Na toevoegen van een equivalente hoeveelheid KOtBu (t.o.v. de katalysator) en verhogen van de temperatuur tot 80 °C werd een kwantitatieve omzetting bekomen. Opmerkelijk was dat enkel 5 mol% van de katalysatoren op zich niet leidde tot conversie van het substraat, zelfs niet bij hogere temperaturen.

Om een goede omzetting van het substraat te bekomen diende ofwel 10 mol% van de katalysator ofwel een combinatie van 5 mol% katalysator met KOtBu (1/1 verhouding) gebruikt te worden bij 80 °C. Katalysator **6** presteerde relatief slecht wat mogelijks veroorzaakt kan worden door sterische hindering. Hoe dan ook, isomerisatie van 2-cyclohexeen-1-ol was niet mogelijk gebruikmakende van deze katalysatoren.

Watde Kharasch additie reactiebetreft, werd de additie van chloroform en tetrachloorkoolstof op n-octeen,n-hexeen en styreen beoogd. Tot onze verbazing, gebruikmakende van 2.5 mol% katalysator bij 80 °C, werden de verwachte Kharasch additieprodukten niet verkregen. Echter werden er in deze condities eveneens isomerisatieprodukten gevonden in geval van n-octeen, n-hexeen. In de reactie van hetzij chloroform of tetrachloorkoolstof met styreen onder dezelfde reactieomstandigheden werd geen enkele omzetting waargenomen na 24 h reactie.

Het falen van katalysatoren **4-6**voor de Kharasch additiereactie kan worden geassocieerd met de aanwezigheid van NHC liganden die een meer basisch karakter bezitten en meer sterisch zijn dan de

fosfineliganden dewelke aanwezig zijn in Grubbs katalysatoren [$RuCl_2$(=CHPh) (PR_3)$_2$] (R = fenyl,cyclopentyl en cyclohexyl).

Het volgende deel van deze studie behandeltde ontwikkeling van heterogene katalysatoren waarbij indenylideen rutheniumkatalysatoren **7** en **8** werden geïmmobiliseerd op silica gedragen niobiumzuur en op silica ondersteund methylaluminoxaan (MAO).

De dispersie van een niobiumzure monolaag op silica werd uitgevoerd door het refluxen van een suspensie van silicagel in een oplossing van niobiumethoxide in hexaan onder argonatmosfeer. De vaste stof werd af gefiltreerd, gewassen met droge hexaan en gedroogd onder vacuüm. De hydrolyse werd uitgevoerd door behandeling van de vaste stof met NH_4OH (1 M). De zuurtegraad van het verkregen $NbOx/SiO_2$ werd gemanipuleerd door behandeling van de materialen met geconcentreerde H_2SO_4 of H_3PO_4 oplossingenom vervolgens $SNbOx/SiO_2$ en $PNbOx/SiO_2$ respectievelijk te verkrijgen. Onder roeren van een suspensie van de verkregen drager met de homogene katalysator in dichloormethaan, werden de katalysatoren **9-14** (Schema 3) bekomen.

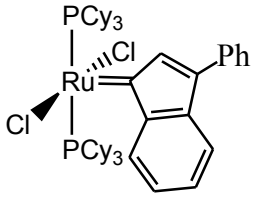

7

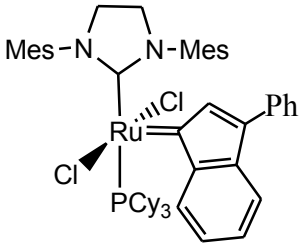

8

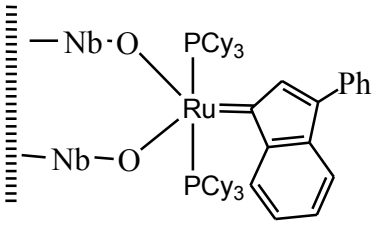

9

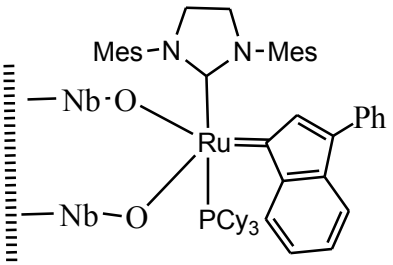

10

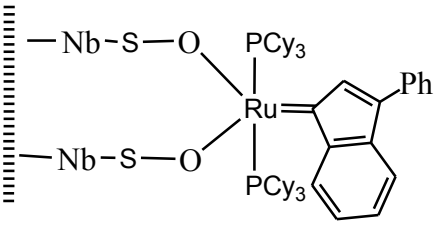

11

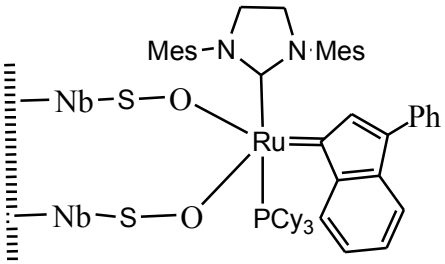

12

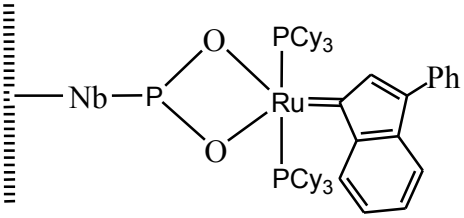

13

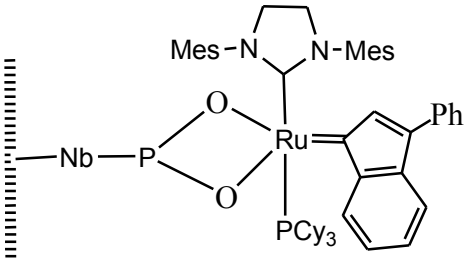

14

Schema 3: Homogene ruthenium indenylideen katalysatoren (**7-8**) en niobiumzuur verankerde katalysatoren (**9-14**).

De drager en de heterogene katalysatoren werden gekarakteriseerd met behulp van diverse technieken, zoals Fourier Transform Infrarood Spectroscopie (FTIR), pyridine adsorptie en

stikstofadsorptie. De FTIR studiebevestigt dat de immobilisatie geslaagd is, uit de pyridine adsorptiestudievolgt dat de immobilisatie het resultaat is van een samenwerking tussen niobium-Brønsted zure plaatsen en het rutheniumcomplex. Anderzijds, uit de stikstofadsorptie studie blijkt dat de structuur van de drager niet gewijzigd is door de katalysatorimmobilisatie. De heterogene katalysatoren vertonen een matige activiteit voor de ring-opening metathese polymerisatie (ROMP) van norborneen en 1,5-*cis*-cis-cyclooctadieën (COD). Helaas, verliezen de katalysatoren langzaam hun activiteit enworden volledig inactief na eenweek als gevolg van de decompositie. Wij veronderstellen dat deze ongewenste deactivering te wijten is aan watermoleculen die vrijkomen uit het dragermateriaal. De deactiveringsnelheid werd gecontroleerd voor ROMP van COD en de gemiddelde afnamesnelheid bleek ongeveer 0.5% per uur voor katalysator **9** en ongeveer 0.7% per uur voor katalysator **10** te zijn.

De verkregen resultaten voor de geïmmobiliseerde katalysatoren op silica gedragen niobiumzuur zetten ons er toe aa om de geschiktheid van methylaluminoxaan (MAO) (een sterk Lewis-zuur)op silica geënt als ondersteuning voor indenylideen ruthenium katalysatoren **7** en **8** (Schema 3) te onderzoeken. Silica ondersteund MAO werd *in situ* bereid via gecontroleerde hydrolyse van trimethylaluminium (TMA) met de silanolgroepen en het gefysisorbeerd water van de silicadrager. De katalysator immobilisatie werd uitgevoerd door aan een geroerde dichloormethaan oplossing met gekende homogene katalysatorconcentratie een passende hoeveelheid dragermateriaal toe te voegen. De katalysatoren op drager **15** en **16** (Schema 4) werden bekomen door filtratie, wassen en drogen onder vacuüm.

Zoals blijkt uit FTIR en stikstofadsorptie, werden de indenylideen ruthenium katalysatoren succesvol geïmmobiliseerd op silica ondersteund MAO zonder vervorming van de structuur van de drager. Zoals in het geval van niobiumzuur gedragen katalysatoren, de MAO katalysatoren vertonen matige activiteit voor de ring-opening metathese polymerisatie (ROMP) van norborneen en 1,5-*cis*-*cis*-cyclooctadieen (COD). Verder bleek dat deze katalysatoren minder stabiel zijn ten opzichte van hun niobiumzuur ondersteunde analogen.

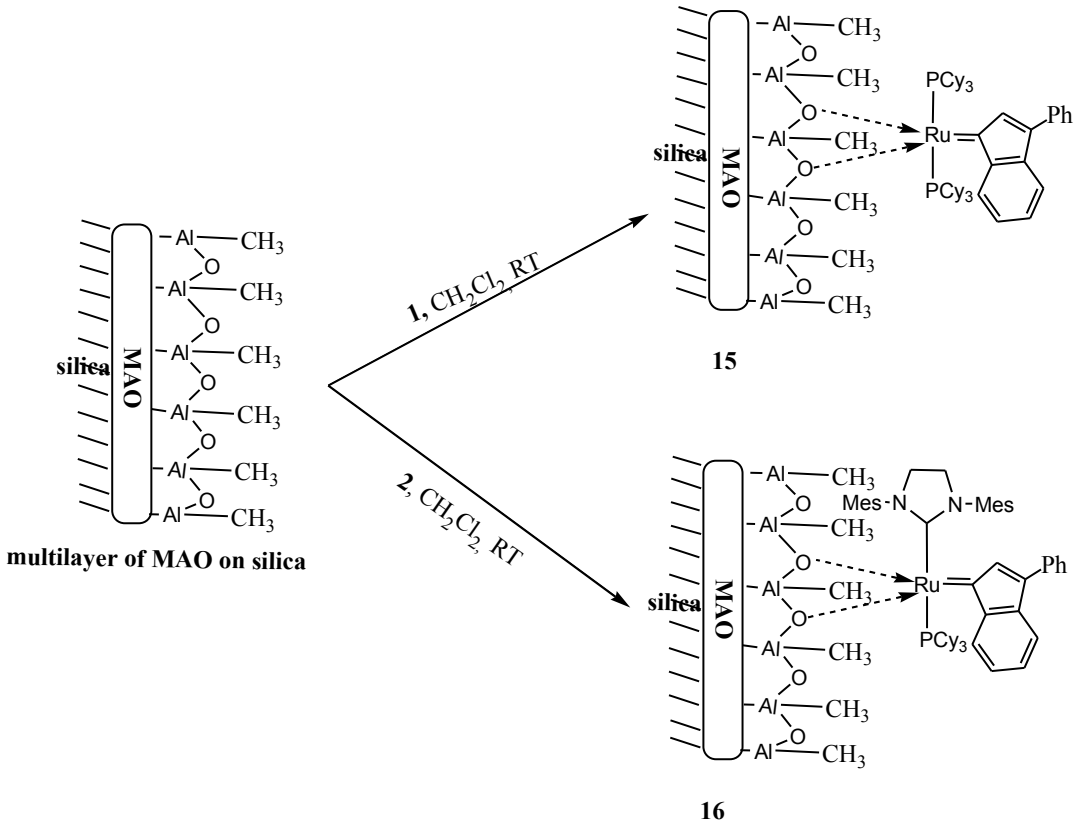

Schema 4: Enten van complexen **7** en **8** op silica ondersteunde MAO.

10.2 Vooruitzichten

Een reeks ruthenium metathese katalysatoren werden tot op heden ontwikkeld en dit omwille van hun toegankelijkheid, opmerkelijke activiteit en selectiviteit, verbonden met een goede tolerantie ten opzichte van polaire organische functionaliteiten en lucht. Rutheniumcomplexen genieten een uitstekend applicatieprofiel in de metathesereacties, meer bepaald in ringsluitingsmetathese (RCM), cross-metathese (CM), ringopening metathese (ROM) en de ring-opening metathese polymerisatie (ROMP). Het nut van ruthenium metathesecomplexen in andere katalytische processen buiten de olefine metathesereactie verdient speciale aandacht. Veel ruthenium carbenen hebben aangetoond dat ze reacties zoals Kharaschadditie, verwijdering van allylgroepen van aminen, de atoomtransfer radicalaire polymerisatie, de hydrogenering van olefinen, de transfer hydrogenering van ketonen, de dehydrogenerende oxidatie van alcoholen, de condensatie van dehydrogenerende alcoholen, en de hydrosilylering van carbonylen katalyseren. De nieuwe toepassingen van deze ruthenium gebaseerde katalysatoren dragen bij tot hun relevantie als een veelzijdig en effectief werktuig in

organische synthese en zal waarschijnlijk de ontwikkeling van nieuwe katalysatoren, zowel voor metathese als voor niet-metathese reacties, in de nabije toekomst stimuleren.

Innovatieve ontwikkelingen in de klasse van de NHC-ruthenium katalysatoren voor de olefinemetathese is vooral gericht op het afstemmen van hun katalytische activiteit en selectiviteit. De asymmetrische NHC liganden, die toelaten om de sterische omvang in de nabijheid van het rutheniumatoom te modificeren,brengen een verandering in de katalytische eigenschappen van de resulterende complexen. Dissymmetrie geïnduceerd door asymmetrische NHC liganden is een sleutel voor hogere selectiviteit in verschillende reacties. Een groot aantal ruthenium complexen met asymmetrisch NHC liganden werden tot nu toe ontwikkeld, maar er is nog steeds behoefte aan nieuwe complexen die niet alleen selectief maar ook stabiel en robuust zijn. Er wordt aangenomen dat de belangrijkste toekomstige focus in dit onderzoeksgebied rust op de ontwikkeling van nieuwe katalysatoren voor selectieve metathese. Voor zover de economische en milieuaspecten betreft, de ontwikkeling van nieuwe NHC-rutheniumcomplexen gekenmerkt door een hoge omzettingsgraad zijn vereist. Deze ontwikkeling moet hand in hand gebeuren met het ontwerp en de synthese van heterogene katalysatoren die kunnen worden teruggewonnen uit het reactiemengsel en hergebruikt worden.

De ontwikkeling van zeer actieve katalysatoren met een goed hergebruik zal helpen om het cruciale probleem van ruthenium verontreiniging in de farmaceutische industrie te overwinnen. Het protocol van Groene chemie vereist niet alleen de ontwikkeling van recycleerbare, efficiënte en stabiele katalysatoren, maar ook het ontwerp van de werkwijze voor het efficiënt verwijderen van metaalsporen uit de producten. Het aanvaardbare ruthenium gehalte in farmaceutisch producten is lager dan 10 ppm. Verschillende technieken werden toegepast om dit doel te bereiken, zoals silica-gel gebaseerde chromatografie, behandeling van het ruwe product met houtskool, DMSO of $Pb(OAc)_4$, enz. Bovendien, de immobilisatie van de katalysator op vaste dragers en het gebruik van een tweefasensysteem werden gebruikt als oplossing voor de zuivering en de terugwinning.

Echter, meestal is het niveau van rutheniumverontreiniging nog steeds hoger dan toegelaten eniseen uitgebreid onderzoek vereist naar de ontwikkeling van verbeteren van het hergebruik van de homogene katalysatoren en het minimaliseren van de verontreiniging in het eindproduct.